" MATHEMATICAL MODELS FOR THE CURE AND VISCOSITY CHARACTERISTICS OF AN EPOXY RESIN AND THEIR APPLICATIONS IN COMPUTER SIMULATIONS OF COMPOSITE MATERIAL MANUFACTURING PROCESSES "

by

WILLIAM RAYMOND JONES BSc, MSc.

A thesis submitted to the

University of Salford

in accordance with the regulations for the degree of

Doctor of Philosophy.

Department of Pure and Applied Physics.

1988

CONTENTS

		PAGE
LIST OF TABLES.		
LIST OF FIGURES.		
ACKNOWLEDGEMENTS.		
ABSTRACT.		
INTRODUCTION.		1
CHAPTER 1 - THE MANUFACTURE OF COMPOSITE MATERIAL COMPONENTS.		
1.1	Use of composite materials.	4
1.2	Manufacturing processes.	6
1.3	Autoclave process.	12
1.4	Process modelling.	15
1.5	Autoclave model.	17
1.5.1	"CURE" model.	20
1.6	BSL914 resin system.	21
CHAPTER 2 - RESIN THERMAL BEHAVIOUR.		
2.1	Cure monitor and resin thermal behaviour.	25
2.2	Differential Scanning Calorimetry.	28
2.2.1	Experimental procedures.	30
2.3	Resin exothermic behaviour.	31
2.3.1	Dynamic exotherm.	32
2.3.1.1	High temperature reactions.	32
2.3.1.2	Dynamic cure exotherm.	34
2.3.1.3	Dynamic baseline options.	38
2.3.1.4	Heat of cure.	39
2.3.2	Isothermal exotherm.	42
2.3.2.1	Autocatalytic reactions.	42
2.3.2.2	Isothermal heat of reaction.	44

CHAPTER 3 - CURE SUB-MODEL DEVELOPMENT.

3.1	Aims of model.	47
3.2	General kinetic analysis.	47
3.3	Kinetic function.	49
3.3.1	n-th order kinetic function.	49
3.3.2	Autocatalytic kinetic function.	51
3.3.3	Practical isothermal reaction rate.	52
3.4	Mathematical formulation.	55
3.4.1	Evaluation of ratio index.	59
3.5	Determination of isothermal rate constants.	61
3.5.1	Method A.	61
3.5.2	Method B.	70
3.6	Summary of kinetic parameters evaluation.	77

CHAPTER 4 - MODEL VERIFICATION AND CURE PREDICTION.

4.1	Methods of isothermal cure prediction.	79
4.2	Master cure curve.	79
4.3	Activation energy from cure curves.	87
4.3.1	FTIR study.	88
4.3.2	Geltime.	92
4.4	Model verification.	94
4.5	Cure prediction.	100
4.5.1	Direct integration.	100
4.5.2	Numerical solution.	105

CHAPTER 5 - VISCOSITY SUB-MODEL.

5.1	Viscosity behaviour.	113
5.2	Viscosity determination.	115
5.2.1	Cone-plate viscometer.	115
5.2.2	Experimental considerations.	118
5.2.2.1	Resin sample shape.	120
5.2.2.2	Meniscus effect.	121
5.3	Experimental results.	122
5.3.1	Shear rate.	122
5.3.2	Isothermal viscosity profiles.	124
5.4	Approaches to viscosity modelling.	126

5.5 Generation of model. 127
5.6 Representation of viscosity data. 136
5.7 Chemorheological model. 138

CHAPTER 6 - COMPUTER SIMULATION.

6.1 Dynamic model. 142
6.2 Models for temperature ramp conditions. 143
6.2.1 Ramp cure model. 143
6.2.2 Exotherm model. 145
6.2.3 Ramp viscosity model. 146
6.3 "VISICURE" computer program. 152
6.3.1 List of variables. 153
6.3.2 Arrays. 154
6.3.3 Function definition. 155
6.3.4 Structure of program. 155
6.4 Computer model output. 157

CHAPTER 7 - APPLICATIONS OF MODELLING TO PRACTICAL PROBLEMS

7.1 Typical manufacturing problems. 168
7.2 Mould cycle design. 168
7.2.1 Voids. 172
7.3 Moulding under temperature ramps. 173
7.4 Optimisation procedures. 175
7.5 Break in cycle. 180
7.6 DSC experiments. 181
7.6.1 Rate constants. 185
7.6.2 n-th order Activation Energy. 186
7.6.3 Verification of model. 188
7.7 Tg measurements. 190
7.8 Region of mouldability. 191

CONCLUSIONS. 193

REFERENCES.
APPENDIX 1 - TABLES.
APPENDIX 2 - VISICURE PROGRAM
APPENDIX 3 - FORMULAE AND CONVERSIONS

LIST OF TABLES.

No.	TITLE
1	Variation of H(iso) with temperature.
2	Reaction rate v Conversion at 140deg.C.
3	Ratio m/n v Temperature.
4(a)-15(a)	Amount and rate of cure at different temperatures.
4(b)-15(b)	Values for rate plots at different temperatures.
16(a)-20(a)	ln(k) v 1/Temperature for a number of conditions.
16(b)-20(b)	Values of n for a number of conditions.
21	Summary of kinetic parameters evaluation.
22,23	Arrhenius plots for ln(Time Shift).
24	ln(Reaction Rate) v 1/Temperature.
25	ln(Geltime) v 1/Temperature.
26-31	Isothermal cure rate calculated from the model at different temperatures.
32	$\log(v_o)$ v Temperature.
33	Coefficient A v Temperature.
34	Coefficient B v Temperature.
35-41	Dynamic Model Results.
42	Preconversion times.
43	Preconversions at 135°C.
44	30% Conversions.
45	Residual exotherms-30% Conversion.
46	Tg of 30% preconverted resin.

LIST OF FIGURES.

TITLE	FIGURE
TAY by-pass ducts.	1
Autoclave process.	2
Autoclave process model.	3
Idealised exotherm.	4
DSC cell crossection.	5
DSC scans.	6 - 8 inc.
Depth of particle removed v Time at 135deg.C.	9
ln(dm/dt) v 1/Temperature.	10
Peak temperature v Heating rate.	11
Dynamic exotherm v Heating rate.	12
Peak signal v Heating rate.	13
DSC scan.	14
Peak time v Temperature.	15
Variation of H(iso) with Temperature.	16
DSC scan.	17
Reaction rate v Conversion at 140deg.C.	18
$y = x^n(1-x)^m$	19
Ratio m/n v Temperature.	20
ln(m/n) v 1/Temperature.	21
ln(dα/dt) v ln(α(1-α)^r).	22,23
f(α) v Temperature.	24
lnK(L) v 1/Temperature.	25
Variation of n(L) with Temperature.	26
lnK(U) v 1/Temperature.	27
Variation of n(U) with Temperature.	28
Variation of n and m with Temperature.	29
lnK(D) v 1/Temperature.	30
Variation of n(D) v Temperature.	31
lnK(LP) v 1/Temperature.	32
Variation of n(LP) with Temperature.	33
lnK(WH) v 1/Temperature.	34
Variation of n(WH) with Temperature.	35
Isothermal cure v Time at 135deg.C.	36

Isothermal cure v ln(TIME) at various temperatures. 37
Arrhenius plot for isothermal ln(TIME SHIFT). 38
Master isothermal cure curve at 145deg.C. 39
Cure v ln(TIME) at different temperatures. 40
Arrhenius plot for ln(TIME SHIFT). 41
Master cure curve at 145deg.C. 42
FTIR trace. 43
Effective combined DICY weight v Time. 44
Arrhenius plot for reacted component. 45
ln(Geltime) v 1/Temperature. 46
Reaction rate v Conversion at temperatures. 47 - 52 inc.
Model conversion v Time (Simpson method) 53 - 58 inc.
Model conversion v Time (Euler method) 59 - 64 inc.
Model conversion v Time at 125deg.C. 65
Iso-conversion curves. 66
Cone and plate. 67
Viscosity v Time at 129.5deg.C. 68
Viscosity v Time at 149deg.C. 69
Shear stress v Shear strain for resin. 70
Experimental viscosity v Time. 71
Viscosity v Time at 138.8deg.C. 72
log(ZERO TIME VISCOSITY) v Temperature. 73
log(ZERO TIME VISCOSITY) v 1/Temperature. 74
Coefficient A v Temperature. 75
log(Coefficient A) v 1/Temperature. 76
Coefficient B v Temperature. 77
log(Coefficient B) v 1/Temperature. 78
Model viscosity v Time. 79
Viscosity v Time at 110deg.C. 80
Viscosity v Time at 139deg.C. 81
Viscosity surface. 82
Iso-viscosity contours(Poise) for BSL914 resin. 83
ln(VISCOSITY) v Conversion. 84
A v 1/Temperature. 85
Cure v Time during a temperature ramp. 86
Heat flow v Time for dynamic run. 87
Dependence of viscosity on integration steps. 88
BSL914 Viscosity profile. 89
Dynamic viscosity v Time. 90
BSL914-Isothermal viscosity at 139deg.C. 91

Viscosity v Time for isothermal hold at 139deg.C. 92
Flow chart. 93
Viscosity and Cure of BSL914 (MODEL OUTPUT).94 - 100 inc.
Model viscosity v Time at 125deg.C. 101
Moulded thickness v Precompression dwell. 102
Void content v Precompression dwell. 103
Viscosity and Cure of BSL 914. 104
Time below 150Poise v Ramp rate. 105
Temperature range with viscosity below 150Poise. 106
Viscosity minimum v Ramp rate. 107
Viscosity and Cure of BSL 914. 108-110 inc.
Residual exotherms-preconverted at 135deg.C. 111
Residual exotherms-30% preconversion. 112
Reaction rate v Conversion at 150deg.C. 113
Index m v Temperature (30% preconversion). 114
lnk v 1/Temperature (30% preconversion). 115
DSC Trace. 116
Cure simulation with break in run. 117
Viscosity and Cure of BSL 914. 118
Region of unmouldable material. 119

ACKNOWLEDGEMENTS.

First of all many thanks go to Rolls-Royce Plc for sponsoring the current research work.

I would also like to express my gratitude to both Professor J.W.Johnson, Rolls-Royce Plc and Professor B.Yates, University of Salford for their continued support and encouragement over the duration of the project.

I am also indebted to colleagues both at Manufacturing Technology-Composites, Alfreton Road and the Training Department, Mickleover for their assistance in support of the modelling exercise.

Last but not least I would like to thank Miss H.Ryder whose word processing expertise enabled the thesis to appear in its final form.

ABSTRACT

Aspects that affect the manufacture of aeroengine components in carbon fibre reinforced epoxy resin composite material are described and in particular factors influencing the process of consolidation of preimpregnated material laminates to final component form are critically assessed. Attention is drawn to the need both to acquire a full understanding of the physics of the consolidation process and to obtain quantitative process control data for efficient development and subsequent production of new components.

All the variables associated with the process of laminate consolidation are dependent on basic matrix resin characteristics especially its cure advancement and the consequent effect on the resin viscosity at all stages of a moulding cycle. To quantify the matrix resin chemorheological behaviour, methods for the generation of mathematical models for the cure and viscosity changes undergone by a dicyandiamide (DICY) cured epoxy resin system are described. By the use of these mathematical models a program for use on a personal computer has been written by means of which the cure,exothermic heat generation and viscosity of the resin may be simulated under both isothermal and linear temperature ramp conditions.

Examples are included of the application of the models in the solution of problems encountered in the autoclave process for composoite material components.

INTRODUCTION

The use of carbon fibre reinforced epoxy resin composite materials for the manufacture of aeroengine components is escalating rapidly. The major reasons for this escalation in their use are that they are both less costly to produce and exhibit performance benefits compared to metallic alternatives in certain regions of an engine.

Up to the present the development phase for components of exacting dimensional and performance requirements included much experimental work which was both time consuming and costly. Experimentation has been generally necessary because of the difficulties encountered in establishing both the design and method of manufacture for particular components. The accumulation of experience gained from the past manufacture of a variety of composite items however has resulted in a substantial reduction in the amount of such development work which is currently associated with new component design and manufacture. In today's environment however it is necessary to reduce even further the manufacturing lead times and also maintain control over the process of manufacture more effectively during the subsequent production of a new component.

Since many candidate processes exist for the manufacture of a composite material artefact e.g. resin injection, matched die or autoclave moulding are three such choices, then it is necessary for a component designer to understand fully the advantages and limitations of all the methods at his disposal at an early stage in the component design. Also, during production, efficient control of a process of manufacture can only be achieved by a thorough understanding of the process itself.

The physics of the process of manufacture

must therefore be fully understood and much activity is currently underway worldwide to develop mathematical models for various aspects of composite manufacture. Such mathematical models enable both the component designer and manufacturer to establish design criteria and modes of control respectively on a quantitative basis. Further, the existence of mathematical models enables computer simulation and automated control of processes to be possible for improved efficiency.

Many processes for advanced component fabrication depend on the use of carbon fibre broadgoods in the form of carbon fibre tapes or sheets preimpregnated with the matrix epoxy resin in its uncured state (commonly known as prepreg materials). These broadgoods are available from a number of commercial suppliers worldwide each of whom incorporates proprietary resin formulations in their prepreg materials. Components are normally manufactured by the stacking of a number of precut, preshaped laminae or plies into a prepreg lay-up conforming to the general shape of a finished component.

All prepreg lay-ups however have to be consolidated by some form of moulding action in order to achieve the void free, high fibre volume fraction composite material which is necessary to maximise the mechanical performance of the moulded component. Consolidation is facilitated by the application of heat in most cases whereby the initially liquid resin allows the required fibre compaction to occur by viscous outflow of excess resin from the prepreg lay-up. On further heating the liquid resin is transformed to the solid phase as a result of the cure reactions undergone by the resin over the duration of the cure cycle.

For the definition of the consolidation process for prepreg materials, factors such as temperature distribution, laminate movement, resin flow and residual void collapse have to be considered. All these factors are however dependent on the basic characteristics of the resin system, namely its cure

advancement and the resulting viscosity changes that occur as a consequence of the application of heat during the moulding cycle.

A prerequisite to the formation of a model for the total consolidation process therefore is that of the generation of mathematical models which are capable of predicting both the state of cure and the viscosity of the resin at all stages during a cure cycle.

In the current thesis the role of cure advancement and the viscosity changes that occur in a resin system commonly used in the U.K. for high performance aeroengine parts is described.

Methods are developed for the generation of mathematical models to describe both the empirically determined cure and viscosity behaviour of this resin system.By means of these models the cure and viscosity of the resin at any time under isothermal or linear temperature ramp condition can be evaluated.

By the incorporation of these mathematical models a code for use on a personal computer is described by means of which the cure and viscosity behaviour of this much used resin system may be simulated under any time-temperature condition.

The final Chapter includes the application of modelling techniques to the solution of typical problems encountered in the manufacture of carbon fibre reinforced epoxy resin composite material components.

CHAPTER 1

THE MANUFACTURE OF COMPOSITE MATERIAL COMPONENTS

1.1 Use of Composite Materials

In the last decade or so carbon fibre composite materials have been increasingly used in the manufacture of aeroengine components. The success in their use is due mainly to their high specific properties i.e. high stiffness and high strength to weight ratios. By the use of lightweight materials the specific fuel consumption of an engine is reduced and the cost of ownership of an aircraft is accordingly lowered.

A further major advantage in the use of the materials is that in nearly all cases the manufacturing costs for composite material components are lower than those for their metallic counterparts. The reason for this lower cost is twofold in that first, less energy is expended in composite manufacture compared to metal work and secondly, less labour costs are incurred compared to the use of the more expensive production routes required for the fabrication of similar metal components.

Although thermoplastic materials have been developed the most favoured matrix materials for carbon fibre composites still are the high performance, thermosetting epoxy resins due to their higher material transition temperatures. Stable composite materials can be produced by their utilisation and these exhibit a long term temperature capability of up to 150°C for continuous use.

Due to the success of composite materials at these lower temperatures much research is currently underway in order to extend the temperature range of composite material application in aeroengines.

Thus, in future we may expect to see matrices such as polyimides, aluminium, glass, titanium and ceramics being reinforced by several candidate reinforcement fibres including silicon carbide and alumina for components with a use temperature up to 1700°C.

Over the years the introduction of these new materials for use in aeroengines has followed a cautious path mainly due to concerns about the low soft and hard body impact resistance experienced with the early development components manufactured in carbon fibre epoxy. As yet therefore no in-flight, core engine or rotating component has been manufactured with carbon fibre composite material and only now is the material being considered for other structural uses in engines. Glass fibre reinforced epoxy and polyimides have however been successfully applied in the compressor blades and casing of the RB162 booster engine and for the nose

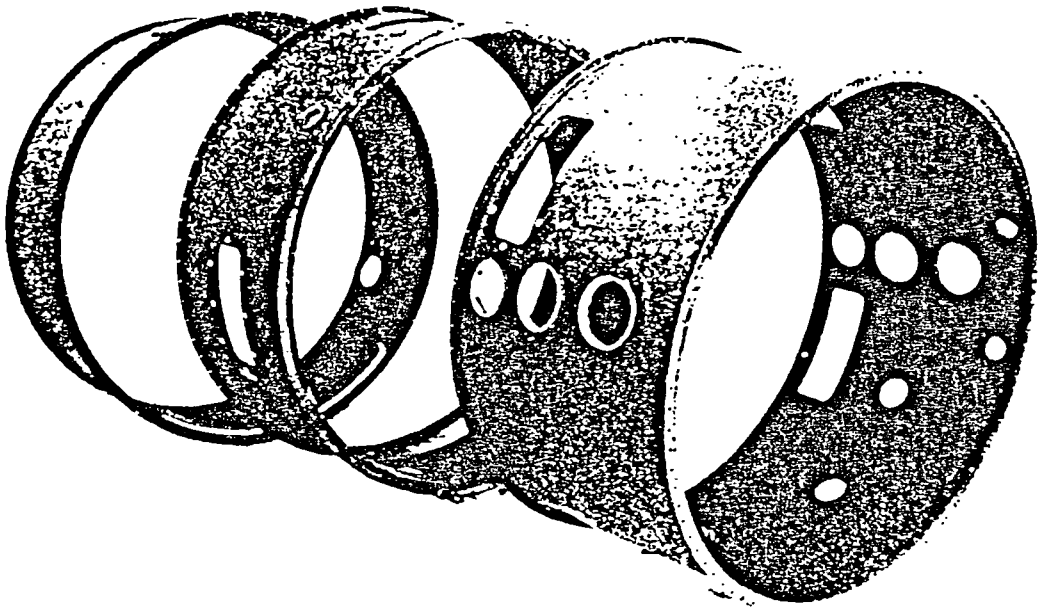

FIG.(1)

spinners of the RB211 engine and its derivitives.

It is more common to find carbon fibre components in the nacelle and installation regions of an engine. A typical example of the use of the

composite is shown in Fig.(1) where a set of by-pass ducts for the Tay engine is shown. The diameter of these ducts is of the order of 1.5m. Other applications include the thrust reverser components of the RB211 engine and a variety of hinges, brackets, fairings, and access doors for use on a number of different engine types.

There is no single, universal process suitable for the manufacture of these various shaped components however. Thus in order to satisfy the design intent in the case of each individual component a number of techniques have to be considered prior to establishing a process selection for the efficient production of a component meeting the design requirements.

1.2 Manufacturing Processes

The high mechanical properties achieved by carbon fibre composite materials depend on the synergistic effect obtained by the reinforcement of the relatively weak and low modulus matrix resin by the high strength, high modulus carbon fibre. Thus if all the fibres were parallel and unidirectional in such a composite then the resulting stiffness in the fibre direction would be proportional to the carbon fibre volume fraction in accordance with the Rule of Mixtures. The strength of the composite in the fibre direction would also increase with increased fibre volume fraction provided no excessive fibre to fibre contact occurred. The mechanical properties are however anisotropic so that in the unidirectional composite as described both the strength and stiffness transverse to the fibre direction are low. In a practical composite therefore laminate properties are optimised in designed directions by the incorporation of laminae of fibre at orientations corresponding to the directions of predicted load paths. Similar results can be obtained by the lamination of orientated cloth laminae the properties of which, individually, are bidirectional.

For the manufacture of carbon fibre-epoxy

composite the matrix resin is initially incorporated or added to the fibre in its uncured or viscous liquid form so that the fibre can be manipulated and draped to the desired configuration of a component. Thereafter, with the aid of thermal processing, cure of the resin is effected whereby it is transformed from the liquid to a solid state resulting in a rigid composite artefact. The time-temperature conditions under which this transformation to the solid state occurs however have to be chosen carefully if a high quality component is to be produced and the design of moulding cycles to achieve this end is therefore of extreme importance in the composite manufacturing environment.

The most favoured starting material for the manufacture of carbon fibre reinforced composite materials is in the form of a fibre tape preimpregnated with epoxy resin; commonly known as prepreg material. For high performance composites the fibres are invariably continuous and may be aligned in the one direction (unidirectional prepreg) or be incorporated in the form of a pre-woven cloth (woven prepreg). The resin in prepregs is normally in the form of a very viscous fluid in order to maintain fibre alignment while at the same time ensuring enough flexibility of the material for drapability purposes.

In all manufacturing processes using prepreg material the thickness of the required component is obtained by stacking a number of precut, prepreg laminae or plies on a rigid surface the shape and lateral dimensions of which correspond exactly to one external surface of the designed component. The natural packing of the fibre in a simple prepreg lay-up is such however that insufficient fibre volume fraction and, consequently, low mechanical properties would be obtained in the finished component.

In order to improve the mechanical performance of the composite therefore a prepreg lay-up is normally consolidated or moulded in a way that a uniform and high fibre volume fraction is achieved. The manner in which this consolidation may be effected for a

specific component is dictated by the design intent for that component.

For instance the main requirement for a component may be that it has to be manufactured within tight geometrical tolerances and have an overall aerodynamic finish on all surfaces. In such a case therefore the required laminate consolidation could only be effected by means of matched-die moulding (or compression moulding) techniques where the consolidation pressure is transmitted to the lay-up via a moveable but rigid top former. During mould closure the mould cavity geometry is controlled by the presence of fixed stops in between the two die surfaces so that when stop contact is achieved the required component geometry is established at the end of the moulding cycle.

The effectiveness of consolidation is determined by both the characteristics of the prepreg material and the rheology of the resin system during the moulding action.

The main characteristic of the prepreg material that affects its mouldability is the amount of excess resin that is incorporated in the tape. Due to the low natural fibre packing in the prepreg ply and in order to minimise the amount of potential voidage due to air entrapment in a moulded component, the inter-fibre free volume in a tape is, normally, substantially filled with resin. In the prepreg material therefore an amount of resin is present which is in excess of that required in a laminate moulded to a higher fibre volume fraction than that in the initial prepreg. The amount of excess resin in commercial material has decreased over the years with the result that, currently, in the "zero bleed" prepregs only a minimal amount of excess resin is present.

A further major requirement during the consolidation phase is that not only does a high fibre volume fraction have to be achieved in the final composite but that fibre orientation in every constituent lamina must be maintained within design limits over the duration of the compression action. Failure to maintain

fibre orientation would result in non-conforming material of low mechanical properties being produced. A minimal amount of voidage is also normally expected in high performance composites since any voidage in the composite results in a material with low interlaminar shear strength.

In essence therefore the consolidation of the fibre lay-up in a matched-die mould to achieve a composite material of high fibre volume fraction involves the removal of excess resin by outflow from the mould. Further the resin flow must occur in such a manner that the fibre orientation is not disturbed during consolidation and that no voidage is present in the final moulded form.

In order to maintain fibre orientation the flow of resin must be low enough at all times in the moulding cycle so that forces acting on individual fibres, produced by the viscous flow, do not exceed the interfibre frictional forces at any time. The interfibre frictional forces are present due to the natural packing of the carbon fibre and are greater the higher the compaction i.e. there is less tendency for fibre movement due to resin flow at higher compaction levels.

The viscous forces acting on the fibres however are dependent not only on the flow rate of the resin but also on its viscosity at all times in the moulding cycle. Thus for a high resin viscosity the flow rate has to be lower than that which could be tolerated with a lower viscosity resin.

Mould closure, which determines the outflow rate of excess resin from the mould, must therefore be undertaken in a controlled manner over a period of time in order to ensure that no fibre wash occurs.

In order to minimise the mould closure time a low viscosity is required and this is normally achieved by heating the mould and lay-up since the viscosity of the initially viscous resin at ambient conditions is substantially reduced at higher temperatures.

There is also a maximum time limit within which mould closure has to be effected at any elevated

temperature. This maximum limit is imposed by the chemorheological characteristics of the resin system. Due to the elevated temperature the chemical reactions associated with cure of the resin are accelerated and the resin viscosity increases at a faster rate than at lower temperatures. Mould closure must therefore be completed before the viscosity rises to such a level so as to inhibit resin flow out of the fibrous lay-up. On the other hand a modest viscosity is desirable at mould closure since a higher hydrostatic pressure can be maintained within the system which would aid in the collapse of residual voidage.

A viscosity-time window thus exists at any elevated temperature during which the successful moulding of a prepreg lay-up can be accomplished. For economic reasons the design of a moulding cycle for components involves the selection of a cure temperature so that this window is of minimum duration compatible with successful consolidation of void free material to the required component geometry.

As soon as the critical process of consolidation has been achieved the material may then be fully cured in the heated mould in order to realise its maximum physical and mechanical properties.

In addition to being dependent on the chemorheological properties of the matrix resin the consolidation of a prepreg lay-up is also a function of the geometry of the component being moulded. This geometry dependence is especially of importance in the moulding of complex shapes with varying sectional thickness and is due to the varying flow requirements of the excess resin from the fibrous lay-up in this case. Since an amount of excess resin is associated with every individual lamina in the lay-up then the viscosity-time window varies from the thicker to the thinner sections of the moulding with the result that, in extreme cases, consolidation cannot be uniformly achieved throughout the component.

Such sectional thickness changes were encountered in the compression moulding of the prototype

RB211 fan blades in the late 1960's and the problems associated with the manufacture of this blade have been described in ref.1. The difficulties experienced in the use of prepreg material in this specific application were so severe that high quality blades could not be consistently moulded to the required dimensions.

The difficulties in the moulding of these blades were overcome only by the application of an entirely different process of manufacture, namely, resin injection. The development of the resin injection technique has been fully described in ref.2.

Briefly in this technique, essentially dry fibre laminae i.e. containing no preimpregnated resin are laid up in a mould. On mould closure the fibrous preform can be consolidated easily to the required final dimensions of the composite article to be manufactured since no resin has to escape in this case. By sealing the mould for both vacuum and internal pressurisation the air within the free volume of the fibre pack can be evacuated and replaced by a fluid resin under pressure. Following cure in the sealed mould a composite artefact, free of voids and having the designed shape and dimensions, can be extracted.

A spin-off from the research and development work described in ref.2 is the successful application of the resin injection technique in the production of flight g.r.p. nose spinners for some versions of the RB211 and RB535 engines.

It is clear from the above that great care has to be exercised in the choice of manufacturing process for components with exacting design requirements on dimensional stability and overall surface finish whereby the use of rigid formers in their manufacture is necessary.

Not all engine components fit this category however. For the by-pass ducts shown in Fig.(1) for instance the main design requirement can be summarised by stating that the diameter of the inside of the duct has to be consistently reproduced with a good surface finish and that the wall material be of high fibre volume

content for maximum strength and stiffness. The surface finish on the outer wall of each duct section is not critical and the need for an outer rigid former in their manufacture can thus be dispensed with. To achieve the necessary inner wall diameter and surface finish the reinforcement material has to be positioned on an inner, solid surface i.e. only one rigid surface is necessary to control the moulding. Consolidation of the material is still required however in order to eliminate voidage and to maximise the mechanical performance of the resulting composite.

From the symmetry of the ducts about their axes the possible routes to their manufacture in this case would be by filament or tape winding techniques. Rubber expansion methods are also used in such cases where consolidation is achieved by the thermal expansion of a male rubber mandrel which consolidates a prepreg lay-up against a solid female mould. Not all engine components that may be moulded by a single surface control method exhibit such symmetry however but most are characterised by being relatively thin walled and of large areal dimensions with possible double curvature.

A common process of manufacture has therefore been established for components of this latter type. In this process consolidation of the material against a rigid former is achieved by means of a flexible bag in an autoclave environment, and the details of this important method are described as follows.

1.3 Autoclave Process

The principle of operation of the autoclave process for carbon fibre epoxy composite material manufacture can be described with the aid of the schematic diagram in Fig.(2). See also ref.3 for a good description of this method of moulding.

The prepreg laminae to be moulded are laid up on the rigid, single control surface as shown. Normally a positive release layer such as reinforced PTFE film is interposed between the lay-up and the tool surface to

facilitate the extraction of the moulded composite following cure.

In practice the control surface is not necessarily flat as shown but is shaped to the required

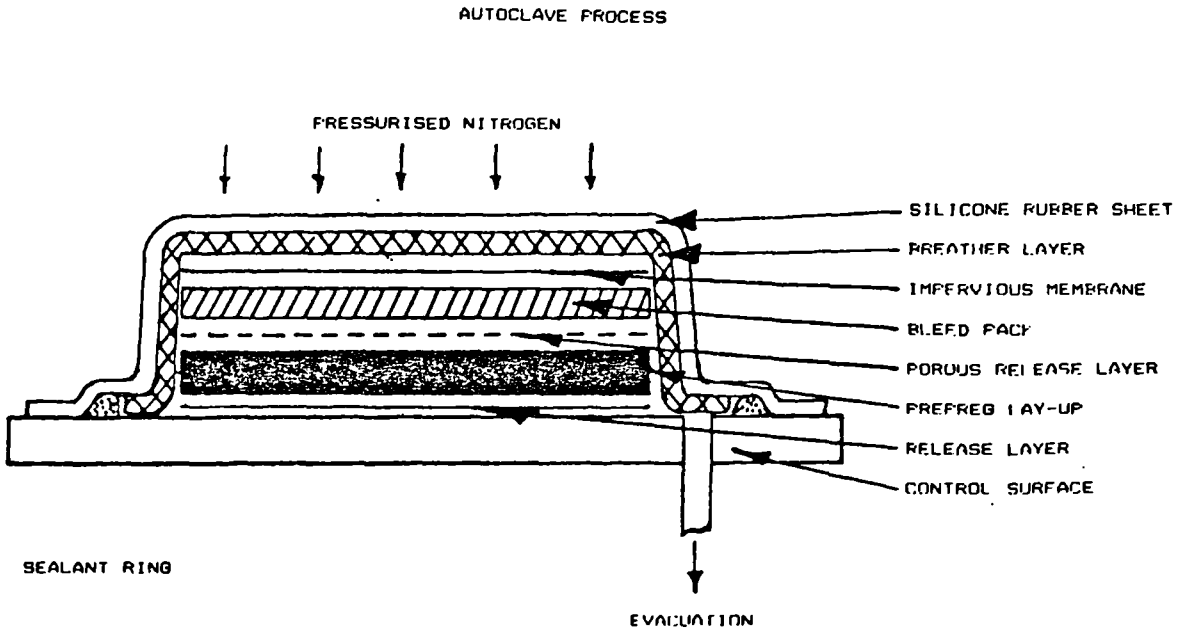

FIG.(2)

component shape. The main requirement demanded of the control surface form and construction material are a) the tool must remain rigid throughout the duration of the moulding cycle, b) the thermal expansion of the tool must preferably match that of the composite article being formed to minimise thermally induced distortions and c) the thermal capacity of the tooling structure must be minimised for controlled and rapid temperature increase to be achieved for economic moulding. It is normal practice therefore to construct the tooling from either relatively thin stainless steel plates or, alternatively, by the use of g.r.p. fabricated parts.

A porous release layer is positioned on top of the lay-up. The function of this release layer is twofold in that, initially, it allows the escape of excess resin from the lay-up into the bleed pack as shown during moulding but subsequently its presence enables

the filled bleed pack and the composite to be easily parted after full cure. The bleed pack consists of a number of glass cloth plies the total porosity within which is sufficient to absorb only the excess resin calculated to be present in the lay-up. The bleed pack is isolated from a further glass cloth, breather layer by an impervious membrane. This whole stack is covered by a silicone rubber sheet the edges of which are sealed to the control surface by strips of sealant as shown positioned at the interface of the rubber sheet and the tool surface.

In the moulding operation air is substantially removed from within the sealed bag by evacuation via the vacuum port, breather layer, bleed pack and thus the prepreg lay-up itself.

For consolidation of the prepreg lay-up the tooling and associated pack is emplaced in an autoclave chamber whereby the temperature of the whole assembly is raised by means of circulating, heated nitrogen gas. Compression of the lay-up is achieved by increasing the pressure of the gas to above that of atmospheric.

On pressurisation the excess fluid resin is forced out of the lay-up into the bleed pack enabling the prepreg laminae to be consolidated to the desired high fibre volume fraction and conformability with the required control surface shape.

For successful application of the process for the consolidation of high quality carbon fibre composites similar considerations have to be applied in the design of suitable moulding cycles for specific components as have already been described for the matched-die or compression moulding process in section 1.2.Thus in order to eliminate fibre wash and voidage and to achieve uniform consolidation throughout a moulded structure a judicious choice of pressurisation and viscosity control temperature conditions has to be made especially if sectional thickness variations occur in the component.

1.4 Process Modelling

Technical considerations of a consolidation process for a component as described above however are not the only factors that affect the choice of one method of manufacture over another for a particular component.

For example consider the choice between the use of the resin injection technique and the autoclave method using prepreg material. For the latter method refrigerated storage of prepreg material is a necessity to minimise cure advancement whereas no such storage problems are associated with the resin injection precursor materials. Thus in the use of prepreg materials the cost of storage and the associated laboratory quality assurance testing has to be considered. Different ply cutting and trimming techniques have to be used for the two types of materials where generally for prepreg individual laminae have to be accurately cut out prior to lay-up whereas in the resin injection case the trimming may be accomplished on a preformed article. The major determining factor in favour of prepreg material however has been the lower cost of tooling especially in the autoclave method for composites requiring only a single control surface in their manufacture.

Historically the introduction of composite materials for engine components was developmental in nature where each step in a method of manufacture had to be individually assessed in an empiricial manner. This approach inevitably meant that a number of full scale pre-production components had to be manufactured by means of a chosen consolidation process prior to the establishment of a method of manufacture.

The cost of such development work is high and since more widespread use of the material is envisaged it is necessary for any manufacturing unit in this area to reduce these costs in order to remain competitive.

There are several ways by which cost reduction may be achieved at all stages during the development and

subsequent production of a proposed new composite material component including the following.

a) From the component designer's point of view it is essential that the various methods of manufacture at his disposal are fully understood and that the limitations of all of the available critical processes of laminate consolidation, when applied to the designed component, can be assessed. Component design can therefore be tailored to a specific, cost effective process of consolidation in the initial design stages.

b) Labour costs may be reduced by the automation of many of the steps encountered in the various methods of manufacture. The relatively high capital cost of full automation in many cases however prohibits implementation unless the total volume of production is of a high order.

c) The main process of composite consolidation used to be regarded as more of a black art than a science and even today many decisions taken during both the design and operation of moulding cycles are more subjective than objective. More efficient control of the process is therefore desirable in order that, preferably, computerised on-line control at all stages of the moulding can be achieved.

By the above means therefore the amount of preproduction development effort would be reduced so that a lower number of both material test pieces and pre-flight engine test components would be required prior to acceptance of a method of manufacture. During subsequent manufacture in production more efficient control would ensure that a lower amount of non-conforming and scrap material would be produced.

The central theme in all of the above considerations is that of the requirement to understand fully the physics of the consolidation process iteself. From the physics of the process a numeric appreciation of the process variables can be obtained from which quantitative component design and process control parameters can be established.

Much materials research and computational work is therefore currently underway worldwide to aid in the generation of mathematical models for composite material consolidation processes. Most of the effort is concentrated on modelling the autoclave process as described for use with prepreg materials incorporating a variety of matrix resin systems.

1.5 Autoclave Model

In order to generate a mathematical model for the autoclave process many factors that affect the processability of prepreg laminates have to be considered.

Of prime importance is the quality of the prepreg materials. Uniform fibre distribution within the lay-up plies is a necessity since the local thickness in any region of a consolidated composite is controlled solely by the fibre content in that region. This is due to the fact that the movement under pressure of the consolidating rubber sheet is restricted only by the inherent packing forces generated by interfibre contact within the plies. The amount of excess resin in the lay-up must also be accurately known since this determines the amount of bleed glass cloth which has to be used during consolidation.

Although the incoming material is controlled within tight specification limits for fibre and resin contents there are still enough variations within these limits to affect the fibre volume fraction of a manufactured component especially if the component is in the form of a thin skin. Quality control testing is therefore a necessity to establish quantitatively the fibre and resin distribution in batches of material.

During the lay-up of the material on the mould control surface the weave construction of a cloth plays an important part since the drapability of the ply in this case is influenced by the construction of the fabric e.g. satin woven materials are generally more drapable than the tighter square woven cloths. The drapability of a cloth therefore determines whether or not radiused

features in the component can be laid up satisfactorily to conform with the mould surface.

The bulk factor of a lay-up is also dependent on the construction of the fibre reinforcement and the bulk factor has a major influence on the quality of fibre positioning and alignment in regions of high curvature in a moulded composite.

Of practical importance also is the tack of the prepreg during lay-up since a certain amount of adhesion between laminae is advantageous at this stage in order to preserve designed laminae orientations during the build. The tack is a function of resin viscosity at lay-up temperatures (normally ambient) and a possible minor amount of cure advancement during prepreg storage.

Ideally, therefore, all of the above factors have to be considered and preferably quantified if a complete model of the autoclave process is to be defined.

Of main concern however is the derivation of a mathematical model to describe the actual consolidation process itself.

For modelling purposes the consolidation process can be divided into a number of discrete sub-models each of which mathematically describes a pertinent material behaviour aspect which critically influences the quality of a moulded component.

The sub-models can be defined with the aid of Fig.(3). The sub-models shown are those for the main variables that affect the processability of prepreg systems and they can be grouped in two main categories as shown i.e. the sub-models that describe the behaviour of the fibre lay-up or composite during consolidation and those which solely describe the matrix resin behaviour.

It will also be noted that a void model is included in Fig.(3). Although the elimination of voids is a necessity in composite fabrication a model for the amount of and distribution of expected voidage is dependent mainly on the reinforcement construction, ply handling history,moisture content and,finally,the efficency of evacuation during moulding. The void model

is therefore substantially independent of resin and fibre behaviour during the consolidation phase.

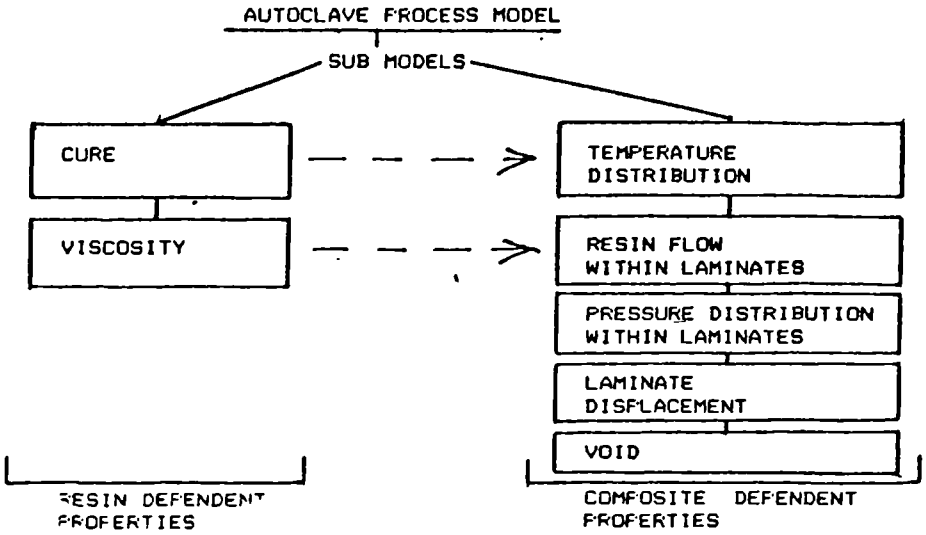

FIG.(3)

Although the sub-models are treated independently they are however all interlinked. For instance the laminate displacement in the consolidation direction during compression is a function of the resin flow through the fibrous network and hence is a function of the resin viscosity. The laminate movement model is thus dependent on the viscosity model.

The flow of resin is also dependent on the pressure gradient within the laminate during the consolidation phase and hence the pressure distribution model is linked to the viscosity model.

The resin viscosity in turn is a function of the state of resin cure at any time and temperature.

Due to the exothermic nature of the cure reaction the temperature distribution within the laminate is not only dependent on heat transfer from the mould tooling but is dependent also on the rate of heat generation within the laminate itself. Hence the temperature distribution model is linked to the model for the degree of cure.

1.5.1 "CURE" Model

A computer model for the autoclave process, called "CURE" has been developed by G S Spinger et al in the USA, see refs.4, 5 and 6. In this computer code the above sub-models have been incorporated and interlinked so that the resin and prepreg behaviour at any time during a simulated cure cycle can be determined. The "CURE" model has been developed for use with Hercules AS/3501-6 graphite fibre reinforced epoxy resin prepreg material which is a system much used in the US aerospace industry. This model however may be adapted for use with other resin systems provided the appropriate material variables and sub-model modifications are incorporated. See the work in refs.7 and 8 for examples of sub-model modifications and generation respectively.

Other notable work on the development and generation of an independent model for the autoclave process is described in ref.9 where the application is again to the Hercules prepreg systems.

In the UK however most aeroengine components are manufactured by the use of BSL 914 resin system for which no such model is available to define the full autoclave process. For reasons already stated in section 1.4 it is important that a model for the process is acquired for more efficient use of BSL 914 prepreg systems in composite manufacture.

All the sub-models necessary to define the total process model are interlinked as described above where the composite behavioural sub-models are all dependent on the matrix resin cure and viscosity at any time and temperature during the process. It is therefore of paramount importance that these characteristics of the resin system are fully defined in order that meaningful numerical variables can be incorporated in the composite sub-models for full process definition.

In the remaining Chapters of the current thesis a description is given of the manner by which mathematical models and computer simulation of the basic

chemorheological behaviour of the BSL 914 resin system are obtained.

A brief description of the BSL 914 resin system is given first as follows.

1.6 BSL 914 Resin System

The BSL 914 resin system (Redux 914) is manufactured by Ciba-Geigy (UK) Ltd. The current system is a generic form of specially formulated resins for use with carbon fibre which were developed in the early 1970's as a result of joint discussions between Rolls-Royce plc and the resin manufacturer, see refs.10 and 11.

This resin system has many unique and advantageous properties for its application in carbon fibre reinforced composite materials.

Of major importance is the capability of the resin when fully cured and in conjunction with the reinforcement fibre to maintain its mechanical properties continuously at elevated temperatures up to 150°C in the harsh environment of a gas turbine engine. In this environment the resinous composite is capable of withstanding moisture, saltspray and engine fluid attack for sustained periods without appreciable degradation in its properties.

In its uncured state, as incorporated in prepreg materials, the resin also exhibits many favourable characteristics from the component manufacturing point of view. These favourable characteristics arise from the special chemical composition of the resin.

The main constituents of the system are MY720 epoxy resin (tetraglycidylated methylene diamine) and DICY (dicyandiamide) hardener. A minor proportion of a difunctional epoxy resin and proprietary additives are also included to modify the cure. Also incorporated is an amount of polyethersulphone for viscosity control purposes.

The DICY hardener, in the form of a white

crystalline powder is physically admixed with the resin prior to being applied to the carbon fibre sheet by the aid of a carrier solvent to form the prepreg. A uniform distribution of DICY hardener particles, approximately 5μm dimension is achieved within the prepreg resin. Under ambient or storage conditions at -18°C the DICY is insoluble in the resin and for this reason the system is known as a latent system since resin cure will not substantially proceed at these temperatures. The latency of the system is of extreme benefit in the use of the material in manufacture since under normal shop floor conditions the absence of cure advancement ensures that component lay-up operations etc are not hampered by adverse changes in resin properties. A long shelf-life for the material is also ensured for the same reason.

Above 100°C however the DICY hardener is soluble in the epoxy and chemical reactions between the DICY and the epoxy which lead to the cure of the resin proceed rapidly above this temperature. Due to the tetrafunctional nature of both the MY720 resin and the DICY hardener the cure mechanism of this system is extremely complex since a combination of reactions between many active molecular sites are possible. The course of these reactions have not been fully determined in the literature but by the use of model compounds however (see refs.12,13 and 61) possible mechanisms have been proposed for the cure of monofunctional epoxies with DICY as follows:-

The initial reaction is the opening of the epoxy ring by the DICY and this reaction can be accelerated by the presence of an organic base. The epoxy ring opening reaction itself however results in the formation of a base by rapid cyclisation and this base further catalyses the ring opening reaction. The reaction is therefore autoaccelerated or autocatalysed and crosslinking of the epoxy molecules proceeds at an accelerated rate once initiated.

The cure mechanism of the MY720 is thought to be of this nature but since the chemistry of the autocatalysed reactions has not been fully elucidated in

this case then, as will be seen in the following text, the cure reactions have to be monitored by indirect, empirical means for modelling of cure advancement to be possible.

The incorporation of polyethersulphone in the system enables control of viscosity throughout the process of manufacture to be maintained. Thus the thermoplastic addition which is in solution in the epoxy resin (the polyethersulphone is initially soluble in the epoxy but this eventually precipitates out to result in a cured material with a two phase structure of high Tg,(see ref.10)) increases the viscosity of the base epoxy resin so that prepreg laminates can be handled without fibre alignment deterioration.

During thermal processing the viscosity of the resin initially decreases with increased temperature to a minimum of approximately 100 Poise at temperatures greater than 100°C. Due to increased crosslinking during cure at elevated temperatures however the viscosity dramatically increases from a minimum to a very large value as the resin eventually solidifies.

From experience it has been found that the moulding of prepreg laminates can be most efficiently carried out when the resin viscosity is in the range 100 to 200 Poise. The polyethersulphone addition ensures that this viscosity can be maintained for sufficiently long periods at elevated temperatures for efficient consolidation of the prepreg laminates to occur i.e. the BSL 914 resin system has a 'tolerant' viscosity-time window as described in section 1.2.

The viscosity behaviour of the resin however cannot be predicted by theoretical means and for the modelling of viscosity behaviour therefore empirical methods will be relied on as will be described in the following text.

In order to maximise the mechanical properties of the composite structure the moulded component is normally postcured for approximately 4 hours at 190°C. During postcure the Tg of the matrix resin increases to within the range 180°C to 190°C as a result of further

crosslinking thus ensuring prolonged, safe use of the component at elevated temperatures up to 150°C.

CHAPTER 2

RESIN THERMAL BEHAVIOUR

2.1 Cure monitor and resin thermal behaviour.

From section 1.6, since the cure mechanism for the BSL_914 system (as with many other resin systems) has not been defined for all possible heating conditions it is impossible to evaluate the kinetic parameters necessary to generate a model for the extent and rate of cure by direct chemical means. Indirect methods are therefore normally used to monitor the cure reaction and the most favoured method for this purpose depends on the exploitation of the exothermic nature of the cure reaction by means of calorimetry (refs.14,15).

IDEALISED EXOTHERM

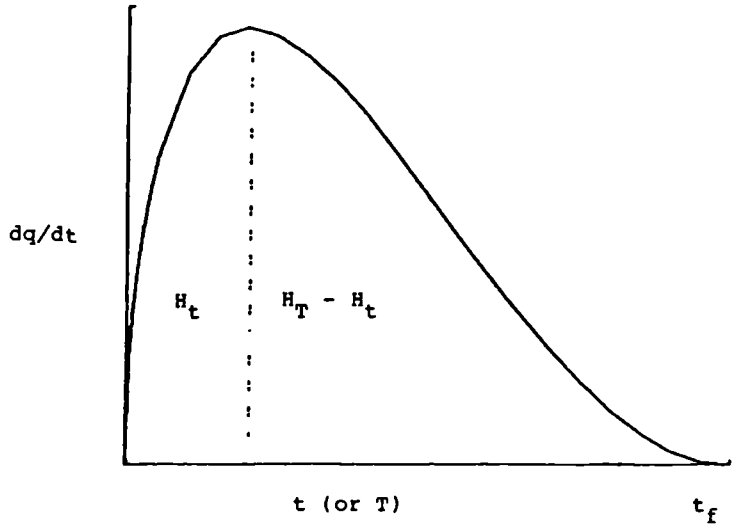

FIG.(4)

The basis of the method can be described by reference to Fig.(4) where a schematic reaction exotherm is shown. During the cure reaction conducted either

under isothermal or alternatively under dynamic rising temperature conditions, heat is evolved. The rate of heat output, dq/dt, increases with time t (or alternatively with temperature, T, which is some function of t under ramped conditions) to a maximum value and subsequently falls to zero on completion of the reaction at time t_f.

In classical chemistry theory the rate of the reaction would be defined by the rate of mass loss, -dm/dt, by which a reactant of initial mass m_o in the system would be consumed during the reaction.

It is assumed in calorimetric methods that the rate of heat generation is proportional to the rate of chemical reaction i.e.

$$dq/dt = -K\ dm/dt \qquad (2.1)$$

where K is the constant of proportionality

At the time of completion of the reaction, t_f, therefore,

$$\int_o^{t_f} dq/dt.dt = -K \int_o^{t_f} dm/dt.dt \qquad (2.2)$$

where $\int_o^{t_f} dq/dt.dt = H_T$ the total area under the exotherm curve

and $\int_o^{t_f} dm/dt.dt = m_o$ the total mass of reactant consumed

thus $H_T = -K.m_o$

Thus substituting for K in (2.2) and integrating to any intermediate time t gives (neglecting negative sign).

$$\int_0^t dq/dt.dt = H_T/m_o \int_0^t dm/dt.dt \qquad (2.3)$$

where $$\int_0^t dq/dt.dt = H_t \qquad (2.4)$$

where H_t is the partial area under the exotherm curve up to time t.

and $$\int_0^t dm/dt = m_t \qquad (2.5)$$

where m_t is the mass of reactant consumed by the reaction up to time t.

Substituting for the integrals in (2.3) and rearranging gives

$$m_t/m_o = H_t/H_T$$

But m_t/m_o is the fractional conversion, α of the reactant.

Thus $$\alpha = H_t/H_T \qquad (2.6)$$

Substituting for H_t in (2.6) from (2.4) gives

$$\alpha = \int_0^t (dq/dt)dt/H_T \qquad (2.7)$$

By differentiation the rate of conversion, $d\alpha/dt$, is obtained at time t.

$$d\alpha/dt = (dq/dt)/H_T \qquad (2.8)$$

Equations (2.6) and (2.8) constitute the basis of

calorimetric methods of cure monitor.

From equation (2.6) the amount of fractional conversion, or alternatively the extent of cure, of an epoxy system at any time during the reaction can be equated to the ratio of the heat liberated up to that time to the total exothermic heat of the reaction.

From equation (2.8) the rate of conversion, or alternatively the rate of cure, of the epoxy system can be equated to the ratio of instantaneous heat output to the total exothermic heat of reaction at any one time.

The most efficient method of evaluating α and $d\alpha/dt$ during the course of the cure reaction is by the use of a commercially available differential scanning calorimeter the operation of which will now be briefly described.

2.2 Differential Scanning Calorimetry

The thermal characterisation of the BSL 914 resin system was conducted by the use of a DuPont 910 Differential Scanning Calorimeter (DSC) connected to a 9900 Computer/Thermal Analyzer. Additional equipment including 943 Thermomechanical Analyser, 981 Dynamic Mechanical Analyser and 951 Thermogravimetric Analyser modules are also incorporated in the total system.

The 910 calorimeter is of the heat-flux type (refs.14,15) and a schematic view of the DSC cell is shown in Fig.(5) (abstracted from the DuPont operating manual).

By its use calorimetric measurements can be undertaken either under isothermal or dynamic (linearly ramped temperature) modes or a combination of both modes may be chosen if so desired.

During operation the calorimeter detects the temperature difference between a reference pan and a sample pan of equivalent heat capacity but which contains a small amount of the material to be analysed. The pans are positioned on a constantan disc through which heat is conducted from the heater block, via the silver ring, into the pans. The chromel wafers fixed to the

constantan disc directly underneath the pans form area thermocouple junctions which measure any temperature

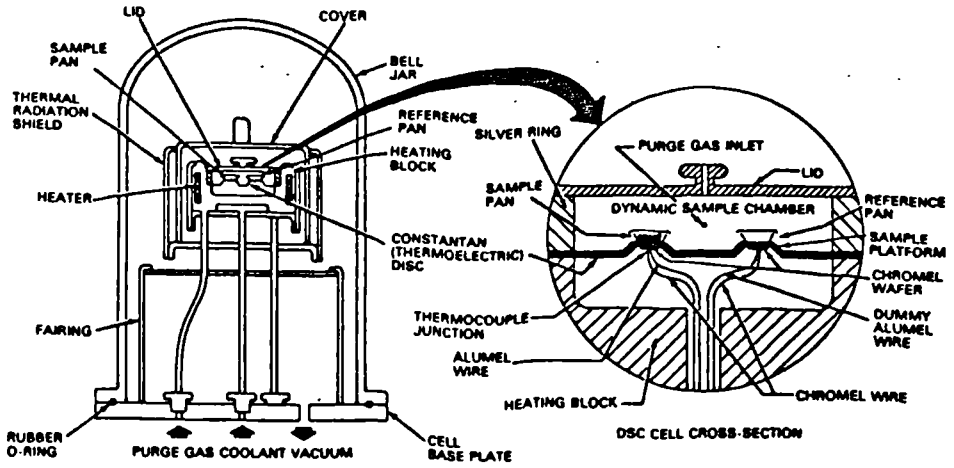

FIG.(5)

difference which may exist between the two pans. Such a temperature difference would be produced by either an endothermic or an exothermic reaction occurring in the sample material. The chromel-alumel wires, also connected to the chromel wafers form the thermocouples necessary to monitor the temperature of the pans directly.

Essentially the evaluation of calorimetric data by the use of the DSC depends on the fact that the temperature difference between the sample and reference pans can be related to the differential heat flow between the two pans (ref.14).

The numerical processing necessary to convert the temperature difference into heat flow is carried out by the thermal analyser computer and associated software. Thus a display of heat flow versus time (or temperature) during an experiment may be observed on the computer screen.

The software facilities additionally incorporate features which allow the fundamental heat flow values to be displayed in chosen units e.g. calories

per second or Joules per gram per second etc.

Also the area under the heat flow curves can be obtained for the thermal analysis requirements as described in section 2.1.

To ensure conformance of instrument operation to that of the manufacturer's specification the DSC is calibrated monthly by measuring the heat of fusion of indium.

2.2.1 Experimental Procedures

In essence the experimental operations required for the generation of calorimetric data by the use of the DSC are minimal in number and relatively easy to perform which attributes make the DSC an extremely useful tool for the thermal characterisation of polymeric materials especially in an industrial environment.

The experimental procedure followed in the course of the current work is described as follows:

First of all similar reference and sample pans were selected. Pure aluminium pans were used and the pan weights were consistently in the range 22.9 to 23.5 mg (ref.16).

A weighed amount of BSL 914 resin film was then transferred into the sample pan and located at the centre of the pan base thus ensuring optimum contact of the resin with the pan base throughout the duration of an experimental run. Sample weights in the range 8 to 12 mg were used and no significant variation in heat flow per unit weight of resin has been detected with this range of sample weights (refs.16,17).

The pan lid was then installed and crimped in position but not sealed airtight. The lid was subsequently perforated by means of a pin which perforation served to further aid in the expulsion of solvents and water from the heated pan during an experiment. Removal of solvents in this manner results in DSC scans with lower associated noise levels in the output signal than would otherwise be the case with sealed pans.

In the case of the BSL 914 resin system less than 0.5% of initial sample weight is lost by evaporation

of solvents and hence this mass loss did not significantly affect the DSC heat flow per unit weight value.Both the sample and reference pans could be transferred to the DSC cell at this stage prior to initiating the chosen heating program for an experiment.

For an isothermal run either one of two methods is generally used for the insertion of the sample pan into the calorimeter (refs.4,35).

In the first method the pan is inserted at ambient temperature. The DSC temperature is then ramped rapidly to the required isothermal temperature. Normally an overshoot to a temperature above the desired isothermal hold is experienced in this method and this leads to the occurrence of an unknown amount of reaction due to both the finite ramp time and also the overshoot.

In the second method and the one which has been preferred in the current work, the DSC is allowed to equilibrate at the isothermal hold temperature prior to insertion of the sample pan. Following pan insertion however rapid fluctuation in the heat flow readings occur. Again in this method as with the former an unknown amount of reaction does occur prior to stabilisation of the sample temperature. Inevitably the errors increase with increased isothermal temperatures.

It has been established (ref.16) that still air conditions in the cell i.e. no enforced air or nitrogen flow, were sufficient for the purposes of this work.

On completion of each experimental run hard copies were obtained of both the screen display and the numerical results generated by means of the software analysis program. Also the output data of the calorimeter were stored on floppy discs.

2.3 Resin Exothermic Behaviour

Before proceeding to evaluate the parameters necessary to generate a kinetic model for the cure of the BSL 914 resin system the general thermal behaviour of the system both under dynamic and isothermal conditions will first be described.

2.3.1 Dynamic Exotherm

2.3.1.1 High Temperature Reactions

In the DSC dynamic mode the sample pans are normally heated with the temperature increasing linearly with time. A typical dynamic scan for the BSL 914 resin system at a heating rate of 10°C/min from 50°C to 375°C is shown in Fig.(6).

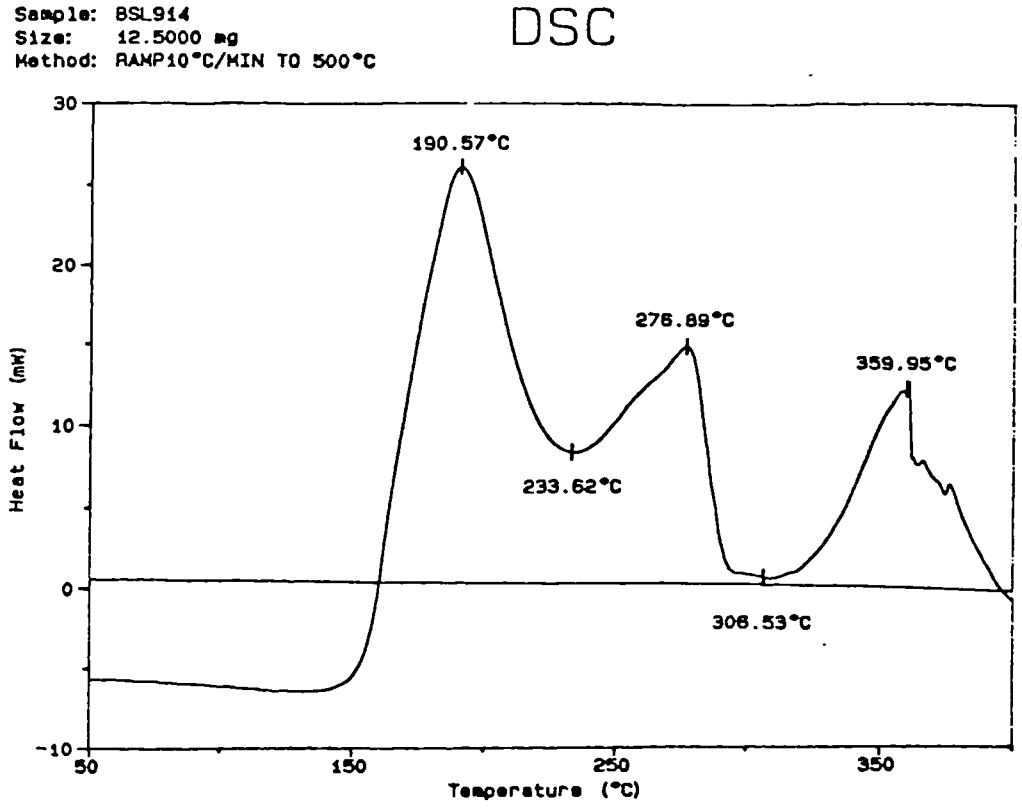

FIG.(6)

The instrumental baseline, generated by dynamically scanning two empty pans, is also shown where, since the pans are identical, hardly any differential heat flow occurs.

If any heat flow does occur however then if the flow is out of the pan this outflow of heat is represented by a positive value of the ordinate compared to the instrumental baseline.

From the sample trace in the range 50°C to 125°C approximately the differential heat flow is therefore into the sample pan and this inward flow is due to the fact that the mass of resin requires heat to maintain the sample temperature at an equivalent level to that of the empty reference pan.

Onset of an exothermic reaction at 125°C however results in the heat flow assuming a positive direction with the flow steadily increasing up to the first peak temperature at 190°C. The heat flow subsequently decreases to a local minimum at 233°C. From section 2.1 it is assumed that the total heat output, which is the area under the first peak, between 125°C and 233°C, can be related to the amount of chemical reaction that has occurred in this temperature range.

On further heating it is observed that two further peaks and hence two main exothermic reactions occur with maximum rates of reaction at 277°C and 360°C respectively.

In order to discriminate cure reactions from resin degradation reactions a thermogravimetric scan (TGA) was conducted on a further resin sample. The TGA scan obtained is shown superimposed on the DSC dynamic scan in Fig.(7). Clearly an accelerated weight loss occurs above 318°C and the third reaction peak can thus be attributed to a degradation reaction.

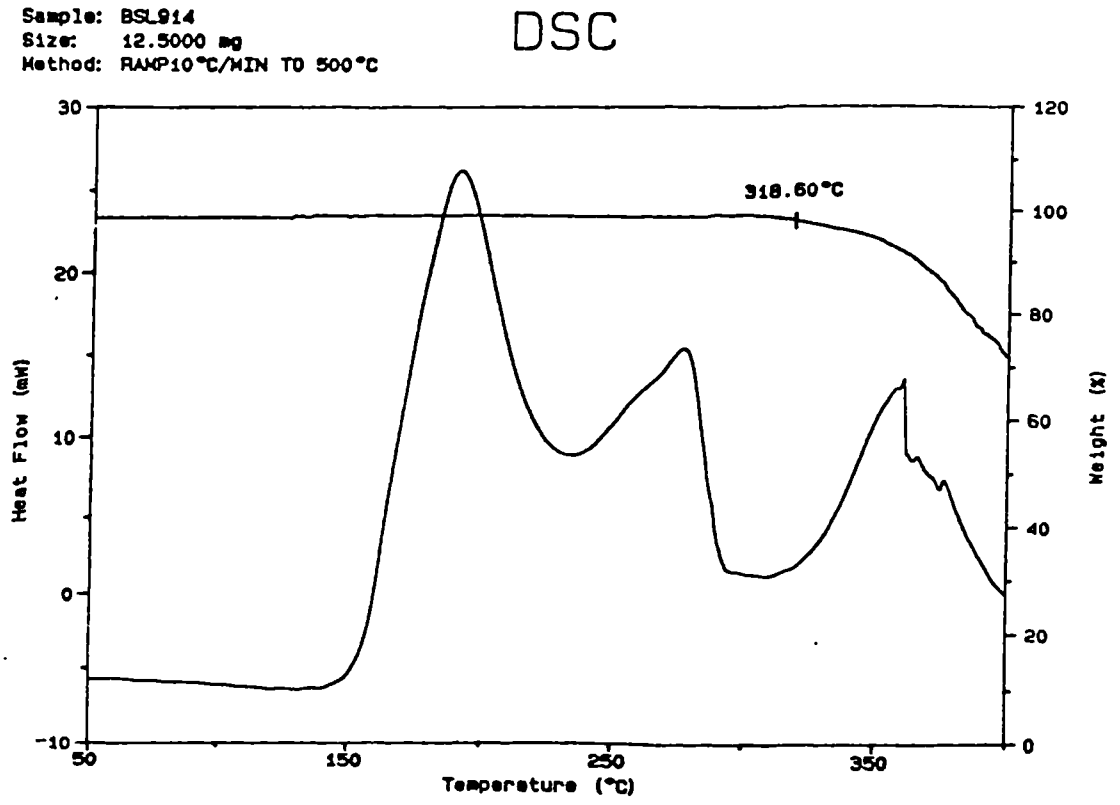

FIG.(7)

Conversely, the cure reactions are therefore represented by the first two peaks of the scan.

Similar exothermic behaviour in dynamic scans has been observed with other DICY cured epoxy systems (refs.14,18,19). In the work described in these references the full or 100% cure of the resins is represented by the area under both cure peaks of the dynamic scan.

In the current work however full or 100% cure is defined as being represented by the area under the first peak only i.e. the resin is deemed fully cured when an amount of heat equivalent to that of the first exothermic reaction has been evolved during a specified cure regime.

The reasons for defining full cure in this manner are based on practical grounds. From section 1.6 the post cure temperature of the resin is normally 190°C. Also carbon fibre components manufactured with this resin system never exceed the postcure temperature for prolonged periods. There is therefore no requirement to account for the presence of the second cure exotherm for the generation of a practical cure model.

With this definition of cure in mind the area of the first exotherm peak must be determined if intermediate cure levels are to be quantified.

2.3.1.2 Dynamic Cure Exotherm

A more detailed view of the above two cure exotherms is shown in Fig.(8). In addition to the dynamic resin scan in this figure, a number of baseline options as generated by the DSC computer are also shown. This figure serves to explain the difficulties encountered in modelling the cure behaviour of the BSL 914 resin system.

On consideration of the resin scan first it is noted that the heat flow accelerates uniformly from a temperature of 125°C until a discernible shoulder or

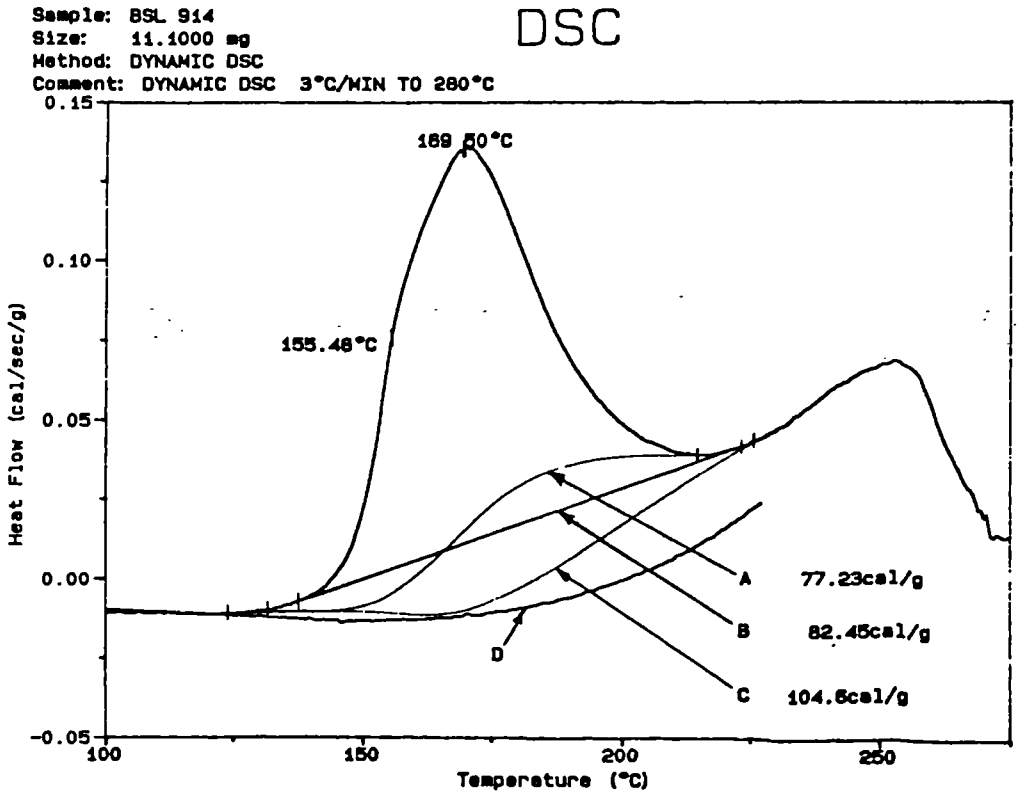

FIG.(8)

inflexion point occurs at a temperature of 155°C . On further heating above 155°C the heat flow decelerates up to the peak maximum at 169°C and subsequently falls to a local positive heat flow minimum value at 220°C.

The occurrence of the inflexion at 155°C is due to a combination of factors as follows:-

a) From section 1.6 the initial stages of cure involve a succession of overlapping chemical reactions with individual associated heats of reaction which have not been quantified (see also refs.18,20, 21). These individual reaction exotherms cannot be resolved by means of the DSC but nevertheless the non-uniform heat output contributes to the overall exotherm profile for the cure reaction in the first peak.

b) The initial stages of the cure reaction are influenced by the amount of hardener available for reaction since this amount

is dependent on the rate of solubility of DICY in the epoxy.

Although the solubility of DICY in epoxy has been quantified (ref.22) no information has been found in the literature as to the rate of solution or as to the heat of solution in this respect. Observations on the time of DICY particle disappearance in resin by hot stage microscopy techniques indicate that, with particle dimensions as currently incorporated in the resin complete solution is not attained for times up to 10 minutes and 100 minutes at isothermal temperatures of 150°C and 125°C respectively. With particle dimensions greater than 70μm DICY particles have been observed that have not entered solution even after a full cure schedule (refs. 19,10,34).

Further experiments aimed at quantifying the rates of dimensional change of DICY particles at a number of temperatures were therefore conducted (ref.24). Hot stage microscopy techniques were again used for these measurements.

The current DICY particle size distribution is such that the size ranges from submicroscopic to 70μm maximum but with a mean value of 4.6μm. Observation and measurement of selected individual particles on the hot stage was however difficult especially since the convective action of the fluid resin at high temperatures induced uncontrollable particle movement in the microscope field of view.

For these reasons a large scatter in the results was obtained as shown in a typical graph of the lateral dimensions lost (or depth removed) due to solubility versus time at 135°C in Fig.(9). From the straight line fit the lateral dimensions removal rate at this temperature is found to be 6.24×10^{-7} cm/sec.

On the assumption that all the particles are spherical and with a mean diamter of 4.6μm then the rate of mass loss may be estimated. An Arrhenius plot of the estimated logarithmic mass loss rate dm/dt versus reciprocal temperature is shown in Fig.(10). From the

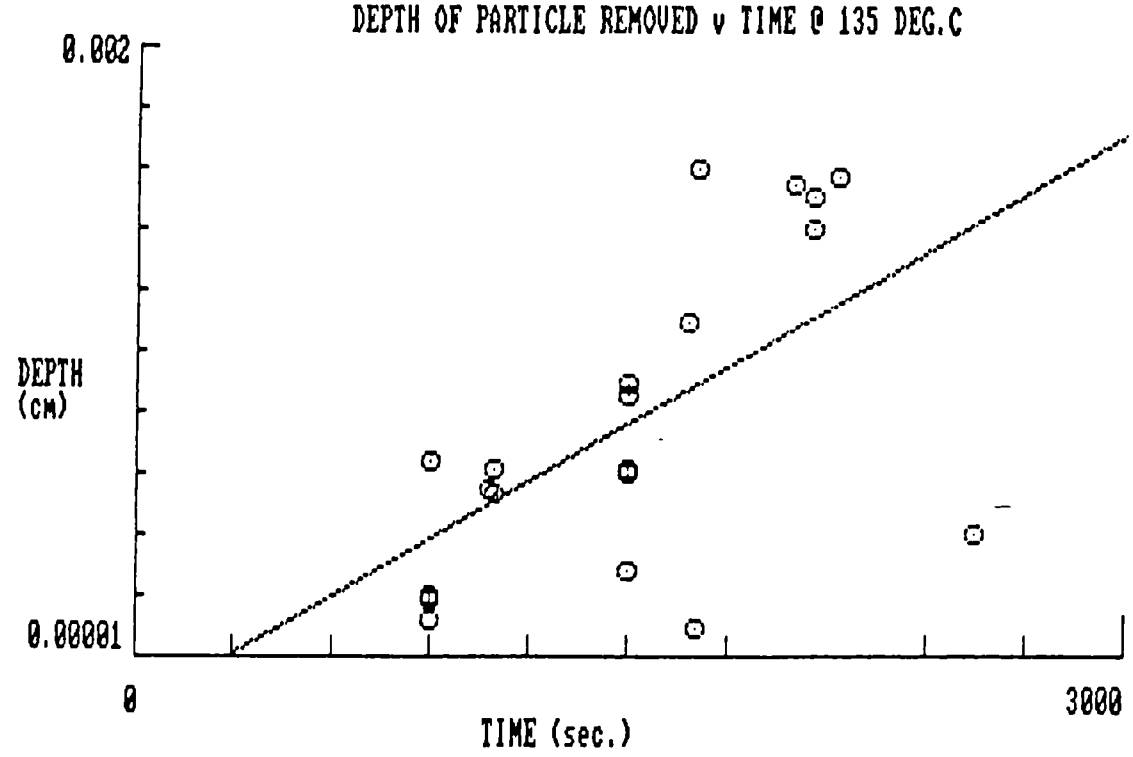

FIG.(9)

straight line fit the activation energy of solution is found to be 172 kJ/mole with a pre-exponential factor of 7.6×10^{9} sec^{-1}.

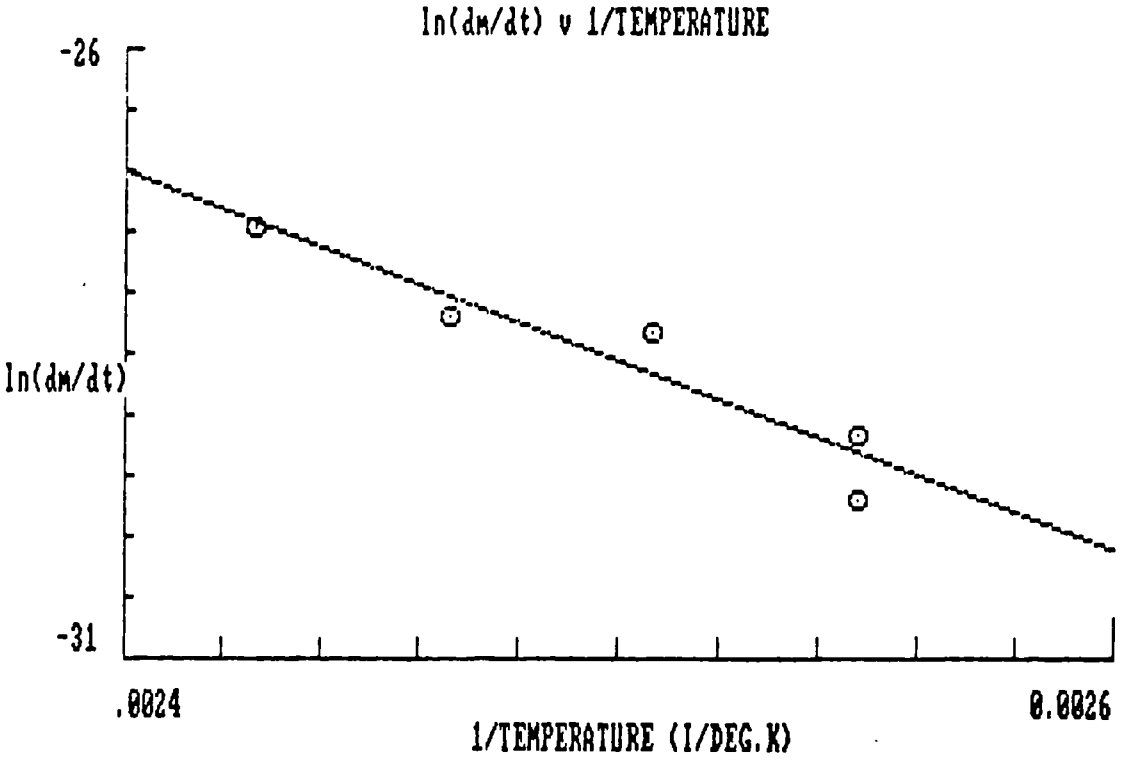

FIG.(10)

The incorporation of the solubility effect into the cure model for BSL 914 resin has however not been attempted as yet since the estimated rate of mass loss, dm/dt, has not been confirmed experimentally.

2.3.1.3 Dynamic Baseline Options

In the DSC dynamic scanning of samples undergoing multiple exothermic reactions as in the case of BSL 914 a major problem encountered is that of defining the correct baseline for the peak integration to represent the state of cure at any temperature during the scan, see also refs.14,15,19,25.

The difficulties in obtaining unambiguous values for the area under the first exotherm peak in order to define full cure can be explained by reference to Fig.(6) and Fig.(8). It is noted from Fig.(6) that the heat flow is negative i.e. into the sample before commencement of the exotherm for reasons already described in section 2.1.3.1. The differential inflow of heat into the sample is substantially constant up to 125°C and is dependent on both the mass of the sample and its specific heat. In this particular case calculations show that the specific heat of the liquid resin is approximately 0.7 cal/g/°C up to 125°C.

Above 125°C however the specific heat is an unknown and possibly a complicated function of temperature (ref.25) during the dynamic cure of the resin.

During the cure reaction the heat flow in the calorimeter is due to contributions from both sample specific heat variations and the exothermic heat produced by chemical reactions. Hence in order to isolate the exothermic heat flow contribution only an estimate of the specific heat inflow can be utilised as a baseline for the purpose of integration of the reaction peak.

Prior to the onset of the exotherm therefore the baseline coincides with the material behaviour trace up to 125°C but above this temperature it is currently indeterminate. The software in the DSC computer however presents three artificial options for a baseline which satisfies the initial conditions at 125°C as shown in Fig.(8).

The first baseline option, B, is a linear baseline which has been subjectively chosen to join points near the beginning and end of the reaction respectively. Baselines A and C, also subjectively chosen, are the horizontal sigmoidal and tangential sigmoidal options respectively.

It is noted from the peak area values in the figure that the integral of the peak is highly dependent on the choice of baseline with the areas varying from a minimum of 77.23 cal/g for baseline A to a maximum value of 104.6 cal/g for baseline C.

Also shown in Fig.(8) is a trace, D, for a material which had undergone a cure reaction so that effectively the first exotherm peak had been removed. It is noted that the cured material behaves similar to the liquid resin up to 125°C but that at higher temperatures the trace gradually curves upwards until eventually the material approaches the second exotherm at approximately 210°C. This trace D, however does not necessarily follow the baseline for the uncured material since the specific heat of the cured material may not be identical with that of the reacting species in the initial temperature scan.

Although there is no theoretical justification in the choice of any of the above baselines it was decided nevertheless that the tangential sigmoidal baseline would be sufficiently consistent for the purpose of practical model generation in this work.

2.3.1.4 Heat Of Cure

A characteristic of dynamic scanning is that the temperature location of the peak maximum depends on the temperature scanning rate. Thus in Figs.(6) and (8) respectively where the scan rates are 10°C/min and 3°C/min the peak maxima occur at approximately 190°C and 170°C. This trend of increased temperature of peak maximum occurrence with increased scan rate is also shown in Fig.(11).

At identical scan rates the area under the first exotherm peak, evaluated by the use of the

tangential sigmoidal baseline as described above has been shown to be reproducible within ±6.5% of the mean value for a number of determinations (ref.16).

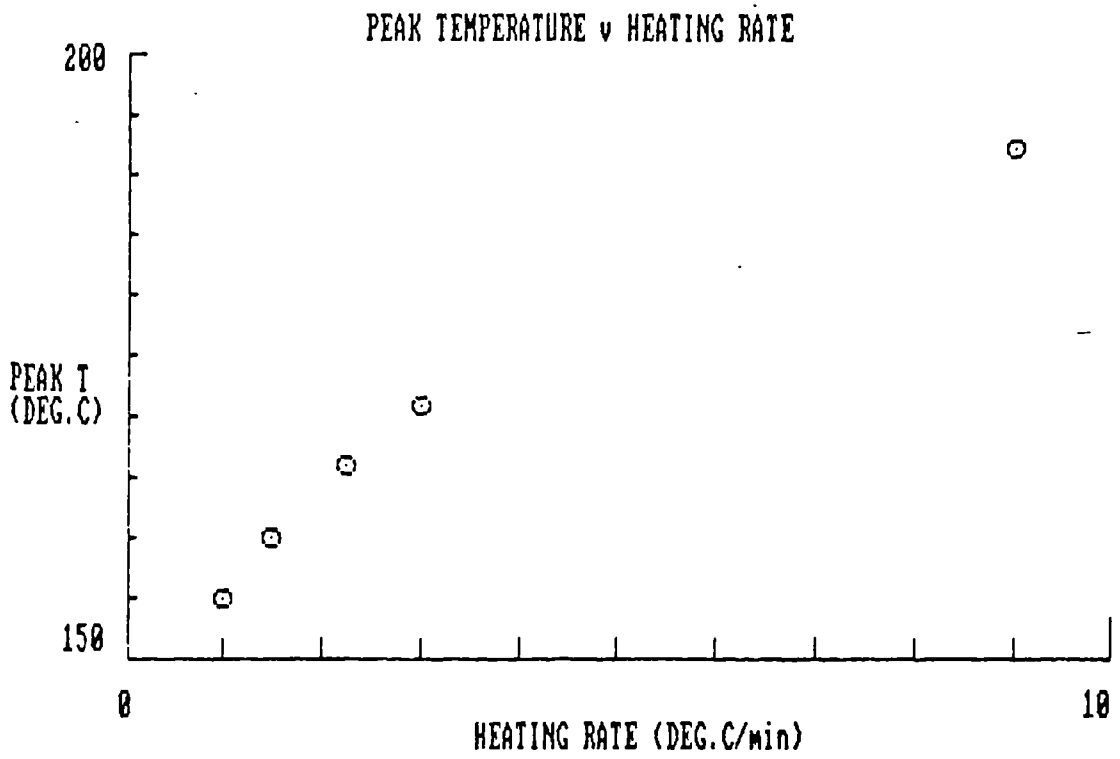

FIG.(11)

The peak area however depends on the temperature scan rate as shown in Fig.(12) where the area under the peak decreases with increased scan rate from approximately 115 cal/g to approximately 90 cal/g for scan rates of 1°C/min and 9°C/min respectively. In ref.18 the reverse trend is indicated whereby the exotherm incorporating both of the two peaks of cure increases with increased scanning rates. The different behaviour in these two cases is attributed to the choice of different baselines and definition of cure.

Since, in practice, the temperature ramp rates in an autoclave are of the order of 1°C/min to 4°C/min then the area under the first exotherm peak, representing 100% cure has been chosen to be 115 cal/g or 481.16 J/g. In the current modelling work therefore intermediate cure levels have been evaluated relative to this value of 115 cal/g as being representative of full cure exothermic heat evolution and will be referred to as H(dyn) in the

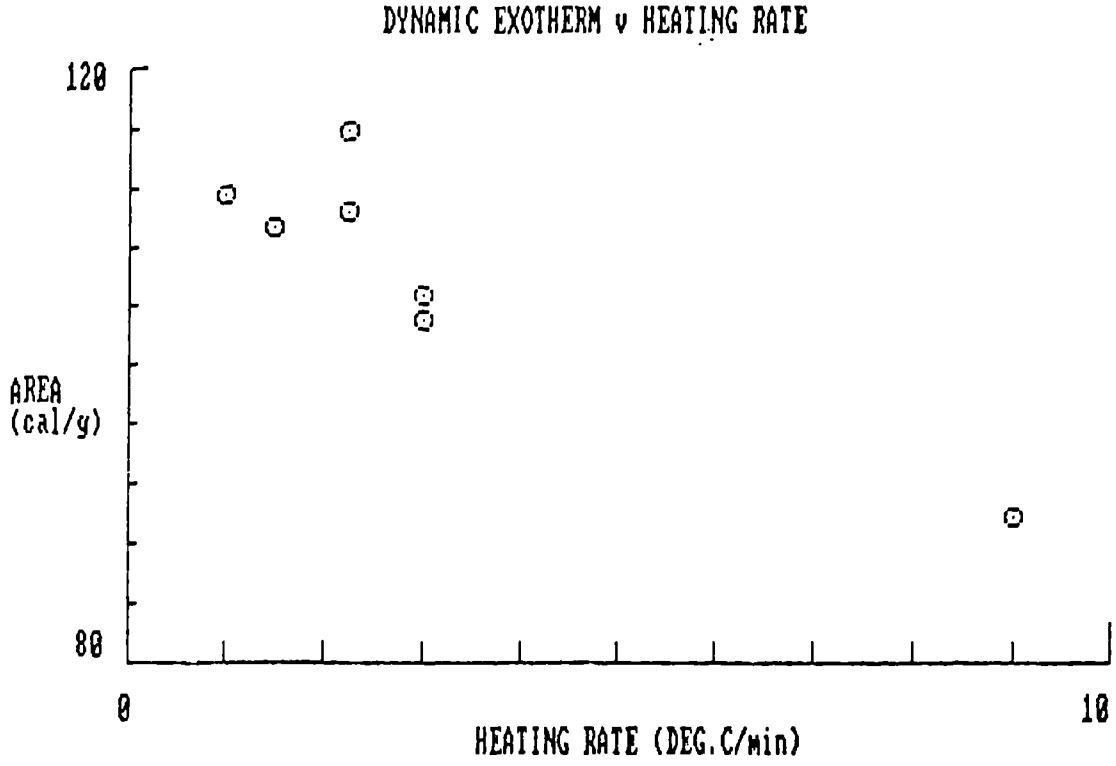

FIG.(12)

rest of the text.

In dynamic scanning the reaction rate is also dependent on the temperature scan rate. The maximum heat flow (maximum peak signal), which occurs at the apex of the exotherm peaks, versus temperature scan rate is shown in Fig.(13). It is noted that the maximum heat outflow, and hence maximum rate of reaction from section 2.1, increases markedly with increased scan rates.

This latter behaviour has an important bearing in the practical considerations of the use of the resin in the moulding of composite materials. For instance should the rate of temperature rise during cure be too high then this would lead to an excessive rate of heat generation within the composite. Failure to dissipate this excessive heat would result in thermally induced damage since the material temperature would rise uncontrollably. In this event the resin might undergo the second and even the third exotherm with resultant catastrophic degradation.

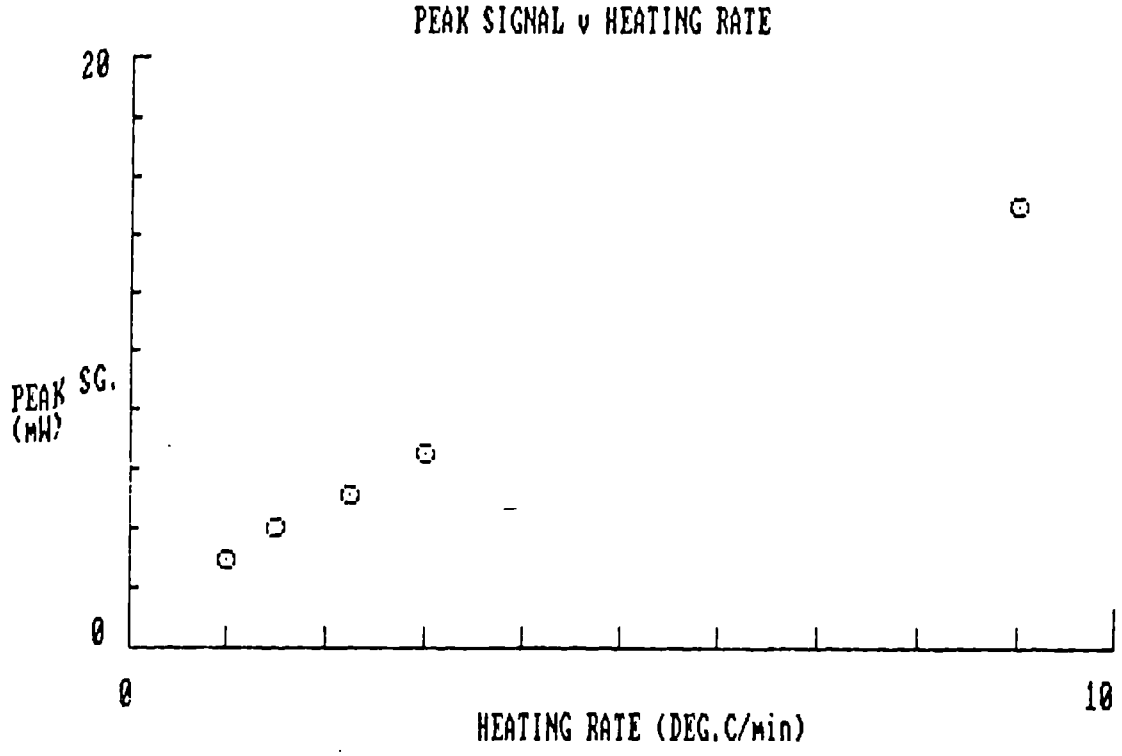

FIG.(13)

2.3.2 Isothermal Exotherm

2.3.2.1 Autocatalytic Reactions

Typical output scans for isothermal runs on the DSC are shown in Fig.(14) for five isothermal hold temperatures in the range 125°C to 150°C. Note the rapid fluctuations in output at the beginning of the scans for reasons described in section 2.2.1.

The main features of all these scans are that the peak maxima do not occur at zero scan time and also, within experimental error, the reaction rate is zero at zero scan time. Peak times are shown for a total of 15 runs at a number of isothermal temperatures in Fig.(15) and it is noted that the lower the temperature the longer it takes for the reaction to attain its maximum rate.

This behaviour of zero initial reaction rate is characteristic of an autocatalysed reaction (refs.26, 27) as opposed to reactions following n-th order kinetics in which case the reaction rate would exhibit a positive

value at zero time. In the case of the BSL 914 resin system the initial rate of reaction is also dependent on the rate of solubility of DICY as well as the

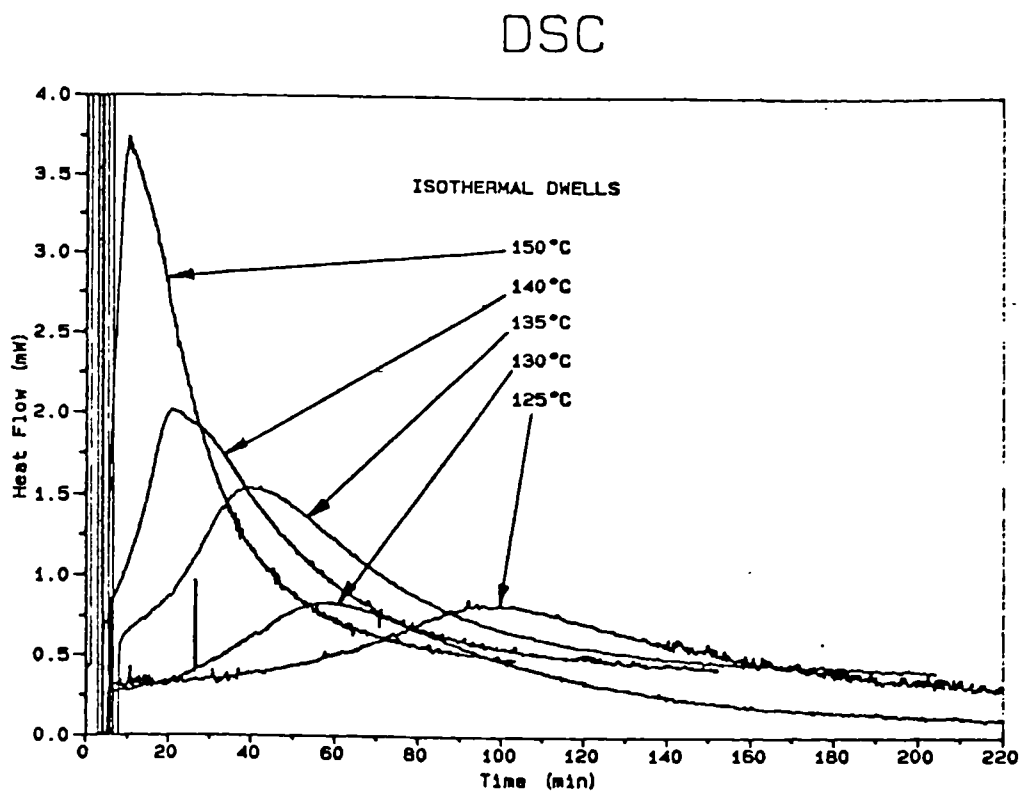

FIG.(14)

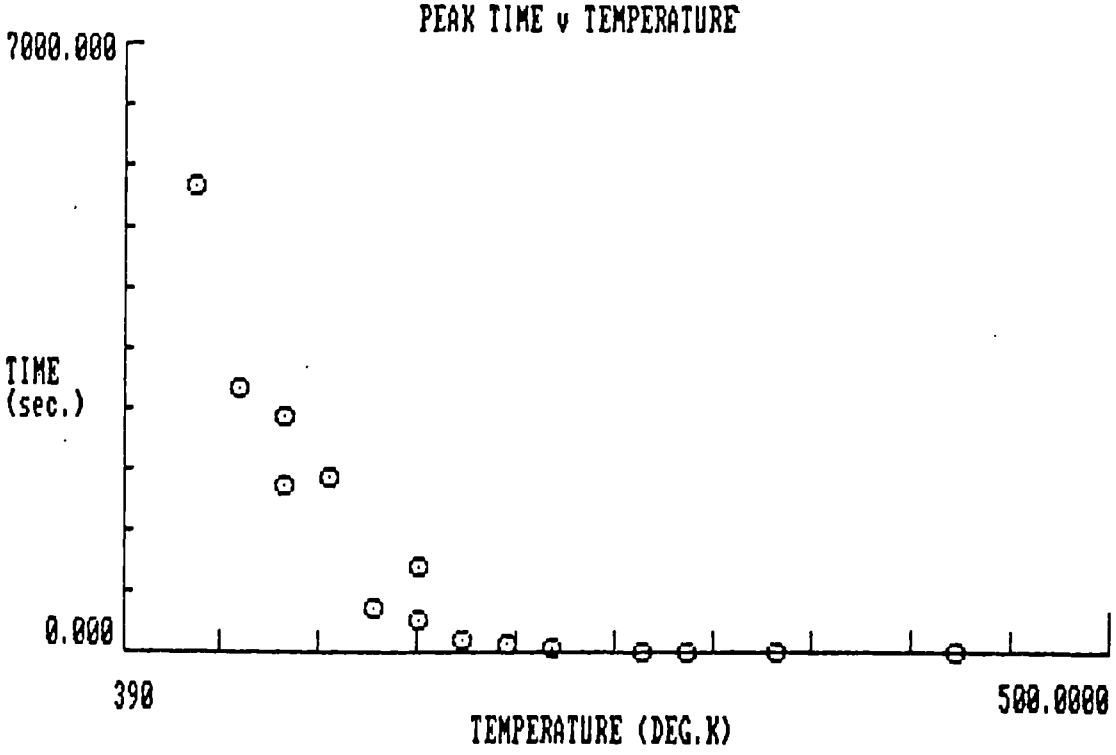

FIG.(15)

autocatalytic reactions which occur in the initial stages of cure (sections 1.6 and 2.3.1.2). Since the rate of solubility of the DICY has not been unambiguously established then the extent to which the solubility effect would give rise to an apparent autocatalytic behaviour has not been determined.

For the purposes of the generation of a practical cure model therefore the reaction will be assumed to be purely autocatalytic.

2.3.2.2 Isothermal Heat Of Reaction

In order to quantify the extent of cure during isothermal scans the areas under individual curves such as those shown in Fig.(14) have to be determined in a similar manner to the dynamically scanned exotherms as already described.

Experimentally, the scans at isothermal hold temperature were conducted for times long enough for the cure reactions to proceed to effective completion at each temperature.

The time to completion of the reaction at any temperature however is difficult to determine exactly for the following reasons:-

a) As cure proceeds at any isothermal temperature the viscosity and hence the glass transition temperature, Tg, of the resin increase. Mobility of the reacting molecules is therefore reduced and the reaction rate becomes diffusion controlled (see also ref.14) and hence extremely low as the Tg approaches the cure temperature. Although the rate of reaction is low under these conditions it is however finite and the resin therefore continues to cure for prolonged periods at any hold temperature and approaches a stable condition asymptotically.

b) As in the dynamic scan case, because the specific heat of the material during the cure is not known then it is difficult both to establish the true baseline for the exothermic reaction and hence how far removed the asymptotic exotherm curve is from this baseline condition at the end of the reaction.

Due to the above difficulties therefore the practice in the current work has been to allow the isothermal runs to proceed to times at which the reaction is subjectively judged to be complete as those shown in Fig.(14). Further the baseline for peak integration purposes has been assumed to be horizontal and passing through the reaction end point as above and intersecting the rising exotherm curve at the commencement of the scan.

On this basis, peak integration can be accomplished at any desired isothermal temperature and the results of total peak integration for 17 conditions are shown in Fig.(16) and tabulated in computer format in Table 1. In Fig.(16) the total isothermal exotherm, H(iso) is plotted versus the isothermal hold temperature.

Due to the difficulties associated with the establishment of the reaction end point and baseline as above there is some scatter in the observed heats of reaction. It is noted however that the heat output significantly increases with temperature in the range 398°K (125°C) to 448°K (175°C) but thereafter decreases with increased temperatures. The decrease in heat output above 175°C is attributed to a substantial amount of reaction taking place before stabilisation of the isothermal conditions as described in section 2.2.1.

On the assumption however that the maximum heat of reaction is observed at 175°C then the variation of H(iso) with temperature can be adequately represented by the quadratic curve as shown (see also refs.25, 33). This quadratic curve was fitted to the data by Lagrange interpolation through the three points indicated in the

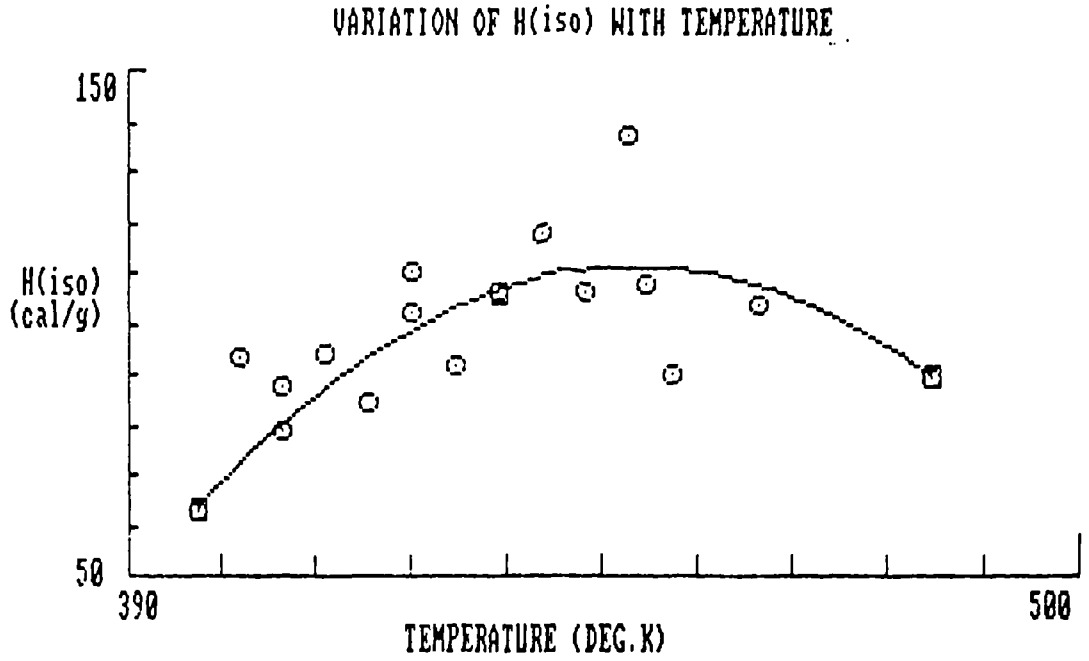

FIG.(16)

figure.

The equation of the quadratic curve is as follows:-

$$H(iso) = (-1.840437 \times 10^{-2})T^2 + (16.53196)T - (3601.842) \quad (2.9)$$

where T is the isothermal temperature in °K.

The maximum of this fitted curve occurs at an isothermal temperature of 449°K (175.9°C) and with a corresponding maximum heat of reaction of 110.7 cal/g.

This maximum isothermal exotherm is nearly identical with the total dynamic exotherm of 115 cal/g which was chosen to represent the full exotherm in section 2.3.1.4.

CHAPTER 3

CURE SUB-MODEL DEVELOPMENT

3.1 Aims Of Model

A mathematical cure sub-model for BSL 914 resin must be capable of predicting the following parameters in the temperature range 125°C to 175°C:-

a) The extent of cure or conversion of the resin at any time and temperature.

b) The rate of cure or conversion of the resin at any time and temperature.

c) The rate of heat output at any time and temperature.

Further, temperature ramp conditions for practical resin cure have to be catered for in addition to isothermal hold conditions at all temperatures in the above range.

A model to satisfy the above requirements can be developed by the analysis of cure reaction kinetics under isothermal conditions.

3.2 General Kinetic Analysis

The general approach to the treatment of kinetic data is to assume that the rate of conversion of the resin at any time and temperature is a function of the conversion at that time and temperature (refs.14, 15)

i.e. $$d\alpha/dt = k\, f(\alpha) \qquad (3.1)$$

where α is the fractional conversion and k is the apparent rate constant or, generally

simply called the rate constant for a reaction proceeding at a velocity or rate of conversion $d\alpha/dt$. The function $f(\alpha)$ is called the kinetic function.

Since the rate of conversion varies with temperature then in common with the analysis of chemical reactions generally (ref.28) the apparent rate constant is assumed to be of the Arrhenius form, thus.

$$k = A \exp(-E/RT) \qquad (3.2)$$

where A is a constant, called the pre-exponential or, alternatively, frequency factor. R is the gas constant and T the absolute temperature at which the reaction proceeds.

For a single specific reaction, E is a constant and the value of which, in a pragmatic sense, indicates how much faster or slower the same reaction would proceed as a result of a change from one reaction temperature to another i.e. E can be regarded as a time-temperature shift factor for an individual reaction.

In chemistry theory where the rates of reactions are defined in terms of absolute concentrations of the reactants, E is known as the Activation Energy. Since $f(\alpha)$ is defined in terms of fractional conversion rather than absolute concentrations in eq.(3.1) then the activation energy does not strictly have this same meaning and hence E is generally referred to as the Apparent Activation Energy in cure kinetics. It is also for these same reasons that k is called the Apparent Rate Constant rather than simply rate constant.

In addition to enabling the rate of conversion of the resin at any temperature to be determined, evaluation of the apparent activation energy will also give information as to possible changes in the nature of the cure reaction mechanism. Thus, if during

the kinetic analysis of a cure reaction the apparent activation energy changes at some temperature then the implication is that the reaction itself has changed at that temperature. The time-temperature conditions at which reaction modifications occur can therefore be identified.

Before the kinetic parameters A and E can be evaluated for a practical resin system however the kinetic function $f(\alpha)$ has to be defined for the cure reaction.

3.3 Kinetic Function

The chemical reactions which lead to epoxy resin cure can be categorised into two main types 1) reactions which follow n-th order kinetics and 2) reactions which follow autocatalysed kinetics (refs.14, 15, 26, 27). The kinetic functions which are applicable in each case are as follows:-

3.3.1 n-th order kinetic function

For cure reactions that follow n-th order kinetics the function $f(\alpha)$ can be generally defined in terms of the fraction of uncured resin as follows:-

$$f(\alpha) = (1 - \alpha)^n \qquad (3.3)$$

where n is the order of the reaction.

The rate of conversion is therefore given by, from eq.(3.1)

$$d\alpha/dt = k(1 - \alpha)^n \qquad (3.4)$$

A number of different epoxy/hardener combinations have been observed to follow n-th order kinetics e.g. the cure of bisphenol A diglycidyl ether (DGEBA) with ethylene-diamine (ref.29), the cure of DGEBA with nadic methyl anhydride (NMA) and benzyldimethylamine (BDMA) (ref.30), the cure of DGEBA with polyamide (ref.31) and the cure of DGEBA with m-phenylene diamine (ref.32).

Numerous methods have been devised for the analysis of dynamic as well as isothermal exotherms as exhibited by systems obeying n-th order kinetics as in eq.(3.4) (refs.14, 15).

Of interest in the current work is the application of two equations for the estimation of the activation energy, E, from two dynamic scans of the material at different heating rates.

The first equation is to be found in ref.15 and is as follows:-

$$E = \frac{-R \quad \Delta \ln\phi}{1.052 \quad \Delta(1/Tp)} \qquad (3.5)$$

where $\Delta \ln\phi$ is the difference in the logarithm of the heating rates ϕ. Tp is the absolute temperature at which peak maxima occur in the two runs and hence $\Delta(1/Tp)$ is the difference in the reciprocal temperature between the two runs. R is the gas constant.

Although eq.(3.5) has been derived for reactions obeying n-th order kinetics it has been found of use for the estimation of E in other cases (ref.15). It is of interest therefore to apply this formula to the two dynamic scans as shown in Fig.(6) and Fig.(8) where the dynamic heating rates are 10°C/min and 3°C/min with corresponding temperatures at peak maxima of 190.57°C and 169.50°C respectively.

Thus $\Delta \ln\phi = 1.20398$

and $\Delta(1/Tp) = 0.10263 \times 10^{-3}$

By substitution in eq.(3.5) then

$$E = 22 \text{ kcal/mole } (92\text{kJ/mole}) \qquad (3.6)$$

The second equation is found in ref.30 as follows:-

$$-E/R = \frac{\Delta \ln(\phi/T^2)}{\Delta(1/T)} \qquad (3.7)$$

Substitution of scan values in eq.(3.7) leads to a value of

$$E = 21\text{kcal/mole (88kJ/mole)} \qquad (3.8)$$

Thus from eqs.(3.6) and (3.8) similar values of E are obtained for the BSL 914 resin system during dynamic scans.

One of the conditions that have to be fulfilled before eqs.(3.5) and (3.7) can be applied to dynamic exotherms is the requirement that the conversion at the peak maximum conditions is constant and independent of heating rate. From a number of runs in the current work with heating rates varying from 1°C/min. to 9°C/min. respectively the conversion at peak maximum has been found to increase from 0.37 to 0.54 (ref.16).

Thus it appears that the amount of conversion at peak maximum is not independent of heating rate in the BSL 914 system with the use of a baseline as described in section 2.3.1.2.

3.3.2 Autocatalytic Kinetic Function

A general form for the autocatalytic kinetic function is given by.

$$f(\alpha) = \alpha^n (1-\alpha)^m \qquad (3.9)$$

By substitution for $f(\alpha)$ in eq.(3.1) therefore

$$d\alpha/dt = k\, \alpha^n (1 - \alpha)^m \qquad (3.10)$$

where $k = A \exp(-E/RT)$

n,m are reaction orders and hence (m + n) is the total reaction order, the other symbols are as already defined in the text.

The autocatalytic kinetic function has been used for the analysis of a number of thermosetting systems. For instance see refs.36, 37 and 38 for its application in polyester systems.

For application in epoxy systems see refs.25, 39 for general description, ref.40 for the cure of DGEBA by m-phenylene diamine, ref.41 for a DICY cured adhesive, refs.42, 43 for the cure of TGDDM resin by DDS and finally refs.33, 44 for filled and modified resin systems.

In the expression for the rate of conversion at any isothermal temperature,eq.(3.10), there are three unknown parameters viz n, m and k.

Two main approaches have been used for the evaluation of these three parameters in the literature. In the first approach use is made of non-linear least squares procedures to fit eq.(3.10) to experimental isothermal data. These fitting procedures are simplified if prior estimates for the values of the reaction orders m and n can be obtained, see refs.37, 25, 42, 36.

The alternative approach depends on the characteristics of the kinetic function see refs.41, 40, 38, 44. In all the latter methods the ratio m/(m+n) is related to the practical exotherm properties.

In the current work both fitting techniques and single point methods have been utilised and compared whereby the ratio of m to n is related to the exotherm properties. As far as is known this form of representation has not been reported in the literature.

Before the mathematical procedure for the evaluation of n, m and k is described however it is necessary to assign a physical meaning to the autocatalysed reaction represented by eq.(3.10).

3.3.3 Practical Isothermal Reaction Rate

From eq.(3.1) the rate of reaction is a function of the conversion with k as the proportionality constant. The rate constant, k, however is dependent on the temperature as defined in eq.(3.2). If therefore the temperature is maintained constant during the course of the reaction, as in the isothermal DSC experiments then a plot of the rate of conversion versus conversion will indicate the main characteristics of the function $f(\alpha)$ since k is a constant in this case.

As described in Chapter 2 both the rate of conversion and conversion can be computed from DSC isothermal scans in the following manner by reference to Fig.(17). In this figure the heat flow versus time is shown for an isothermal run at 140°C. Also shown are computer generated ordinates intersecting the curve and the baseline at selected times. By means of the software facilities on the DSC the area bounded by any two adjacent ordinates and the curve can be evaluted. Also the total heat of reaction at 140°C can be obtained from the total area under the curve and this value corresponds to H(iso) as described in section 2.3.2.2. In this particular example H(iso) is 94.35 cal/g.

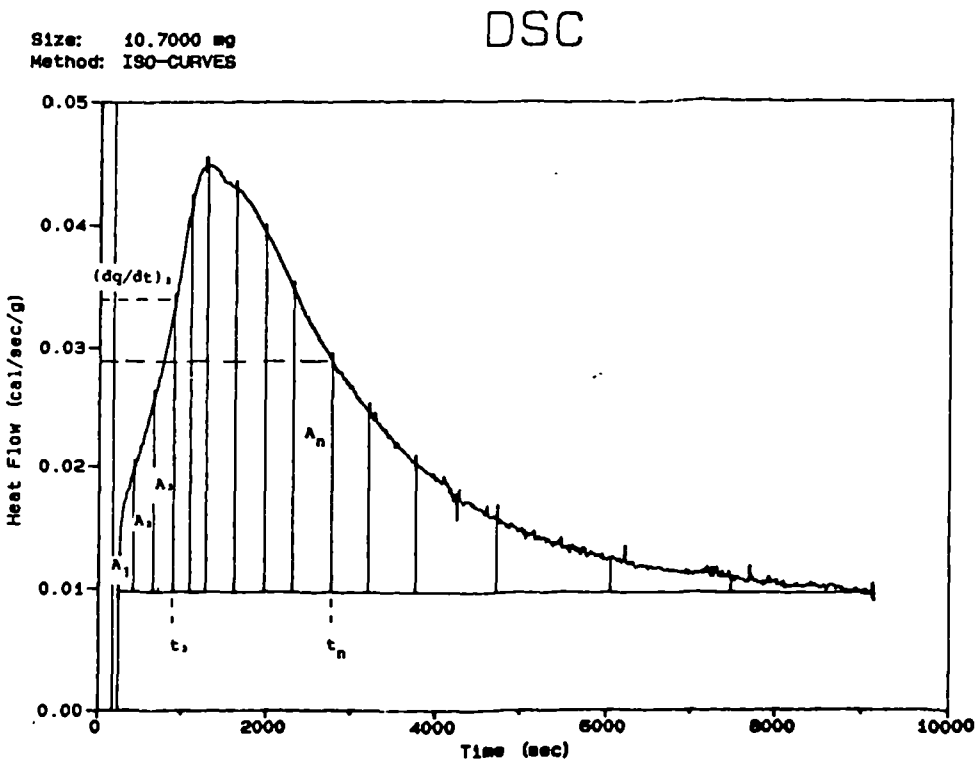

FIG.(17)

Thus in Fig.(17) the rate of conversion after the reaction has proceeded for a time $t = t_3$ is

$$(dq/dt)_{t3}/H(iso)(140)$$

where H(iso)(140) is the isothermal heat of reaction at 140°C as described and $(dq/dt)_{t3}$ the instantaneous heat flow at time t_3.

The conversion is given at time t_3 by

$$(A_1 + A_2 + A_3)/H(iso)(140)$$

Note that in order to characterise the autocatalytic function at one temperature both the rate of conversion and conversion are defined relative to the total isothermal exotherm at that temperature i.e. H(iso).

Let ß and dß/dt therefore represent the conversion and rate of conversion respectively relative to the isothermal heat of reaction as distinct from α and dα/dt which are defined as fractional conversion and rate of reaction respectively relative to the total heat of reaction H(dyn) as defined in section 2.3.1.3.

Generally then in Fig.(17).

Rate of isothermal reaction at time t = t_n is

$$(d\beta/dt)_{tn} = (dq/dt)_{tn}/H(iso)(140)$$

Conversion at time t_n is

$$\beta_{tn} = \sum_{i=1}^{n} A_i/H(iso)(140)$$

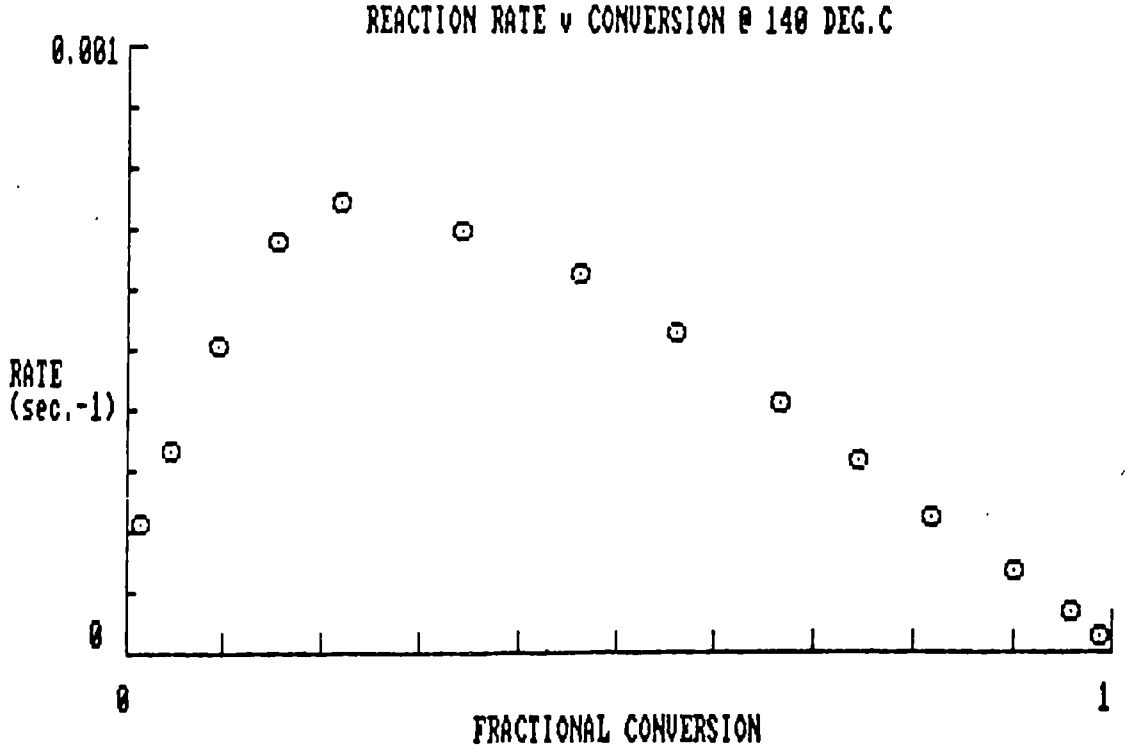

FIG.(18)

Values for the rates and the corresponding conversions so computed for the exotherm in Fig.(17) are tabulated in Table 2 and plotted as shown in Fig.(18).

It is noted that the reaction rate accelerates with increased conversion from zero to a maximum value. This initial acceleration in the reaction rate gives rise to the terms autoacceleration or autocatalysis to describe these reactions. Note that the fractional conversion ß is unity at the end of the reaction.

3.4 Mathematical Formulation

The mathematical process for evaluation of the three variables m, n and k in eq.(3.10) can be described by first considering the characteristics of the function f(α) in eq.(3.9) in the following manner.

$$\text{Let} \qquad y = x^n (1-x)^m \qquad (3.11)$$

Values of x and y for two combinations of m and n are shown in Fig.(19). For the two curves shown the ratio of m to n is constant and equal to 4.

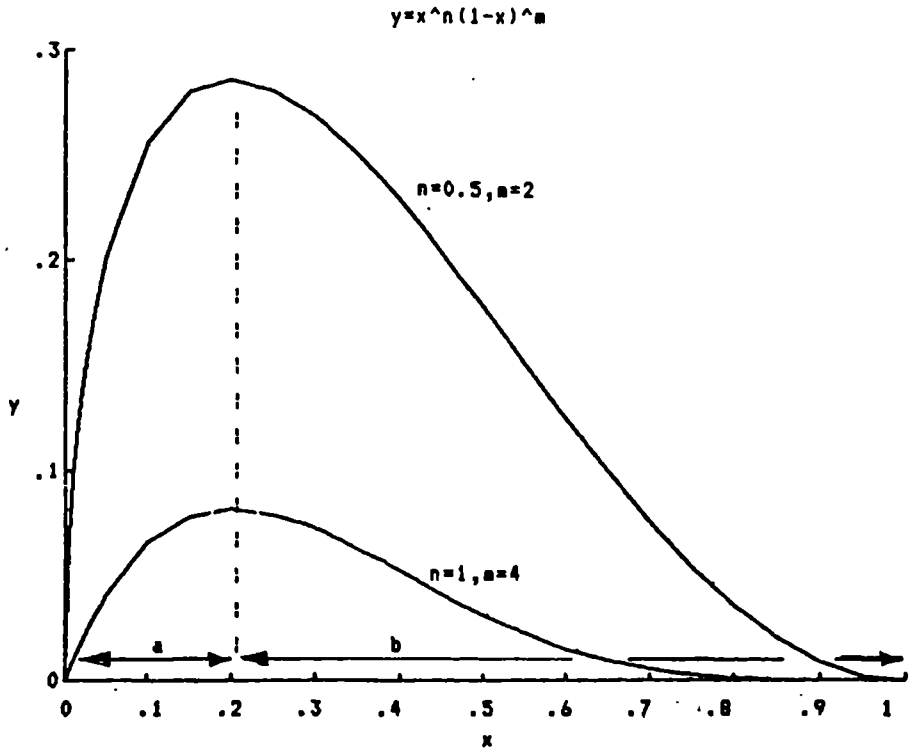

FIG.(19)

It is noted that the two curves exhibit characteristics which are similar to the reaction rate versus conversion curve of Fig.(18) i.e.

a) the curves in Fig.(19) pass through the origin corresponding to the commencement of the reaction in Fig.(18).

b) the curves in Fig.(19) exhibit a maximum value at some positive value of x corresponding to peak reaction rate which occurs at a value of conversion greater than zero in Fig.(19).

c) subsequent to the maxima in peak heights the value of y decreases gradually to zero at x = 1 in Fig.(19) and this corresponds to the point at which the fractional conversion of the resin is complete in Fig.(18).

By differentiating eq.(3.11) by the product rule (ref.45) then

$$dy/dx = nx^{n-1}(1-x)^{m} - mx^{n}(1-x)^{m-1} \qquad (3.12)$$

At the peak maximum let x = a, (1-x) = b and y = c then, since dy/dx = o at maximum, by substitution in eq.(3.12) we obtain

$$na^{n-1}b^{m} - ma^{n}b^{m-1} = 0$$

thus $$a^{n-1}b^{m-1}(nb - ma) = 0$$

so $$nb = ma$$

i.e. $$m = nb/a \qquad (3.13)$$

From eq.(3.13) therefore the ratio of the indices, m to n, can be determined from a knowledge of

the ratio a to b and this fact is illustrated in Fig.(19) where the peak maxima occur at the same value of x for the same ratio of m to n in the two cases.

It is therefore assumed that the characteristics of the experimentally derived plot in Fig.(18) can be adequately represented by an expression based on eq.(3.11).

Incorporating the autocatalytic function in eq.(3.10) modified so that the conversion and rate of conversion respectively are relative to the isothermal heat of reaction as described above gives

$$d\beta/dt = k\beta^n (1 - \beta)^m \qquad (3.14)$$

The values b and a in eq.(3.13) can be related to the isothermal exotherm properties as follows:-

For a typical exotherm as shown in Fig.(17) the conversion β_p at peak maximum is defined by:

$$\beta_p = Q_p/H(iso) \qquad (3.15)$$

where Q_p is the area under the exotherm up to peak maximum.

$$(1 - \beta_p) = 1 - (Q_p/H(iso)) \qquad (3.16)$$

From (3.15) and (3.16) $(1-\beta_p)/\beta_p = Q_R/Q_p$

where Q_R is the area under the curve from the location of the peak maximum to the point of conclusion of the reaction.

Both Q_R and Q_p are computed directly on the DSC.

But β is equivalent to a in Fig.(19) and $1 - \beta$ is equivalent to b and thus from eq.(3.13).

$$m/n = Q_R/Q_p = r \qquad (3.17)$$

where r is the ratio of the areas Q_R/Q_p

Substituting for m in eq (3.14) gives

$$d\beta/dt = k\beta^{n}(1 - \beta)^{nr}$$

$$= k\,(\beta(1 - \beta)^{r})^{n} \qquad (3.18)$$

We require to establish however the rate of reaction relative to the total heat of reaction i.e. $d\alpha/dt$ at the corresponding conversion α relative to the total heat of reaction H(dyn).

If Q_t is the area under the exotherm and $(dq/dt)_t$ the heat flow respectively at any time t then by definition.

$$(d\beta/dt)_t = (dq/dt)_t/H(iso)$$

and

$$(d\alpha/dt)_t = (dq/dt)_t/H(dyn)$$

then generally

$$d\beta/dt = (H(dyn)/H(iso)).d\alpha/dt$$

Similarly by definition

$$\beta = Q_t/H(iso)$$

and

$$\alpha = Q_t/H(dyn)$$

so that $\beta = (H(dyn)/H(iso)).\alpha$

If we denote $H(dyn)/H(iso) = F$ (3.19)

then by substitution for β and $d\beta/dt$ in (3.18)

$$F\,d\alpha/dt = k\,(F\alpha(1 - F\alpha)^{r})^{n} \qquad \text{where } \alpha = \beta/F$$

or $$d\alpha/dt = (k/F)(F\alpha(1 - F\alpha)^{r})^{n} \qquad (3.20)$$

which relates $d\alpha/dt$, α and the isothermal rate

constant k.

Equation (3.20) can be linearised by taking logarithms.

$$\ln(d\alpha/dt) = \ln(k/F) + n \ln(F\alpha(1 - F\alpha)^r) \quad (3.21)$$

Thus, provided that F and r are known at the reaction temperature, then by plotting $\ln(d\alpha/dt)$ v $\ln(F\alpha(1 - F\alpha)^r$ the values of the isothermal rate constant k and the reaction order n can be obtained at the isothermal reaction temperature.

F can be simply evaluated at any temperature since H(dyn) is a constant in eq.(3.19) as defined in section 2.3.1.3 and H(iso) can be evaluated by the use of the quadratic equation (2.9).

The index r has to be determined experimentally as follows:-

3.4.1 Evaluation Of Ratio Index

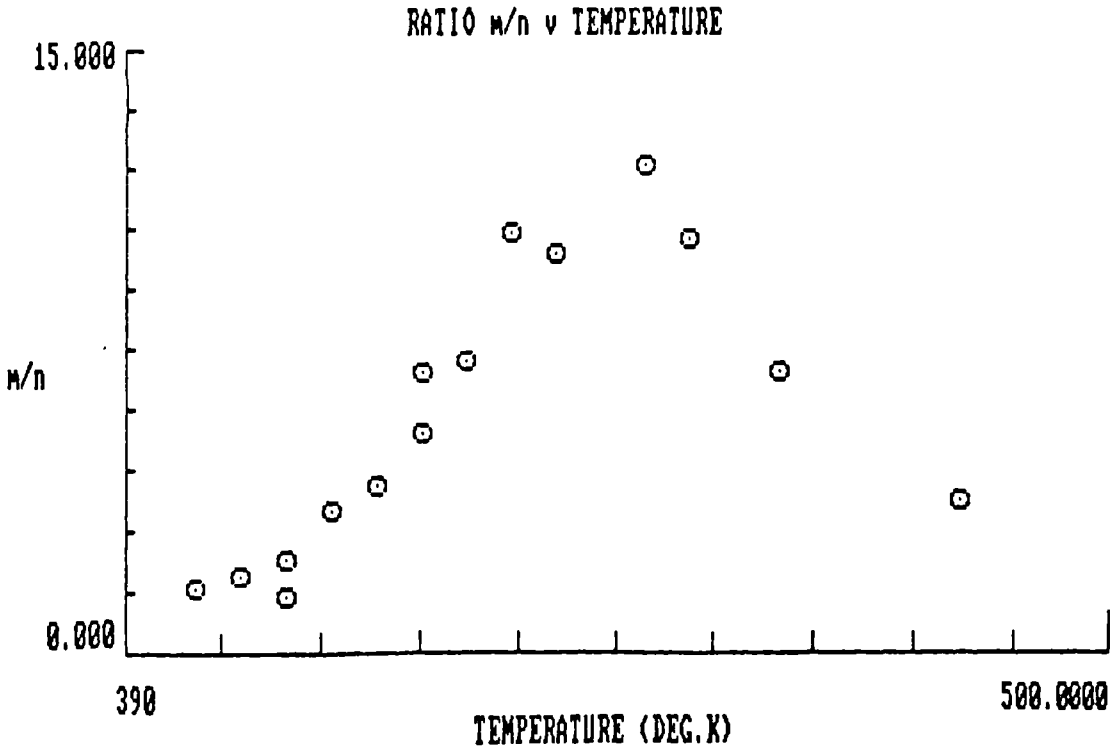

FIG.(20)

From eq.(3.17) the ratio r is given by

$$r = Q_R/Q_P$$

and this ratio was evaluated for a total of 15 different isothermal runs in the temperature range 125°C to 210°C.

The values of r at the respective temperatures are tabulated in Table 3 and plotted in Fig.(20). It is noted in Fig.(20) that the ratio m/n gradually increases with increased temperature up to a temperature in the region of 175°C but thereafter decreases sharply. The temperature at which this sudden change in the behaviour of the reaction order ratio coincides with the turning point in the H(iso) v temperature curve as described in section 2.3.2.2.

Due to these difficulties in the measurement of H(iso) and ratio r above 175°C then this temperature of 175°C is the upper limit of the current model applicability.

Ratio r however can be related to temperature as can be observed in the graph of lnr versus reciprocal temperature as shown in Fig.(21). The least squares fit straight line through the points is shown and the equation for r is given by

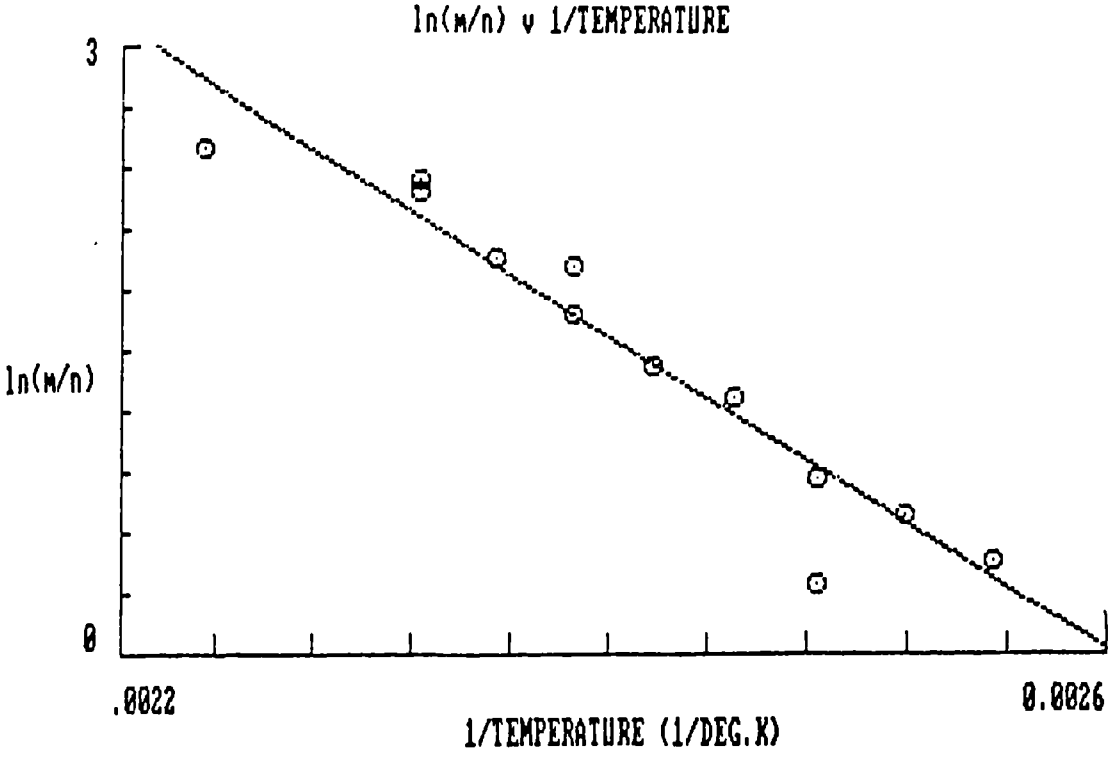

FIG.(21)

$$\ln r = (-8796.092)(1/T°K) + 22.46026 \qquad (3.22)$$

3.5 Determination Of The Isothermal Rate Constants

Two approaches have been used for the evaluation of the isothermal rate constant, k and the indices m and n. In the first approach, Method A below, curve fitting techniques have been used whereas in Method B the parameters are estimated from the characteristics of a single point on the exotherm profile viz the peak maximum.

3.5.1 Method A

In order to determine the isothermal rate constant at a constant temperature by Method A then, since F and r have been established, the experimental values for α and $d\alpha/dt$ at that temperature have to be incorporated in eq.(3.21). Also since k is a function of temperature as described in section 3.2 then in order to obtain E and A in eq.(3.2) the procedure for the evaluation of k has to be repeated at a number of temperatures.

A total of twelve conditions were analysed in the current work. The determination of the practical values of α and $d\alpha/dt$ at each temperature followed similar procedures to those for the determination of β and $d\beta/dt$ in section 3.3 but where α and $d\alpha/dt$ are defined relative to the total heat of reaction H(dyn) as follows.

$$\text{Rate of reaction} = d\alpha/dt = (dq/dt)/H(dyn)$$

$$\text{Conversion} = \alpha = \Sigma A_i/H(dyn)$$

The practical values are tabulated in Tables 4(a) to 15(a) inclusive.

From knowing α and $d\alpha/dt$ at each temperature therefore $\ln(d\alpha/dt)$ and $\ln(F\alpha(1 - F\alpha)^r$ as defined in eq.(3.21) can be computed. These values are tabulated in Tables 4(b) to 15(b) inclusive. Also shown in these Tables are the values of H(iso) and the ratio r as determined by eqs.(2.9) and (3.22) respectively.

The computed values of $\ln(d\alpha/dt)$ for $\ln(F\alpha(1-F\alpha)^r) > -10$ are shown plotted in Figs.(22) and (23) for six isothermal temperatures.

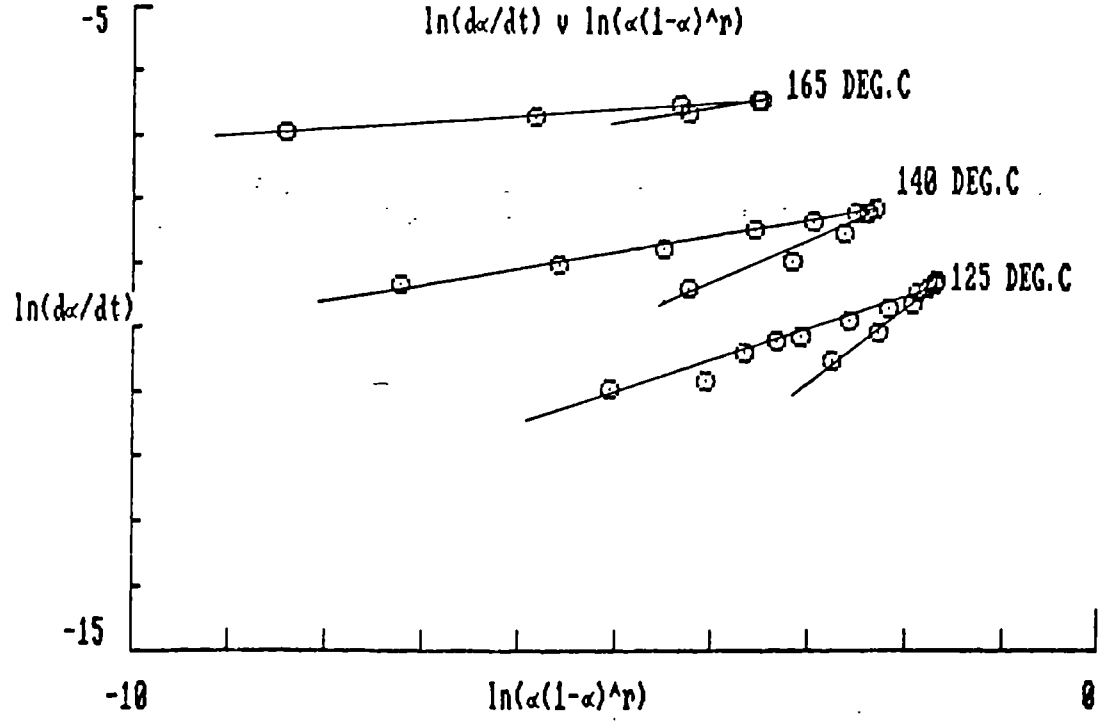

FIG.(22)

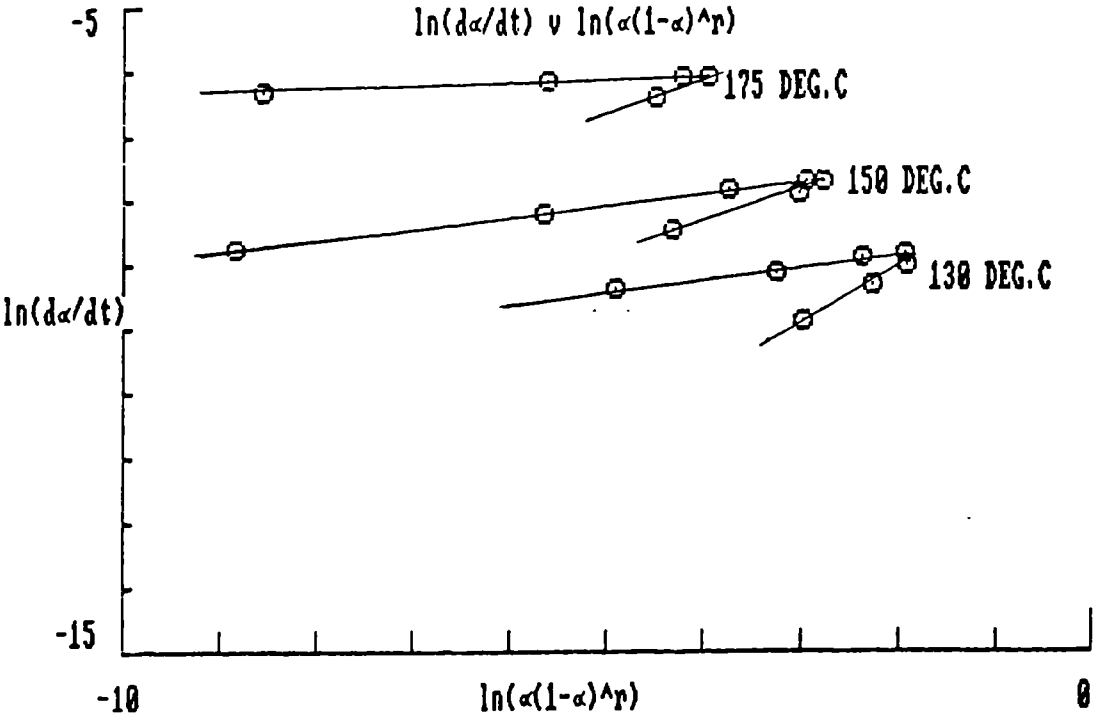

FIG.(23)

From Figs.(22) and (23) the plots at each temperature are bifurcated with upper and lower limbs

having different slopes. The sequence of plotting in these graphs is that the first point, corresponding to the start of the cure reaction occurs at the minimum ordinate value on the lower limb at each temperature. As the reaction proceeds the plotted points move up the lower limb with increased ordinate values towards the apex of the bifurcation. For points beyond the apex however the plotting direction is revesed so that decreased ordinate values are obtained as the reaction proceeds towards completion along the upper limb of the curve.

The x-coordinate of the bifurcation apex decreases gradually with increased temperature and this can be explained as follows by cosidering the behaviour of the function f(α) given by

$$f(\alpha) = \ln(F\alpha(1 - F\alpha)^r) \qquad (3.23)$$

$$= \ln(u)$$

$$\text{where } u = F\alpha(1 - F\alpha)^r \qquad (3.24)$$

f(α) attains a maximum value when $df(\alpha)/d\alpha = 0$

Since $df(\alpha)/d\alpha = df(\alpha)/du.du/d\alpha$

where $df(\alpha)/du = 1/u$

and $du/d\alpha = [F(1-F\alpha)^r - F^2\alpha r(1-F\alpha)^{r-1}]$

$$= F(1-F\alpha)^{r-1}(1-F\alpha(1 + r)) \qquad (3.25)$$

then, since $0 < \alpha < 1$ during the reaction, $df(\alpha)/du \neq 0$ and thus $df(\alpha)/d\alpha = 0$ when $du/d\alpha = 0$
i.e. when

$(1-F\alpha(1 + r)) = 0$ from eq.(3.25)

or when $$F\alpha = \frac{1}{r+1} \qquad (3.26)$$

Recalling that $F\alpha = \beta$ from section 3.4 then from eq.(3.26) the value of $f(\alpha)$ attains a maximum at any temperature at a point where the isothermal conversion is given by $1/(r + 1)$. It will be shown later (section 3.5.2) that the conversion equivalent to $1/(r + 1)$ occurs at the peak of the exotherm. Since r increases with temperature, Fig.(20) then the value of $f(\alpha)$ maximum decreases with increased temperature.

In order to establish the value of $f(\alpha)$ in the practical case at the bifurcation apex, the points in the upper and lower limb of each curve were independently connected by least squares fit lines as shown in Figs.(22) and (23). The x-coordinate of the point of intersection of the upper and lower limbs could thus be determined.

The theoretical value of $f(\alpha)$ in eq.(3.23), with $F\alpha$ as computed from eq.(3.26) where r is given by eq.(3.22) is plotted against temperature in Fig.(24). Also plotted are the x-coordinates of the bifurcation apex at the temperatures shown.

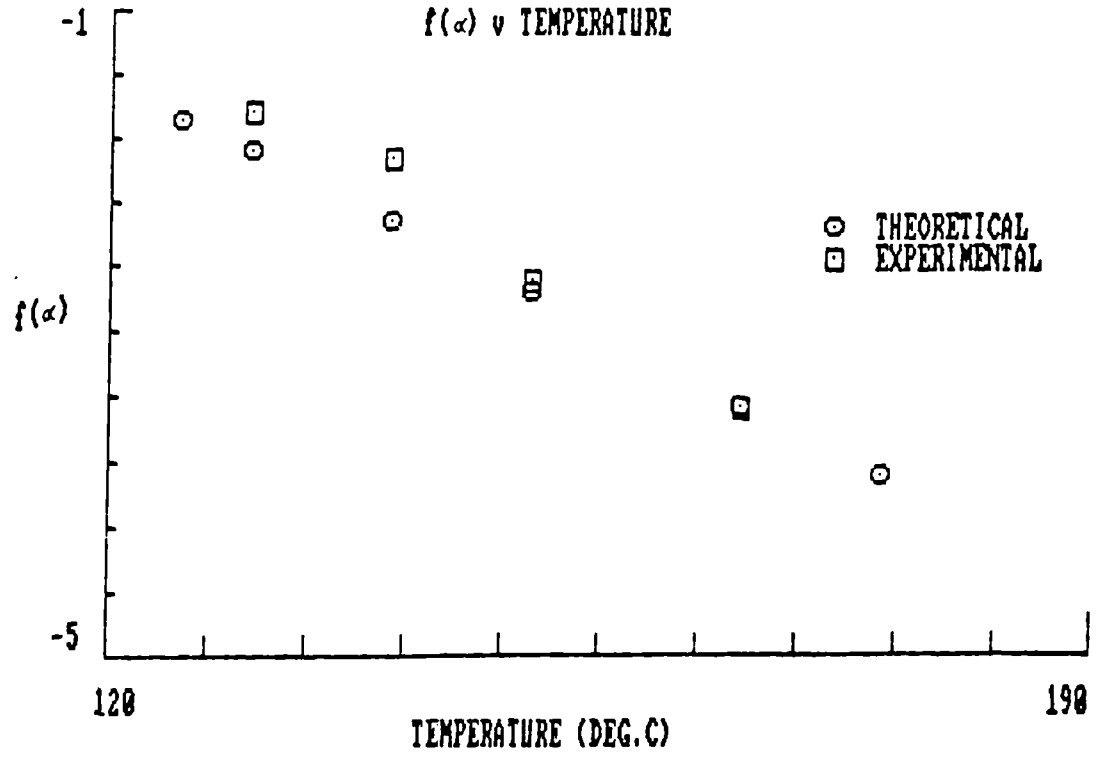

FIG.(24)

There is reasonable agreement between the theoretical and practical values of f(α) in this case and hence the apex of each bifurcation occur at conversions given by eq.(3.26) at the appropriate temperatures.

On recalling eq.(3.21) however which gives a linear dependance of ln(dα/dt) on ln(Fα(1 - Fα)^r then the bifurcation as observed in the above plots of these two variables would not be expected. The fact that these bifurcations occur indicate therefore that the incorporation of the practical values of dα/dt and α respectively in the variables lead to deviations from the expected theoretical behaviour.

The reasons for this deviation from theory is due to a combination of the following factors:-

a) From section 2.3.2.2 the reaction becomes increasingly diffusion controlled the higher the resin conversion. The reaction rate dα/dt would therefore not necessarily follow the same dependance on α at low conversion in a relatively liquid medium compared to the higher conversion in a gelled resin.

b) Also from section 2.3.2.2 the baseline for the isothermal DSC measurements has been assumed to be horizontal. For reasons already stated the evaluation for α and dα/dt may therefore be in error.

c) From section 2.3.1.2 the solubility of DICY in the epoxy resin initially influences the heat output and hence the apparent reaction rate.

For whatever reason however there are apparently two distinct reaction mechanisms occurring in each of the isothermal traces in Figs.(22) and (23). Kinetic parameters were thus determined for each of the apparent reactions corresponding to the upper and lower

limbs of the bifurcated curves in these figures.

The rate constant at each temperature for the reaction occurring during the initial portion of the exotherm up to the peak maximum can be obtained from the slope and the intercept of the straight line fit to the points in the lower limbs of the curves shown in Figs. (22) and (23). From eq.(3.21) the slope of the line is equal to the reaction order n, which will be denoted n(L) for the lower limbs. The intercept is equal to K/F, which will be denoted by K(L)/F for the lower limbs, where K(L) is the isothermal rate constant and F is the numerical ratio of the dynamic to the isothermal heat of reaction at that temperature as already defined in eq.(3.19).

Since k is expressed in terms of the activation energy E and the pre-exponential factor A in eq.(3.10) then an Arrhenius plot of lnk(L) v 1/T°K can be constructed as shown in Fig.(25) with the values tabulated in Table (16a).

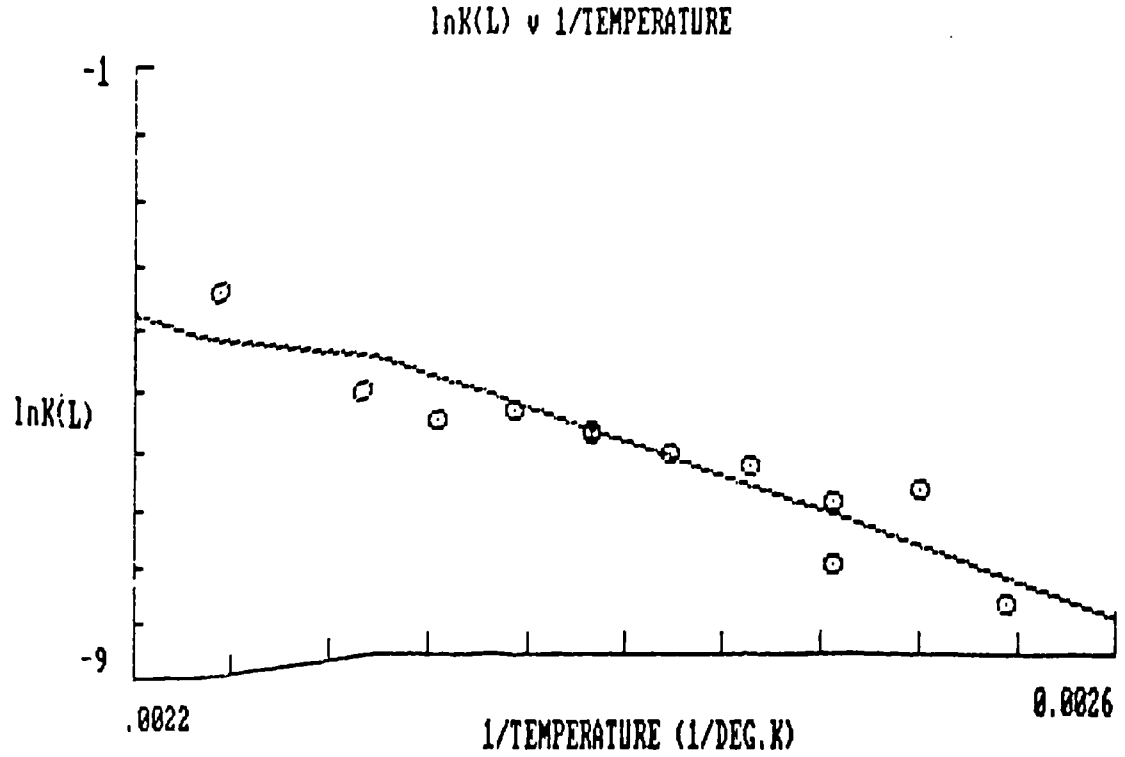

FIG.(25)

The equation of the straight line fit joining the points is given by:-

$$\ln k(L) = (-12989.99)(1/T°K)+(24.58238) \quad (3.27)$$

from which an apparent activation energy E(L) can be obtained as:-

$$E(L) = 25.8 \text{ kcal/mol } (108 \text{kJ/mol}) \quad (3.28)$$

and the constant A(L) given by:-

$$\ln A(L) = 24.58 \text{ sec}^{-1} \quad (3.29)$$

The plot for n(L) against temperature is shown in Fig.(26) and the values tabulated in Table 16(b). The index n(L) therefore decreases linearly with temperature and can be defined by the straight line.

$$n(L) = (-1.515142E-02)T°K + (6.870618) \quad (3.30)$$

Since the ratio of the two indices m to n has been defined in eq.(3.22) then m can be evaluated at any temperature.

A similar analysis for the points in the upper limbs of the curves in Figs.(22) and (23) leads to an Arrhenius equation given by:-

$$\ln k(U) = (-8379.384)(1/T°K)+(13.02864) \quad (3.31)$$

where the plot is shown in Fig.(27) and tabulated in Table 17(a).

A linear variation of n(U) with temperature is also obtained as

$$n(U) = (-6.571918E-03)T°K + (2.994045) \quad (3.32)$$

which is shown plotted in Fig.(28) and tabulated in Table 17(b).

In eqs.(3.31) and (3.32) k(U) and n(U) refer respectively to the rate constant and reaction order for the latter portion of the exotherm peak beyond the peak maximum.

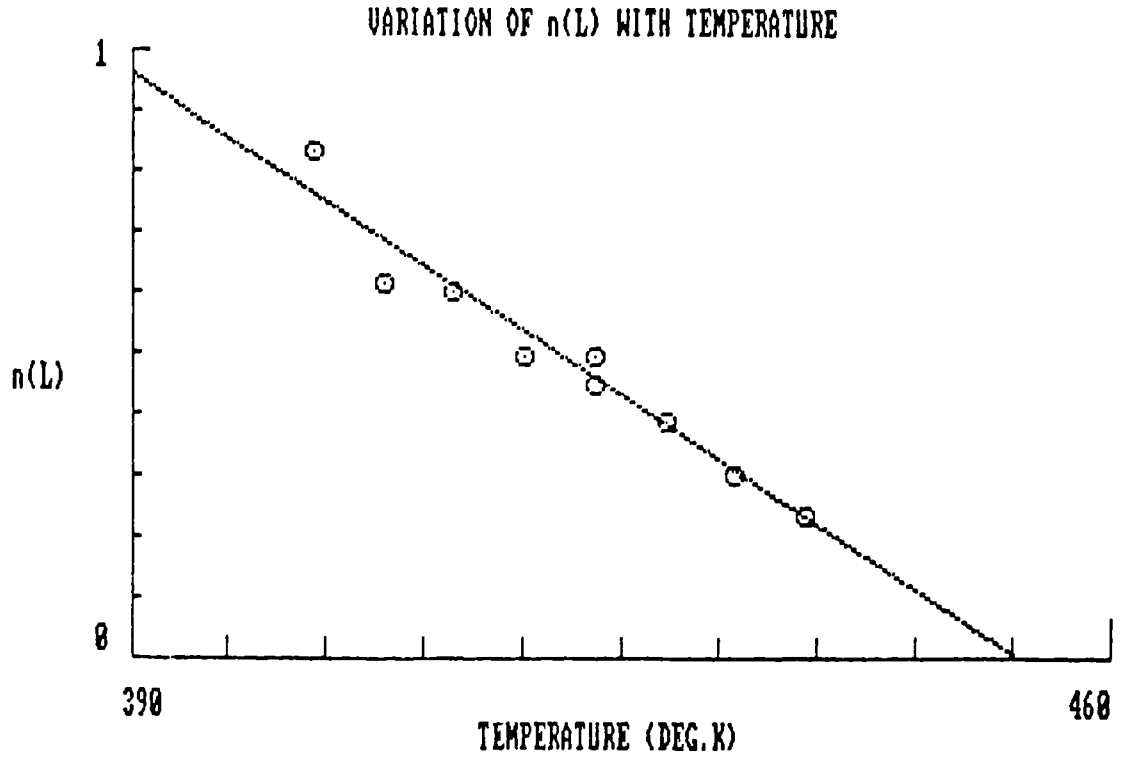
VARIATION OF n(L) WITH TEMPERATURE
1
n(L)
0
390
460
TEMPERATURE (DEG.K)

FIG.(26)

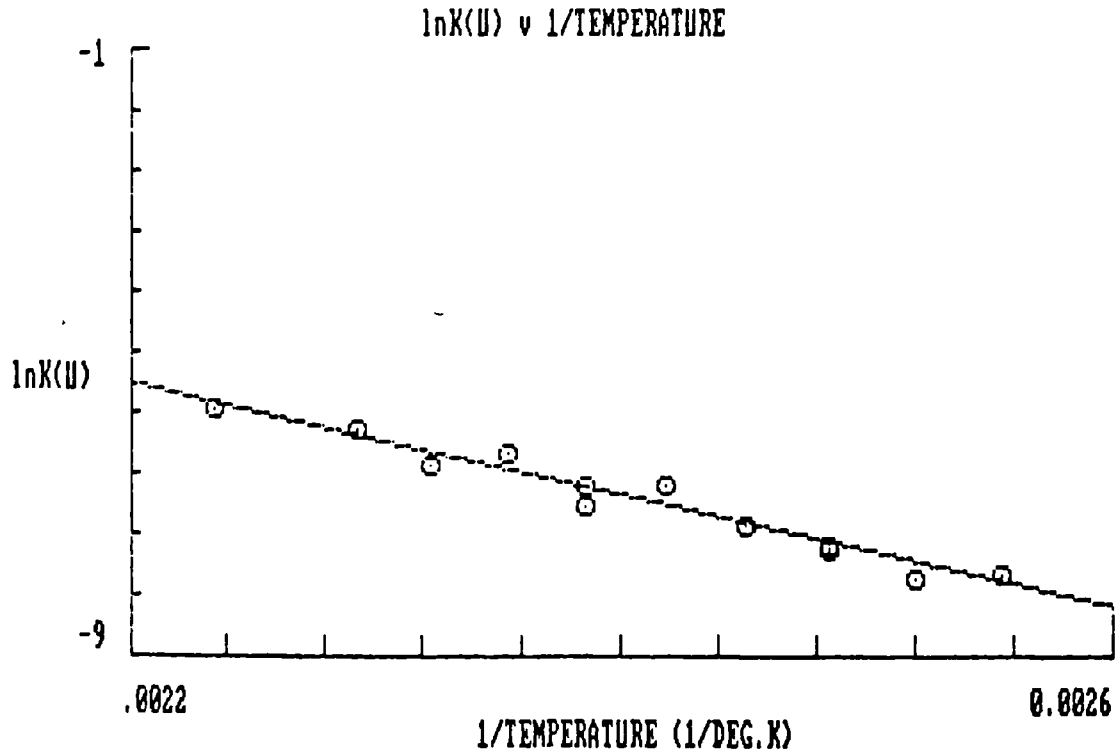
lnK(U) v 1/TEMPERATURE
-1
lnK(U)
-9
.0022
0.0026
1/TEMPERATURE (1/DEG.K)

FIG.(27)

The slope corresponds to an apparent activation energy E(U) of

$$E(U) = 16.65 \text{ kcal/mole (70kJ/mole)} \qquad (3.33)$$

and the constant.

$$\ln A(U) = 13.03 \text{ sec}^{-1}$$

Similarly the index m(U) can be obtained at any temperature and, specifically the variation of m and n for the case of the upper limbs reaction is shown in Fig.

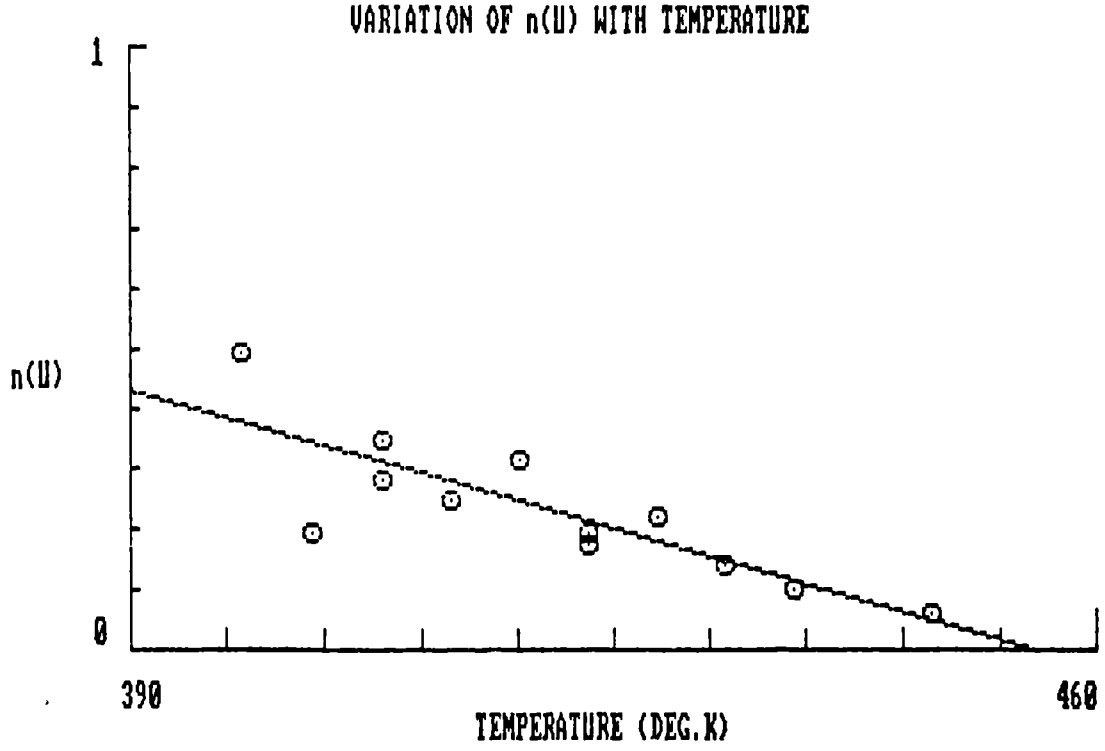

FIG.(28)

(29). It is noted that m behaves in a reasonably linear manner over most of the temperature range of interest but decreases rapidly at temperatures above approximately 165°C.

From the above it is clear that there is a significant difference in the kinetic parameters so evaluated between the initial and final stages of the

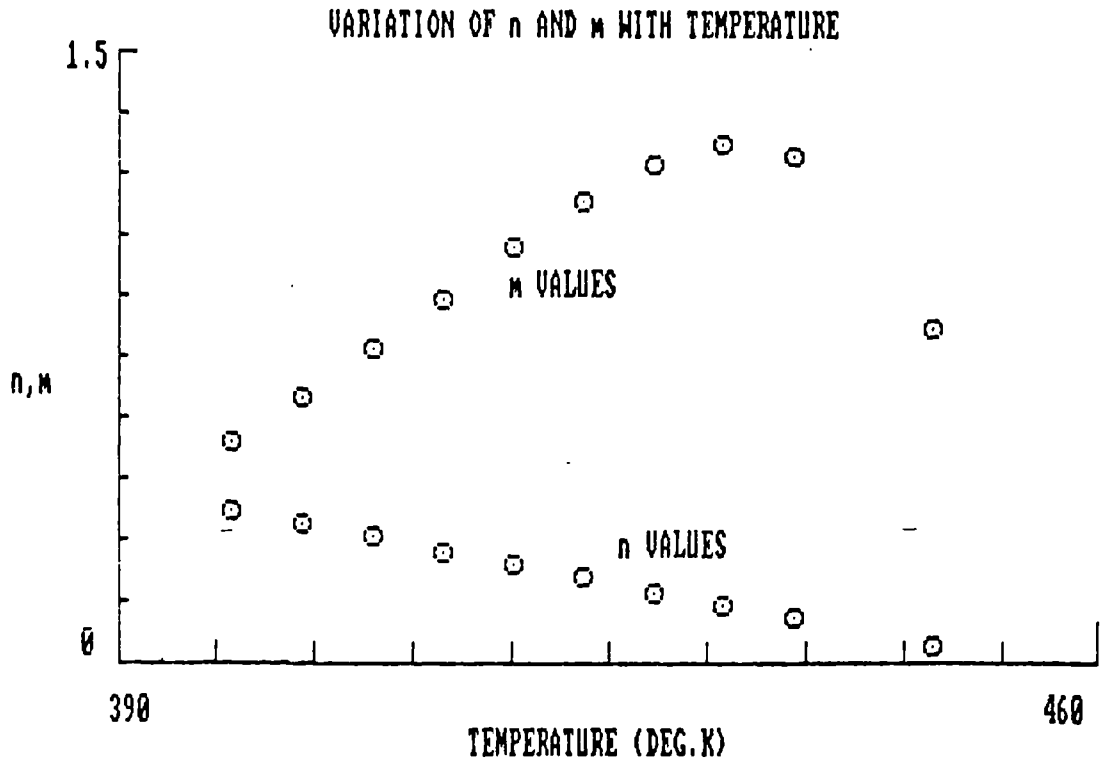

FIG.(29)

cure reaction. A single point method of evaluation was therefore used to independently check these values as follows.

3.5.2. Method B

The evaluation of m, n and k by Method A necessitates the time consuming operation of measuring the incremental areas under the exotherm so that $d\alpha/dt$ can be calculated at successive time intervals during the course of the reaction. The single point method overcomes this difficulty as follows:-

Consider again the expression for the rate of reaction in the form

$$d\alpha/dt = (k/F)(F\alpha(1 - F\alpha)^{r})^{n} \qquad (3.34)$$

with symbols as already defined in previous sections.

On differentiating eq.(3.34) with respect to time

$$d^2\alpha/dt^2 = (k/F)[n(F\alpha(1-F\alpha)^{r})^{n-1}((1-F\alpha)^{r}-rF\alpha(1-F\alpha)^{r-1})] \qquad (3.35)$$

At the exotherm peak maximum then

$$d^2\alpha/dt^2 = 0,\ \alpha = \alpha_p \text{ and } d\alpha/dt = d\alpha_p/dt$$

Thus $d^2\alpha/dt^2 = 0$ when R.H.S. of eq.(3.35) is zero

i.e when $((1-F\alpha_p)^r)-rF\alpha_p(1 - F\alpha_p)^{r-1}) = 0$

or when $r = (1-F\alpha_p)/F\alpha_p$ (3.36)

or alternativly when:

$$F\alpha_p = 1/(r + 1) \quad (3.37)$$

It is noted that eqs.(3.37) and (3.26) are identical hence confirming the fact that the bifurcation in the plots in Method A occur at the exotherm peak maximum.

If we now substitute for $F\alpha_p$ in eq.(3.34) from eq.(3.37) at peak maximum we obtain

$$d\alpha_p/dt = (k/F)((1/(r+1)).(r/(r+1))^r)^n$$

$$= kr^{rn}/F(r+1)^{rn} \quad (3.38)$$

or alternatively

$$k = (F.(d\alpha_p/dt)(r + 1)^{rn})/r^{rn} \quad (3.39)$$

Since $d\alpha_p/dt$ and r are obtained from the experimental data for the peak maximum and F is known from the total peak area then the isothermal rate constant k can be determined if n is evaluated as follows.

By integration of eq.(3.34) the time t_p from the start of the reaction to the peak maximum can be obtained since

$$F/k\int_o^{\alpha_p} d\alpha/(F\alpha(1-F\alpha)^r)^n = \int_o^{t_p} dt = t_p \quad (3.40)$$

Substituting for k in eq.(3.40) from eq.(3.39)

$$\frac{r^{rn}}{(d\alpha_p/dt)(r+1)^{rn}} \int_0^{\alpha_p} d\alpha/(F\alpha(1-F\alpha)^r)^n = t_p \qquad (3.41)$$

Since t_p can be obtained from experimental data then eq.(3.41) can be numerically solved by trial substitution for n. In the current work the integral was solved numerically by Simpson's method and the L.H.S. of eq.(3.41) was evaluated to the fourth decimal place.

Since the value of n can thus be determined then the isothermal rate constant k can be evaluated by the substitution for n in eq.(3.39) following which m can be directly evaluated from the ratio r.

The integral in eq.(3.41) is however applicable to any portion of the cure exotherm. For instance t_m is the experimentally observed time at the end of the isothermal reaction then since the fractional isothermal conversion is unity or $\alpha_m = 1/F$ where α_m is the maximum conversion relative to the dynamic exotherm then

$$\frac{r^{rn}}{(d\alpha_p/dt)(r+1)^{rn}} \int_{\alpha_p}^{1/F} d\alpha/(F\alpha(1 - F\alpha)^r)^n = (t_m - t_p) \qquad (3.42)$$

or similarly for the whole isothermal exotherm.

$$\frac{r^{rn}}{(d\alpha_p/dt)(r+1)^{rn}} \int_0^{1/F} d\alpha/(F\alpha(1 - F\alpha)^r)^n = t_m \qquad (3.43)$$

In order for the integrals in eqs.(3.42) and (3.43) to remain determinate it is necessary for $F\alpha < 1$ and so in the current work the final conversion at the time t_m was assumed to be $((1/F) - 0.001)$. Due to this limitation the derivation of the kinetic parameters by eqs. (3.42) and (3.43) are not as precise as by the use of eq.(3.41) but nevertheless the parameters can be estimated to any desired degree of accuracy.

Thus the indices m and n and the rate constant k can be determined relatively quickly by the use of the characteristic properties of the peak maximum values only. In order to obtain the activation energy of the reaction then an Arrhenius plot of lnk versus reciprocal absolute temperature can be obtained by repeat of the above procedure at a number of temperatures.

The Arrhenius plot for the rate constants k(D) determined by eq.(3.41) i.e. integrating from zero conversion at the start of the reaction to the conversion at the peak maximum is shown in Fig.(30) with the values tabulated in Table 18(a). The equation of the straight - line fit in Fig.(30) is given by

$$\ln k(D) = (-9109.057)(1/T°K)+(14.27517) \quad (3.44)$$

giving the activation energy of

$$E(D) = 18.1 \text{ kcal/mole } (75.7 \text{kJ/mole}) \quad (3.45)$$

and the constant

$$\ln A(D) = 14.28 \text{ sec}^{-1} \quad (3.46)$$

From the Table 19(b) and the plot of n(D) versus temperature in Fig.(31) the linear variation of n(D) with temperature is obtained and given by

$$n(D) = (-2.732677 \times 10^{-3})(T°K)+(1.267957) \quad (3.47)$$

Similarly by the use of eq.(3.42) on the area of the exotherm between the peak maximum and the end of the reaction both k(LP) and n(LP) can be obtained where the subscript (LP) refers to the values calculated by means of this integral. The values of lnk(LP) and n(LP) are tabulated in Tables 19(a) and 19(b) respectively and plotted in Figs.(32) and (33).

The respective equations for lnk(LP) and n(LP) are

$$\ln k(LP) = (-9242.84)(1/T°K)+(14.61344) \quad (3.48)$$

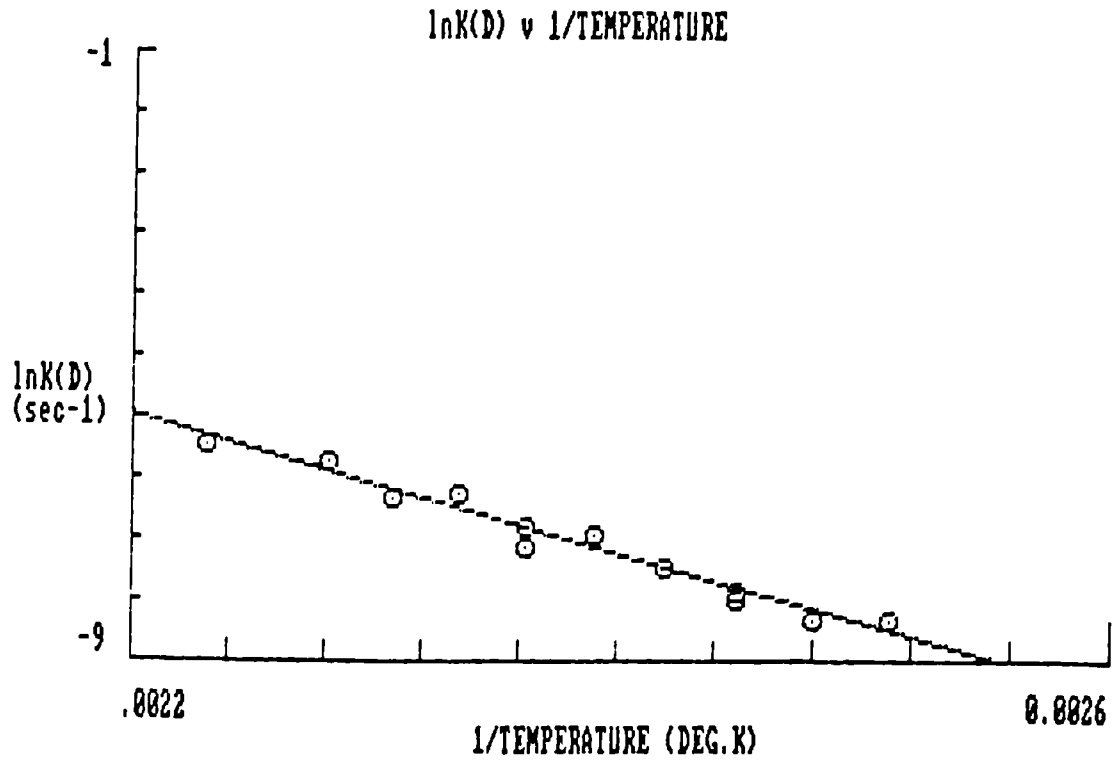
lnK(D) v 1/TEMPERATURE
-1
lnK(D)
(sec-1)
-9
.0022
0.0026
1/TEMPERATURE (DEG.K)

FIG.(30)

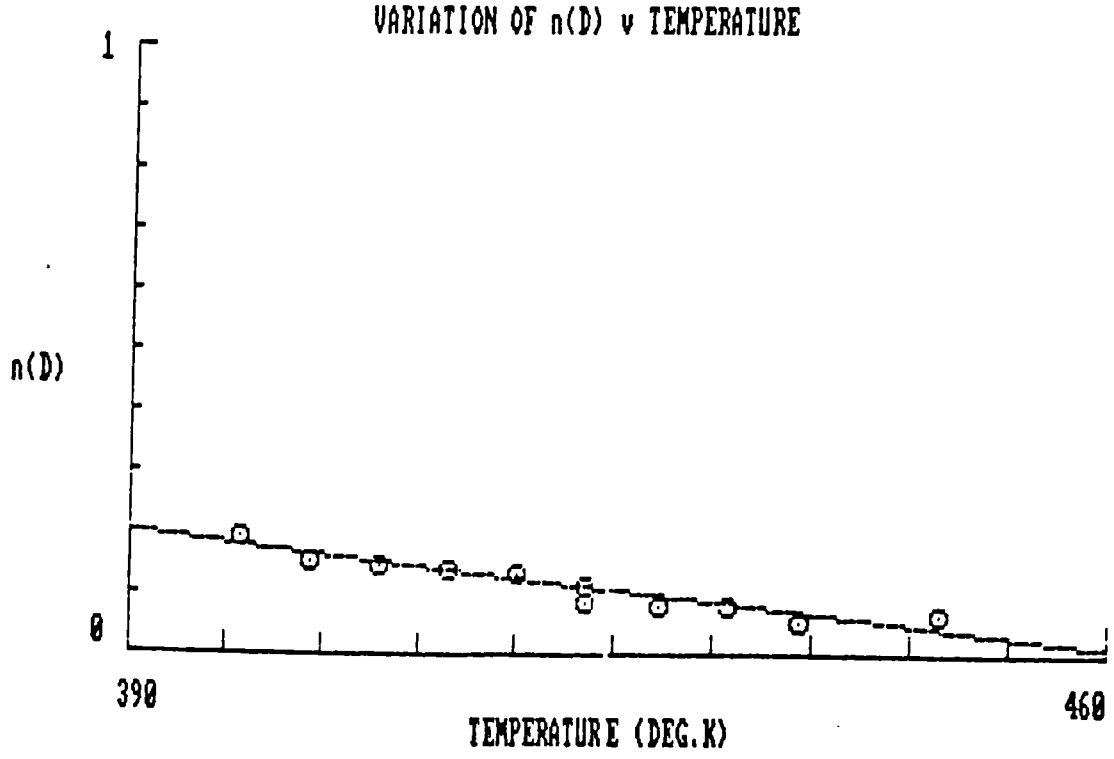
VARIATION OF n(D) v TEMPERATURE
1
n(D)
0
390
460
TEMPERATURE (DEG.K)

FIG.(31)

and

$$n(LP) = (-4.422515 \times 10^{-3})(T°K)+(1.984559) \quad (3.49)$$

giving an activation energy of

$$E(LP) = 18.37kcal/mole\ (76.8kJ/mole) \quad (3.50)$$

and the constant

$$\ln(A(LP) = 14.61sec^{-1} \quad (3.51)$$

Finally by the application of eq.(3.43) for the complete exotherm then, if the subscript (WH) refers to the values so calculated, then from the tabulated values in Tables 20(a) and 20(b) and the plots of Figs.(34) and (35) the Arrhenius equation can be obtained as

$$\ln k(WH) = (-8782.488)(1/T°K)+(13.57461) \quad (3.52)$$

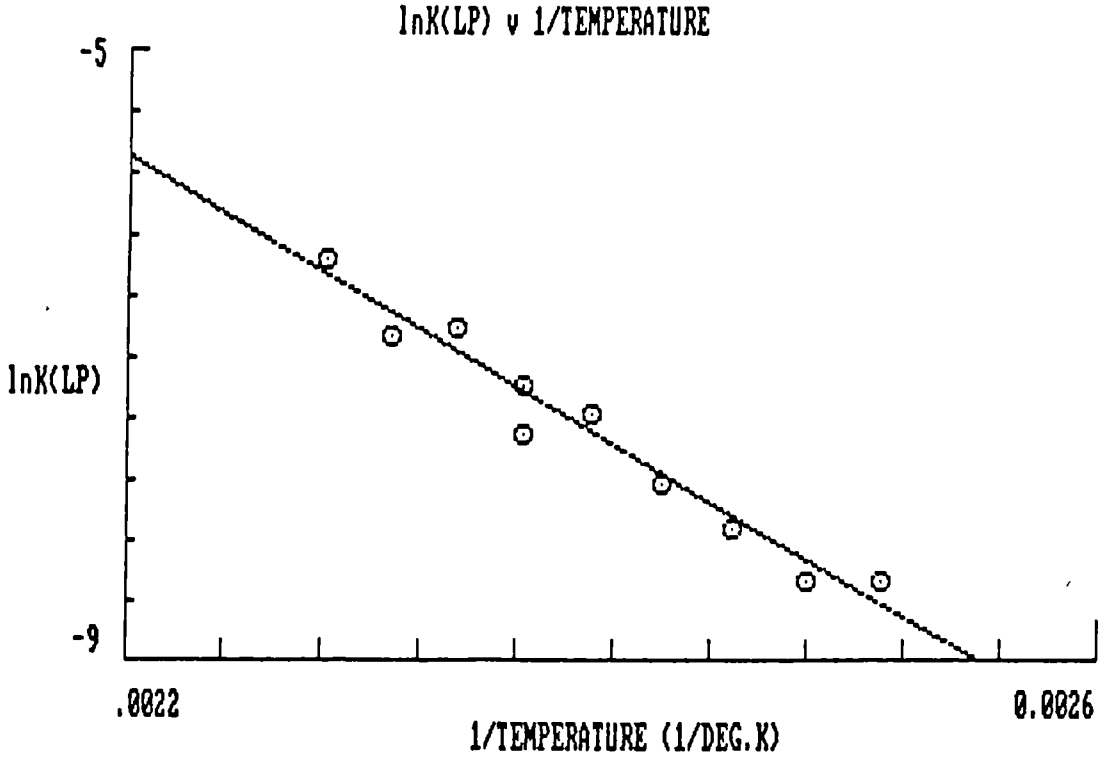

FIG.(32)

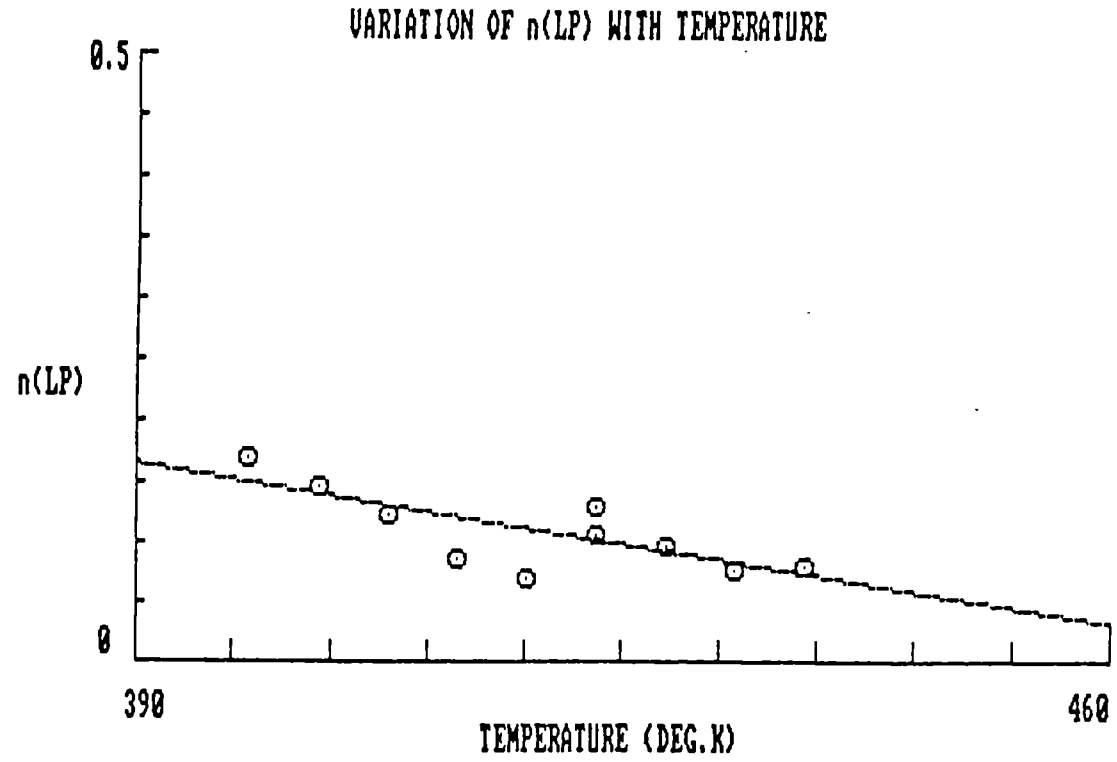
VARIATION OF n(LP) WITH TEMPERATURE
0.5
n(LP)
0
390
460
TEMPERATURE (DEG.K)

FIG.(33)

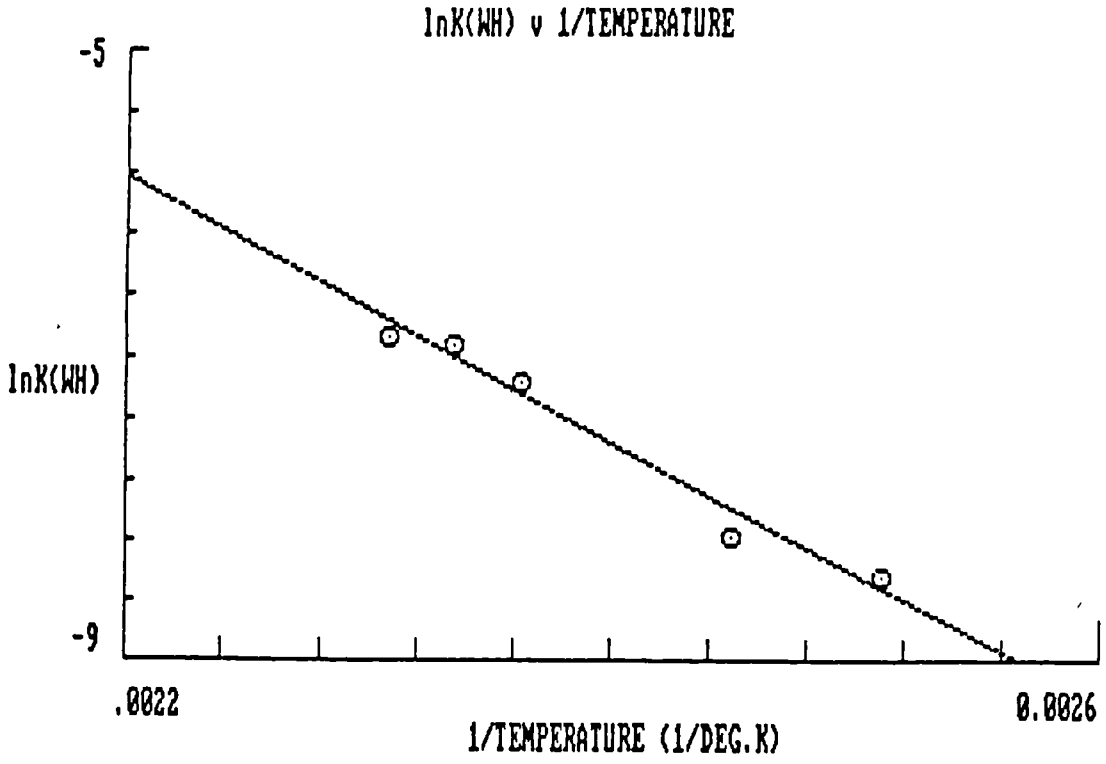
lnK(WH) v 1/TEMPERATURE
-5
lnK(WH)
-9
.0022
0.0026
1/TEMPERATURE (1/DEG.K)

FIG.(34)

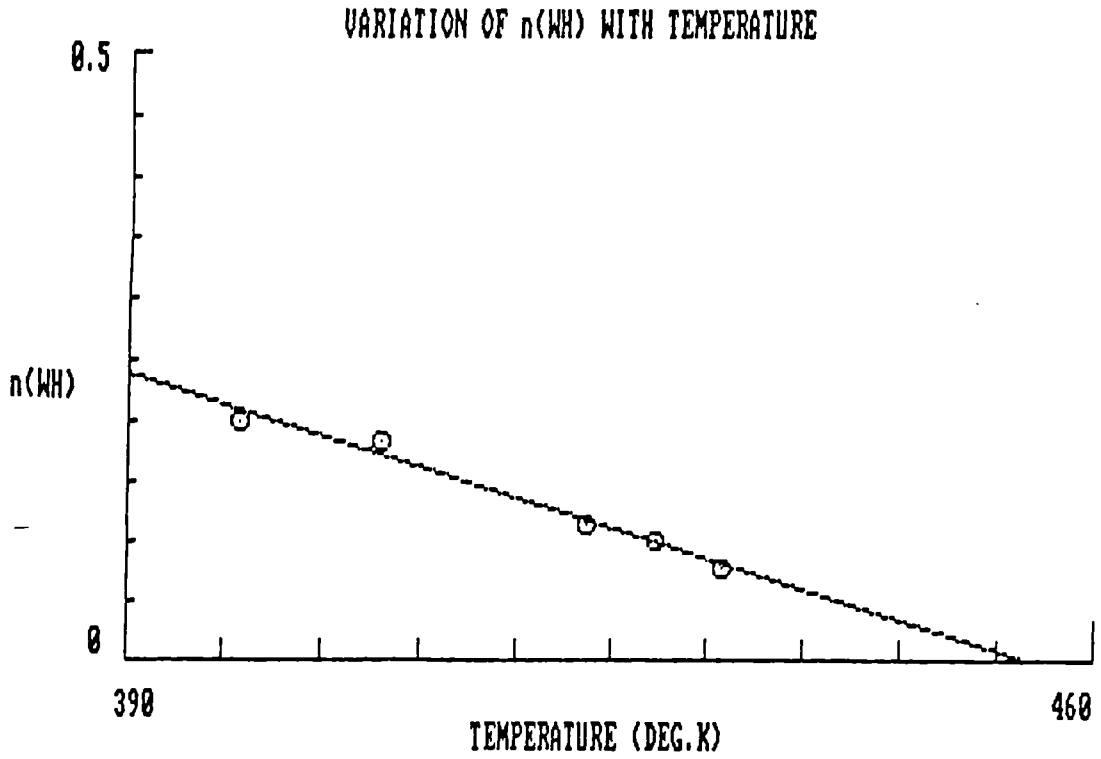

FIG.(35)

and the linear equation

$$n(WH) = (-4.82504 \times 10^{-3})(T°K)+(2.176593) \quad (3.53)$$

Thus in this case the activation energy is

$$E(WH) = 17.45 \text{ kcal/mole } (73\text{kJ/mole}) \quad (3.54)$$

and the constant

$$\ln A(WH) = 13.57\text{sec}^{-1} \quad (3.55)$$

3.6 Summary Of Kinetic Parameters evaluation

So far a number of values for the rate constant and the index n have been obtained by different techniques and it is of interest at this stage therefore to summarise and compare these different values.

The values of the apparent activation energy E, and the pre-exponential factor, A together with their method of determination and relevant equations in the text are shown in Table (21). The values of the slope and intercept of the line givng the dependence of the

reaction order n on temperature is also included in each case where applicable.

From Table (21) it will be observed that there is good agreement between the values E, A and n parameters as calculated by the single point evaluation in Method B to those as calculated by Method A for the (U) series values.

It is to be noted however that the parameter values calculated by Method A for the (L) series values are significantly different. This difference is due to the critical portion of the exotherm profile being complicated for reasons of DICY solubility and superimposed heats of reaction as described in the text.

It is to be noted also that the activation energies obtained from the dynamic exotherms are higher than those as derived by the isothermal methods as described above but the dynamic methods nevertheless give a useful initial guide to the value of the activation energy to be expected of autocatalytic reactions of this kind.

For the current model the values of the A, E and n parameters as generated from the (U) series of calculations were chosen to represent the course of the reaction. This model will be verified in the following Chapter and its use in cure prediction under isothermal conditions will be described.

CHAPTER 4

MODEL VERIFICATION AND CURE PREDICTION

4.1 Methods Of Isothermal Cure Prediction

In this Chapter the cure or conversion of the resin will be considered and techniques will be described to show how the degree of cure at any time may be predicted under isothermal conditions.

Cure prediction by the use of a master cure curve will first be described. In practice this method gives a relatively quick and useful guide to the extent of cure to be expected for a resin that has been heated for a known time at any isothermal temperature (see also ref.14).

In the latter part of the Chapter the kinetics model as described in Chapter 2 and 3 will be verified and the use of this model for cure prediction will be assessed.

4.2 Master cure curve

A typical, experimentally determined isothermal cure curve for BSL 914 resin at 135°C is shown in Fig.(36). The cure in this case is defined relative to the isothermal exotherm giving the conversion ß as described in section 3.3. It is observed that the cure curve is S-shaped with cure accelerating with respect to time in the initial stages of the reaction but subsequently decelerating with time at more advanced cure due to the reaction being increasingly diffusion controlled. This S-shape is characteristic of the cure curves at all isothermal temperatures as is evident in Fig.(37) where the fractional isothermal cure at the temperatures indicated are plotted against ln(time).

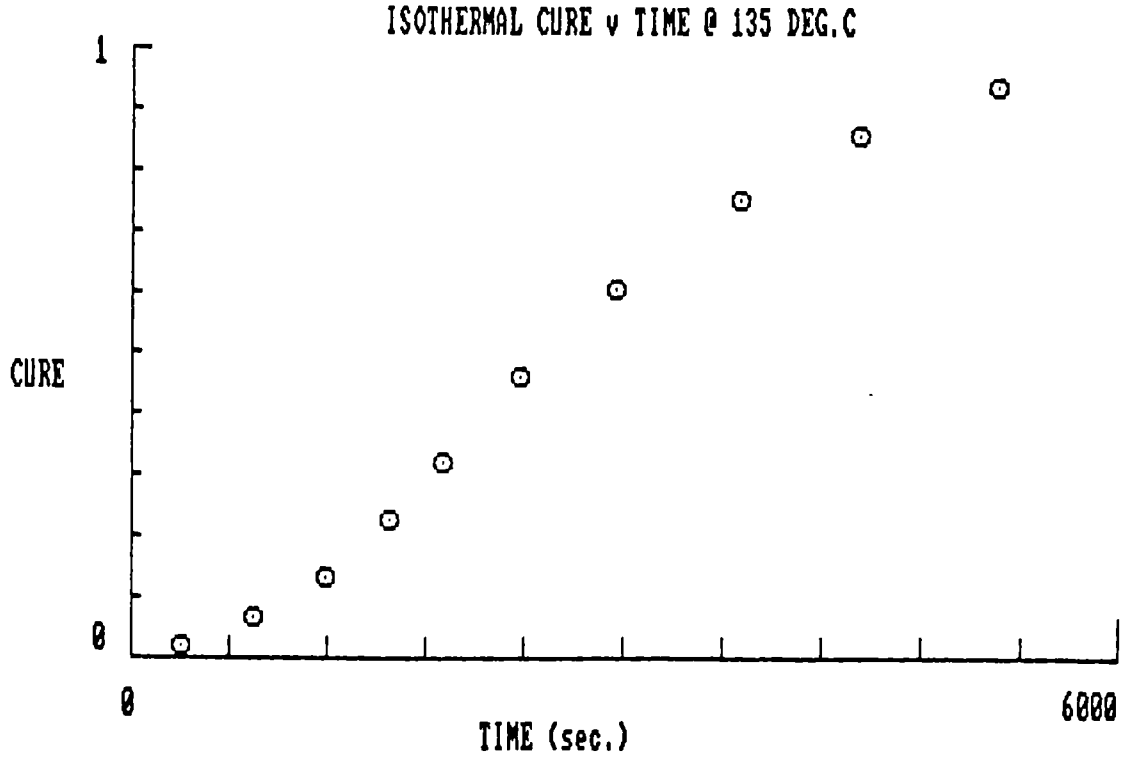
ISOTHERMAL CURE v TIME @ 135 DEG.C
1
CURE
0
0
6000
TIME (sec.)

FIG.(36)

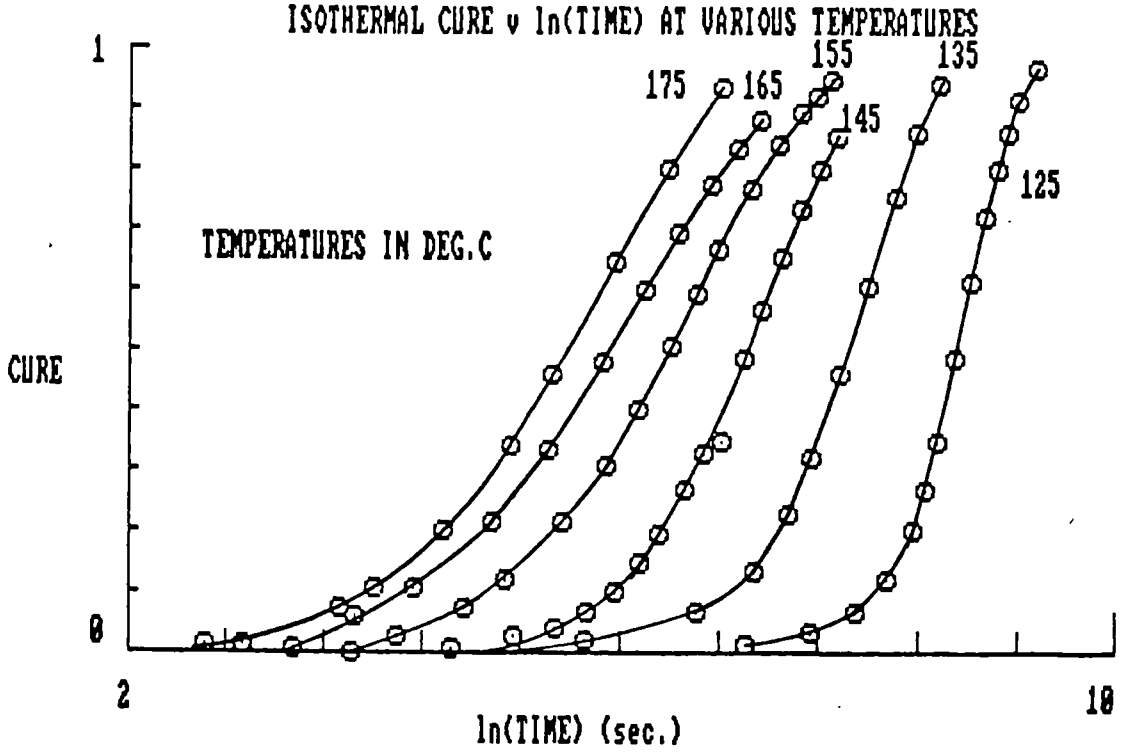
ISOTHERMAL CURE v ln(TIME) AT VARIOUS TEMPERATURES
1
CURE
0
2
10
ln(TIME) (sec.)
TEMPERATURES IN DEG.C
175
165
155
145
135
125

FIG.(37)

All the curves are nearly identical in profile in Fig.(37) the only difference being in their location on the ln(time) axis and where the curve position is clearly dependent on temperature.

Thus if any one of the above curves is arbitrarily chosen then the shift in ln(time) of all the curves relative to the chosen curve can be evaluated. Therefore by constructing the cure curve at one temperature the cure at any other temperature can be obtained. This evaluation of ln(shift) is the basis of a prediction method for cure by the use of a master cure curve the generation and use of which will be described as follows:-

Consider the isothermal cure curve at 145°C(418.2°K) in Fig.(37) where the logarithm of the time t for the resin to attain a fractional isothermal conversion ß can be denoted by

$$\ln t(ß,418.2)$$

Similarly at any other absolute temperature, T, the time for the same isothermal conversion ß to be attained is given by.

$$\ln t(ß,T)$$

At conversion ß therefore the time shift factor, relative to the 418.2°K times, can be denoted by $\Delta \ln t_{(ß=ß)}$ and is given simply as

$$\ln(SHIFT) = \Delta \ln t_{(ß=ß)} = \ln t(ß,T) - \ln t(ß,418.2) \quad (4.1)$$

for any temperature T.

By choosing an arbitrary value of conversion ß equal to 0.3 then $\Delta \ln t_{(ß=0.3)}$ can be obtained from the curves in Fig.(37) for the six discrete temperatures plotted. From these values of ln(SHIFT) an Arrhenius plot of ln(SHIFT) versus reciprocal absolute temperature can be obtained as shown in Fig.(38) from the tabulated values in Table 22.

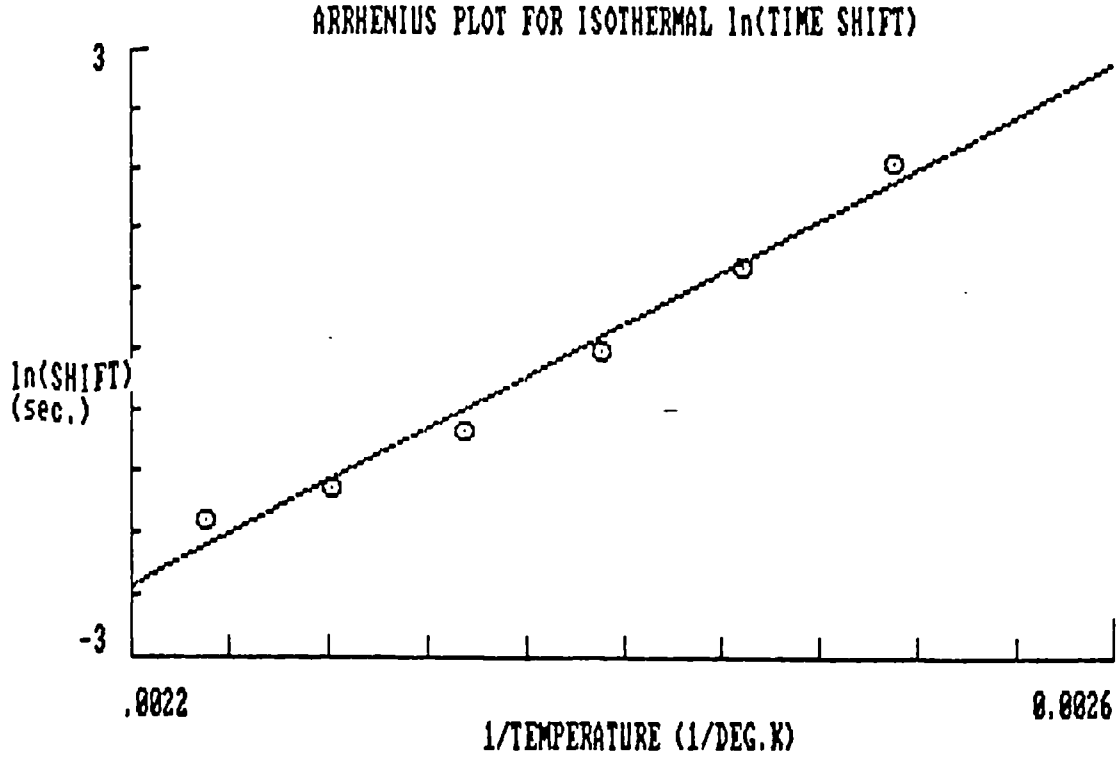

FIG.(38)

The equation joining these points is given by

$$\Delta \ln t_{(\beta=0.3)} = (12909.27)(1/T°K)-(30.72263) \qquad (4.2)$$

The validity of eq.(4.2) can be ascertained by the addition of the time shift so evaluated by eq.(4.2) to the experimental time values shown in Fig.(37) in which case every value of corrected time would be expected to lie on the cure curve at 145°C which is therefore the master curve.

The master curve so constructed is shown in Fig.(39) and, although ideal superposition of the curves is not obtained, it can be inferred that eq.(4.2) is a reasonable representation for the time shift at any temperature in the range of 125°C to 175°C.

To illustrate the application of the master curve and eq.(4.2) for cure prediction consider that an estimate of the time for the resin to attain an

isothermal conversion of 0.5 at 135°C is required.

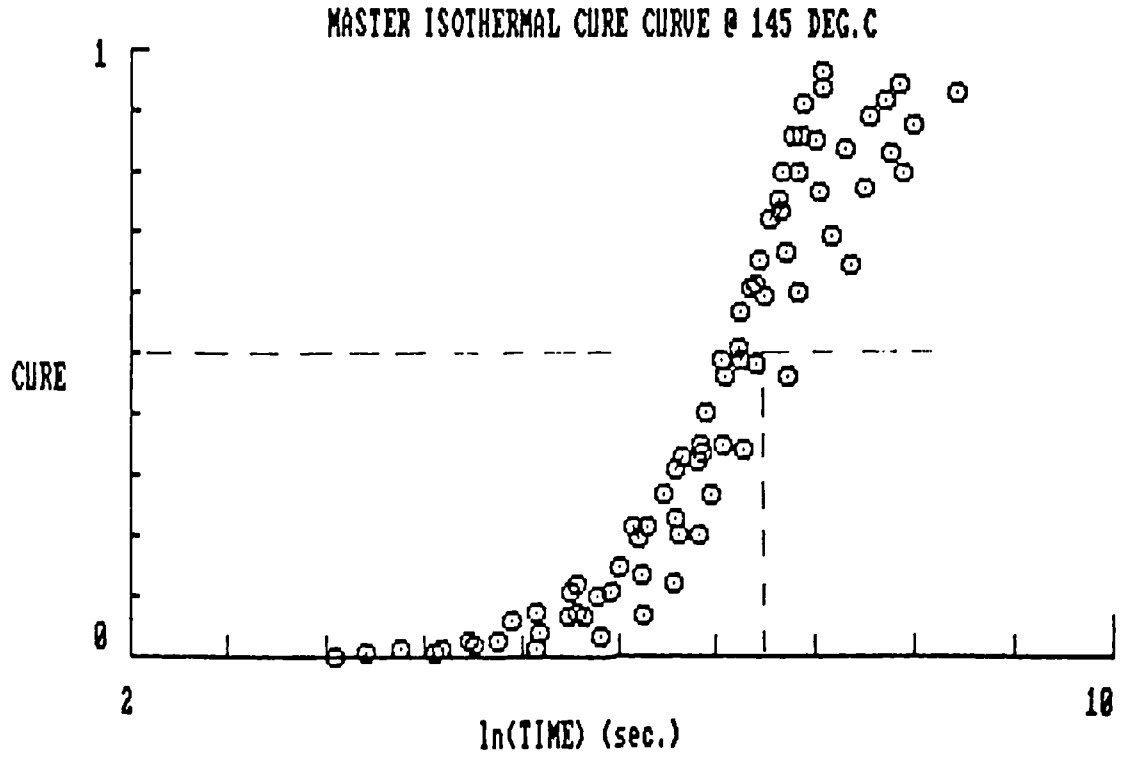

FIG.(39)

The first step is to note the value of ln(time) at which 0.5 conversion is reached from the master curve shown in Fig.(38). From the figure

$$\ln t(0.5,145) = 7.2$$

From eq.(4.2)

$$\Delta \ln t_{(B=0.5)} = 0.9022$$

From eq.(4.1)

$$\ln t(0.5,135) = \ln t(0.5,145) + \Delta \ln t_{(B=0.5)}$$

$$= 7.2 + 0.9027$$

$$= 8.1022$$

$$t = 3302 \text{ sec}$$

where t is the predicted time to achieve 0.5 conversion at 135°C.

On inspection of the experimental curve at this temperature in Fig.(36) the actual time to attain 0.5 conversion is seen to be of the same order of magnitude as that predicted.

The predicted and actual times however are not exactly equal since the accuracy of the predictive method is limited due to the fact that eq.(4.2) has been applied over such a large temperature range viz 125°C to 175°C. Nevertheless reasonable estimates of the time to attain desired cures at any temperature within the above range can be obtained.

For the same reasons exact superposition of the points in the master curve at 0.3 conversion is not achieved with the result that the ln(time) values at 0.3 conversion are scattered about the mean 145°C values.

It is also observed that the scatter of the points is greater the higher the conversion and this is due to the increased diffusion control at higher conversion. The formula for the shift factor would therefore be different from eq.(4.2) if calculated at a higher level of conversion than 0.3. For instance by choosing a conversion of 0.8 an analogous equation to eq.(4.2) is obtained and given by

$$\Delta \ln t_{(\beta=0.8)} = (9229.322)(1/T°K)-(21.90453) \qquad (4.3)$$

where the shift is again relative to the cure curve at 145°C.

Similarly at the commencement of the reaction the conversion would be influenced by hardener solubility effects and by choosing a conversion of 0.05 an equation for the shift factor of the following form is obtained

$$\Delta \ln t_{(\beta=0.05)} = (15901.88)(1/T°K)-(37.98324) \qquad (4.4)$$

The fact that different equations apply at different levels of conversion is also clear by observation of the curves in Fig.(37). The curves at the different temperatures are not perfectly "parallel" i.e. they tend to converge with increased conversion. Thus

the time shifts are less at higher conversion levels compared to those at the lower conversion values.

Following similar procedures as above a master cure curve can be generated but with the conversion defined relative to the total reaction exotherm i.e. conversion α as defined in section 3.4.

The curves of cure against ln(time) in this case are shown in Fig.(40). The tabulated values of ln(time shifts) with reciprocal absolute temperatures are included in Table 23. The resultant Arrhenius plot is shown in Fig.(41) from which the following equation is obtained for the time shift dependence on temperature evaluated for a conversion $\alpha = 0.3$.

$$\Delta \ln t_{(\alpha=0.3)} = (13853.98)(1/T°K)-(33.02942) \quad (4.5)$$

The master cure curve in this case is shown in Fig.(42).

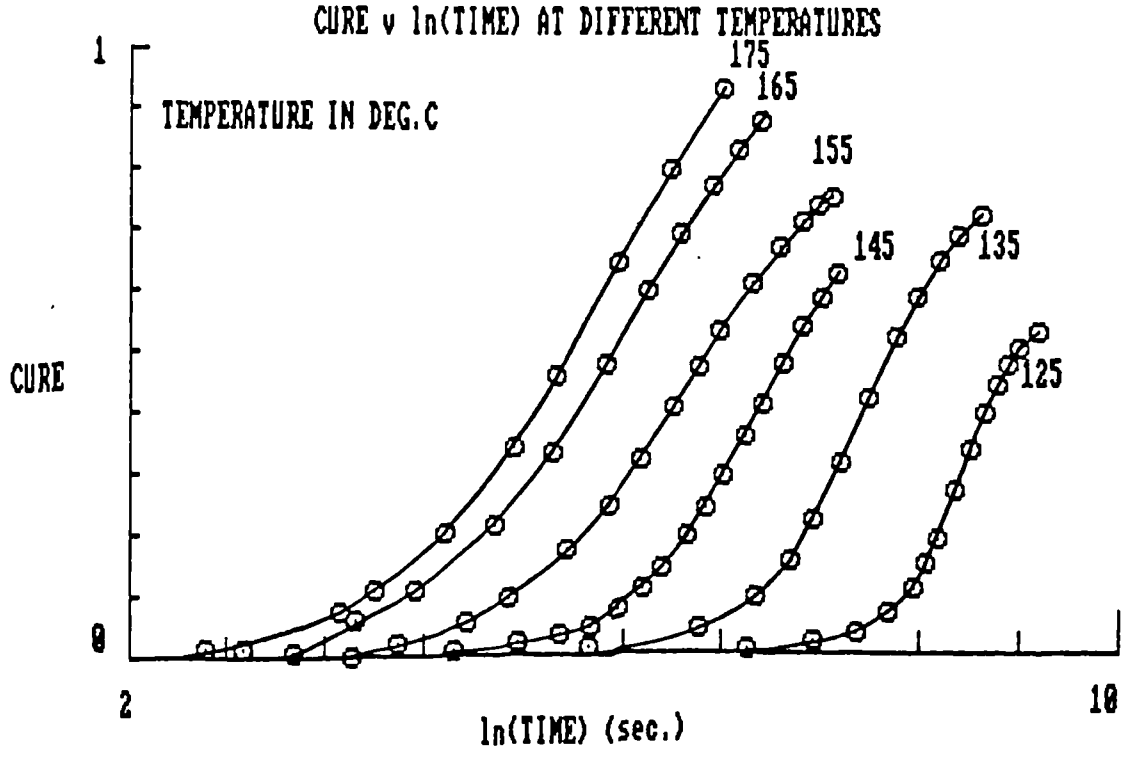

FIG.(40)

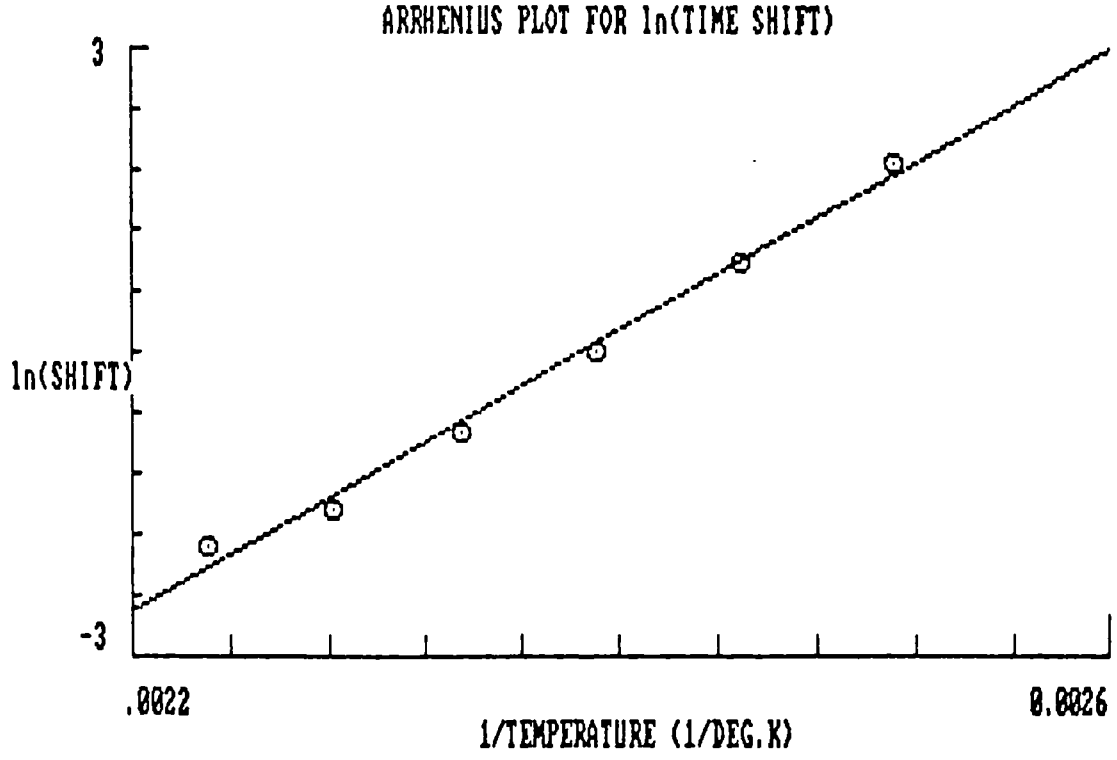
ARRHENIUS PLOT FOR ln(TIME SHIFT)
3
ln(SHIFT)
-3
.0022
0.0026
1/TEMPERATURE (1/DEG.K)

FIG.(41)

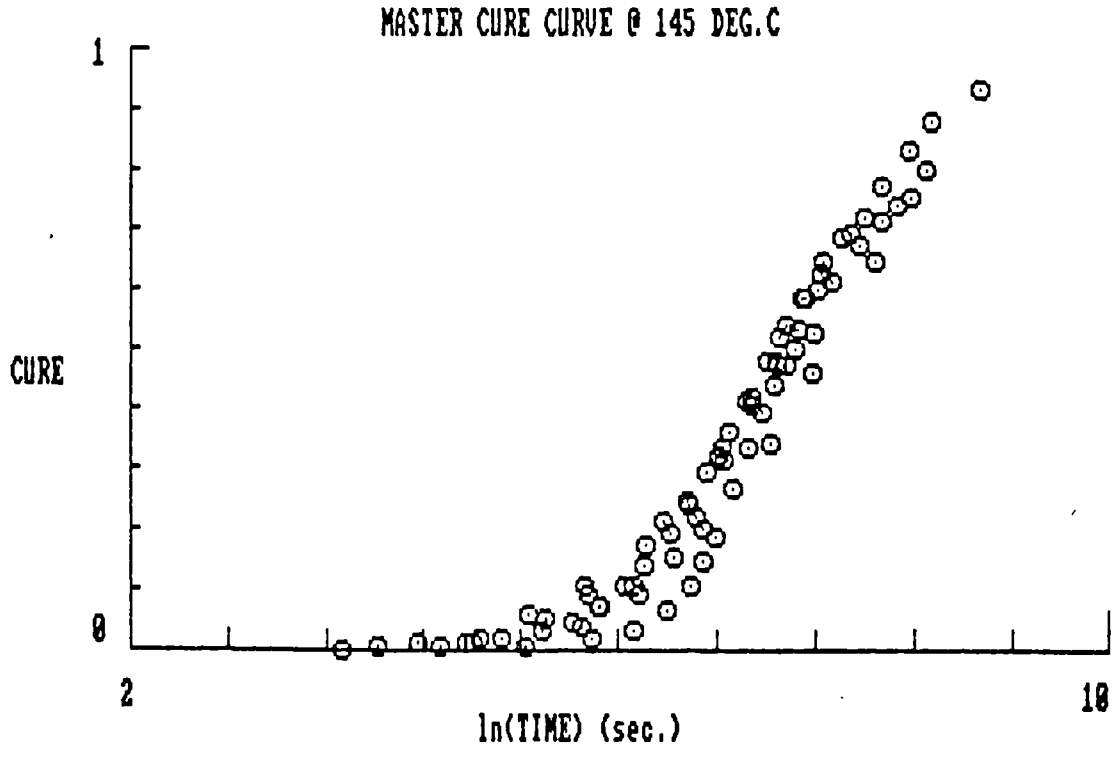
MASTER CURE CURVE @ 145 DEG.C
1
CURE
0
2
10
ln(TIME) (sec.)

FIG.(42)

4.3 Activation energy from cure curves

Since eqs.(4.2), (4.3) and (4.4) define the time shifts for constant but different levels of conversion at any tempeature then the activation energies for iso-conversion can be evaluated.

Consider eq.(4.3) which relates the time shift to temperature at an isothermal conversion of 0.8 then the activation energy obtained from the slope is given by

$$E_{\beta=0.8} = 18.3\text{kcal/mole (76.7kJ/mole)}$$

It is interesting to note that this activation energy is close to the values as calculated by methods A and B in Chapter 2 at similar conversion levels. In Table 21 for instance the activation energy calculated for the upper limb plots of Method A, which relate to conversion beyond the exotherm peak, is 70kJ/mole. Also the (LP) series values of Method B give an activation energy of 77kJ/mole and this value is an average for the reaction occurring at conversion between the exotherm peak maximum and the end of the reaction and hence includes 0.8 conversion.

Similarly the activation energy calculated from eq.(4.2) for a conversion of 0.3 is

$$E_{\beta = 0.3} = 25.7 \text{ kcal/mole (107.3 kJ/mole)}$$

This activation energy is similar to that calculated for the upper limb plots in Method A as shown in Table 21 where the activation energy is 108 kJ/mole. The upper limb values in Method A correspond to the average values at the low conversion levels i.e. up to approx 0.3 conversion.

This trend of increasing activation energy with decreased conversion is maintained to even lower conversion since the activation energy at 0.05 conversion from eq.(4.4) is given by.

$$E_{\beta = 0.05} = 31.6 \text{ kcal/mole (132.2 kJ/mole)}$$

This value of the activation energy at the commencement of the reaction is high but this value has been confirmed by an independent method using infra-red spectroscopy as follows.

4.3.1 FTIR Study

In this study the activation energy for the rate of combination of DICY hardener and the epoxy resin was estimated at low conversion levels during the initial stages of the cure reaction by a chemical analysis technique. This method of cure analysis is therefore not dependent on the analysis of exotherms as so far described.

The basis of the chemical analysis method depends on the fact that DICY becomes more soluble in certain solvents, in this case methylene chloride, as soon as it commences to react with the epoxy resin.

The experimental procedures can be briefly described as follows (refs.17, 46).

1.5g of the as received resin film containing the dispersed DICY hardener particles was placed in a test tube containing 20cc methylene chloride. The epoxy component of the system is soluble in methylene chloride whereas the DICY is not and the particles therefore settled to the bottom of the tube. This particle separation was further aided by centrifuging the mixture for up to 10 minutes. The supernatant solution of epoxy in methylene chloride was then decanted and discarded.

Following further washing by pure methylene chloride and drying the residual DICY particles were then dissolved in 20cc methanol, the solution of which was aided by ultrasonic agitation.

Since DICY is an organic chemical then it exhibits a strong characteristic infra-red spectrum due to chemical bond vibrations having resonant frequencies in the infra-red range. On transmission through a sample of DICY a broadband infra-red beam will therefore exhibit increased absorbance at these characteristic frequencies due to energy absorbtion by the organic molecules.

One of the bonds in the DICY molecules

exhibiting a strong absorbance peak is the nitrile or, C ≡ N bond at a characteristic frequency in the wave number range 2150-2200 cm^{-1}. The amount of DICY in the methanol solution as above (and hence the amount of DICY in the original resin sample) could therefore be quantified by measurement of the area of the absorbance peak of the nitrile group.

For the purpose of calibration and analysis a double beam Fourier Transform Infra Red Spectrometer (FTIR) was used. By its means the nitrile peak area was measured for solutions of known concentrations of DICY in pure methanol. For liquid containment purposes during the course of the analysis and in order to maintain a constant optical path for the infra red beam for all the experiments, the DICY/methanol solution for each analysis was enclosed in a sodium chloride constant volume cell supplied with the spectrometer.

Having established a calibration curve of the nitrile group peak absorbance area against DICY/methanol solution concentration the progress of the DICY reaction with the epoxy could be evaluated as follows.

Samples of resin were heated for various times under isothermal conditions at a number of temperatures. All the processed samples were then analysed according to the above procedure.

A typical result of these experiments is shown in Fig.(43). In this figure the decrease in transmittance of the beam in the wavenumber range 2100-2230cm^{-1} is shown for methanol solutions of two resin samples which had been heated for 20 minutes and 90 minutes respectively at 125°C. It is observed that the area of the peak for the resin processed for the longer time of 90 minutes is significantly less than that for the 20 minutes sample.

This difference in peak area is due to the fact that the nitrile group is a functional group of the DICY and which therefore reacts with the active molecular groups in the epoxy. As the cure reaction proceeds the amount of this group in the sample thus gradually disappears due to the chemical reaction and the areas

under the peaks in Fig.(40) are equivalent to the amount of unreacted DICY in the resin mass at the time at which the respective reactions were suppressed on cooling.

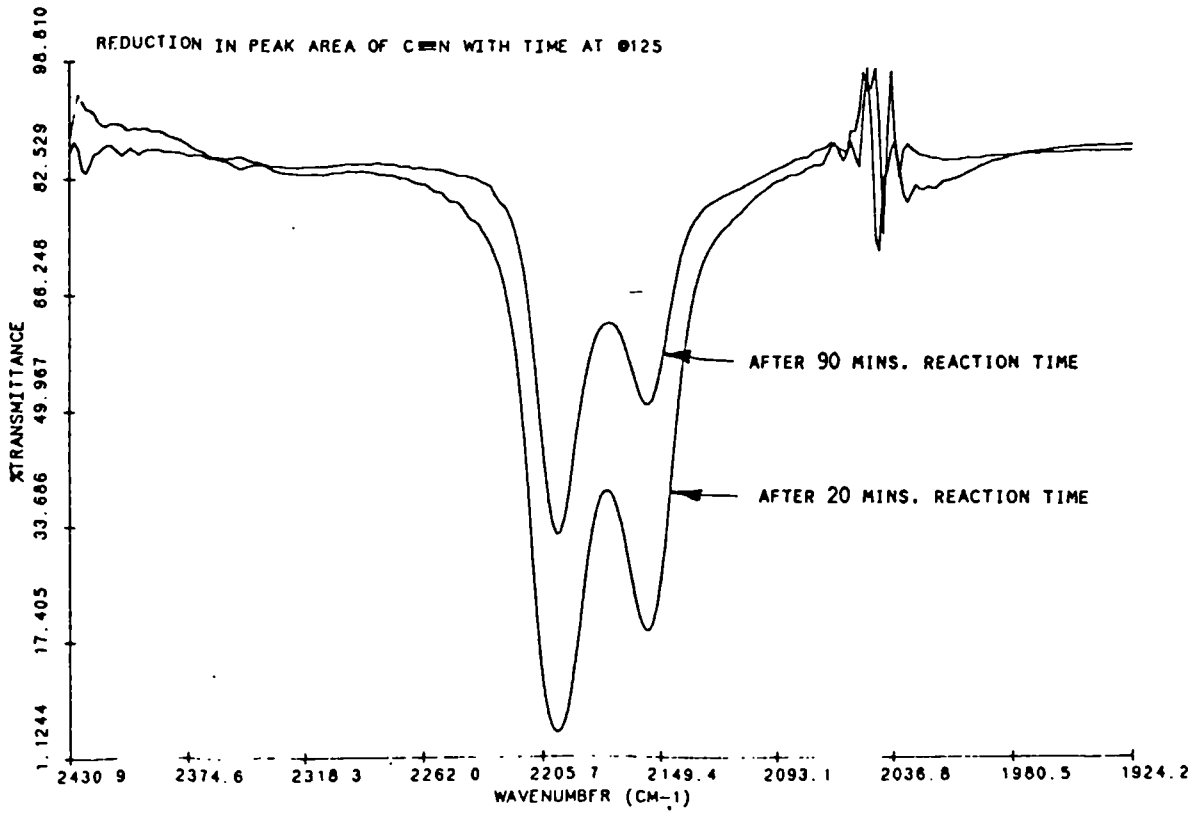

FIG.(43)

By subtraction of the unreacted DICY content as measured above from the original content the amount of DICY reacted at any time can therefore be obtained.

A plot of the reacted DICY content expressed in w/v of methanol solution versus time at four different temperatures is shown in Fig.(44). All the plots are reasonably linear over the relatively low duration of the reaction at each temperature. Unfortunately the measurements as undertaken in the above manner are limited to the maximum times shown in Fig.(44) at each temperature due to the fact that as the reaction proceeds the methylene chloride solution of the reacted material becomes increasingly more viscous with the result that extraction of DICY by centrifuging becomes increasingly more difficult.

From the values plotted in Fig.(44) however the rate of reaction at low conversion at each of the temperatures can be obtained from the slopes of the best fit lines shown.

An Arrhenius plot of ln(reaction rate) versus reciprocal temperature can hence be generated as shown in Fig.(45) from the values tabulated in Table 24.

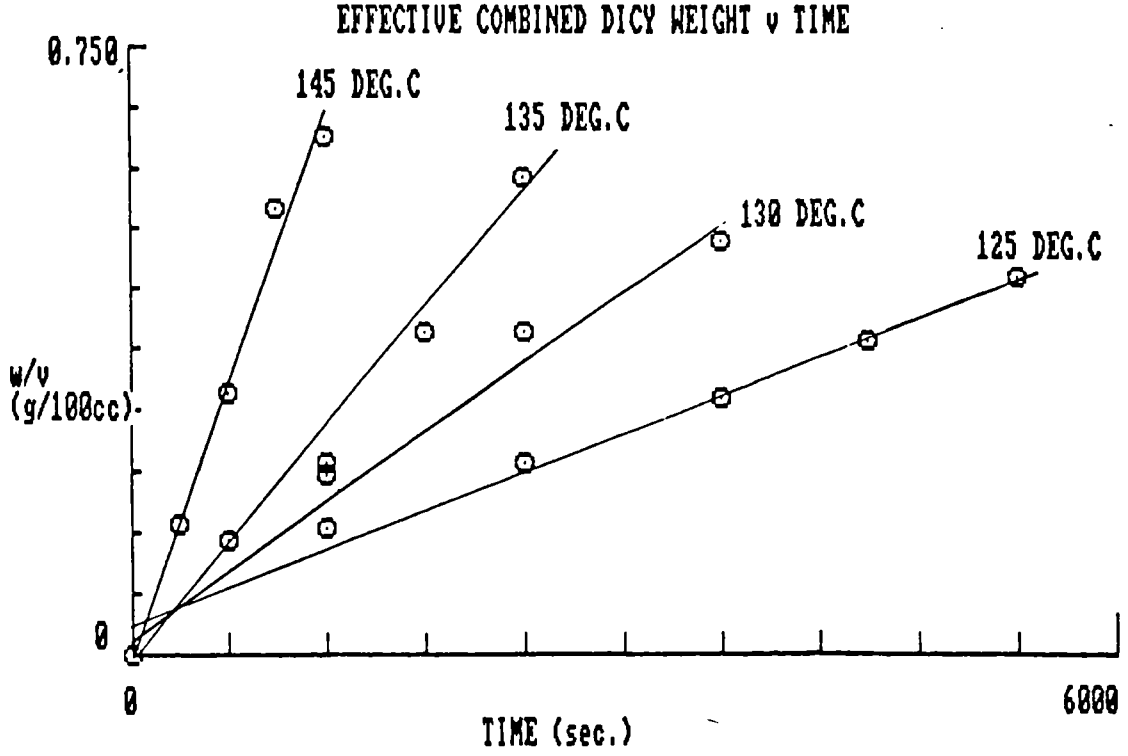

FIG.(44)

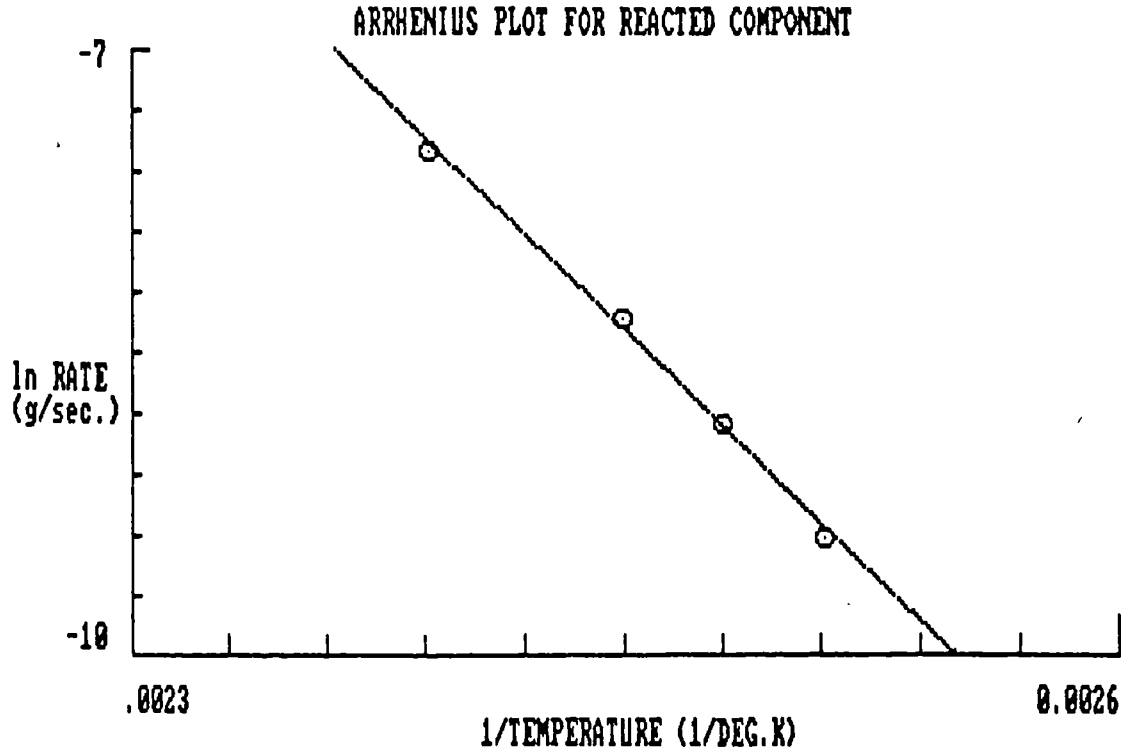

FIG.(45)

The equation joining the points shown is given by

$$\ln(\text{Rate}) = (-15902.79)(1/T°K)+(30.56721) \quad (4.6)$$

from whih an activation energy of

$$E = 31.6 \text{ kcal/mole } (132\text{kJ/mole})$$

is obtained.

It is noted that the activation energy so derived by this analysis method is close to the value as evaluated for $E_{\beta=0.05}$ above.

4.3.2 Gel Time

During the initial stages of the cure of an expoy resin the formation and growth of linear polymer chains occur in the liquid resin. These chains soon branch and cross links between previously independent chains are formed as the cure reaction proceeds. The time at which the growing, three dimensional network of crosslinked chains becomes infinite in extent i.e. extends throughout the resin volume undergoing cure is called the gel time. Reaction beyond the gel point enables further crosslinks to be established within the network thereby increasing the rigidity of the resin.

Physically, at the gel point the resin is in a gelled or rubbery state and the polymer does not normally flow and is generally not processable beyond this point (see also ref.15).From a practical point of view the gel time is thus an important characteristic of the resin system.

For epoxy resins generally the gel point occurs above 0.5 conversion (ref.15).

For current model purposes therefore it is of interest to evaluate the activation energy of the reaction at the gel point and this was accomplished as follows.

The isothermal gel times were obtained at a number of temperatures by the use of a hot bench technique. A small amount of resin was placed on a hot

bench which consisted of a horizontal rectangular heated plate with a nominally linear surface temperature gradient from one end to the other. Actual temperatures at selected positions on this hot plate were calibrated by means of materials with known melting points being placed at the corresponding locations.

During the test, as the resin is probed periodically by a sharp instrument such as a pin a filament of resin can be drawn from the main bulk of the sample resting on the bench surface. At the gel point however when the resin attains the rubbery state such a drawn filament easily snaps and the time at which this occurs, the gel time, is recorded.

The test was repeated a minimum of three times at each isothermal temperature (ref.17) and from these mean values an Arrhenius plot of ln(gel time) versus reciprorcal temperature can be plotted as shown in Fig.(46) from the tabulated values in Table (25).

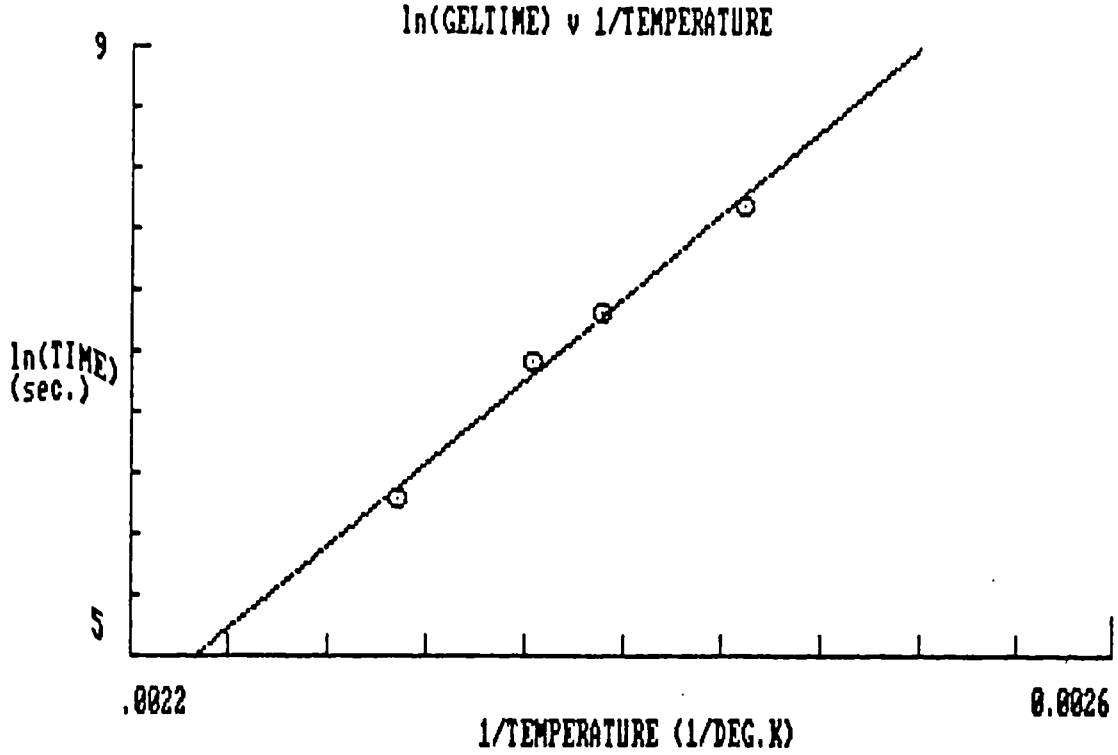

FIG.(46)

The linear relationship in this case is given by

$$\ln(\text{gel time}) = (13636.86)(1/T°K)-(25.3658) \quad (4.7)$$

from which an activation energy of

$$E = 27.1 \text{ kcal/mole } (113.4 \text{ kJ/mole})$$

is obtained.

It is noted that this activation energy is close to the value of 109kJ/mole as evaluated from the lower limb plots of Method A in Table 21. It is also close to the value for $E_{\beta=0.3}$ of 107.kJ/mole as obtained above from the master curve.

This result implies therefore that gel in the case of BSL 914 resin system as with other epoxy system occurs at isothermal conversion of the order of 0.5.

4.4 Model Verification

From previous sections in this Chapter, estimates of cure under isothermal conditions could be obtained by the use of the master curves generated. Due to the scatter of the values in these master curves for the reasons described however the cure predictions so obtained would not be precise enough to fulfill the requirements of a practical model as described in section 3.1.

For the generation of a cure model in the current work therefore use will be made of the generalised autocatalytic function, the derivation of which was described in Chapter 3.

For convenience the relevant equations from previous text which form the basis of the model can be summarised as follows.

From eq.(3.14) the rate of cure $d\beta/dt$ where the conversion β is defined relative to the isothermal heat of reaction H(iso) is given by

$$d\beta/dt = k\beta^n(1 - \beta)^m \quad (4.8)$$

where k is the isothermal rate constant.

Eq (4.8) is modified so that the cure α is defined relative to the total heat of reaction, H(dyn) as follows

$$d\alpha/dt = (k/F)(F\alpha)^n(1 - F\alpha)^m \qquad (4.9)$$

where F is defined by

$$F = H(dyn)/H(iso) \qquad (4.10)$$

From section 2.3.2.2 the value of H(dyn) is constant with

$$H(dyn) = 115 \text{ cal/g}$$

Variation of the parametrs k, F, n and m in eq.(4.9) with absolute temperature, T are defined as follows.

From eq.(2.9) the variation in the isothermal exotherm is

$$H(iso)=(-1.840437 \times 10^{-2})(T^2)+(16.53196)(T)-(3601.842) \qquad (4.11)$$

From eq.(3.32) the variations in the index n, is given by

$$n = (-6.571918 \times 10^{-3})(T) + (2.994045) \qquad (4.12)$$

From eq.(3.22) the ratio r of the two indices, m/n is given by

$$\ln r = (-8796.092)(1/T)+(22.46026) \qquad (4.13)$$

From eqs.(4.12) and (4.13) the index m can be evaluated.

Finally from eq.(3.31) the isothermal rate constant, k is given by

$$\ln k = (-8379.384)(1/T)+(13.02864) \qquad (4.14)$$

for which an apparent activation energy E, and pre-exponential factor A, apply and are defined by

$$E = 70 \text{ kJ/mole}$$

and

$$\ln A = 13.03 \text{ sec}^{-1}$$

The model defined by eq.(4.9) can therefore be verified by comparing the theoretical rate of conversion $d\alpha/dt$ for any α in the range 0 to 1 in eq.(4.9) with the practically observed values from the DSC experimental work as described in Chapters 2 and 3.

This comparison between theoretical prediction and the practical results was undertaken at six tempeatures as follows in the temperature range 125 to 175°C inclusive.

At 125°C the practical values of rate of conversion are tabulated in Table 4(a) and the theoretical values evaluated by means of eq.(4.9) and the associated eqs.(4.10) to (4.14) inclusive are tabulated in Table 26.

The comparison plot of these values is shown in Fig.(47). It will be observed that a fair comparison exists between the theoretical and experimental points.

Both the maximum rate of reaction and the conversion at which this maximum rate of reaction occurs are predicted satisfactorily.

The maximum conversion, approximately 0.55, achieved on completion of the reaction at 125°C is also satisfactorily predicted.

It will be noted however that the theoretical rates of reaction prior to the peak in the curve is greater than those in the practical case. This slight difference between the practical and theoretical values in the region of low conversion is due to the problems associated with the evaluation of the kinetic parameters as described in Chapter 3.

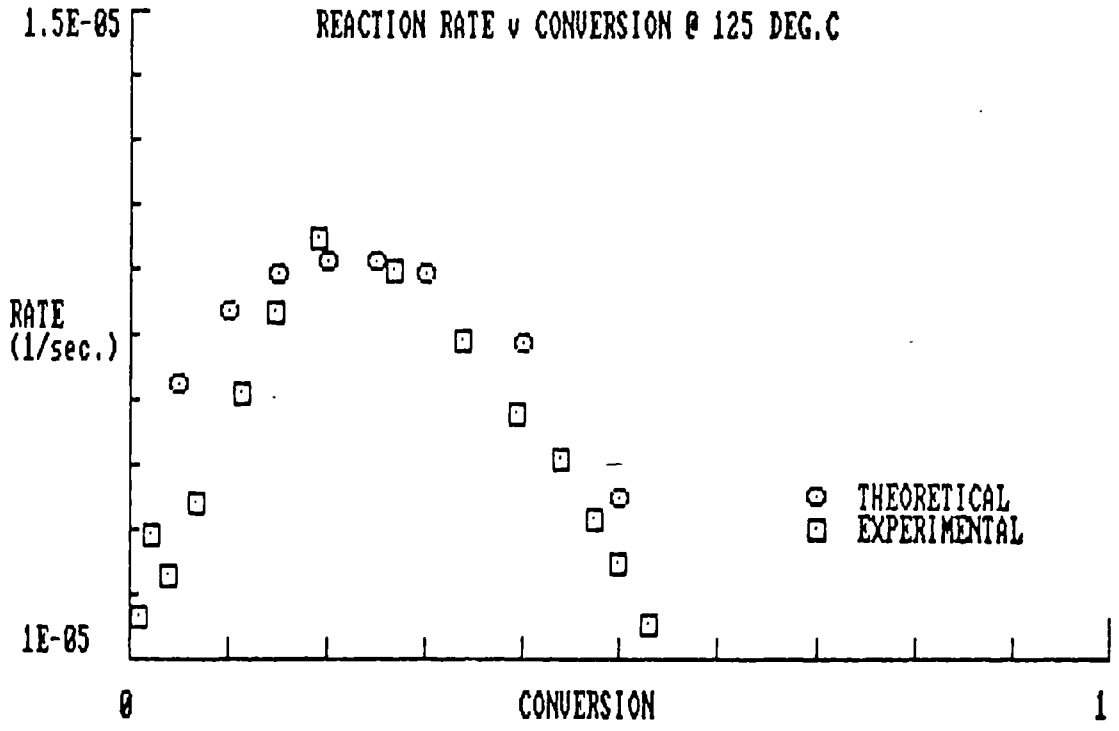

FIG.(47)

The comparison plot for the theoretical and practical cases at 130°C is shown in Fig.(48) plotted from the tabulated practical values in Table 5(a) and the tabulated theoretical values in Table 27.

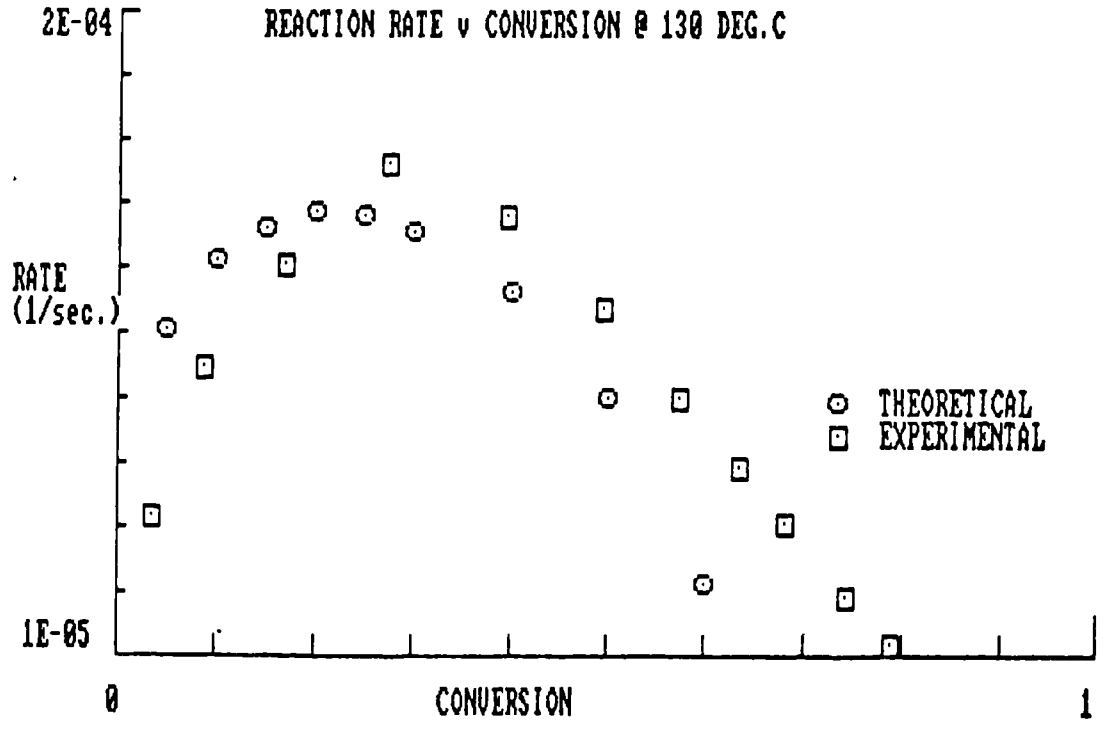

FIG.(48)

Similarly the plots at 140°C, 150°C, 165°C and 175°C are shown in Fig.(49) to Fig.(52) inclusive from the respective Tables 6(a), 11(a), 14(a) and 15(a) for the practical values and Tables 28 to 31 inclusive for the theoretical values.

From these figures it is clear that satisfactory predictions of the rates of isothermal cure can be obtained in the temperature range 125°C to 175°C inclusive. The model as described by eqs.(4.9) to (4.14) can therefore be used with confidence to evaluate the cure of the resin at all isothermal conditions in this temperature range as will be described below.

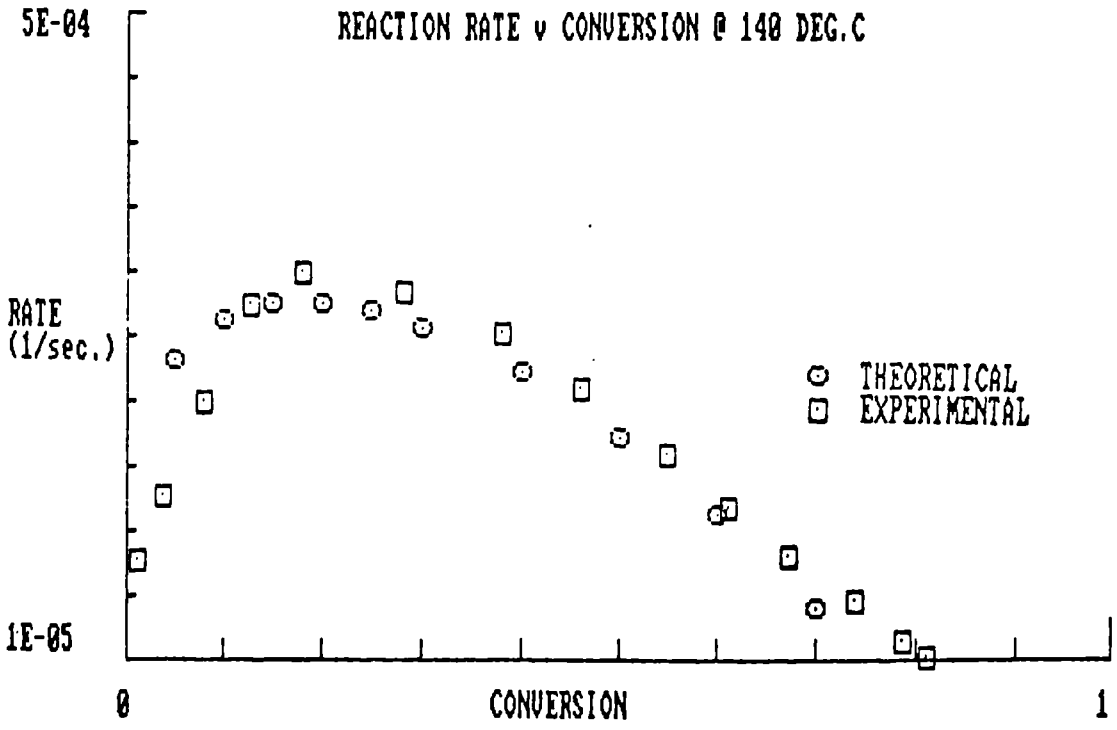

FIG.(49)

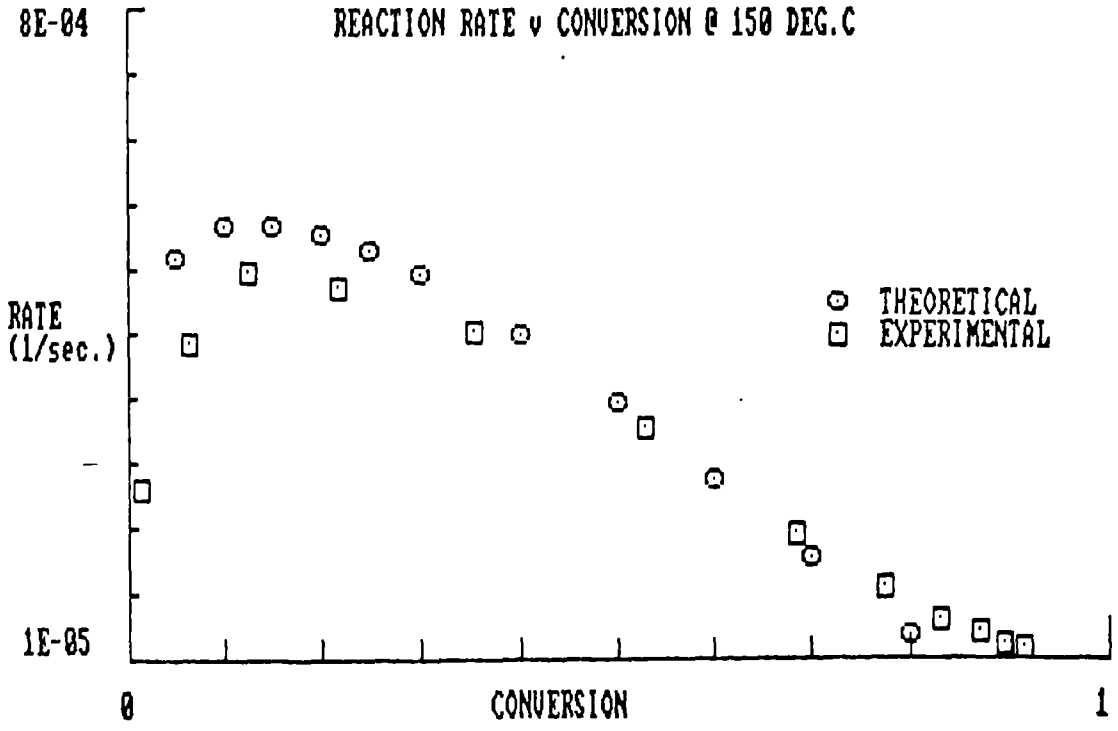
8E-04
REACTION RATE v CONVERSION @ 150 DEG.C
RATE
(1/sec.)
THEORETICAL
EXPERIMENTAL
1E-05
0
CONVERSION
1

FIG.(50)

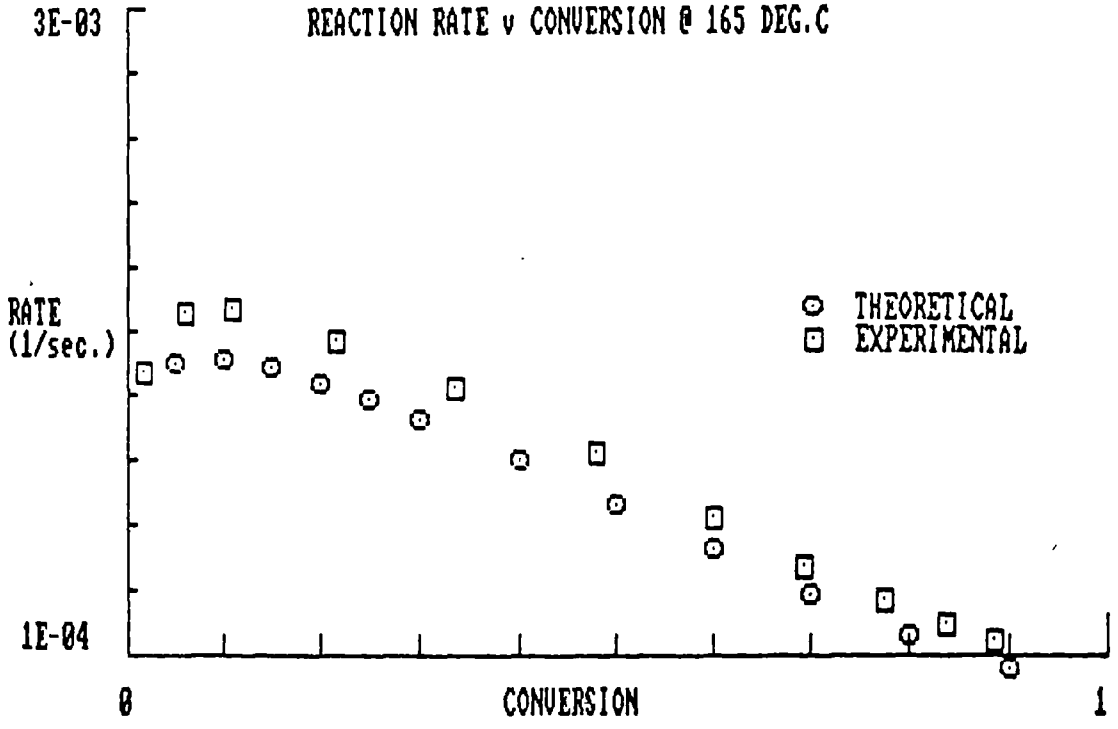
3E-03
REACTION RATE v CONVERSION @ 165 DEG.C
RATE
(1/sec.)
THEORETICAL
EXPERIMENTAL
1E-04
0
CONVERSION
1

FIG.(51)

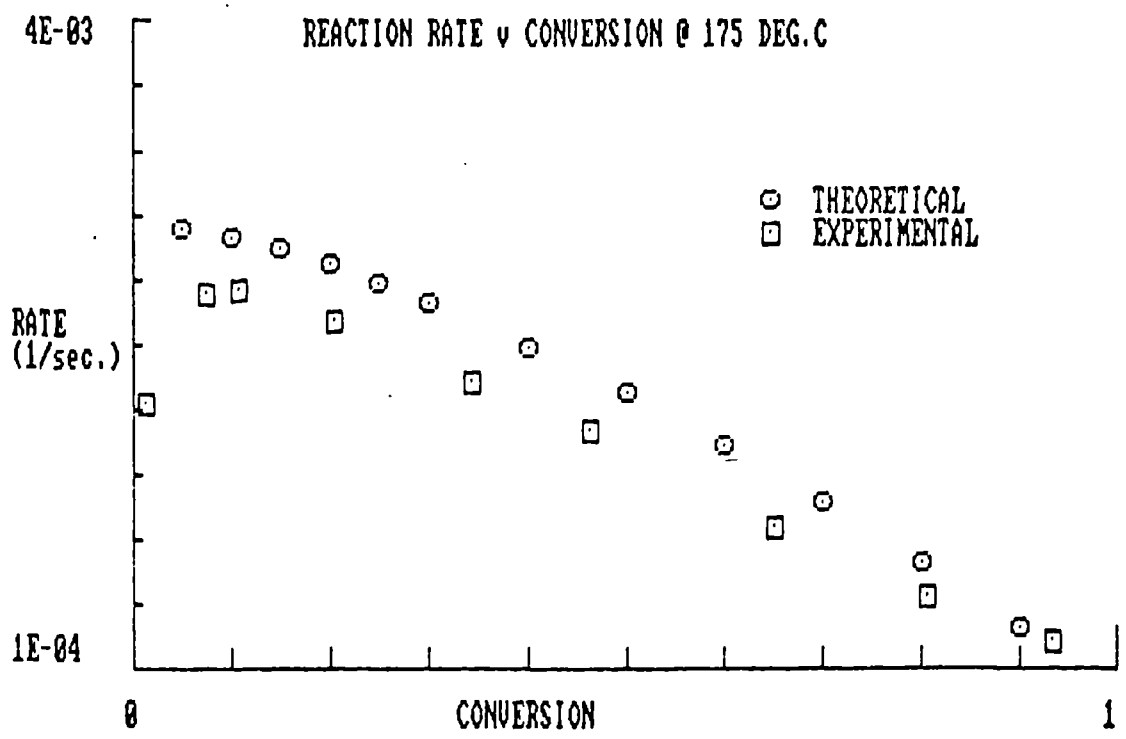

FIG.(52)

4.5 Cure Prediction

Eq.(4.9) is a first order, first degree differential equation expressing the rate of conversion or cure as a function of cure. The solution of this differential equation therefore should enable the cure to be evaluated at any time during the course of the reaction under isothermal condition. Eq.(4.9) can be solved either directly by integration since the variables are separable or alternatively by numerical techniques.

The two methods of solution will be described as follows.

4.5.1 Direct Integration

From eq.(4.9)

$$d\alpha/dt = (k/F)(F\alpha)^n(1 - F\alpha)^m$$

then by separating the variables

$$d\alpha/(k/F)(F\alpha)^n(1 - F\alpha)^m = dt \qquad (4.15)$$

Integrating eq (4.15) between limits of conversion α_o and t_o at the onset of the reaction and α_F at a subsequent time t.

$$\int_{\alpha_o}^{\alpha_F} d\alpha/(k/F)(F\alpha)^n(1 - F\alpha)^m = \int_{t_o}^{t} dt = t - t_o$$

$$\approx t \text{ when } \alpha_o \rightarrow 0 \text{ at } t_o = 0 \qquad (4.16)$$

The integral on the LHS can be numerically integrated.

The numerical method chosen in the current work was Simpson's method (ref.45) by means of which the area under the curve of the function $f(\alpha)$ is obtained for a range of $0 < \alpha < 1/F$ where $f(\alpha)$ is defined by

$$f(\alpha) = 1/(k/F)(F\alpha)^n(1 - F\alpha)^m \qquad (4.17)$$

The mathematical procedure consists of dividing the range of α into an even number, N, intervals so that each interval is of equal length h given by

$$h = (\alpha_F - \alpha_o)/N \approx \alpha_F/N \text{ when } \alpha_o \rightarrow 0 \qquad (4.18)$$

The reason for the limit $0 < \alpha < 1/F$ in eq.(4.17) is due to the fact that the integral becomes indeterminate when $\alpha = 0$ and that the maximum isothermal conversion never attains a value of 1/F.

Simpson's rule for integration in this case is therefore

$$\int_{\alpha_o}^{\alpha_F} f(\alpha)d\alpha = (h/3)[f(\alpha_o)+4f(\alpha_o + h)+2f(\alpha_o + 2h)+4f(\alpha_o + 3h)$$

$$+.....+4f(\alpha_o + (n - 1)h) + f(\alpha_F)] + err \qquad (4.19)$$

where err is an error term.

A computer program enabled twenty discrete points per reaction to be displayed so that the resulting theoretically determined values of conversion against time could be plotted as shown in Figs.(53) to (58) inclusive for the temperatures indicated in the figures.

In these plots also the practical values of conversion and time are shown and these were obtained from Tables 4(a), 5(a), 6(a), 11(a), 14(a) and 15(a) for the relevant temperatures.

On inspection of these figures it is seen that there is good agreement between the theoretical and practical values of the conversion at any time during the course of the reaction at isothermal temperatures in the range 125°C to 175°C inclusive.

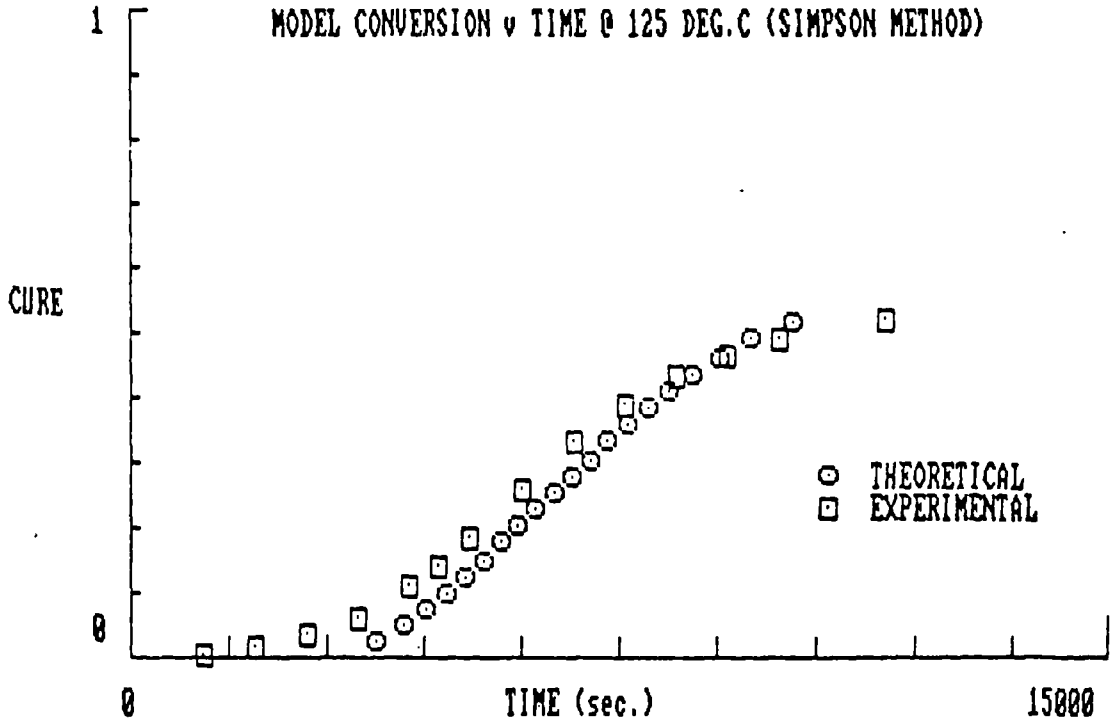

FIG.(53)

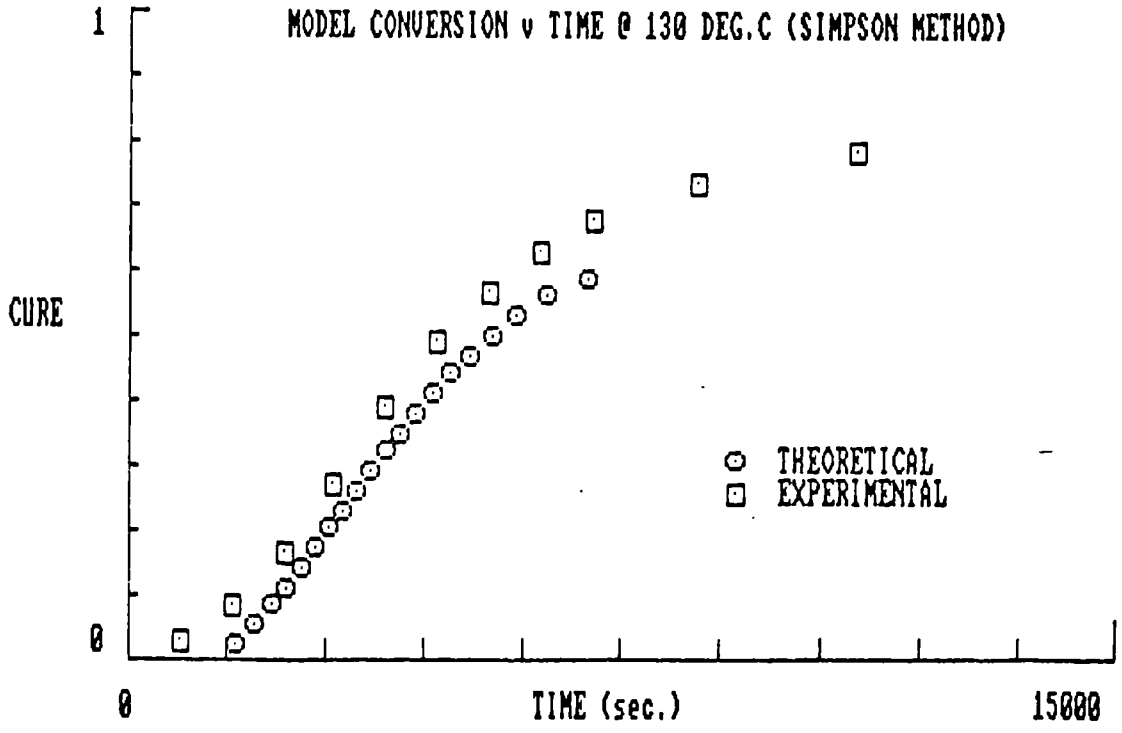
MODEL CONVERSION v TIME @ 130 DEG.C (SIMPSON METHOD)
1
CURE
0
THEORETICAL
EXPERIMENTAL
0
TIME (sec.)
15000

FIG.(54)

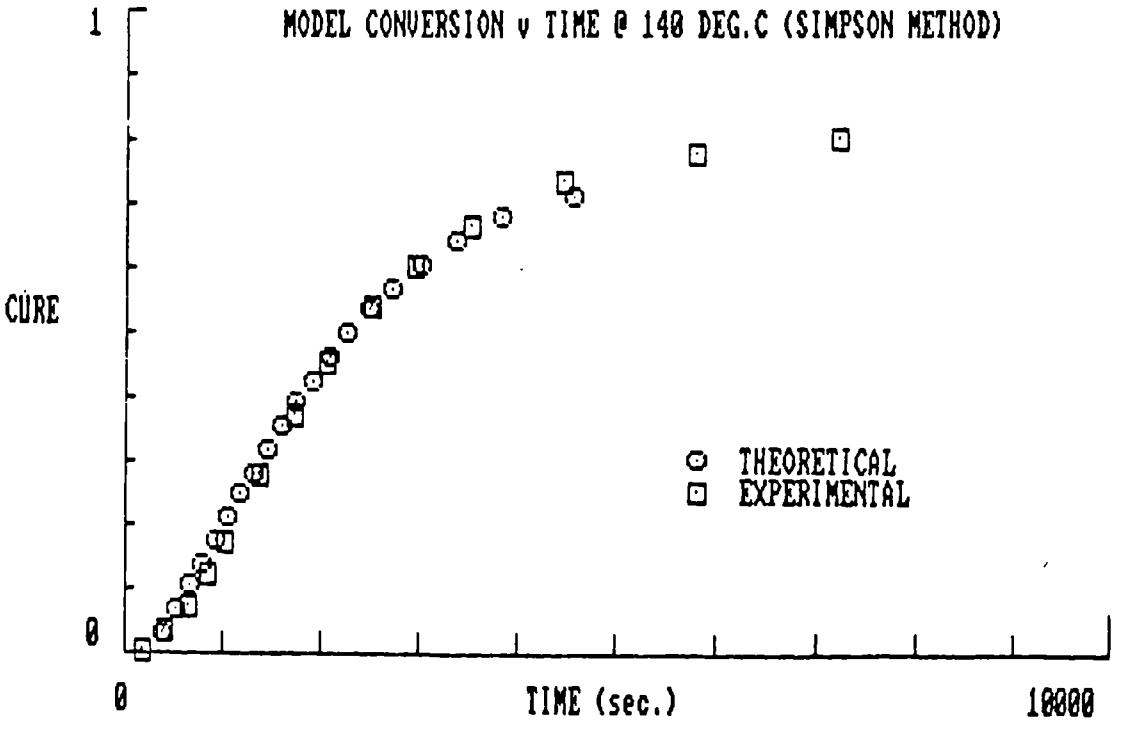
MODEL CONVERSION v TIME @ 140 DEG.C (SIMPSON METHOD)
1
CURE
0
THEORETICAL
EXPERIMENTAL
0
TIME (sec.)
10000

FIG.(55)

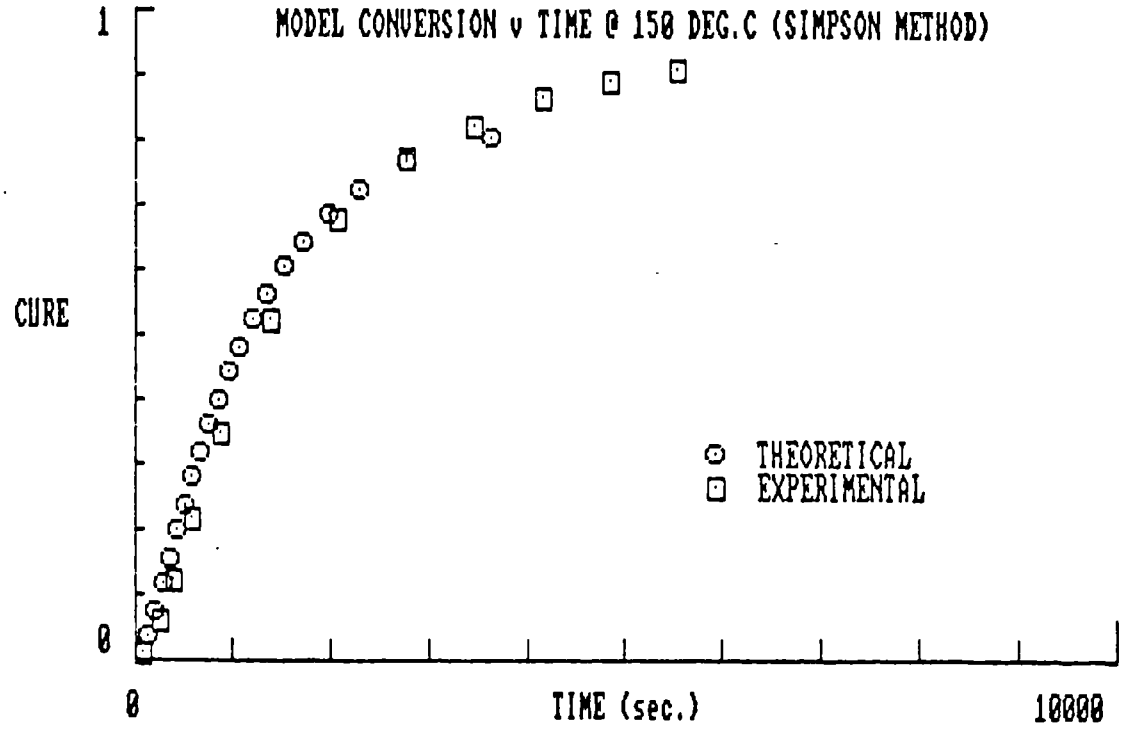
MODEL CONVERSION v TIME @ 150 DEG.C (SIMPSON METHOD)
1
CURE
0
THEORETICAL
EXPERIMENTAL
0
TIME (sec.)
10000

FIG.(56)

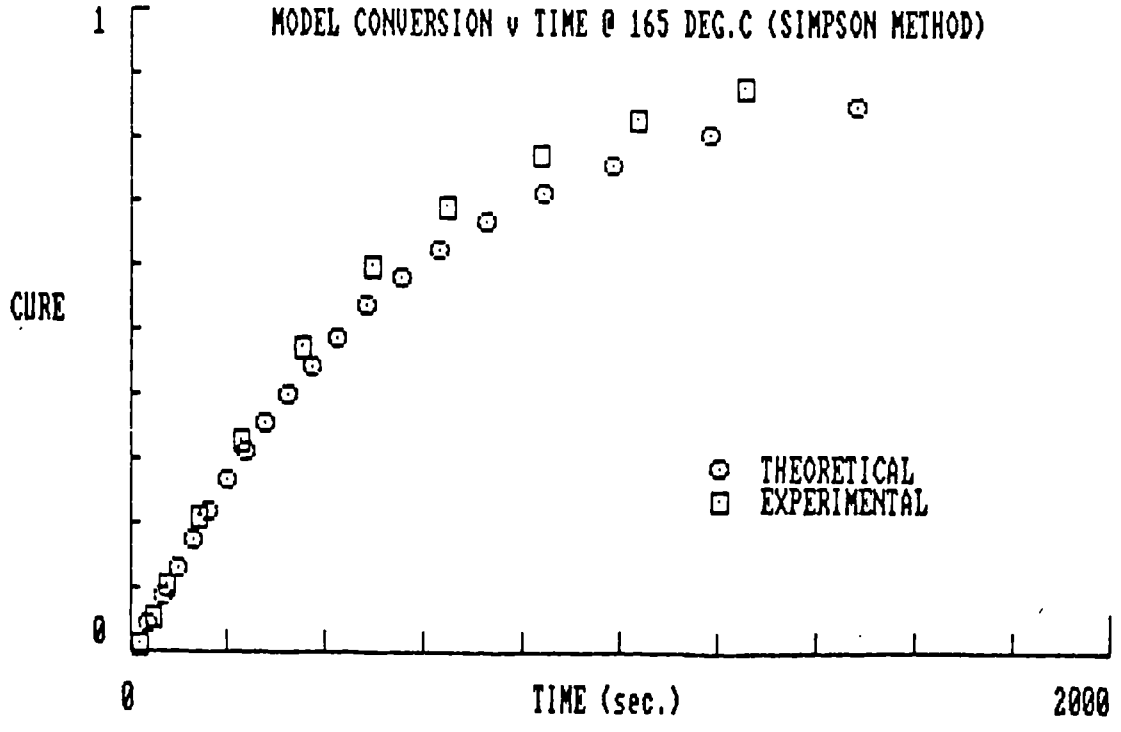
MODEL CONVERSION v TIME @ 165 DEG.C (SIMPSON METHOD)
1
CURE
0
THEORETICAL
EXPERIMENTAL
0
TIME (sec.)
2000

FIG.(57)

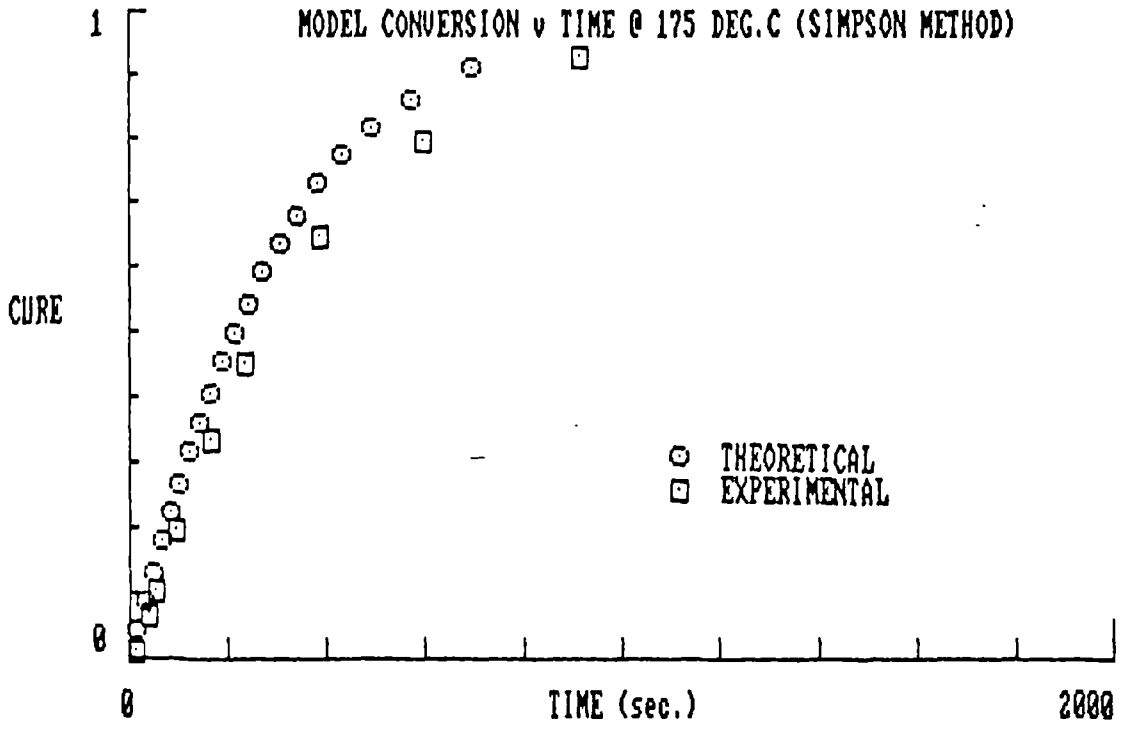

FIG.(58)

4.5.2 Numerical Solution

There are several methods in the literature by which differential equations may be solved numerically. The simplest of these is the Euler method (ref.45) which can be simply described as follows.

Consider eq.(4.9) for the rate of reaction. Since this equation is of first order and first degree then its particular solution requires one initial or start condition and this is

$$\alpha = \alpha_o \approx 0 \quad \text{at} \quad t = t_o \approx 0 \qquad (4.20)$$

where α_o and t_o are as defined in section 4.5.1

If we assume that the solution of eq.(4.9) at any time $t = t_i$ is given by $\alpha = \alpha_i$ then the Euler method gives the solution after a further time increment dt where $t = t_{i+1}$ as follows

$$\alpha_{i+1} = \alpha_i + (d\alpha/dt)_{t=ti} \cdot dt \qquad (4.21)$$

In particular at the onset of the reaction

$$\alpha_1 = \alpha_0 + (d\alpha/dt)_{t=to} \cdot dt \qquad (4.22)$$

where α_o is defined by eq.(4.20) and $(d\alpha/dt)_{t=0}$ is defined by the application of eq.(4.9) so that

$$(d\alpha/dt)_{t=to} = (k/F)(F\alpha_o)^n(1 - F\alpha_o)^m \qquad (4.23)$$

Successive application of eqs.(4.21) and (4.23) will thus lead to the solution of eq.(4.9).

The error in these successive approximations is of the order of $(dt)^2$ (ref.45) and a better approximation to the solution is obtained by the use of a modification of the Euler method where the error is of the order of $(dt)^3$.

In the modified Euler method the term for the conversion α_{i+1} in eq.(4.21) is given by

$$\alpha_{i+1} = \alpha_i + (1/2)[(d\alpha/dt_{t=t1+1} + (d\alpha/dt)_{t=ti}].dt \qquad (4.24)$$

This is a two step method whereas the basic Euler method is only a single stage which therefore requires less labour in the computation.

No significant difference in the solutions to the rate equation were observed however between those obtained by the Euler and the modified Euler methods. Only the comparison between solutions obtained by the latter method and the practically determined values from the Tables listed in section 4.5.1 will therefore be drawn.

These comparison plots shown in Figs.(59) to (64) inclusive indicate reasonable agreement between the practical and theoretical values at all temperatures apart from the slight overestimate of the cure during the early part of the reaction at 125°C in Fig.(59). Note that by the Simpson method the conversion is underestimated in the same region in Fig.(53).

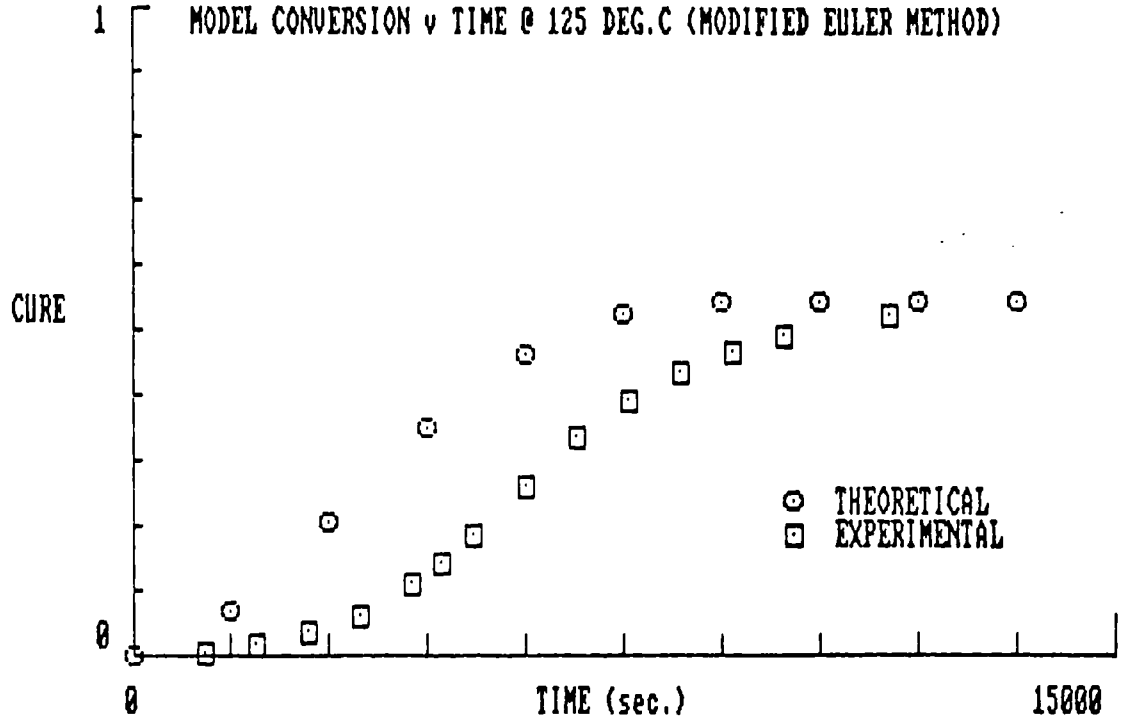
1
MODEL CONVERSION v TIME @ 125 DEG.C (MODIFIED EULER METHOD)
CURE
THEORETICAL
EXPERIMENTAL
0
0
TIME (sec.)
15000

FIG.(59)

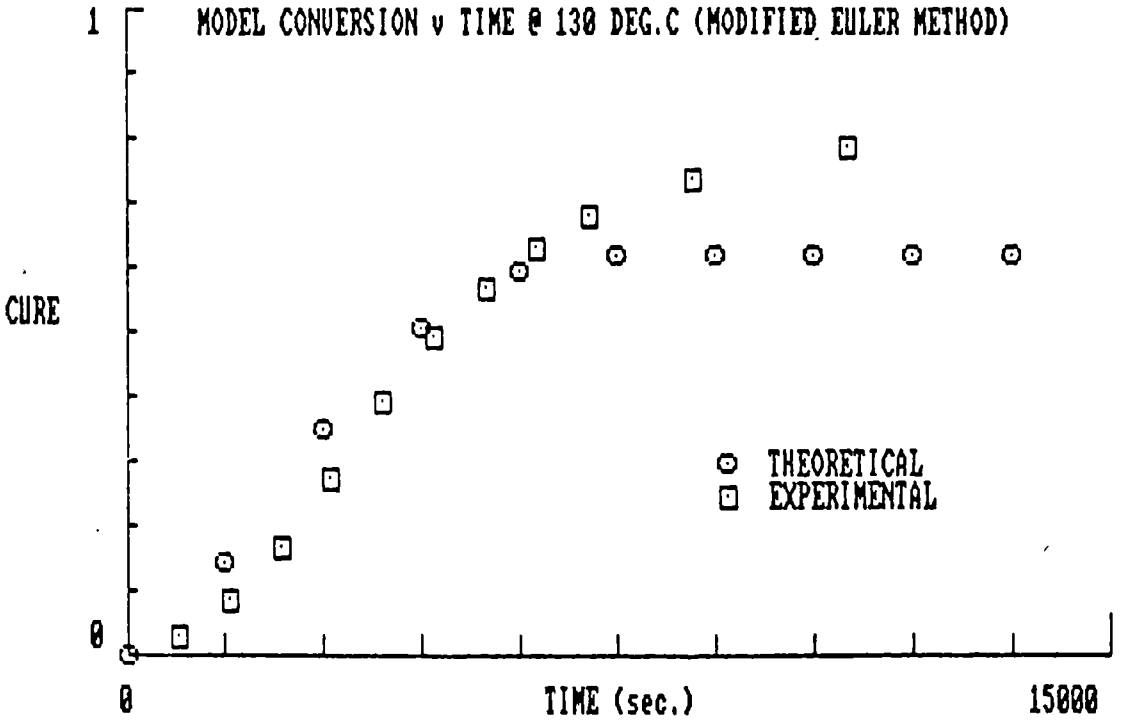
1
MODEL CONVERSION v TIME @ 130 DEG.C (MODIFIED EULER METHOD)
CURE
THEORETICAL
EXPERIMENTAL
0
0
TIME (sec.)
15000

FIG.(60)

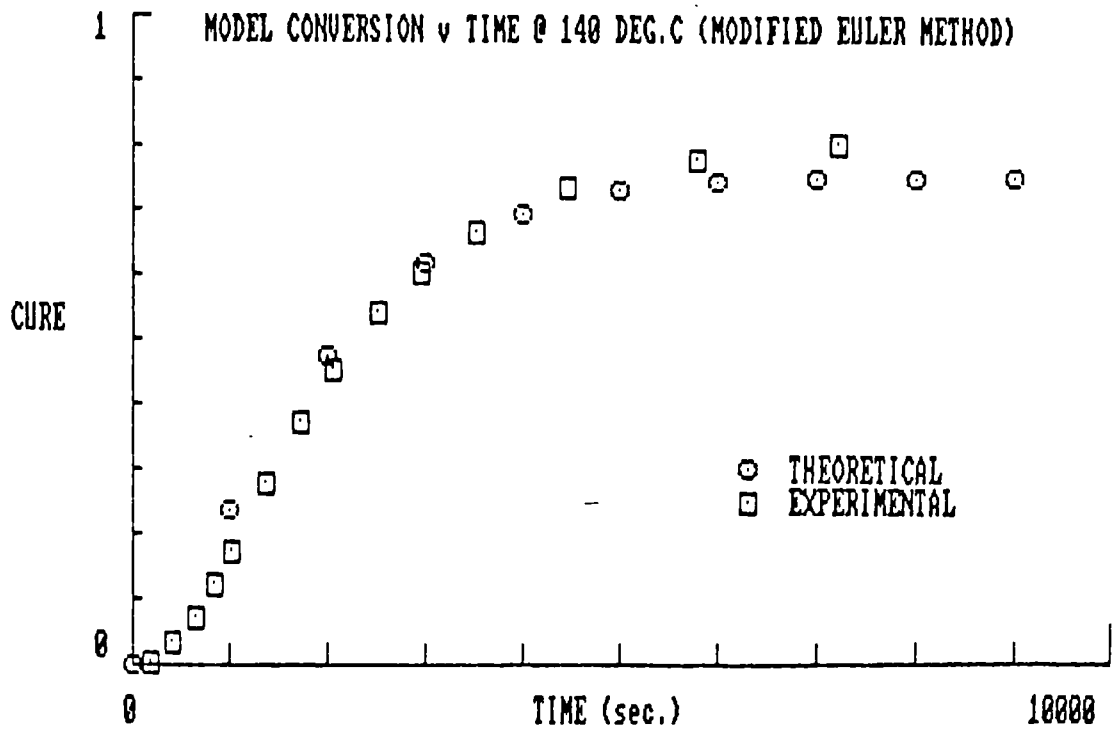
MODEL CONVERSION v TIME @ 140 DEG.C (MODIFIED EULER METHOD)
1
CURE
0
THEORETICAL
EXPERIMENTAL
0
TIME (sec.)
10000

FIG.(61)

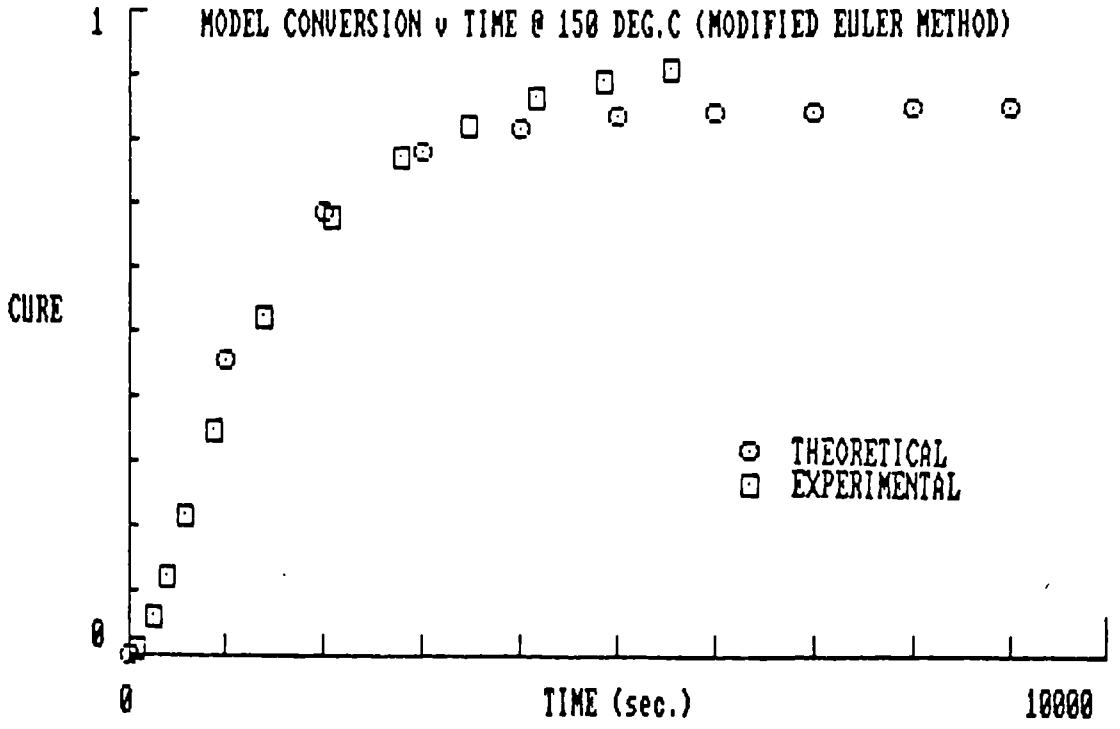
MODEL CONVERSION v TIME @ 150 DEG.C (MODIFIED EULER METHOD)
1
CURE
0
THEORETICAL
EXPERIMENTAL
0
TIME (sec.)
10000

FIG.(62)

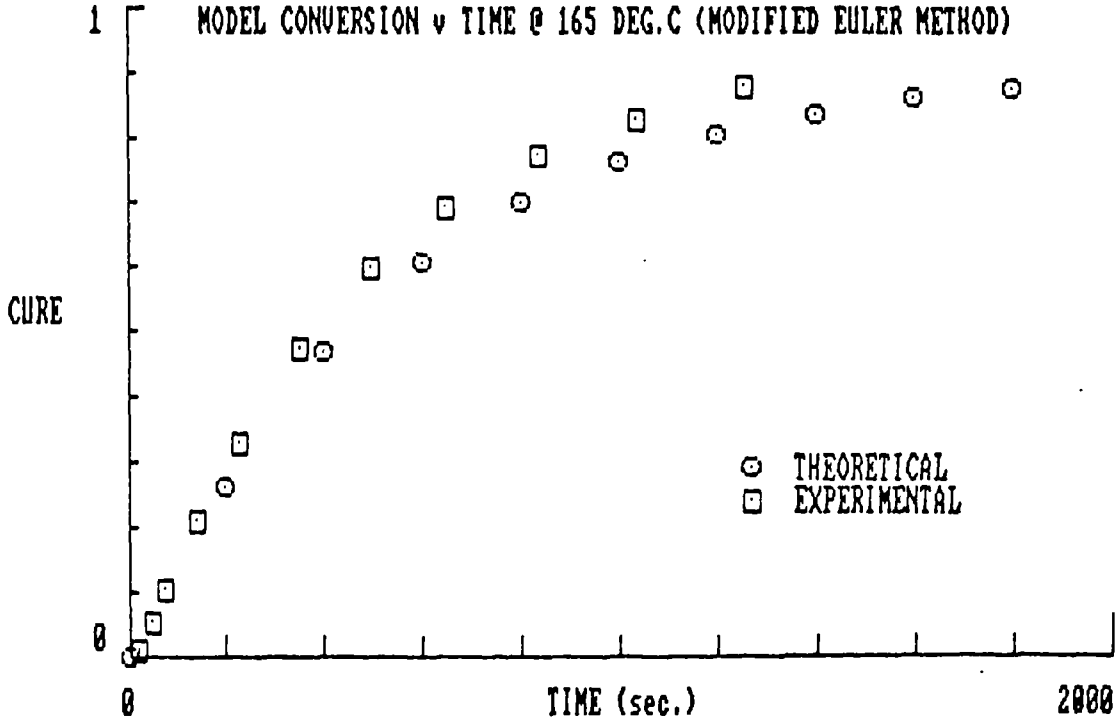
1
MODEL CONVERSION v TIME @ 165 DEG.C (MODIFIED EULER METHOD)
CURE
THEORETICAL
EXPERIMENTAL
0
0
TIME (sec.)
2000

FIG.(63)

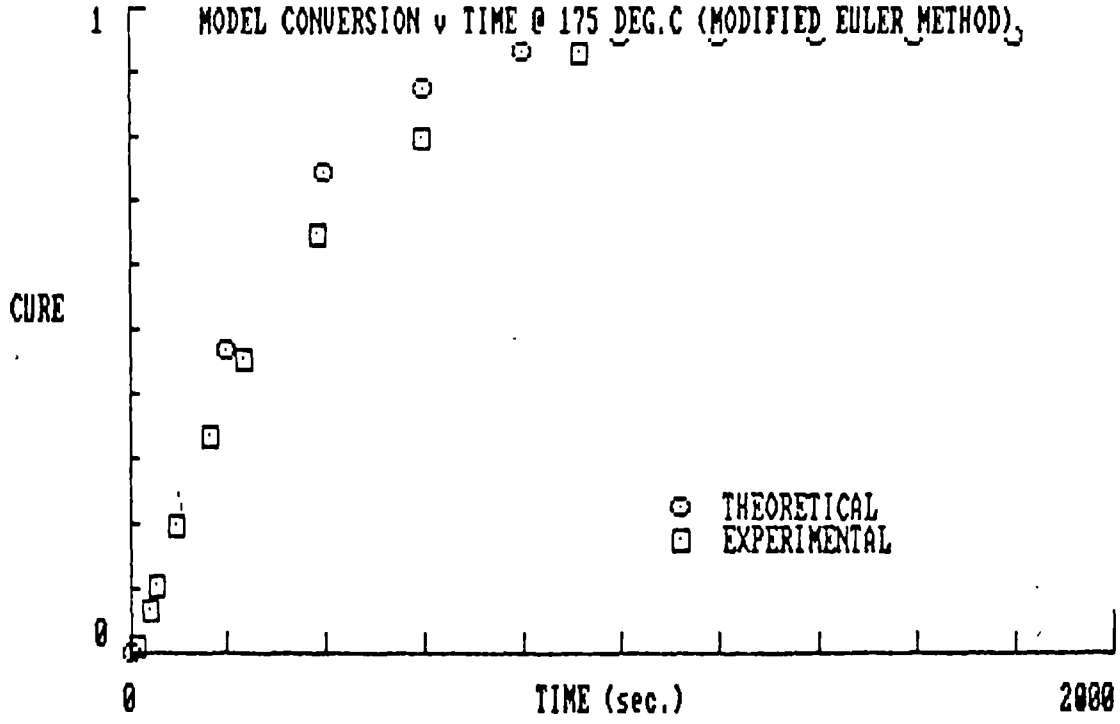
1
MODEL CONVERSION v TIME @ 175 DEG.C (MODIFIED EULER METHOD)
CURE
THEORETICAL
EXPERIMENTAL
0
0
TIME (sec.)
2000

FIG.(64)

In order to investigate this discrepancy further between the Simpson and the modified Euler methods of solution at 125°C the rate equation was solved by a Runge-Kutta fourth order method which is considered to be of much higher accuracy of the order $(dt)^5$.

The formulae for the solution is as follows: For a time increment of Δt then

$$k_1 = f(t_i, x_i).\Delta t$$
$$k_2 = f(t_i + (1/2)\Delta t, \alpha_i + (1/2)k_1).\Delta t$$
$$K_3 = f(t_i + (1/2)\Delta t, \alpha_i + (1/2)k_2).\Delta t$$
$$K_4 = f(t_i + \Delta t, \alpha_i + k_3).\Delta t$$
$$\Delta\alpha_i = (1/6)(k_1 + 2k_2 + 2k_3 + k_4)$$

where $f(\alpha,t)$ is given by $d\alpha/dt$ in eq(4.9).

This value of α_{i+1} corresponding to $t = t_i + \Delta t$ is given by

$$\alpha_{i+1} = \alpha_i + \Delta\alpha_i$$

The plot of this solution is shown in Fig.(65) and it is noted on comparison with Fig.(59) that this solution is hardly any different from the solution as obtained by the modified Euler method. Thus the discrepancy between these methods and the Simpson method is attributed to the round off errors in the numerical calculations at very low conversion levels.

From the comparisons shown in Figs.(53) to (65) inclusive it is considered that all of the methods described for the integration of the rate equation, eq.(4.9) are of sufficient accuracy to predict the cure of the resin system under isothermal conditions in the temperature range 125°C to 175°C. Thus if the value of time is required for a given amount of cure then the use of the Simpson method of section 4.5.1 would be preferred for the solution whereas if a value of cure is required at a given time then the modified Euler method would be the preferred solution method due to its reasonable accuracy and relative ease of manipulation.

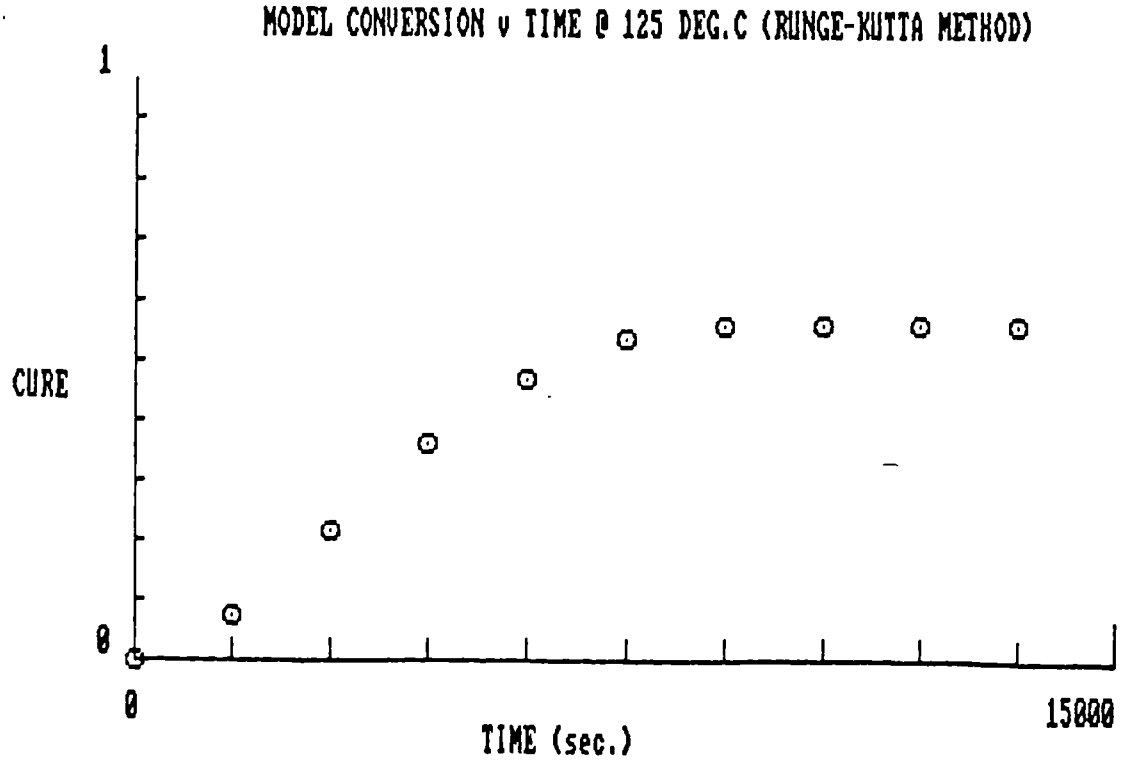

FIG.(65)

An example of the use of the Simpson method of integration is in its application for the evaluation of the half-life of the material at various isothermal temperatures. The half-life is defined as the time at which the resin achieves a 0.5 conversion level at any isothermal temperature. This is a useful value in practice since it gives a rough guide as to the state of cure at any temperature.

The half life is evaluated by the Simpson method by putting $\alpha_F = 0.5$ as the upper limit of the integral in eq.(4.16).

The half life curve so determined is shown in Fig.(66) together with the 0.3 iso-conversion curve derived in a similar manner by having $\alpha_F = 0.3$.

An example of the use of the modified Euler method will be described later in Chapter 6 where the development of a dynamic cure model will be dealt with.

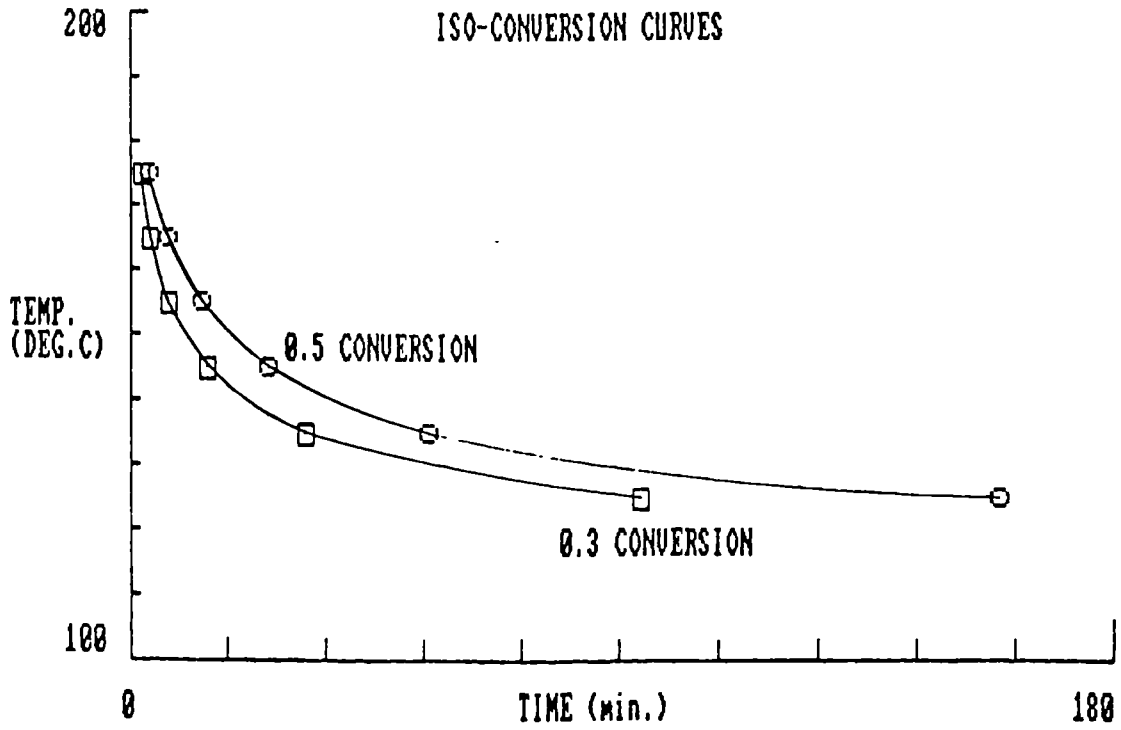
ISO-CONVERSION CURVES
200
100
TEMP.
(DEG.C)
0.5 CONVERSION
0.3 CONVERSION
0
TIME (min.)
180

FIG.(66)

CHAPTER 5

VISCOSITY SUB-MODEL

5.1 Viscosity Behaviour

From Chapter 1 the rheological behaviour of the resin is a major factor to be considered if successful application of the autoclave method to the moulding of carbon fibre prepregs is to be achieved.

Due to the fact that the matrix resin undergoes a change from a low viscosity liquid to a solid during the process of moulding then in order to attain the correct laminate consolidation conditions this variation in resin viscosity has to be appreciated and quantified for its rheological behaviour to be determined.

Viscosity is therefore a necessary parameter and which can be defined for a Newtonian fluid as follows (see also refs.47, 48, 49).

$$\tau = v \, ds/dy \qquad (5.1)$$

where τ is the shear stress in a liquid undergoing laminar flow where the velocity gradient normal to the flow direction is given by ds/dy. v is a constant called the coefficient of viscosity or simply viscosity.

Thus for a Newtonian liquid the shear stress is directly proportional to the rate of change of velocity with distance. The velocity gradient can however be equated to the time rate of change of the shear strain in the liquid, thus

$$\tau = v \dot{\theta} \qquad (5.2)$$

where $\dot{\theta} = d\theta/dt = ds/dy$

where $\dot{\theta}$ is called the shear rate.

It will be shown later (section 5.3.1) that the resin system behaves like a Newtonian fluid at the lower levels of chemical conversion which are applicable during the initial stages of the cure process. Methods for the evaluation of the melt viscosity of polymers obeying the Newtonian fluid eqs.(5.1) and (5.2) can therefore be used for the generation of viscosity data for the modelling of the current BSL 914 resin system viscosity.

The resin melt viscosity however is a function of time and temperature due to two main characteristics of the resin viscosity behaviour. The first characteristic, in common with most simple liquids, is a physical phenomenon whereby the viscosity decreases with increased temperature. This lowering of the viscosity on heating is due to increased mobility of molecular chains in the resin as a result of heat energy input during the temperature risetime.

The second effect arises as a result of the chemical changes accompanying the cure reaction. Thus if the resin is maintained at an elevated temperature for a time both the molecular weight of and the crosslink density within the resin increase due to the cure reaction. As a result the viscosity rises with time with the rate of increase escalating rapidly at the gel point when the crosslinks become infinite in extent.

Thus at any isothermal temperature the resin behaviour is characterised by an initial zero-time viscosity which decreases the higher the temperature but with time at the same temperature however the time-dependent viscosity increases to values greater than the zero-time viscosity. Further the rate of rise of the time-dependent viscosity is greater the higher the isothermal temperature.

Before the mathematical model of this viscosity behaviour is formulated however the method of viscosity determination as used in the current work will be described.

5.2 Viscosity Determination

Many viscometers are commercially available for the determination of fluid viscosities and these can be classified as to the type of physical measurement employed in their use.

Typical methods of measurement include the measurement of the rate of flow of fluids in tubes as in the capillary flow type of viscometers; the measurement of the rate of motion of a rigid body in a liquid as in the falling sphere viscometer and the measurement of the damping of a vibrating element immersed in a fluid in a vibrational viscometer. Rotational viscometers belong to another class whereby either the velocity of, or the torsional couple exerted on a solid rotating cylinder or other rigid element immersed in the liquid is measured. The cone-plate viscometer belongs to the rotational class where the measurement of the reaction torque due to viscous traction on a solid element rotating at a constant rate in the fluid of interest is used.

The viscosity data generated for the current model were obtained by the use of a Ferranti-Shirley cone-plate viscometer the description and principle of operation of which will now follow.

5.2.1 Cone-Plate Viscometer

In the cone-plate viscometer the sample of resin the viscosity of which is required is contained in the space between a cone of large apical angle, rotating abouts its axis, and a stationary horizontal flat surface normal to the axis of cone rotation. A schematic cross-section of the instrument is shown in Fig.(67a).

The essential feature of this instrument is that the rate of shear is uniform throughout the sample and this is ensured by the existence of a small angle, A radians, between the conical surface and the flat base plate surface when the apex of the cone is contiguous with the latter plate as shown in the figure.

During operation the cone is rotated at a fixed angular velocity, Ω rad sec^{-1}, relative to the fixed, flat plate and the rate of shear, $\dot{\theta}$, at a distance r from

the central axis is given by the ratio of linear velocity to the separation of the two surfaces i.e.

$$\dot{\theta} = r\Omega/rA = (\Omega/A) \text{ sec}^{-1} \qquad (5.3)$$

The shear rate $\dot{\theta}$ is therefore independent of r.

In this viscometer the shear rate is maintained constant by means of a velocity servo system which maintains constant rotational speed of the cone irrespective of the amount of reaction torque produced by the liquid in between the rigid surfaces. This reaction torque is measured by a torque dynamometer and from this measurement the shear stress in the resin can be evaluated.

Since the shear rate is constant the shear stress τ in the resin is also constant and the total reaction torque, T, is given by

$$T = \int_0^R \tau.r.2\pi r \, dr$$

$$= 2\pi R^3\tau/3 \qquad (5.4)$$

where R is the radius of the cone.

From eq.(5.4) the shear stress τ is given by

$$\tau = 3T/2\pi R^3 \qquad (5.5)$$

The viscosity v of the resin is therefore obtained from eqs.(5.2), (5.4) and (5.5).

$$v = (3T/2\pi R^3)/(\Omega/A)$$

$$= (3TA)/(2\pi R^3\Omega) \qquad (5.6)$$

For the current viscosity data generation a cone of diameter 2cm and cone angle of 0.006 radians was

used.

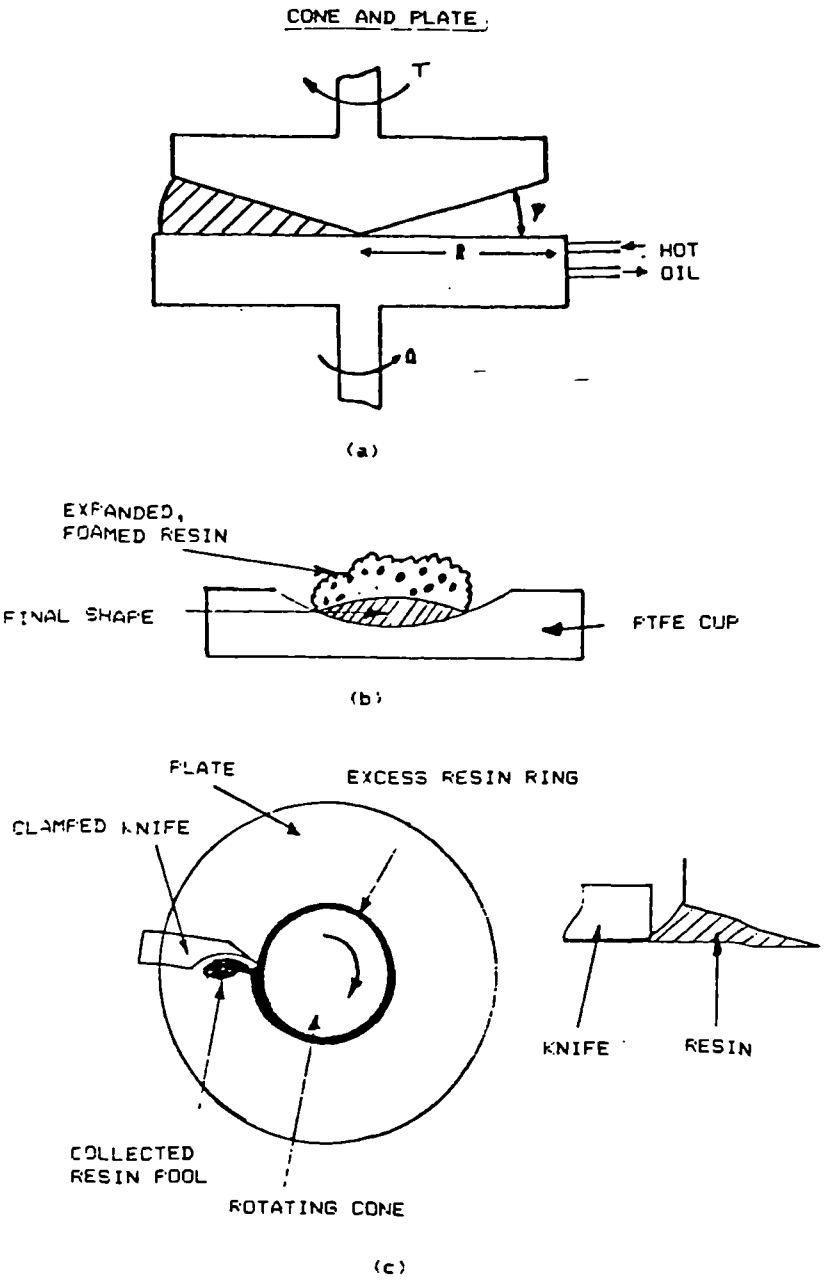

FIG.(67)

Viscosities at higher temperatures than ambient can be obtained by means of the viscometer and this is achieved by the circulation of hot oil at a controlled temperature through the base plate as shown in Fig.(67a). Only isothermal conditions could be satisfactorily obtained by this heating method however and the viscosity behaviour during ramped temperature conditions could not be ascertained by the use of this viscometer.

Temperature control under isothermal conditions is estimated to be within ±2°C of the set temperature throughout the duration of an experimental run.

5.2.2 Experimental Considerations

In practice the viscometer is simple to use in that only a small amount of sample fluid is required in between the cone and the base plate. In the case of epoxy resin samples at high isothermal temperatures the resin approaches and may even exceed gelation during an experimental run. The fact that the resin sample is small (approximately 0.5g) therefore is a major advantage of the instrument in that the surfaces of the cone and plate respectively can be easily cleaned on separation of the cone from the plate prior to further use of the instrument.

Due to the fact that the BSL 914 resin system is a partially filled epoxy resin system (due to the dispersion of DICY particles in the as-received resin film) which undergoes a substantial viscosity increase, especially with dwells at high temperatures greater than 100°C, then special measures have to be taken for the successful use of the viscometer for this application.

The difficulties associated with viscosity determination in this case can be explained by reference to Figs.(68) and (69). In these log-linear plots the viscosity profiles with time for a number of runs at each of the isothermal temperatures 129.5°C and 149°C are shown. These plots were generated by following normal practice whereby the viscometer was preheated to the required temperature prior to placement of the standard resin sample (weight 0.3g) onto the base plate. Subsequent to positioning the sample under the cone apex the latter was lowered so as to contact the flat plate and the instrument was allowed to equilibrate for three minutes before commencement of cone rotation at zero time in the above plots.

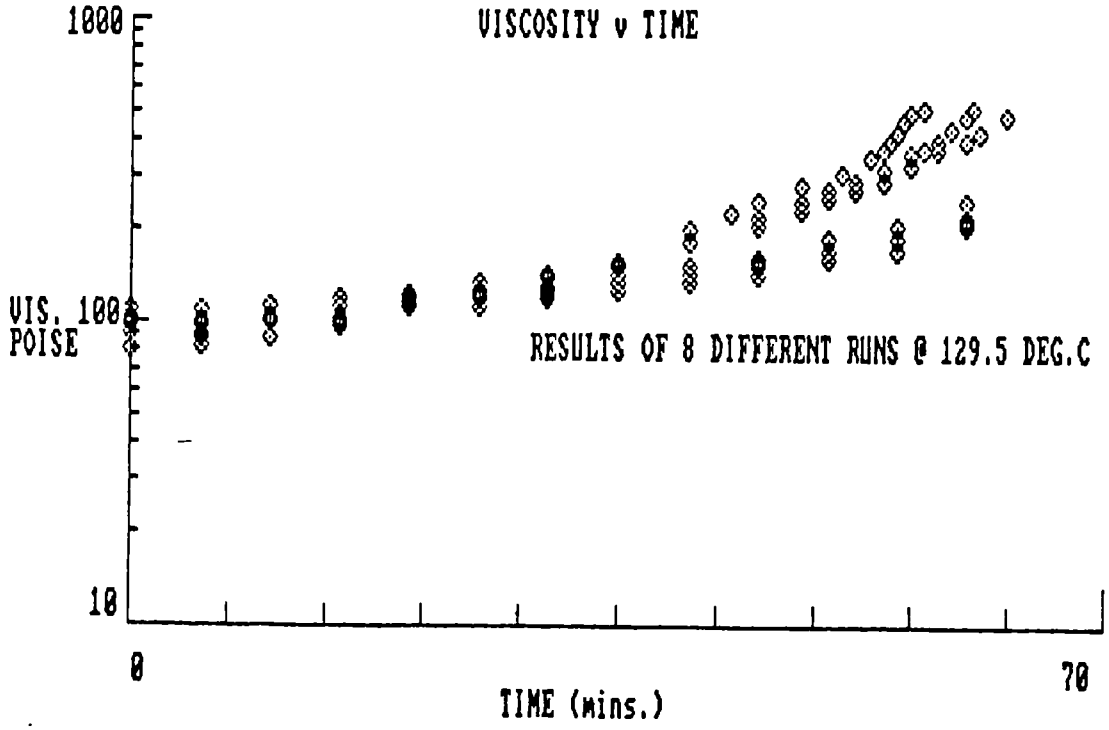
VISCOSITY v TIME
1000
VIS. 100
POISE
10
RESULTS OF 8 DIFFERENT RUNS @ 129.5 DEG.C
0
70
TIME (mins.)

FIG.(68)

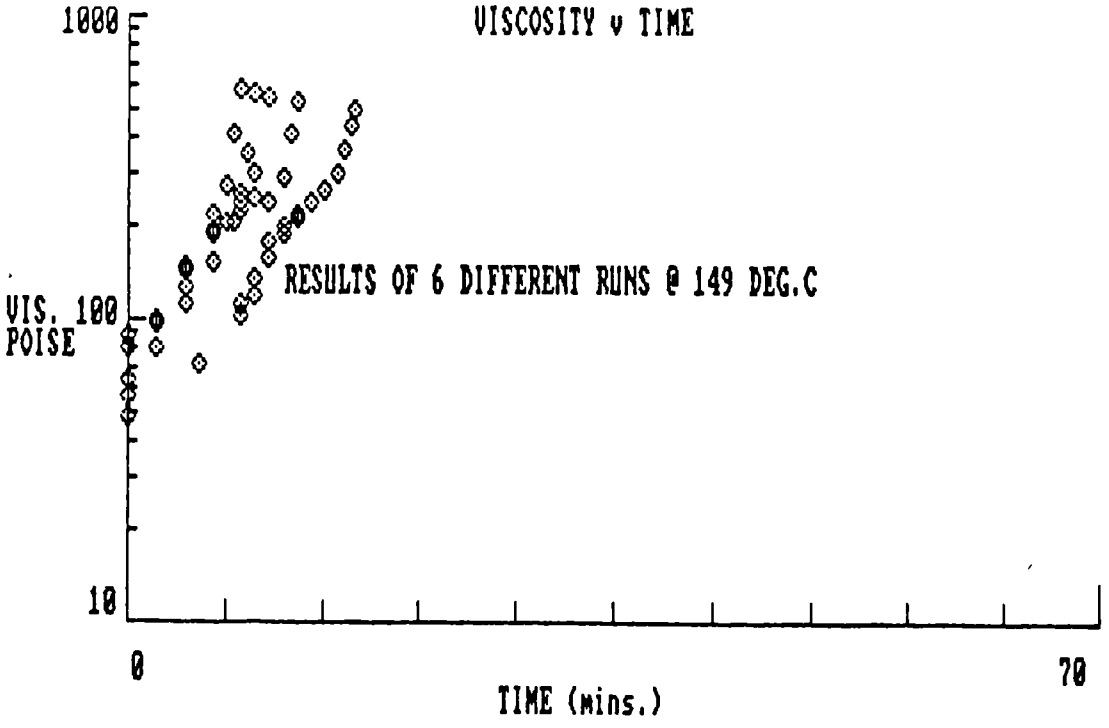
VISCOSITY v TIME
1000
VIS. 100
POISE
10
RESULTS OF 6 DIFFERENT RUNS @ 149 DEG.C
0
70
TIME (mins.)

FIG.(69)

The resin samples for these experiments were selected over a period of months and originated from different batches and the behaviour in these plots is therefore representative of that expected of the BSL 914 resin system.

It is noted in the above plots that the scatter both in the zero-time viscosity and in the time-dependent viscosity values increase with increased temperature. Further the scatter in the time-dependent viscosity increases with increased time at temperature.

In order to minimise these effects the following two modifications to normal experimental procedures were developed.

5.2.2.1 Resin Sample Shape

At ambient temperature the resin sample is normally in the form of a small irregular shaped blob of gummy material following its removal off the backing release paper of the resin film rolls. Such blobs of resin contained an uncontrolled amount of entrapped air. Further entrapment of air occurs on placement of the resin on the viscometer hot plate as the resin, due to the lowering of its viscosity, spreads outwards in an irregular manner thereby trapping bubbles. The temperatures at which the viscosity determinations are undertaken are never high enough for the viscosity to decrease sufficiently for the natural escape of these air bubbles during the three minutes dwell prior to lowering the cone into contact with the flat plate.

Under such circumstances therefore a sample to sample variation in the viscosity would be expected since entrapped air would influence the reaction torque on the rotating cone. This effect would be more severe near zero time in the experiment as air bubble re-distribution within the resin would require time to stabilise.

This problem was substantially overcome by deaeration of the resin in a specially designed container so that after de-aeration a lenticular shaped lozenge of resin was obtained. For this purpose a shallow depression was machined in a PTFE block as shown in the

cross-sectional view in Fig.(67b). During evacuation in an oven at 70°C for 10 minutes the resin frothed and expanded in volume initially as shown but finally collapsed to the convex lenticular shape shown with no entrapped air bubbles inside.

After cooling the resin sample is easily removed and on placement on the viscometer hot plate the resin flows outwards from its point of contact with the plate without any air being trapped.

The zero-time viscosity scatter was reduced by the use of this technique. Some scatter in the zero-time viscosity still persists however and this is probably due to sample variation in DICY particle size in the proximity of the cone apex.

5.2.2.2 Meniscus Effect

During cone rotation the resin contained in between the cone and plate as shown schematically by the hatched region in Fig.(67a) has normally a convex meniscus as indicated at the outer periphery of the cone. For optimum performance of the viscometer it is required that the resin be in contact with the whole of the cone surface from the apex up to the outer rim.

On the other hand no excessive amount of resin should exude out from in between the surfaces since the effect of which would be to introduce a thick ring of resin surrounding the cone. This peripheral ring of resin, outwards of the cone, would differentially rotate with the cone due to the laterally transmitted viscous traction forces. Thus, unknown forces act on the cone's outer diameter.

Further in the case of the resin measurements at temperatures higher than ambient the effective diameter at which these forces act is variable due to the fact that the resin is cooler in the meniscus surface since the latter is exposed to air at ambient temperature. Near zero-time therefore the viscosity in the outer resin ring would be higher that that of the resin in between the viscometer surfaces and the effective diameter at which the peripheral forces act

would be minimised. As cure advances however the reverse is the case since the viscosity in the resin ring would be less than that of the bulk and hence the effective diameter would increase in this case.

These variable traction couples acting in the vicinity of the outer edge of the cone would have a marked effect on the measured reaction torque with an attendant variability in the derived viscosity values. These factors would be more severe during advanced cure and result in the observed scatter of the time-dependent viscosity in Figs.(68) and (69).

In practice it is impossible to weigh exactly an amount of resin to ensure a constant meniscus profile in the test. The volume of resin in the differentially rotating ring was therefore maintained constant by the addition of a scavenging knife the purpose of which was to remove excess resin in a manner as can be described by reference to Fig.(67c).

A steel knife with the profile shown in the plan view of the cone and plate was clamped to the hot plate. During cone rotation the inertial forces in the differentially rotating ring enabled the excess resin to be collected in a pool in front of the knife edge as shown. At optimum position of the knife, approximately 0.5mm from the cone rim the shape of the resin meniscus is as shown in the sectional view in Fig.(67c).

By this means less scatter in the time-dependent viscosity is obtained especially at the longer times. The time-dependent viscosities so obtained are generally at the lower bound of the scatter bands as observed in Figs.(68) and (69) as expected due to the removal of the excess resin.

5.3 Experimental Results

5.3.1 Shear Rate

The flow rate of resin within prepreg laminates during their compaction is generally low since the moulding actually takes place over a relatively extended period of time of the order of tens of minutes. The rate

of shear of the resin is therefore low at all times during the consolidation process and hence the viscosities in the current work were all evaluated at a low cone rotation of 6 r.p.m. corresponding to a shear rate of $95sec^{-1}$. At this low shear rate, shear heating effects can be neglected. Also the viscosity is independent of shear rate at these low cone rotations up to 36 r.p.m. as can be seen in Fig.(70) where the shear stress in the resin is plotted against the corresponding shear rate at an isothermal temperature of 130°C. The plot is linear indicating that at these low shear rates the resin is behaving as a Newtonian fluid.

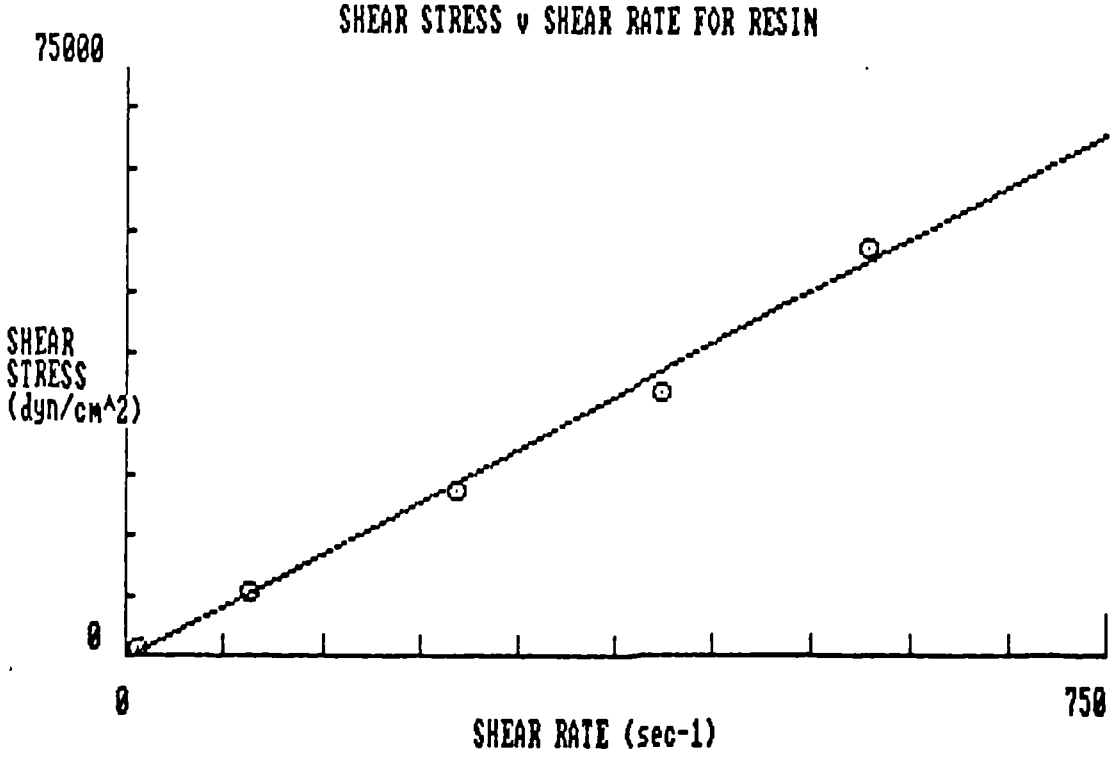

FIG.(70)

The best fit straight line through these points is given by

$$\tau = (86.5)\dot{\theta} - 381$$

with symbols as defined in section 5.2.1.

From the slope of this line the viscosity at 130°C in this specific test is therefore 86.5 Poise.

5.3.2 Isothermal Viscosity Profiles

In the current work the viscosity determinations were restricted to isothermal temperatures in the range 110°C to 150°C. Viscosities at temperatures outside this range were not determined for the following two reasons.

a) Viscosities below 110°C are not required since no prepreg consolidation should be attempted below this temperature due to the probability of the filtration of the insoluble DICY hardener at low temperature.

b) Above 150°C the cure reaction occurs at too fast a rate for the viscosity results to be meaningful above this temperature.

The isothermal viscosity profiles obtained within this temperature range will therefore be used to generate the mathematical model.

On comparison of Figs.(68) and (69) it is noted that the zero-time viscosity is lower at the higher temperature than that at the lower temperature. Also the time-dependent viscosity increases at a greater rate at the higher temperature following the behaviour as described in section 5.1.

This behaviour applies generally throughout the temperature range 110°C to 150°C as can be observed in Fig.(71) where typical experimentally determined viscosity profiles at various isothermal temperatures are shown.

For these viscosity determinations a time limit of 70 minutes was established for the experimental runs at temperatures lower than 130°C since longer times at any temperature are not normally encountered in the autoclave moulding cycle. Further, tests at higher temperatures than 130°C were arrested at times at which the viscosity approached 1000 Poise since it is currently considered that negligible resin flow occurs in prepreg laminates at higher viscosities than this level. There

is also a viscometer use aspect in that if the resin cures in between the cone and the plate then extreme difficulty in their separation would ensue if cure were to advance too far.

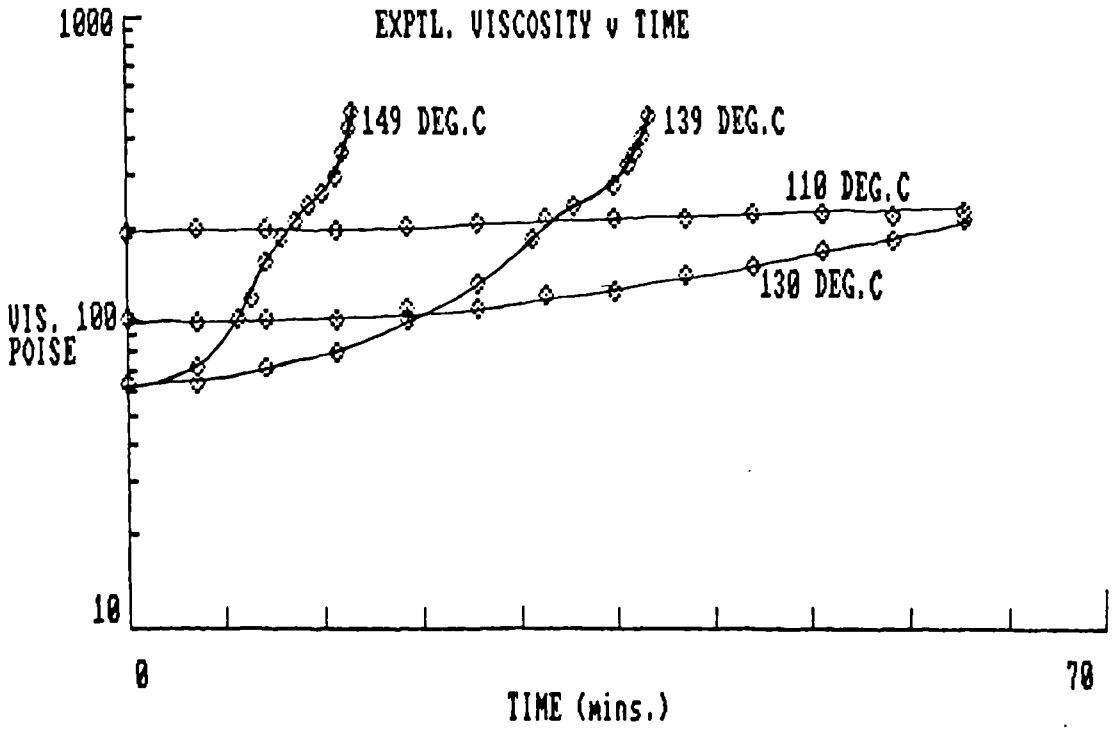

FIG.(71)

On returning to Fig.(71) it will be observed that at 110°C and 130°C the viscosity profiles are smooth curves whereas the curves at 139°C and 149°C exhibit humps at the 200 Poise level. The existence of these humps (which do not consistently occur in repeat runs at the same temperature) has not been satisfactorily explained but they could arise due to either torque measurement non-linearity or material effects occurring during the solution of the DICY hardener in the resin. For the purpose of modelling in the current work therefore the viscosity profiles will be assumed to be smooth at all isothermal temperatures.

Numerous experimental determinations of viscosity at a number of isothermal temperatures were carried out during the course of this work with the result that the experimentally determined values will only be shown graphically in the following sections to

avoid excessive tabulation of data.

The experimental results on which the mathematical model is based include those derived by the modified methods as described in sections 5.2, 5.1 and 5.2.2.2 as well as values determined prior to the incorporation of these modifications.

The model as will be described in the following sections will reasonably represent the viscosity behaviour of the BSL 914 resin system in its practical environment.

5.4 Approaches To Viscosity Modelling

Broadly speaking there are two approaches to the modelling of the melt viscosity behaviour of polymeric materials.

In one approach the viscosity is related to one or more of the fundamental properties of the material i.e. the viscosity is related to the molecular weight of the polymer, its molecular free volume or molecular chain lengths (ref.47).

A notable example is in the use of the Williams, Landel and Ferry (WLF) equation where the viscosity of a thermoplastic polymer is related to the basic material property, the glass transition temperature, Tg, of the polymer as follows (ref.47).

$$\log(v/v_{Tg}) = -C_1(T-Tg)/(C_2 + T-Tg) \qquad (5.7)$$

where v is the viscosity at temperature T and v_{Tg} that at Tg, C_1 and C_2 are material dependent parameters. This equation is applicable in the range $Tg < T < (Tg + 100)$

Eq.(5.7) can be modified for use with epoxy resins as described in refs.50 and 8.

An approach based on any of the fundamental properties of the materials as above requires experimentation in addition to that of viscosity determination as undertaken in the current work.

The alternative approach is to develop a model based on the phenomenological behaviour of the viscosity

with time and temperature. In essence this approach involves the application of curve fitting techniques to the experimentally determined viscosity time profiles at a number of isothermal temperatures.

A number of equations so derived can be found in the literature to describe the time-temperature viscosity behaviour of epoxy resins. Two such equations are given below:-

From ref.51

$$\log v = C_1.\frac{[10^{A_1/T}]}{T^2}\ (t) + \log[C_2.\frac{(10^{A_2/T})}{T^2}]$$

where C_1, C_2, A_1 and A_2 are constants and t, T are time and temperature respectively.

From refs.52 and 5

$$\ln v(t) = \ln v_\infty + E_v/RT + tk_\infty \exp E_k/RT$$

where v_∞, k_∞ are empirical constants, R is the gas constant, E_v and E_k are apparent activation energies.

In the current work a phenomenological model will be developed where the viscosity time profile at any isothermal temperature can be adequately described within the limits of viscosity and time as described in section 5.3.2 by means of quadratic equations with time as the independent variable.

Also in common with all of the above models the zero-time viscosity at any isothermal temperature will be found to follow an Arrhenius form.

5.5 Generation Of Model

Due to the large changes in viscosity from 10 to 10^3 Poise in the practical situation during the time of measurement then it is standard practice to display the viscosity in logarithmic form (to base 10) as shown in Figs.(68), (69) and (71). The initial steps in the development of the model was to fit quadratic curves to these empirical viscosity curves. A typical quadratic

fit to experimental data is shown in Fig.69 for an isothermal temperature viscosity profile at 138.8°C.

The Lagrange interpolation technique was used to evaluate the coefficients of the quadratic. The procedure was to choose three data points inclusive of the zero-time value so that a best fit curve could be obtained by subjective judgement, typically as shown in Fig.(72). The Lagrange method was preferred to least squares techniques since it enabled curves to be plotted which were not influenced by the presence of humps in some of the experimental plots as described in section 5.3.2.

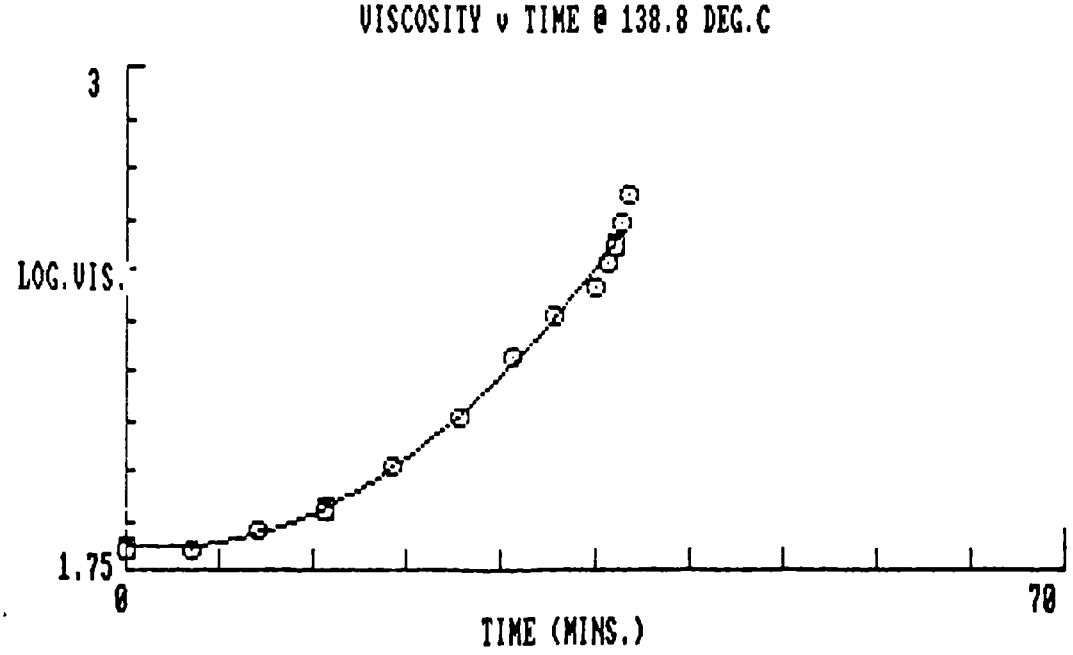

FIG.(72)

The equation of the viscosity curve at any isothermal temperature is therefore of the form

$$\log v = At^2 + Bt + C$$

where the coefficients A,B and C are constants and v is the viscosity at time t.

At zero-time however

$$C = \log (\text{zero-time viscosity}) = \log v_o$$

and the equation for the viscosity profile therefore takes the form

$$\log v = At^2 + Bt + \log v_o \qquad (5.8)$$

The terms involving t in eq.(5.8) thus represent the time-dependent viscosity behaviour.

All the coefficients in eq.(5.8) are functions of temperature as follows.

In Fig.(73) the values of log v_o are plotted versus temperature from the tabulated values in Table 32. As can be observed from the figure the value of log v_o (and hence zero-time viscosity, v_o) decreases with temperature. The Arrhenius form of this temperature dependency is shown in Fig.(74) where the equation of the least squares best fit line is given by

$$\log v_o = (2566.243)(1/T°K)-(4.42193) \qquad (5.9)$$

fitted with a correlation coefficient of 0.8300.

From eq.(5.9) an apparent activation energy for viscous flow is obtained and is given by

$$Ev_o = 11.74 \text{ kcal/mole } (49\text{kJ/mole}) \qquad (5.10)$$

The variation in the coefficient A with temperature is as shown in Fig.(75) from the values in Table 33. From this plot the value of A increases rapidly at temperatures above 130°C. This behaviour is consistent with the fact that the time-dependent viscosity increases at a faster rate the higher the temperature and hence At^2, the predominant time dependent viscosity contribution in eq.(5.8), increases accordingly.

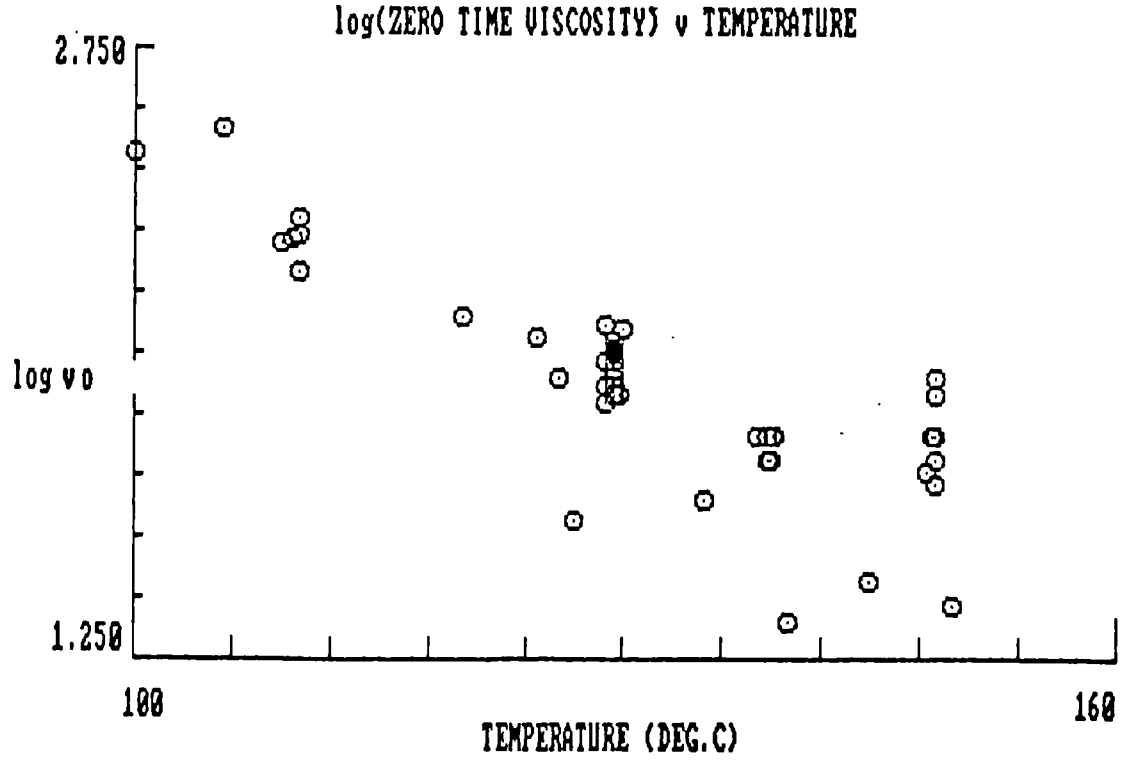
log(ZERO TIME VISCOSITY) v TEMPERATURE
2.750
log v o
1.250
100
160
TEMPERATURE (DEG.C)

FIG.(73)

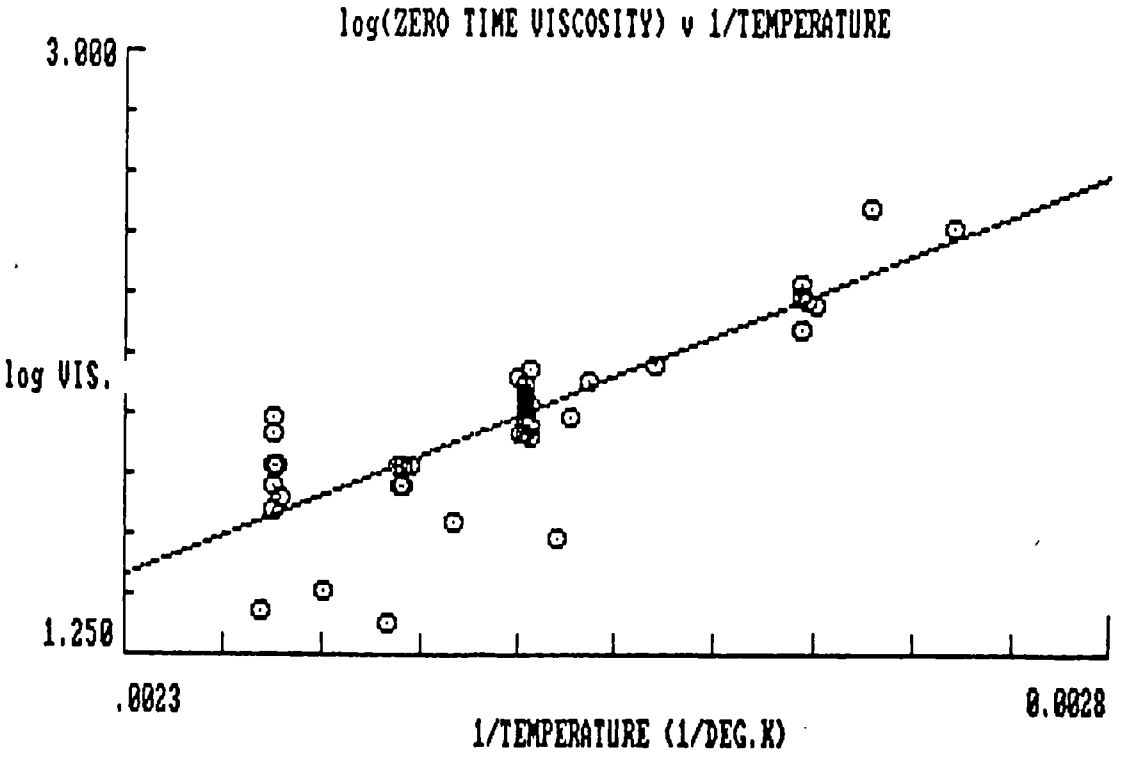
log(ZERO TIME VISCOSITY) v 1/TEMPERATURE
3.000
log VIS.
1.250
.0023
0.0028
1/TEMPERATURE (1/DEG.K)

FIG.(74)

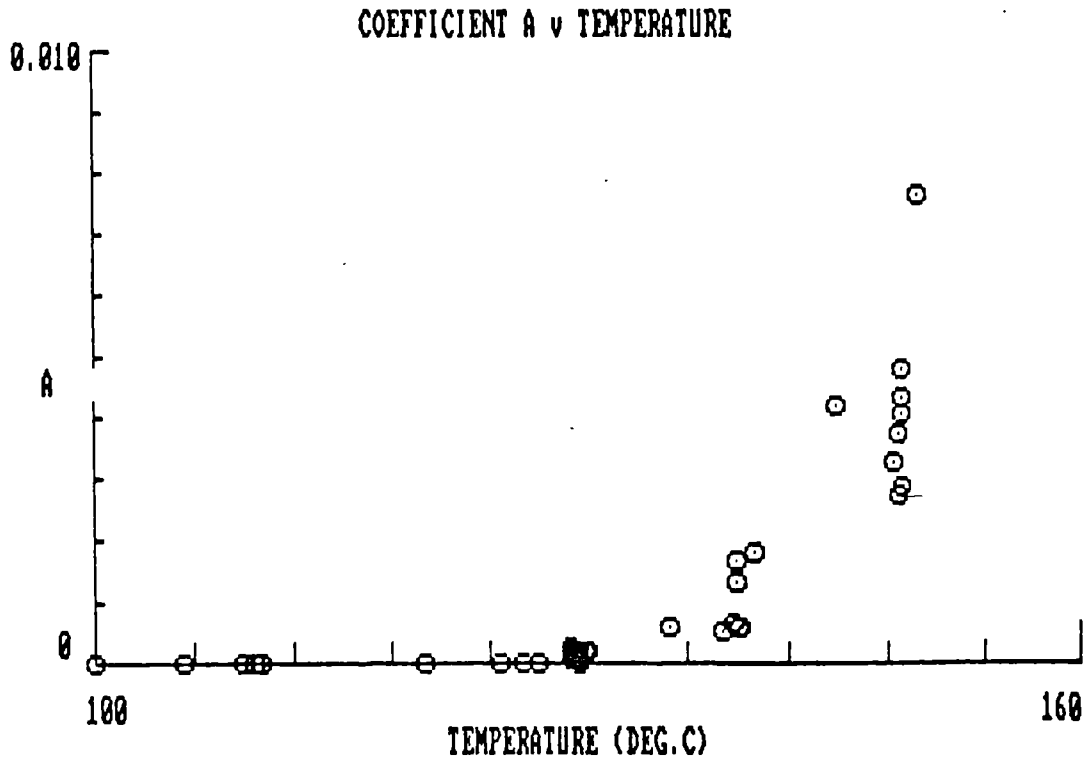
COEFFICIENT A v TEMPERATURE
0.010
A
0
100
160
TEMPERATURE (DEG.C)

FIG.(75)

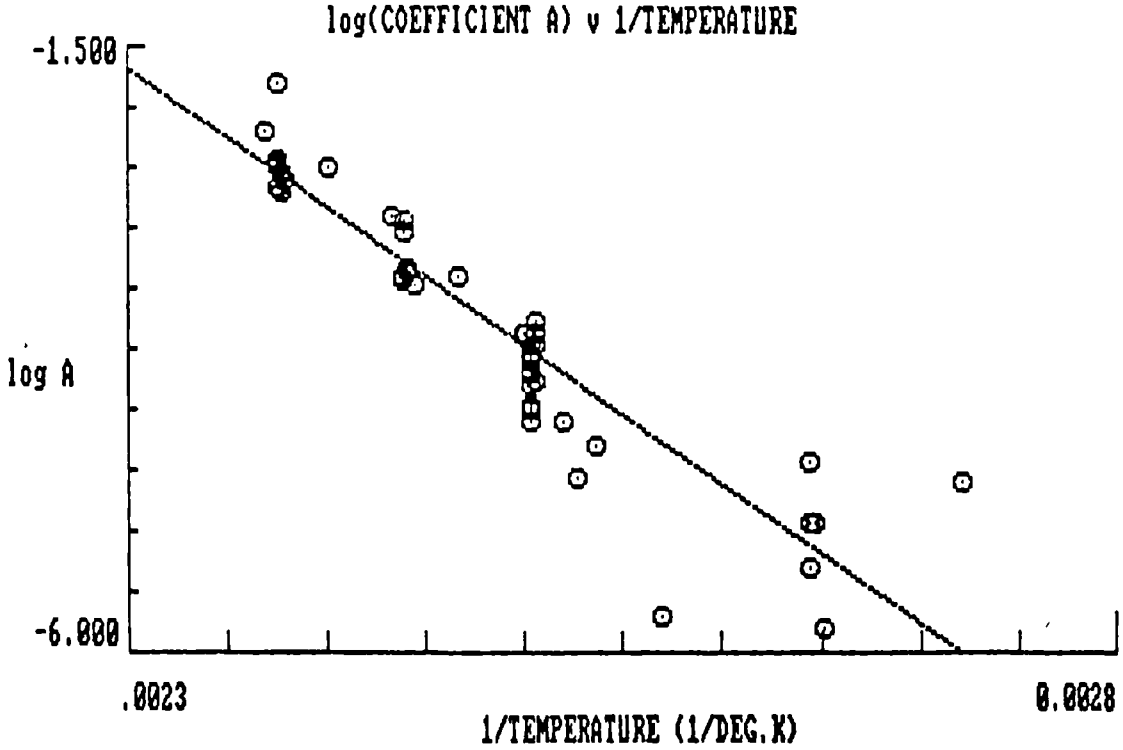
log(COEFFICIENT A) v 1/TEMPERATURE
-1.500
log A
-6.000
.0023
0.0028
1/TEMPERATURE (1/DEG.K)

FIG.(76)

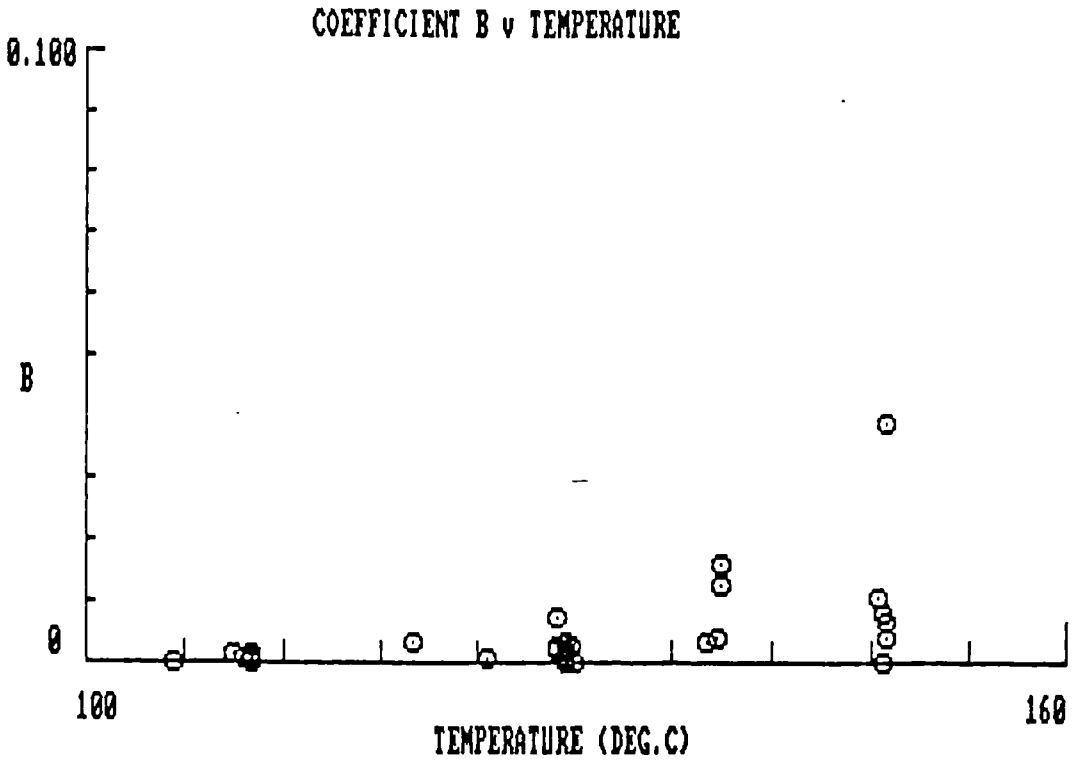
COEFFICIENT B v TEMPERATURE
0.100
B
0
100
160
TEMPERATURE (DEG.C)

FIG.(77)

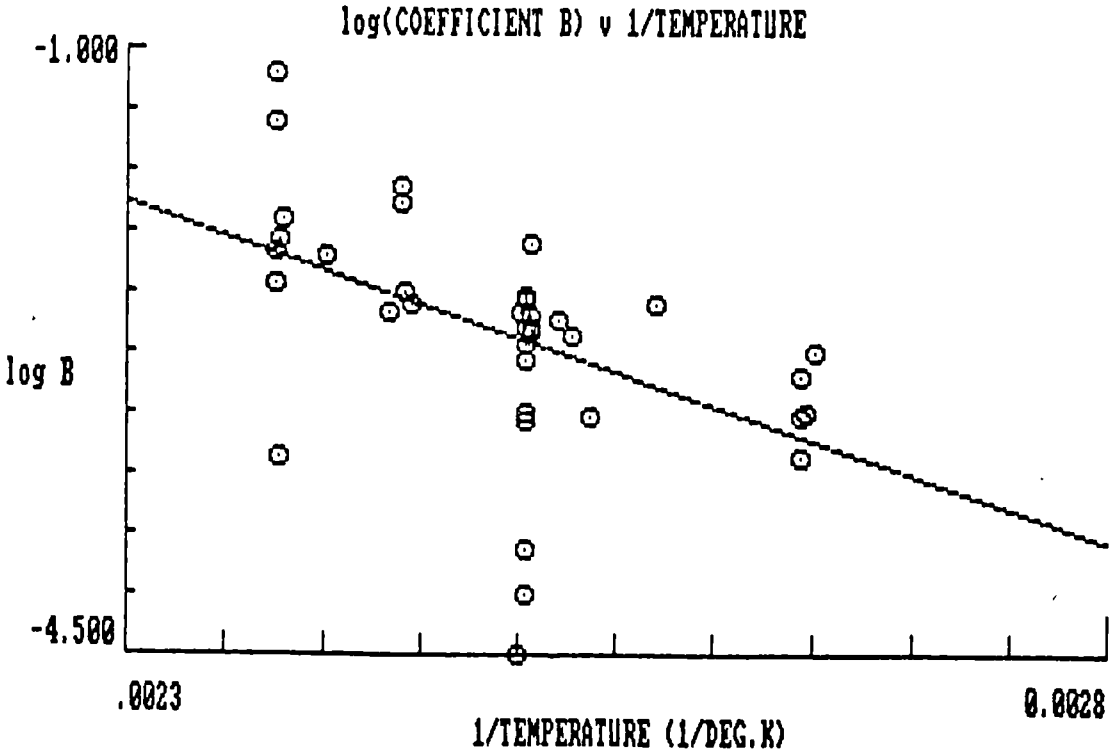
log(COEFFICIENT B) v 1/TEMPERATURE
-1.000
log B
-4.500
.0023
0.0028
1/TEMPERATURE (1/DEG.K)

FIG.(78)

If log A is plotted against reciprocal temperature a plot as shown in Fig.(76) is obtained. The equation of the straight line fit is given by.

$$\log A = (-11457.69)(1/T°K)+(24.69417) \quad (5.11)$$

fitted with a correlation coefficient of 0.9185.

In the same manner by plotting coefficient B against temperature in Fig.(77) from Table 34 and log B versus reciprocal absolute temperature in Fig.(78) the dependence of B on absolute temperature is given by

$$\log B = (-4387.629)(1/T°K)+(8.210288) \quad (5.12)$$

fitted with a correlation coefficient of 0.4839.

In the above plots, Figs.(73) to (78) inclusive a fair degree of scatter in the plotted values is observed. Reasonable correlations however exist in the equations for the temperature dependence of the zero-time viscosity and the coefficient A respectively in eqs.(5.9) and (5.11). The correlation coefficient for the coefficient B in eq.(5.12) is however low but since B varies much less than A with temperature the error associated with the determination of B will not seriously affect the viscosity value.

Due to the scatter as above care must be exercised when comparing individual experimental viscosity profiles with that predicted by the model incorporating the above parameters which are based on average values of a large number of experimental tests. From the scatter in Fig.(74) it is estimated that the zero-time viscosity is accurate to within ±30 Poise with the maximum error occurring at 150°C.

Equations (5.8), (5.9), (5.11) and (5.12) thus constitute a model by means of which the viscosity behaviour of the BSL 914 resin system can be predicted with reasonable accuracy.

Typical outputs of the model with parameters as

defined above are shown in Fig.(79) in the range 100°C to 170°C. Values outside of the range 110°C to 150°C are extrapolated values obtained by the use of the same model parameters. The curves shown are similar in form to the experimental results in Fig.(71).

Direct comparison of the model output at two isothermal temperatures viz 110°C and 139°C are shown in Figs.(80) and (81) respectively. From Fig.(80) it is noted that the model prediction lies within the scatterband of experimental results. The same conclusion can be applied to the comparison at 139°C as shown in Fig.(81) although more scatter is evident in the experimental plot at this temperature.

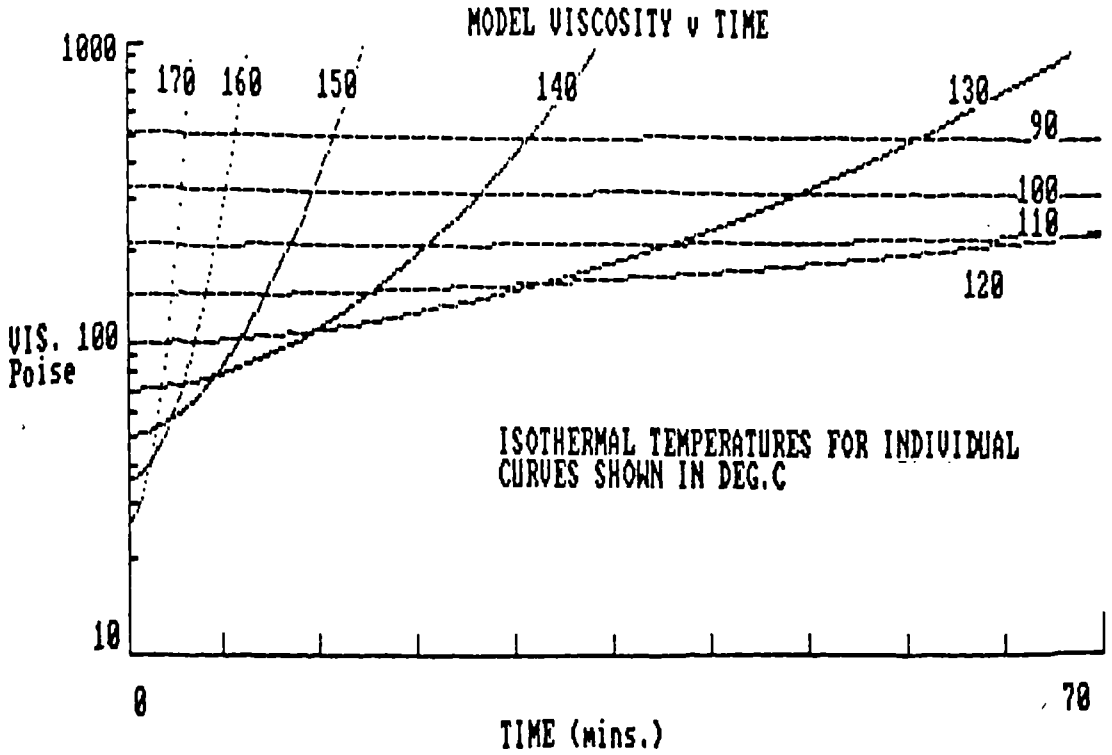

FIG.(79)

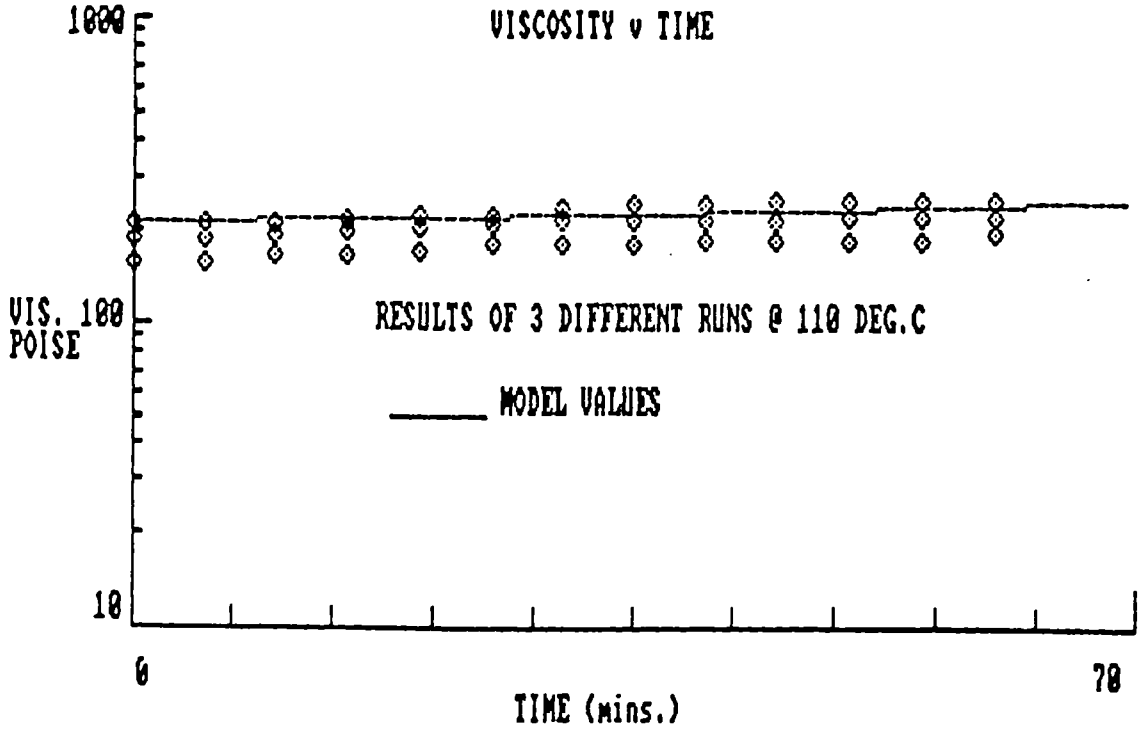
1000
VISCOSITY v TIME
VIS. 100
POISE
RESULTS OF 3 DIFFERENT RUNS @ 110 DEG.C
MODEL VALUES
10
0
70
TIME (mins.)

FIG.(80)

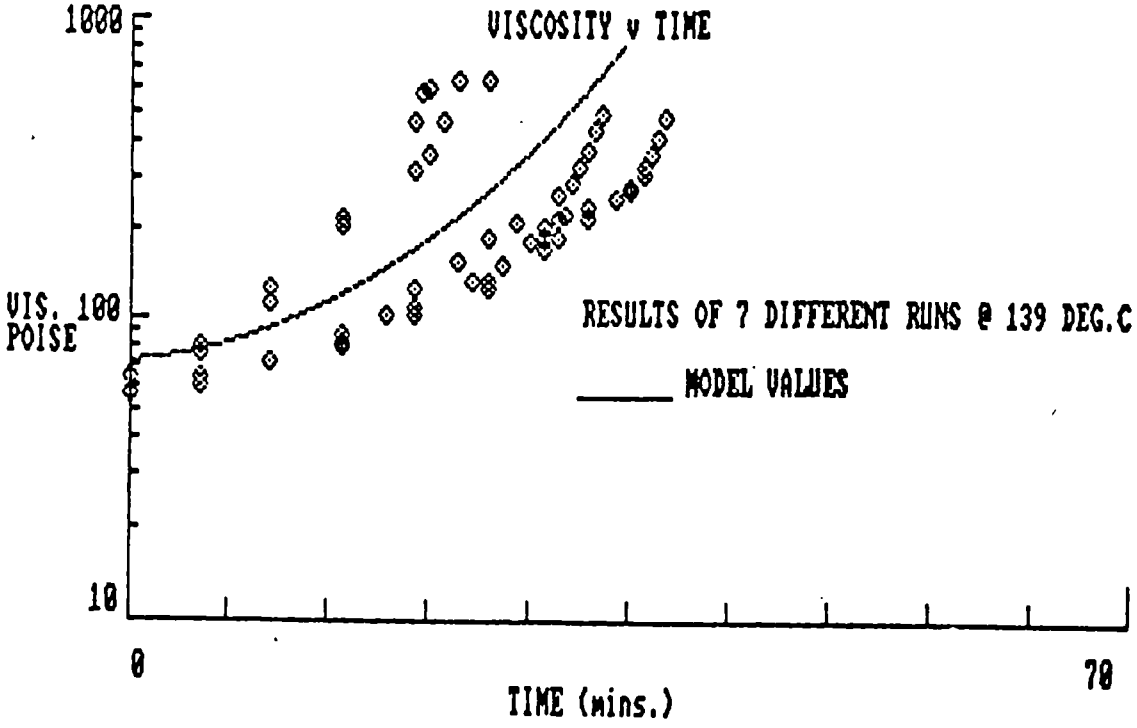
1000
VISCOSITY v TIME
VIS. 100
POISE
RESULTS OF 7 DIFFERENT RUNS @ 139 DEG.C
MODEL VALUES
10
0
70
TIME (mins.)

FIG.(81)

5.6 Representation Of Viscosity Data

A clearer representation of viscosity predictions by use of the model can be obtained by means of a 3-D surface plot as shown in Fig.(82) where the viscosity variation with time and temperature can be visualised.

Of more interest however is the iso-viscosity contour plot as shown in Fig.(83) where contours of viscosities in Poise as indicated are mapped onto the temperature-time plane. In the hatched region in this figure the resin viscosity has a value in between 100 and 200 Poise. This region of the diagram is of practical significance in that these contours define the viscosity limits between which compaction of the prepreg laminates can be successfully accomplished in the autoclave cycle i.e. the viscosity time windows in Chapter 1.

Practical experience has indicated that it is difficult to obtain void free composites if the resin viscosity is lower than 100Poise during pressurisation of the lay up. The reason for potential void generation with lower resin viscosities is that excessive outflow of resin would occur from the lay up with consequent depletion of matrix resin. On the other hand if the viscosity exceeds 200 Poise inadequate consolidation will occur due to insufficient resin outflow during the compaction period prior to resin gelation.

The hatched region therefore represents a time-temperature 'window' of conditions by which laminate consolidation can be successfully accomplished.

On consideration of the shape of the hatched region the advantages of the BSL 914 resin system in comparison to other commercially available resins for practical applications become apparent. Due to the thermoplastic addition in the epoxy resin the viscosity is generally higher at all temperature than the viscosity of alternative resin systems. Also the BSL 914 resin

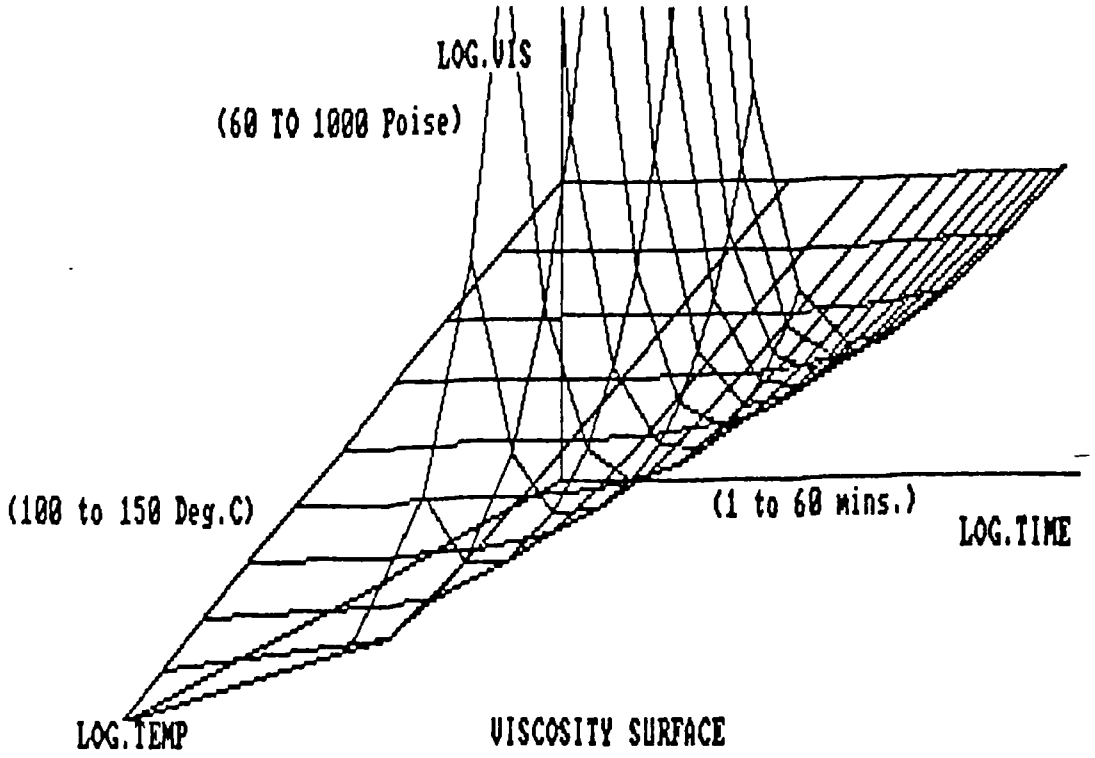
LOG.VIS
(60 TO 1000 Poise)
(100 to 150 Deg.C)
(1 to 60 mins.)
LOG.TIME
LOG.TEMP
VISCOSITY SURFACE

FIG.(82)

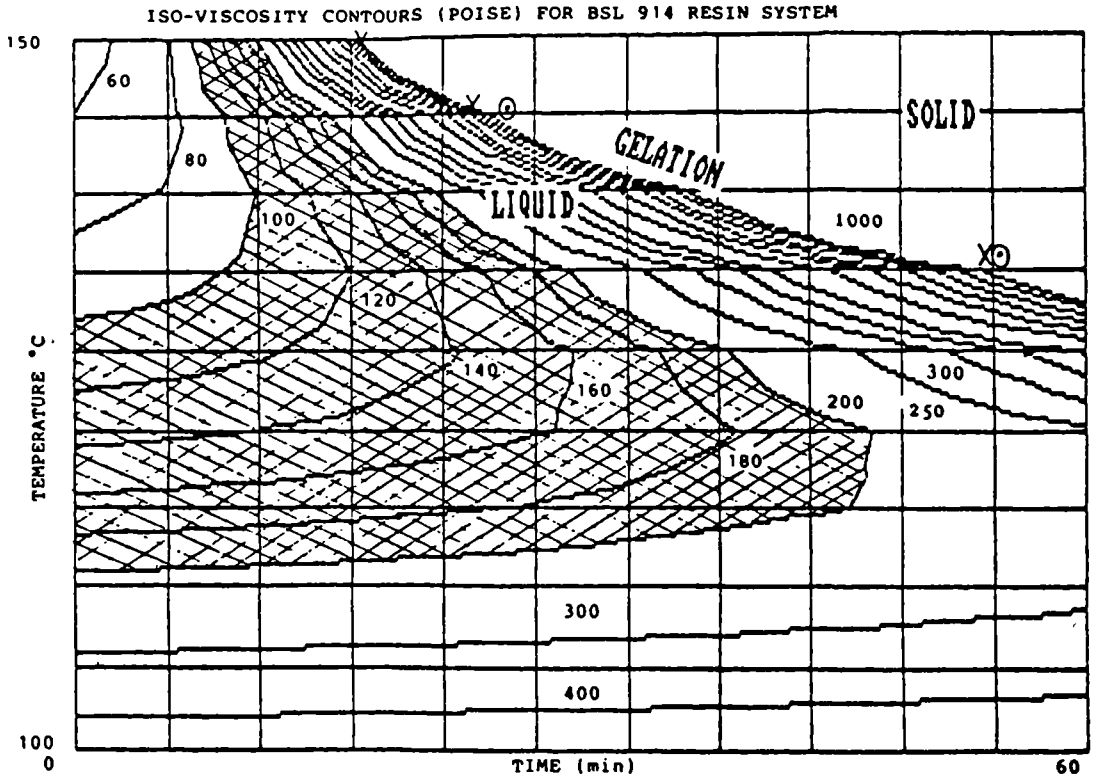
ISO-VISCOSITY CONTOURS (POISE) FOR BSL 914 RESIN SYSTEM
150
100
0
TEMPERATURE °C
TIME (min)
60
SOLID
GELATION
LIQUID
60
80
100
120
140
160
180
200
250
300
1000
300
400

FIG.(83)

system has a long residence time at all temperatures between 110°C and 130°C prior to the resin viscosity exceeding 200 Poise. For the above two reason therefore the BSL 914 resin system is a 'tolerant' system in that in practical applications, especially in the moulding of large structures, ample leeway exists in the dwell time for controlled viscosity flow at all temperatures. Laminate consolidation can therefore be successfully achieved with the added advantage that process control is not overcritically dependent on temperature ramp rate or isothermal dwells at temperatures.

The diagram in Fig.(83) can be regarded as a minor portion of a wider time-temperature-transformation (TTT) diagram by which material phase changes can be visualised (see also refs.53 and 54). Thus in Fig.(83) the viscosity contours are increasingly compressed together as the 1000 Poise contour is approached indicating that the resin viscosity is rising at a faster rate in this region. It is noted if the gel time at temperature, as measured in section 4.3.2, is plotted as shown by X on the diagram that the gelation time essentially coincides with the viscosity contour in the region of 1000 Poise. It is therefore clear from this diagram that the gelation line represents the boundary between the liquid and the solid phases of the resin.

It is of interest also to note that by plotting the half-life of the resin indicated by 0 points as computed by means of the cure sub-model described in the previous chapter that the half-life time also coincides with the gelation line. Thus from this diagram gelation occurs at approximately 0.5 conversion of the resin.

5.7 Chemorheological Model

The models for resin cure and viscosity as described in the previous sections have defined the cure and viscosity as independent functions of time. It has been shown that both viscosity and the cure behaviour with time under isothermal conditions can be represented reasonably accurately for the BSL 914 resin system.

These models are most useful therefore for shop floor practice since the chemical and rheological properties of the resin can be directly linked to the process time.

Since however both the viscosity and the cure are functions of the same single variable, time, then the viscosity can be expressed as a function of conversion whereby a chemorheological model will be obtained. From refs.5, 55, 56 and 6 the viscosity v at a resin conversion α can be represented by

$$v = v_\infty \exp(U/RT + K\alpha) \qquad (5.13)$$

where v_∞ is a constant, U is the activation energy of viscosity and T is the absolute temperature.

In natural logarithmic form eq.(5.13) takes the form

$$\ln v = \ln v_\infty + (U/RT + K\alpha) \qquad (5.14)$$

Eq.(5.14) can be rewritten as

$$\ln v = A + K\alpha \qquad (5.15)$$

where

$$A = U/RT + \ln v_\infty \qquad (5.16)$$

Thus by plotting lnv versus α the values of A and K can be obtained from the intercept and slope respectively in eq.(5.15).

Values of cure and viscosities at various times at a number of isothermal temperatures were obtained by the use of the cure-time and viscosity-time models already described and plots of lnv versus α so obtained are shown in Fig.(84). It will be observed that these plots are linear up to 0.3 conversion at all temperatures. Also the best fit lines for individual temperature plots are essentially parallel and from the slope of the lines therefore the constant K is

independent of temperature as already stated.

From eq.(5.16) by plotting the values of A obtained from the intercepts of the graph in Fig.(84) against reciprocal temperature then from eq.(5.16) a linear graph as shown in Fig.(85) is obtained and the equation of the straight line fit is given by.

$$A = (5633.715)(1/T°K)-(9.324397) \qquad (5.17)$$

From eq.(5.17) the activation energy for viscosity is found to be

$$U = 11.2 \text{ kcal/mole } (46.8\text{kJ/mole})$$

and the constant v_∞ is

$$v_\infty = 8.92 \times 10^{-5} \text{ Poise}$$

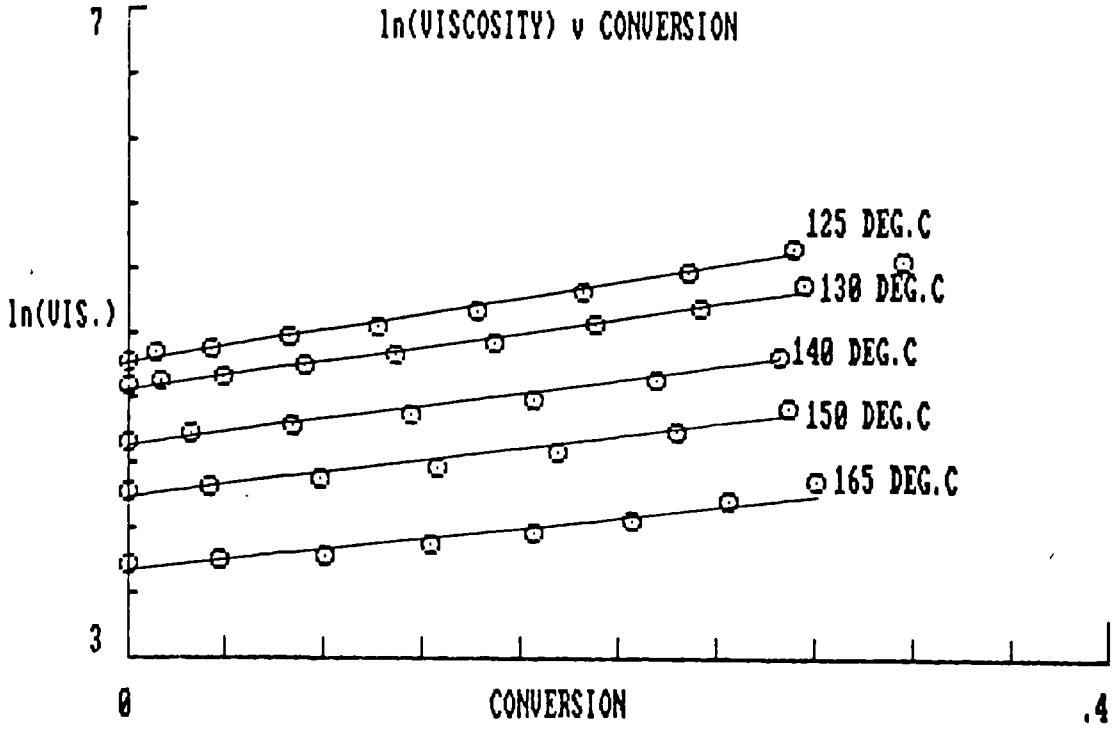

FIG.(84)

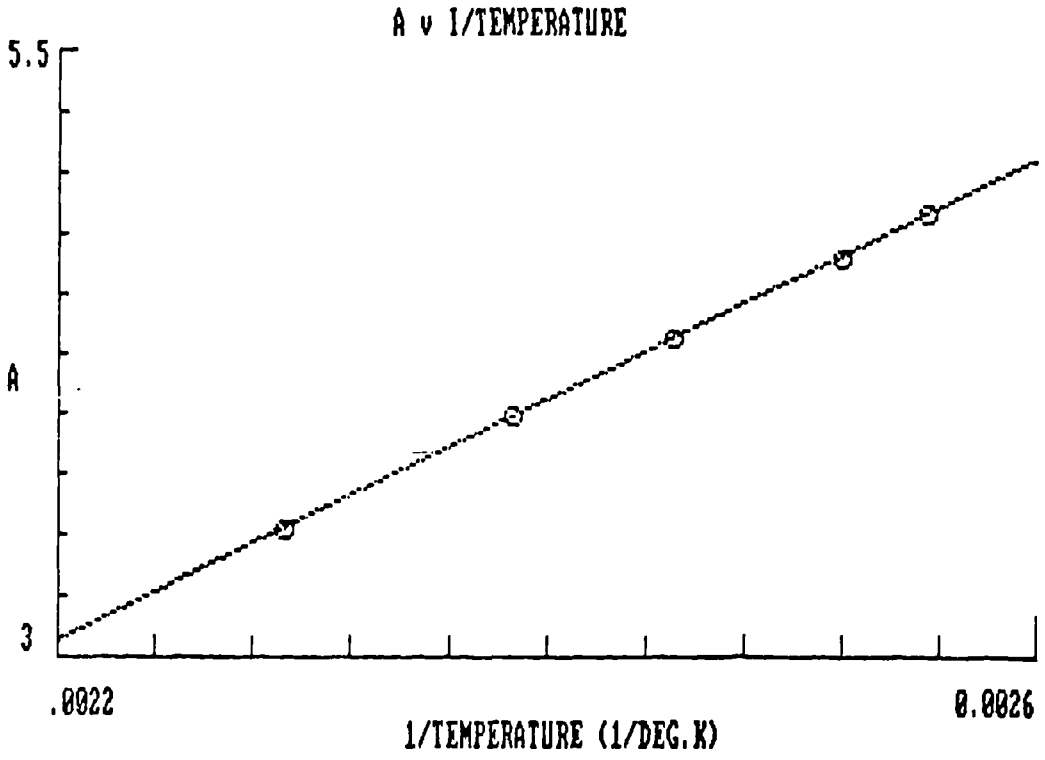

FIG.(85)

All the constants in eq.(5.13) are therefore known and a chemrheological model relating the resin viscosity to its degree of cure at any isothermal temperature is obtained up to a maximum resin conversion of 0.3. At degrees of conversion greater than 0.3 the plots in Fig.(84) become non-linear due to the fact that resin gelation is approached and eq.(5.13) becomes inapplicable.

CHAPTER 6

COMPUTER SIMULATION

6.1 Dynamic Model

So far in the text models for the prediction of BSL 914 resin system cure and viscosity behaviour under isothermal conditions have been developed. In practical moulding situations however artefacts are seldom manufactured under solely isothermal conditions. Normally temperature ramps are encountered in addition to isothermal holds; the choice of moulding cycle being dependent on the overall dimensions and wall thickness of the moulded component.

In the case of the moulding of small structures for instance, rapid temperature rise of the combined tooling and lay-up can be achieved in an autoclave. In order to dissipate the exothermic heat of reaction an isothermal dwell is incorporated in the moulding cycle. In the case of large structures however isothermal dwells may even be excluded altogether since low temperature ramp rates up to full cure temperatures have to be used in order to ensure that the tooling attains its correct temperature at all times during the moulding cycle. As a result of the slow temperature rise in such cases the resin attains maximum cure at the end of the ramp time.

In order for a mathematical model to be useful for the simulation of the physical and chemical changes that occur in the resin during a moulding cycle,it must be able to accommodate the varied temperature profiles that may be encountered in shop floor practices.

In this Chapter the manner by which a dynamic computer model is generated will be described by means of which the prediction of cure and viscosity for BSL 914 resin system can be predicted following thermal

treatments of the form of isothermal dwell only, or a linear temperature ramp only or a combination of a linear temperature ramp followed by an isothermal dwell. The exothermic heat of reaction will also be simulated by the computer model under the same temperature conditions as above.

The computer program generated has been written in IBM BASIC language and is suitable for use on an IBM, or compatible, personal computer with printout and high resolution graphics facilities. The programme requires only 6737 bytes of memory and can therefore be stored on a flexible or floppy disc.

6.2 Models For Temperature Ramp Conditions

The cure and viscosity behaviour of the resin can both be modelled for a linear temperature ramp by representing the ramp as a series of isothermal steps of short duration. The manner by which these models for cure and viscosity respectively in the dynamic mode are generated will be described as follows.

6.2.1 Ramp Cure Model

From eq.(4.9) the rate of cure with time under isothermal conditions is given by

$$d\alpha/dt = (k/F)(F\alpha)^n(1-F\alpha)^m \qquad (6.1)$$

with symbols as defined in section 4.4.

By integration of eq.(6.1) as described in Chapter 4 the cure at any time during an isothermal dwell can be obtained if the values of the constants k, F, n and m for that temperature are included.

By representing a linear temperature ramp as a series of isothermal steps and applying eq.(6.1) with the appropriate values of k, F, n and m for each step then the cure at the end of the ramp time can be approximated by the summation of the contribution to cure evaluated by integration of eq.(6.1) for each step.

Thus if α_R is the cure at the end of the ramp then

$$\alpha_R = \sum_{i=1}^{N} \left[\int_0^t (k(T_i)/F(T_i)(F(T_i)\alpha)^{n(T_i)}(1-F(T_i)\alpha)^{m(T_i)}\, dt \right] \quad (6.2)$$

where the ramp is divided into N intervals of time each equal to t. At the isothermal step temperature T_i, the values of the other constants for the i-th step viz $k(T_i)$, $F(T_i)$, $n(T_i)$ and $m(T_i)$ are evaluated by the appropriate equations from Chapters 2 and 3.

The value of α_R in eq.(6.2) is dependent on the number of intervals, N, to which the total ramp time (or temperature) has been divided. Thus by applying eq.(6.2) to a ramp of 3°C/min in the temperature range 110°C to 175°C then the value of α_R is 0.3399 when N is chosen to be 20. If N is chosen as 100 and 300 then the value of α_R is found to be 0.3436 and 0.3440 respectively. Therefore from the value of α_R calculated for these three different N values as described it is concluded that the integration converges satisfactorily for N greater than 100 and that α_R is constant to the third decimal place.

The cure versus time for a ramp rate of 3°C/min from 110°C to 175°C is shown in Fig.(86) calculated by means of eq.(6.2) where the value of N was 200. The integral in eq.(6.2) was calculated numerically for each step by means of the modified Euler method as described in section 4.5.2.

In Fig.(86) the theoretically determined cure profile is compared to experimental values obtained from a DSC dynamic exotherm produced by a resin sample at the same ramp rate of 3°C/min. The experimental values were determined as described in section 2.3.1 with α defined relative to the heat of reaction H(dyn) as described in section 3.4.

From Fig.(86) therefore it is seen that good agreement exists between the model prediction and experimentally determined values of cure advancement with time under conditions of a linear temperature ramp.

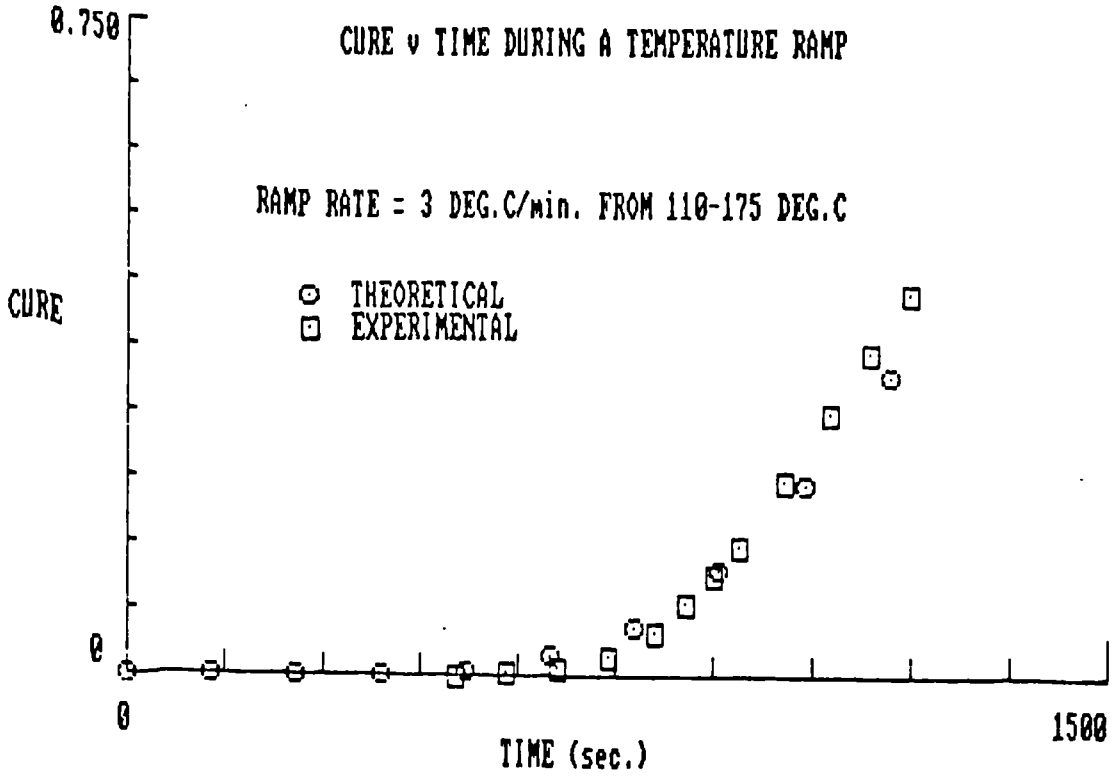

FIG.(86)

6.2.2 Exotherm Model

From section 6.1 it is important that the exothermic heat generated by the cure reaction is dissipated by heat transfer to the autoclave tooling at all stages during the moulding cycle otherwise uncontrolled reactions would occur in the matrix resin with consequent degradation in its physical and mechanical properties. In practice this heat dissipation is achieved by limiting the temperature ramp rate or by introducing isothermal dwells as described.

A knowledge of the exothermic heat generation to be expected in any moulding cycle is therefore useful for the design of moulding cycles and this can be obtained from the cure model as follows.

In eq.(6.1) the rate of reaction $d\alpha/dt$ is given in terms of conversion α, with both $d\alpha/dt$ and α being defined relative to the total heat of reaction H(dyn) (see section 3.5.1).

From section 3.4 however

$$d\alpha/dt = (dq/dt)/H(dyn)$$

where dq/dt is the heat flow which is therefore

given by

$$dq/dt = H(dyn)d\alpha/dt$$

In the case of a linear temperature ramp therefore the heat outflow at the end of each time step in eq.(6.2) can be evaluated by simply inserting the conversion calculated at the end of each step into eq.(6.1) with the relevant k, F, n and m values for the step temperature and multiplying by H(dyn).

Similar calculations apply for the isothermal dwell.

A comparison of the model prediction with experimental results obtained from DSC at a ramp rate of 3°C/min in the temperature range 110°C to 175°C is shown in Fig.(87) where it can be observed that reasonable predictions of both exotherm onset and heat flow over the whole of the temperature range is obtained.

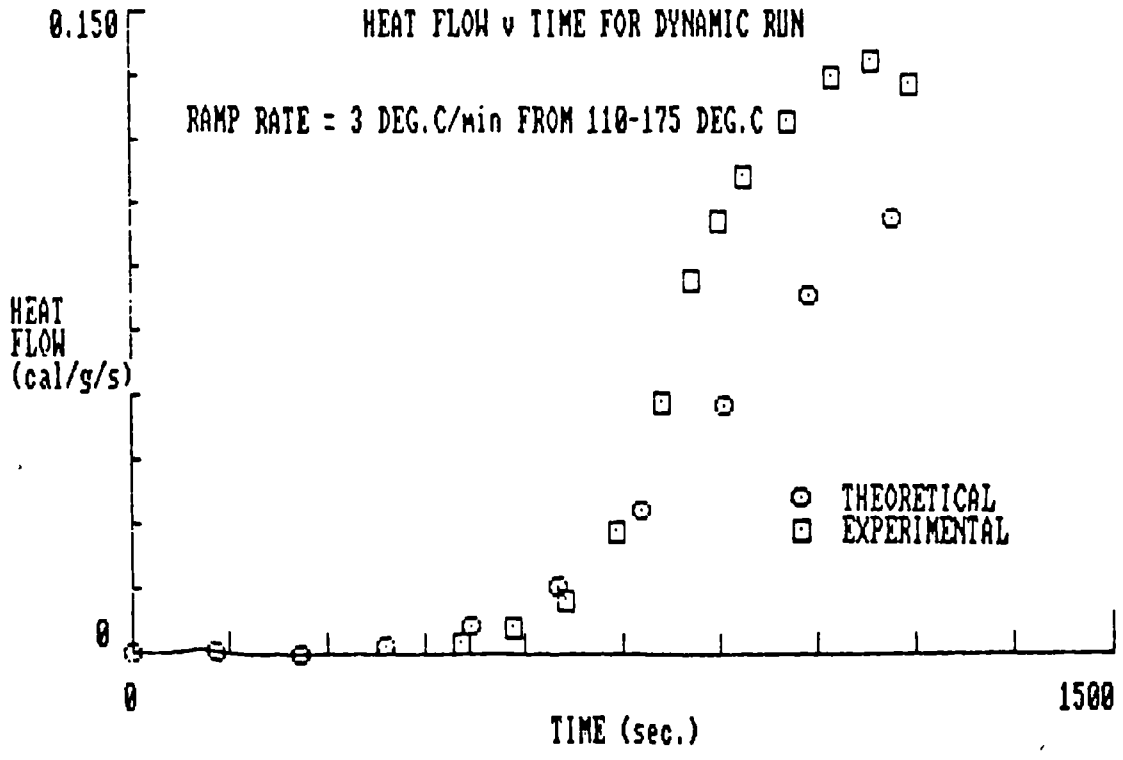

FIG.(87)

6.2.3 Ramp Viscosity Model.

The viscosity changes of the resin under linear temperature ramp conditions can also be modelled in a similar manner to the cure modelling by representing the

temperature ramp by a series of isothermal steps of short duration as follows.

From Chapter 5 it will be recalled that the viscosity of the resin at any time under isothermal conditions can be considered as the sum of the zero-time viscosity and a time dependent viscosity at that temperature.

From eq.(5.8) by rearrangement the viscosity v at time t is given by

$$\log v = \log v_o + (At^2 + Bt) \qquad (6.3)$$

with coefficients as described in Chapter 5 and where the bracketed terms represent the time dependent viscosity.

For a temperature ramp represented by N isothermal steps each of duration t the viscosity , v_R at the end of the ramp is given by

$$\log v_R = \log v_{OR} + \sum_{i=1}^{N} [A(T_i)t^2 + B(T_i)t] \qquad (6.4)$$

where v_{OR} is the zero time viscosity at the end of the ramp which is evaluated by means of eq.(5.9); $A(T_i)$ and $B(T_i)$ are the coefficients of the quadratic equation eq.(6.3) at the isothermal step temperature T_i obtained by dividing the ramp temperature range by N and multiplying by i.

The viscosity, v_R, so evaluated is a function of the number of intervals, N, as shown in Fig.(88) where the variation of viscosity with tempeature in the range 110°C to 175°C for different values of N in the range 20 to 400 is shown. The summation in this case does not converge to a limit with the result that the viscosity apparently increases at a faster rate with temperature the higher the value of N. Further the minimum viscosity for each curve occurs at a lower temperature the greater the value of N. The optimised value of N in this case therefore has to be determined by comparison of the

theoretical curves, obtained by varying N, with an experimentally determined viscosity profile under identical ramp conditions.

It will be recalled from Chapter 5 however that viscosities under isothermal conditions only could be determined by the cone and plate viscometer. In order to obtain resin viscosity behaviour under linear temperature ramp conditions for the evaluation of N therefore a dynamic mechanical spectrometer was used.

The specific instrument used was a Rheometrics Dynamic Spectrometer, RDS-7700. This spectrometer is useful for the dynamic mechanical testing of materials whereby the viscoelastic properties of the test material can be determined.

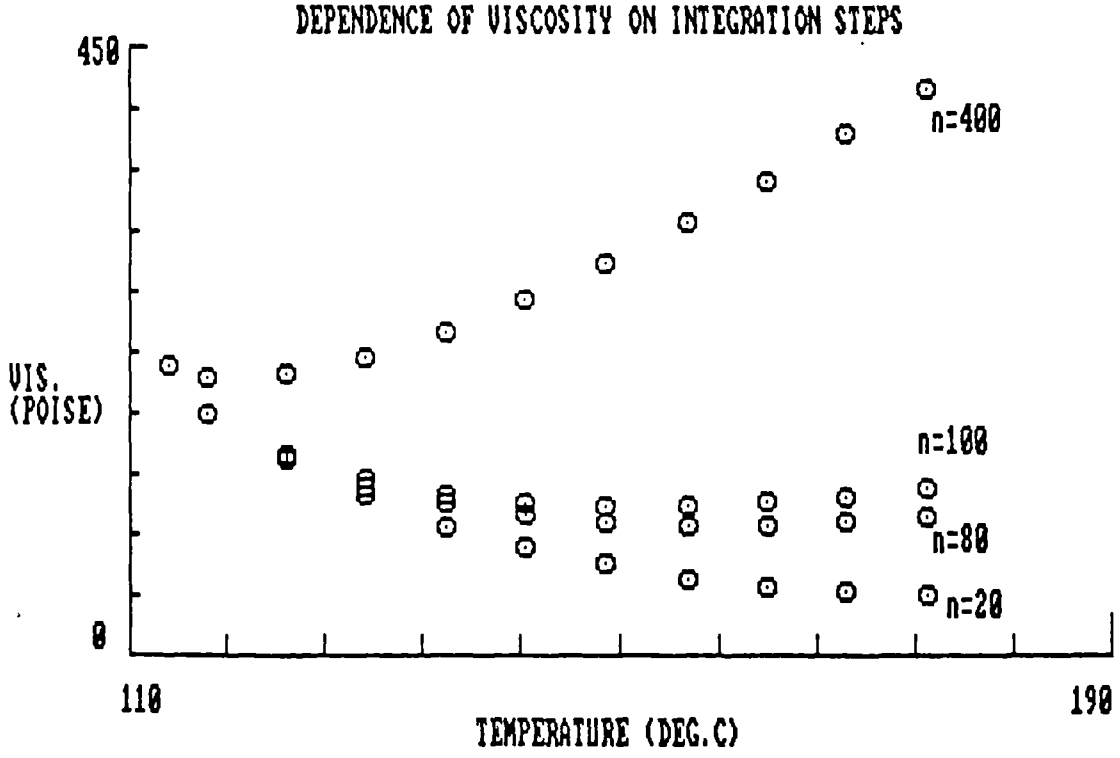

FIG.(88)

For the test in the current work a sample of resin was placed in the controlled gap in between the faces of two equidiameter, 50mm, circular plates. One of the circular plates oscillated at a controlled frequency and amplitude relative to the fixed plate. The whole was enclosed in a tubular furnace by means of which a controlled linear temperature rise could be maintained.

During the test the restoring torque acting on

the sinusoidally oscillating plate was continuously monitored and from the torque, frequency and amplitude values the complex viscosity v^* of the resin is obtained which mathematically consists of a real and imaginary part as follows (see ref.47).

$$v^* = v' - iv''$$

where the real part v' is given by

$$v' = G''/W$$

and the imaginary part v" is given by

$$v'' = G'/W$$

In these expressions G' and G" respectively are the storage and loss moduli of the material and W is the frequency of oscillation. For the storage modulus the shear stress in the resin is in phase with the applied strain whereas for the loss modulus the resulting stress is 90° out of phase with the strain.

The in-phase or real component v' above is the dynamic viscosity of the resin and at low frequencies of oscillation v'approaches the values of the ordinary steady flow viscosity or shear viscosity as determined by means of a cone and plate viscometer.

In the current work a strain of 10% (corresponding to the amplitude of the circular plate oscillation) was imposed on the resin and the frequency of oscillation was 100 radians/sec.

A typical viscosity profile obtained by means of the mechanical spectrometer is shown in Fig.(89) (ref.57). In this figure the viscosity profile for the BSL 914 resin system is shown when thermally processed under a linear temperature ramp of 3°C/min in the range of 40°C to 175°C. It will be noted that the viscosity (ETA axis) decreases with time until a minimum viscosity is reached at approximately 42 minutes corresponding to a temperature of 166°C. Thereafter the viscosity increases

rapidly with time.

A comparison of these experimentally determined values with those theoretically predicted by means of eq.(6.4) with N equal to 200 is shown in Fig.(90) in the temperature range 110°C to 175°C. From this figure it is noted that both the time of occurrence and the value of the minimum viscosity is predicted reasonably accurately for this value of N.

From the practical moulding point of view knowledge of this viscosity minimum and its time of occurrence is of fundamental importance since the consolidation of prepreg laminates can be accomplished most efficiently at this point in a moulding cycle.

In Fig.(90) it is observed that an overestimate of the viscosity at times less than the viscosity minimum time is obtained by means of the model whereas viscosities are underestimated at times greater than that of the viscosity minimum. This behaviour is attributed to the differences in the two experimental techniques used for viscosity determinations. This conclusion is confirmed by consideration of Figs.(91) and (92).

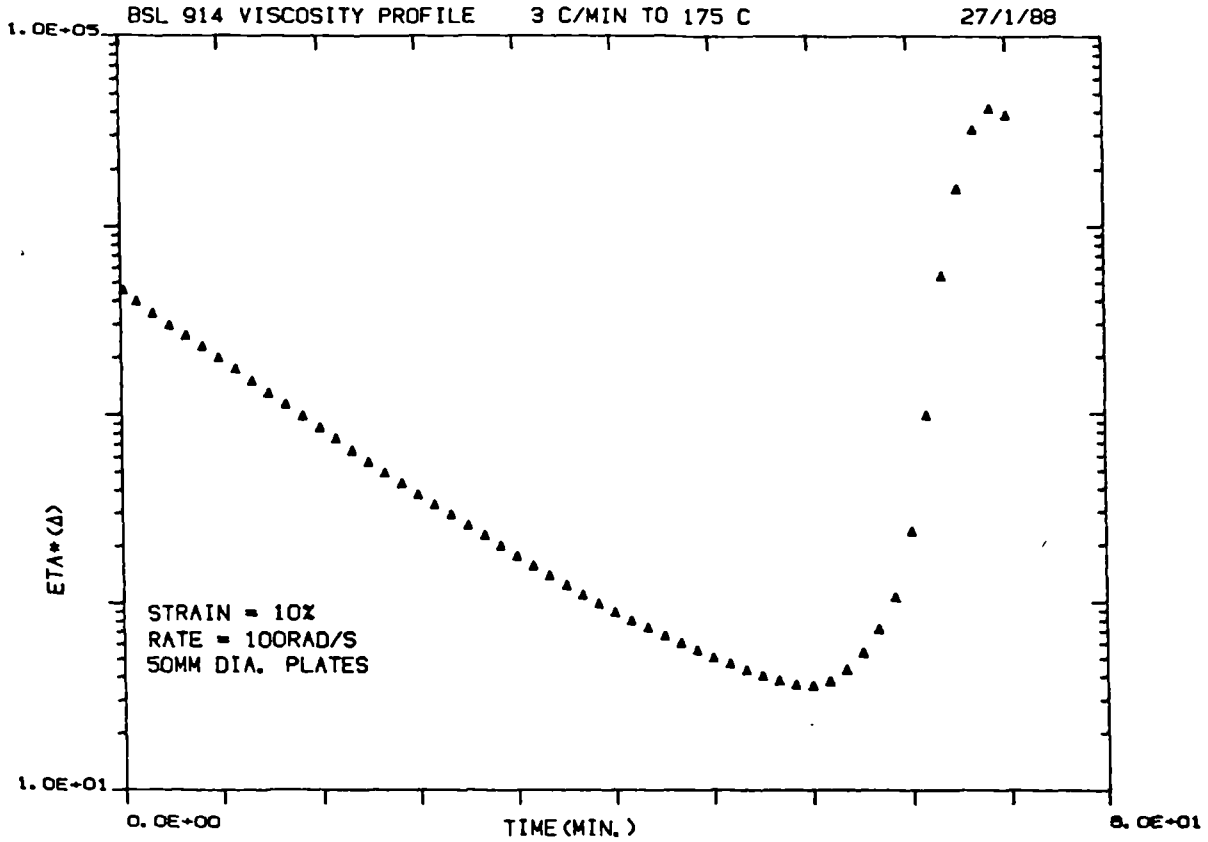

FIG.(89)

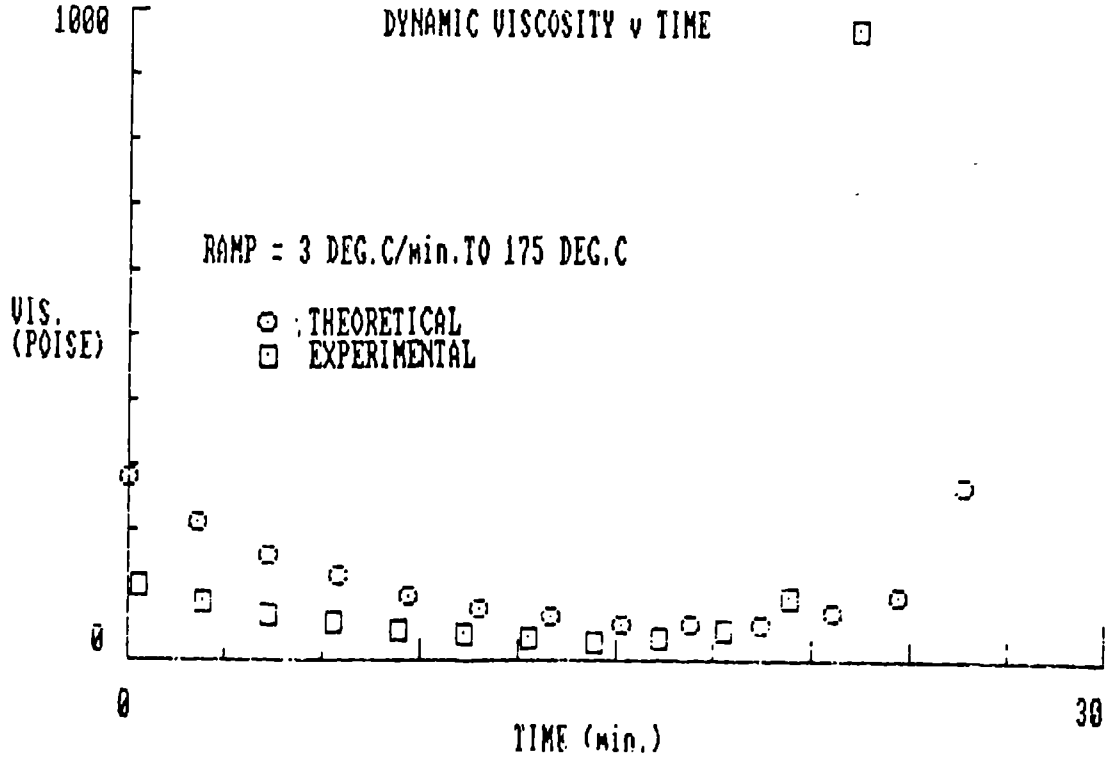
1000
DYNAMIC VISCOSITY v TIME
RAMP = 3 DEG.C/min.TO 175 DEG.C
VIS.
(POISE)
THEORETICAL
EXPERIMENTAL
0
0
30
TIME (min.)

FIG.(90)

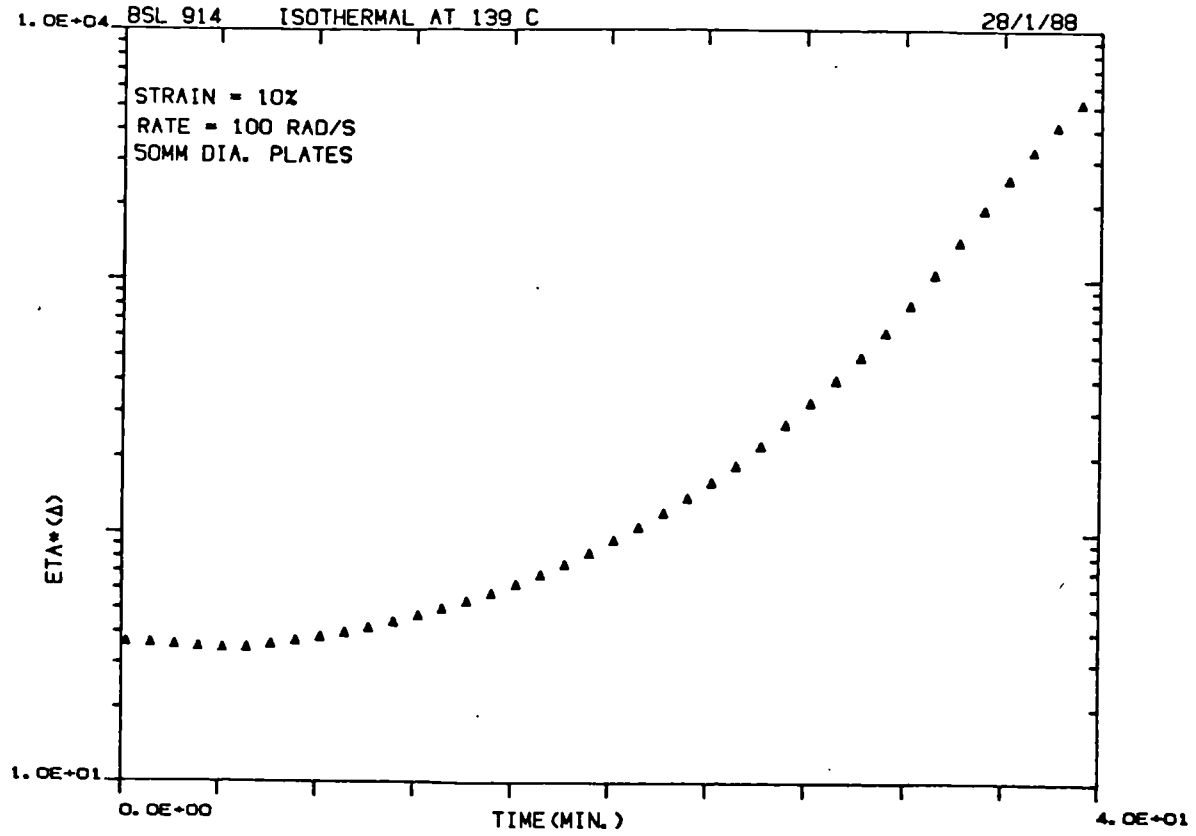
1.0E+04
BSL 914
ISOTHERMAL AT 139 C
28/1/88
STRAIN = 10%
RATE = 100 RAD/S
50MM DIA. PLATES
ETA*(Δ)
1.0E+01
0.0E+00
TIME(MIN.)
4.0E+01

FIG.(91)

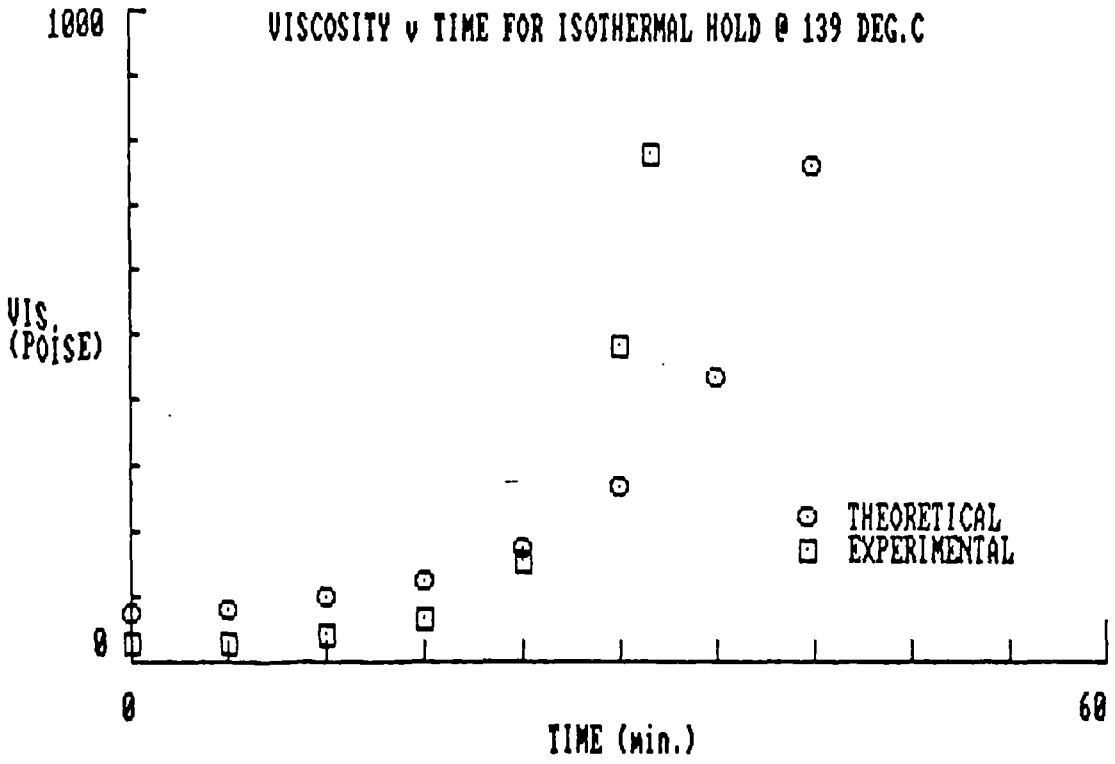

FIG.(92)

In Fig.(91) the resin viscosity profile obtained by the mechanical spectrometer at an isothermal temperature of 139°C is shown. This profile is compared with the model prediction at the same isothermal temperature in Fig.(92) and it is noted that the viscosity as experimentally measured by means of the spectrometer rises at a faster rate than that predicted by the model which is based on cone-plate viscometry results as described in Chapter 5.

Bearing in mind the slight discrepancies in these experimental results obtained by the two different techniques it is therefore considered that by means of the model based on isothermal cone-plate viscometry reasonable prediction of the resin viscosity both under isothermal and dynamic temperature conditions can be obtained.

6.3 'VISICURE' Computer Program

In this section the details of a computer program, titled 'VISICURE' will be given. By means of this program cure advancement and viscosity changes in the resin during a simulated cure cycle can be obtained.

The program is based on the mathemtical models for cure, viscosity and exotherm characteristics of the BSL914 resin systems as described in the text.

The program is written in IBM BASIC version 2.0 and can be run on an IBM personal computer or compatible.

A listing of the program is included in Appendix 2 and pertinent explanations as to structure and content are given as follows:-

6.3.1 List Of Variables

A list of the variables with their definitions is given.

Input Variables

R = Temperature ramp rate, °C/min
TF = Final ramp temperature, °C
TH = Isothermal hold time, minutes

Major Programme Variables

TX = Total run time, sec.
TR = Ramp time from 110°C to TF, sec.
TS = Isothermal dwell, sec.
SX = x-axis scale factor for total run time
ST = y-axis scale for factor for temperature in range 110°C to 200°C
SC = y-axis scale factor for conversion in range 0 to 1
SV = y-axis scale factor for viscosity in range 0 to 1000 Poise
SH = y-axis scale factor for heat outflow in range 0 to 0.3 cal/g/sec/
NR = number of intervals for ramp vicosity integration
NI = number of intervals for viscosity determination during isothermal dwell
NT = total number of intervals for viscosity determination
TP = temperature step for each interval in ramp,°C

TV = step temperature for viscosity determination, °C
XO = coefficient B as defined by eq.(5.12)
XI = initial viscosity as defined by eq.(5.9)
XT = coefficient A as defined by eq.(5.11)
Q = antilog (base 10) of XT
SR = time into isothermal dwell, minutes
W = time squared
B = antilog (base 10) XO
ZT = time dependent viscosity, Poise
VI = initial viscosity, Poise
VT = total viscosity, Poise
XL = initial time for conversion plot, sec.
YL = initial conversion at XL = 0
XH = total cycle time, sec.
N = total number of intervals in cycle
NS = number of subintervals in a single main interval
C = time
D = conversion
H = interval time, sec.
X, XV, XE, Y, YV, YE, AB, BC are plotting variables

6.3.2 Arrays

The following arrays have been used in the program.

V((NT,2) - for storage of time and corresponding viscosity at the end of each interval

A((N+1),2) - for storage of time and the corresponding conversion at the end of each interval

C(N,(NS+1) - temporary array for storage of time and the corresponding conversion at each Euler integration step

H(CN+1),2) - for storage of time and the corresponding heat flow at each step

N((N+1),2))
BV((N+1),2))For storage of graph coordinates
BH((N+1),2))

6.3.3 Function Definition

The autocatalytic function for determination of cure is defined in subroutine 30,000 as follows:-

FNRAT (C) given by eq.(3.20) or its equivalent and the auxillary variables are defined by:-

HT = isothermal heat of reaction as defined by eq.(2.9)
NT = value of index as defined by eq.(3.32)
LR = ratio of indices as defined by eq.(3.22)
RA = antilog (base e) of LR
M = value of index m
F = ratio of dynamic exotherm (115 cal/g) to HT
LNK = activation energy and pre-exponential factor as defined by eq.(3.31)

6.3.4 Structure of Program

The flow chart of the program is shown in Fig.(93).

The moulding cycle to be simulated is defined by the input parameters in subroutine 5000.

The calculations for the cure and exothermic heat evaluation are carried out in subroutine 24000. The temperature ramp is divided into (NS*N/2) isothermal dwells in line 24137. The conversion is calculated for each N/2 step and stored for plotting purposes in lines 24260 and 24270. The conversion is obtained by use of the modified Euler method carried out over NS step within each main interval as in lines 24164 to 24240 inclusive.

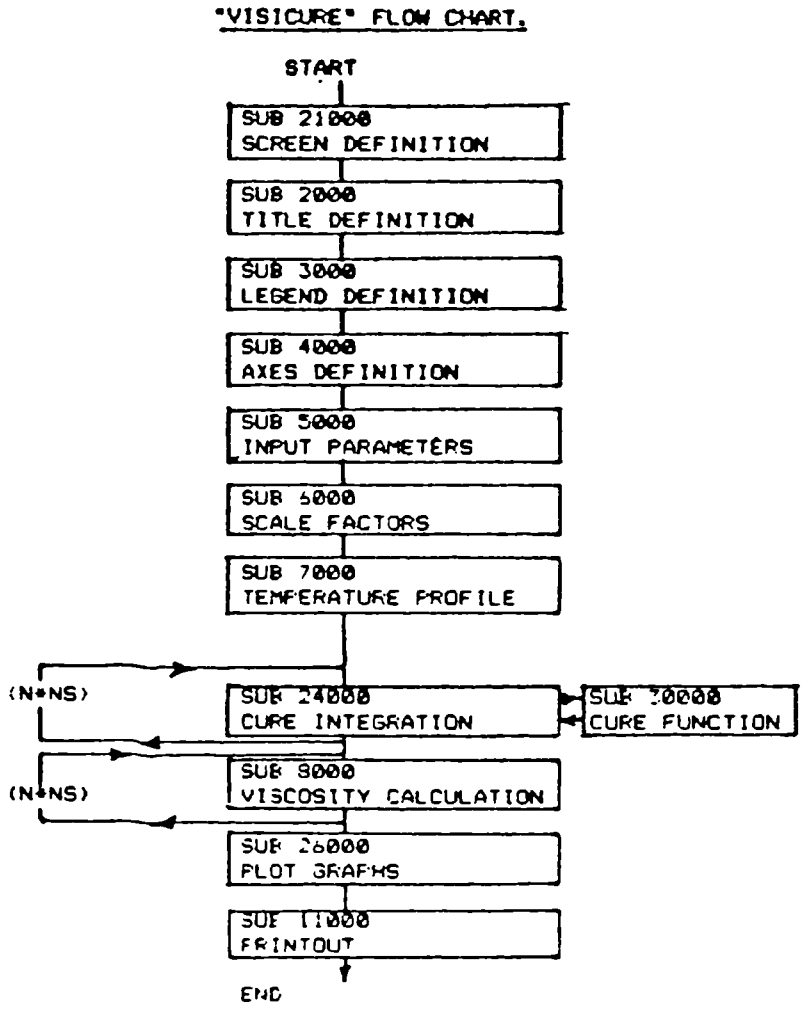

FIG.(93)

The isothermal dwell region of the simulated moulding cycle is divided into a total of (NS x N/2) time steps in lines 24139 and the integration follows the same procedure as for the ramp conversion except that since the temperature is constant, the evaluation of the autocatalytic function as defined in subroutine 30000 is not required and is therefore bypassed in line 24142.

Line 24175 defines the saturation level of the conversion.

The heat output is evaluated at the end of each main step in line 24272.

The calculations for the viscosity profile are carried out in subroutine 8000. The ramp is divided into NR steps so that increments of temperature TP as in lines

8060 are obtained with each step temperature TV being defined in line 8070. During the ramp rise time the coefficients of the quadratic viscosity equation are evaluated at each step in lines 8720, 8130 and 8740. During the isothermal dwell however the calculations are bypassed as defined in line 8090 for the remaining steps defined by SR in line 8170. Line 8295 defines the maximum viscosity limit imposed to maintain calculations within the numerical range of the computer.

The plotting of the values so calculated is controlled by subroutine 26000 and the printout by subroutine 11000.

6.4 Computer Model Output

In the concluding figures of the current Chapter , Figs.(94) to (100) inclusive examples of the output from the 'VISICURE' program are shown in the form of graphics screen prints and the accompanying numerical printout for each respective computer screen display are tabulated in Tables 35 to 41 inclusive.

In Fig.(94) the results of a simulation for an isothermal hold at the highest temperature, 175°C, of program applicability is shown. The isothermal level of 20 minutes is simulated by incorporating an initial arbitrary high rate of temperature rise, in this case 10000°C/min as shown in the simulation details at the bottom of the screen display. With such a high initial ramp rate negligible conversion and viscosity changes occur prior to the start of the isothermal dwell.

In the graphics window a grid is observed with the total scan time, rounded to the nearest minute, being represented by the horizontal axis.

The cure advancement, viscosity change, instantaneous heat output and the temperature profile for the simulation are all represented in the vertical axis with the following ranges.

The simulation temperature conditions are in the range 110°C to 200°C as shown in the legend on the right hand side of the screen and are represented by the T curve in the graph.

VISCOSITY AND CURE OF BSL914

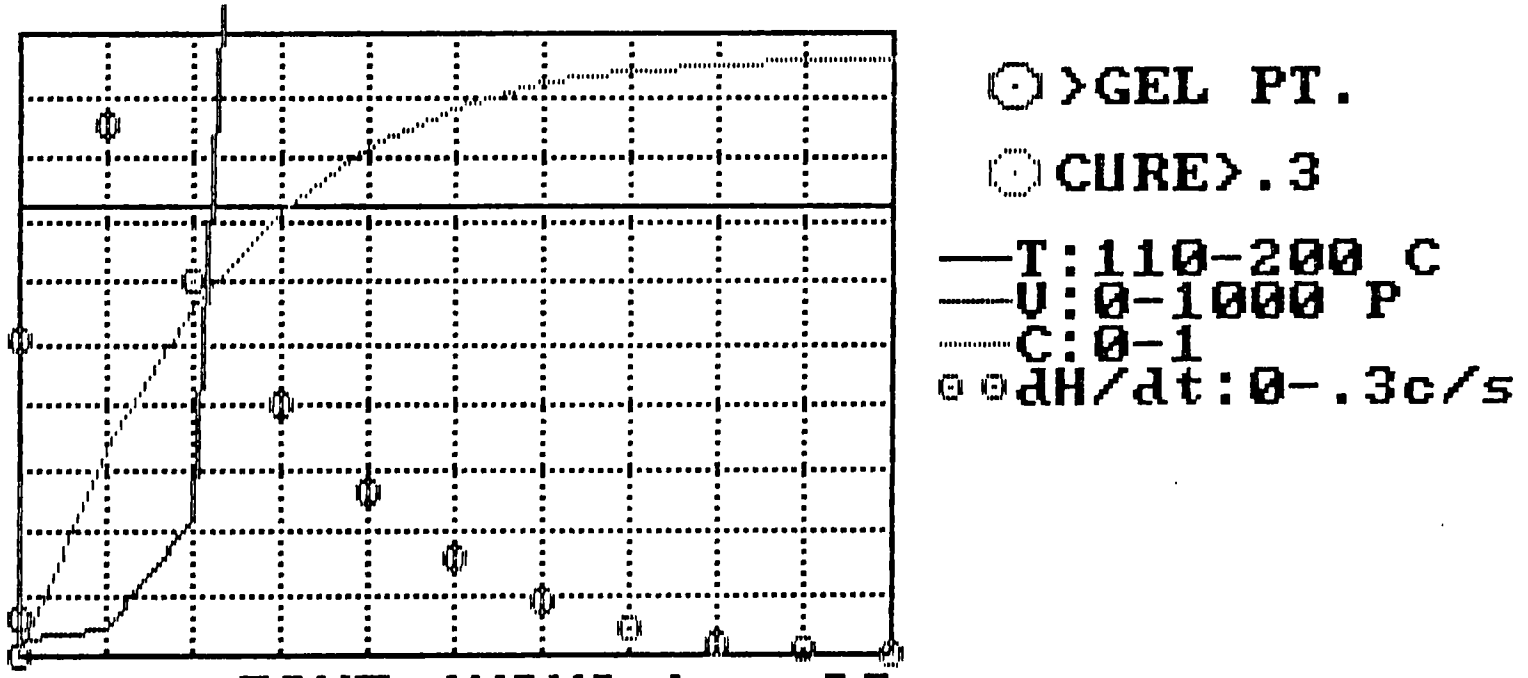

TEMP.RAMP RATE (DEG.C/MIN.)=10000
FINAL RAMP TEMPERATURE (DEG.C)=175
ISOTHERMAL HOLD TIME (MINS.)=20

FIG.(94)

The viscosity, V, range is between 0 and 1000 Poise and the conversion, E, curve is in the range 0 to 1 where 1 represents full cure of the resin.

The instantaneous heat output, dH/dt, is shown by the discrete circles and the values are in the range 0 to 0.3 cal/g/sec as shown in the legend.

The flags indicating that the gel point has been reached i.e. viscosity has exceeeded 1000 Poise and that a cure greater than 0.3 has been achieved in the simulated cycle appear on the screen at the location shown at the appropriate time during the simulation.

The curves described above are displayed in different colours and are therefore easier to visualise on the computer screen as compared to the screen prints included in the figures.

From the display shown in Fig.(94) it will be noted that at an isothermal temperature of 175°C the exothermic heat flow is extremely high and the maximum of nearly 0.3 cal/g/sec occurs within 2 minutes of run time. Also over 90% cure occurs within 10 minutes and the viscosity of the resin has exceeded 1000 Poise and therefore gelled, within 5 minutes. As full cure is approached it is noted that the rate of heat output decreases accordingly.

In the printout accompanying this simulation in Table 35 the simulated cycle details are printed and the tabulated numerical values for the ramp and isothermal portions of the run are independently indicated. Note that in the Table, and as described in section 6.3.4 the limiting viscosity of 1000 Poise is imposed after 10 minutes into the run in order to ensure that the calculated viscosity value does not exceed the maximum numerical range, 1.7×10^{38}, of the computer.

In contrast to the relatively fast reactions that occur at 175°C in the above simulation hardly any changes occur at an isothermal temperature of 111°C which is at the lower end of the temperature range for which the program is applicable as shown in Fig.(95). In this simulation only a minimal rise in viscosity and cure is observed. Hardly any exothermic heat is evolved,

VISCOSITY AND CURE OF BSL914

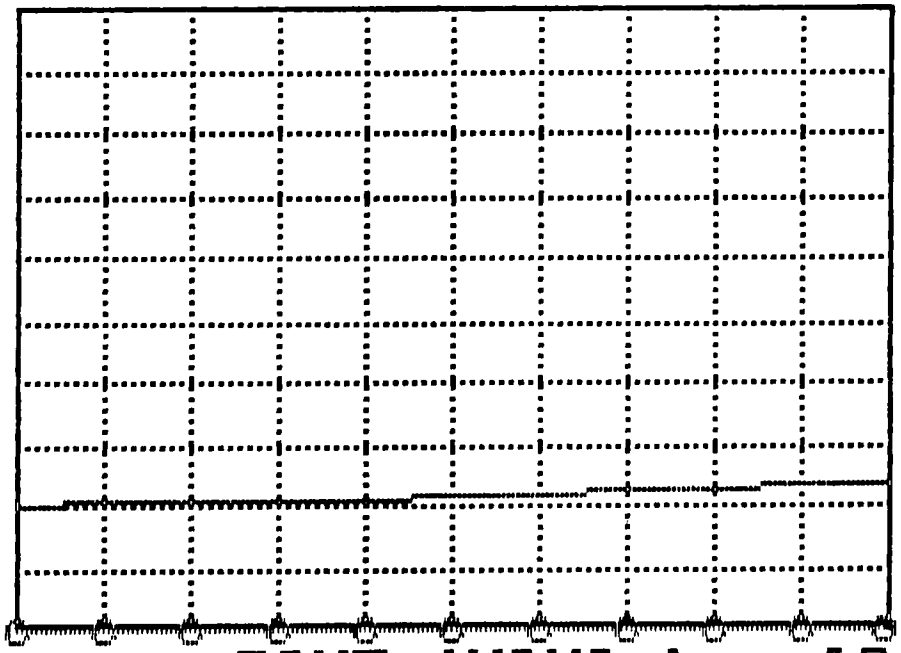

TEMP.RAMP RATE (DEG.C/MIN.)=10000
FINAL RAMP TEMPERATURE (DEG.C)=111
ISOTHERMAL HOLD TIME (MINS.)=60

FIG.(95)

consequently the gel point is not reached and cure is below 0.3 as indicated by the absence of the appropriate warning flags in the top right hand side of the screen.

From these two simulations at 111°C and 175°C therefore the program outputs are in agreement with expected resin behaviour at these isothermal temperatures i.e. qualitatively speaking hardly any reaction occurs at low temperatures around 110°C whereas the resin would be expected to cure extremely fast at such a high temperature as 175°C.

A simulation of a tempeature ramp over the whole range of program applicability in the temperature range 110°C to 175°C is shown in Fig.(96). A ramp is simulated by the incorporation of a relatively low isothermal hold time, in this case 0.1 minute as shown. At a ramp rate of 1°C/min resin cure appreciably commences about 20 minutes into the run corresponding to a temperature of 130°C. Over 80% cure is however achieved before the end of the ramp is reached with attendant solidification of the resin. The instantaneous heat output never exceeds 0.06cal/g/sec for this ramp condition.

A typical simulation of an initial temperature ramp followed by an isothermal hold is shown in Fig.(97) where the ramp time at 1°C/min is equal to the isothermal dwell time of 50 minutes at 160°C. It is noted that the resin gels at the beginning of the isothermal hold time in this case. If however the temperature ramp rate is lowered to 0.1°C/min i.e. ten times slower, then the resin cures much earlier in the ramp as shown for this simulation in Fig.(98) but with a much reduced heat flow.

Increasing the ramp rate by 10 times to 10°C/min up to 160°C however introduces increased heat flow problems as indicated for this simulation in Fig.(99). During the initial ramp the heat flow accelerates and the heat flow problem is only alleviated by the onset of the isothermal dwell at 160°C. Under such unstable ramp conditions in practice uncontrolled exotheric heat evolution would lead to resin degradation.

Finally, in Fig.(100) a typical autoclave moulding cycle for a large structure is simulated. In this case the moulding cycle consists of a temperature ramp of 3°C/min from 110°C to 175°C followed by an isothermal hold of 20 minutes. It is observed that the evolution of exothermic heat is positively increasing during the ramp time but in practice this does not become uncontrolled due to its dissipation by thermal transfer to the tooling. The cure in this case is effected in the early stages of the isothermal dwell.

VISCOSITY AND CURE OF BSL914

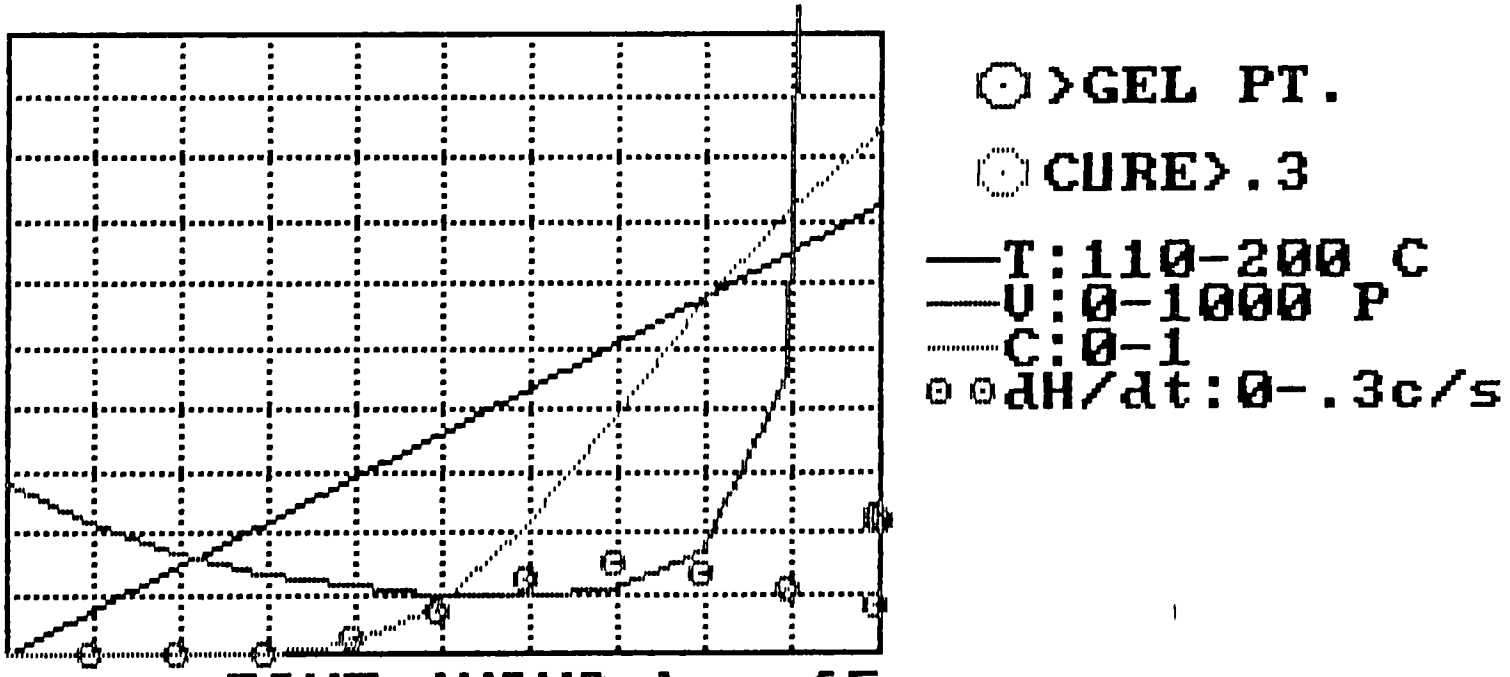

TEMP.RAMP RATE (DEG.C/MIN.)=1
FINAL RAMP TEMPERATURE (DEG.C)=175
ISOTHERMAL HOLD TIME (MINS.)=.1

FIG.(96)

VISCOSITY AND CURE OF BSL914

TEMP.RAMP RATE (DEG.C/MIN.)=1
FINAL RAMP TEMPERATURE (DEG.C)=160
ISOTHERMAL HOLD TIME (MINS.)=50

FIG.(97)

VISCOSITY AND CURE OF BSL914

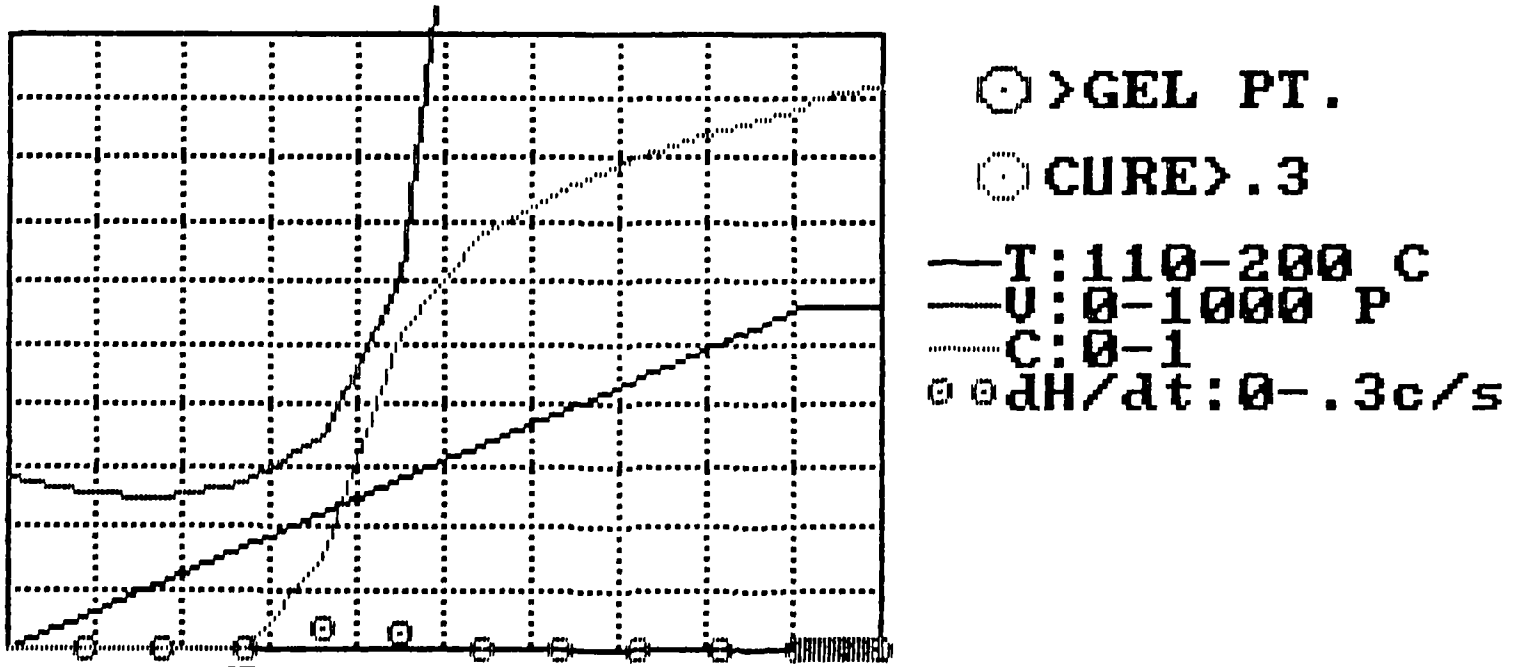

TEMP.RAMP RATE (DEG.C/MIN.)=.1
FINAL RAMP TEMPERATURE (DEG.C)=160
ISOTHERMAL HOLD TIME (MINS.)=50

FIG.(98)

VISCOSITY AND CURE OF BSL914

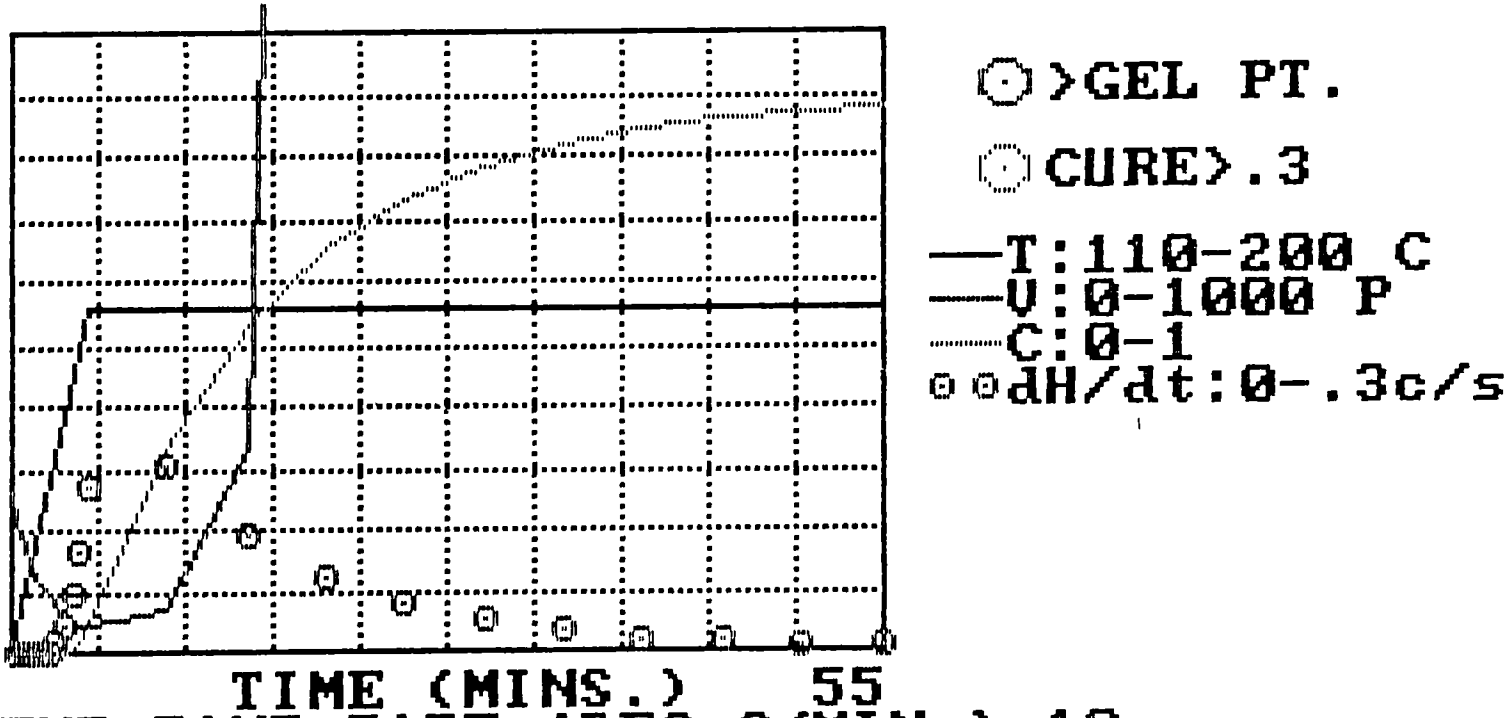

TEMP.RAMP RATE (DEG.C/MIN.)=10
FINAL RAMP TEMPERATURE (DEG.C)=160
ISOTHERMAL HOLD TIME (MINS.)=50

FIG.(99)

VISCOSITY AND CURE OF BSL914

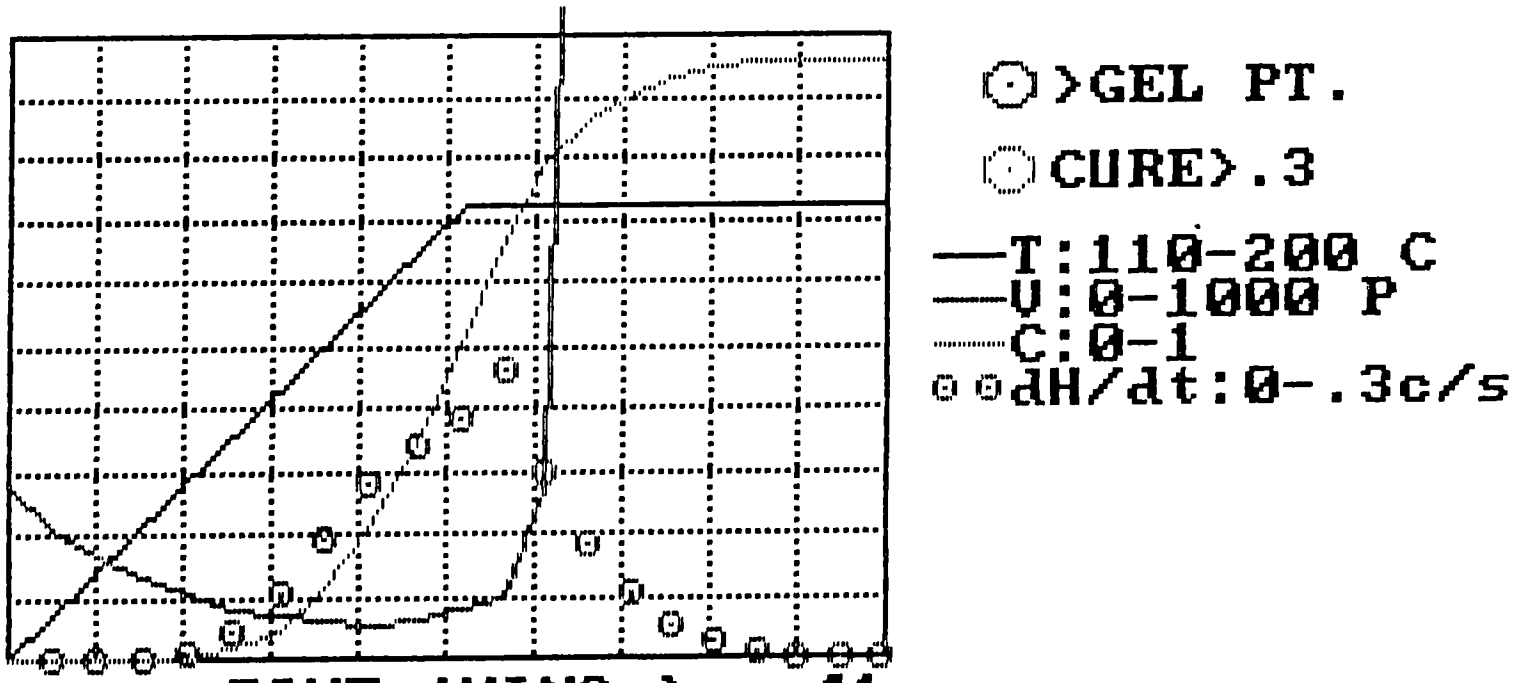

TEMP.RAMP RATE (DEG.C/MIN.)=3
FINAL RAMP TEMPERATURE (DEG.C)=175
ISOTHERMAL HOLD TIME (MINS.)=20

FIG.(100)

CHAPTER 7

APPLICATIONS OF MODELLING TO PRACTICAL PROBLEMS.

7.1 Typical Manufacturing Problems.

In the current Chapter the application of modelling techniques to the solution of two typical problems encountered in the autoclave manufacture of carbon fibre reinforced epoxy composites will be described.

In the first problem the application of the 'VISICURE' computer program in the design of a specific moulding cycle will be described.

The second problem is that of deciding how to proceed with the moulding operation following a catastrophic failure during a planned cycle in a production situation. This second problem necessitated further modelling and development of the 'VISICURE' program.

7.2 Mould Cycle Design.

A typical mould cycle design problem is as follows:-

It is required to mould a flat panel with dimensions 200 x 100 x 5.03mm (corresponding to a fibre volume fraction of 0.58) and consisting of a balanced lay-up of 18, 5-shaft satin woven cloth laminae in an autoclave which is being heated at a ramp rate of 0.61°C/min. from ambient to 190°C. It is required to know at what time in the moulding cycle and for how long should the consolidation pressure be applied for effective moulding to be achieved at the end of the moulding cycle.

The first step in the solution of this problem is that of the determination of the viscosity limits within which the moulding may be effectively carried out. As described in section 1.2 a low viscosity level is initially required so that outflow of resin from the lay-up into the bleed pack is achieved. Following the required outflow however the resin viscosity has to be such that a high enough hydrostatic pressure exists in the matrix resin to aid in the removal of residual voidage. To obtain an estimate of these viscosity limits the following experiments were conducted.

Calculations indicated that six glass cloth bleed layers were required to absorb the excess resin from the lay-up in order to achieve a fibre volume fraction of 0.58 in the final composite.

Five panels each containing this number of bleed layers and the approriate separation release films were then consolidated in a laboratory version of the autoclave.(refs.58,59).

The experimental conditions were such that the individual panels received different dwell times at 125°C prior to lay-up evacuation and application of a consolidation pressure of 100psi being effected. Evacuation and pressure were then maintained for a further 1 hour at 125°C in each case in order to consolidate the lay-up. At the end of this period of time the positive pressure was reduced to atmospheric but evacuation was maintained for the rest of the cycle which consisted of a temperature ramp of 3.5°C/min. to 190°C to cure the composite in its consolidated form.

Because the initial dwell at 125°C was different in each case then the resin viscosity at the onset of consolidation was different in the respective panels. The dwell times for the panels were 10, 20, 40, 80 and 120 minutes with corresponding viscosities at the end of each dwell being 126, 138, 186, 291 and 534 Poise as calculated by the viscosity sub-model. The model viscosity profile at 125°C is as shown in Fig.(101).

On the assumption that no further compaction (or lay-up relaxation) occurs under evacuation during

the final cure ramp above 125°C then the effectiveness of the moulding operation at 125°C may be measured.

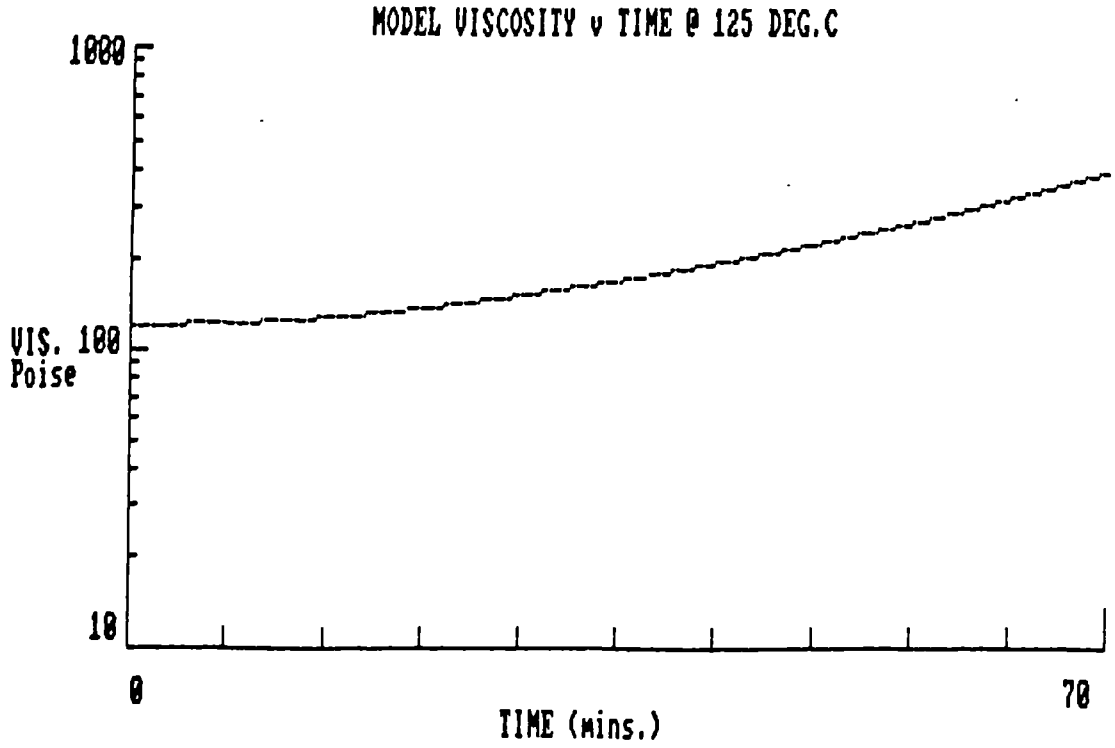

FIG.(101)

The amount of consolidation that occurred during the pressurisation stage at 125°C may be determined from the ratio of the moulded thickness to that of the theoretical value of 5.03mm. This ratio is shown plotted against precompression dwell in Fig.(102) for the 100psi consolidation conditions. The ratio for the as laid up thickness was of the order of 1.37 in each case.

From the plot at 100psi it is clear that hardly any compaction occurs following a dwell of 120 minutes.

Thus the amount of compaction that may be obtained is negligible if the initial viscosity of the resin exceeds 534 Poise.

Laminate movement does occur however at dwell times less than 120 minutes with the amount of compaction increasing with decreased precompression dwell in an approximately linear manner. It is observed in this plot that only dwell times less than 20 minutes result in panels approaching the required moulded thickness where the ratio is unity. Dwells of this order correspond to

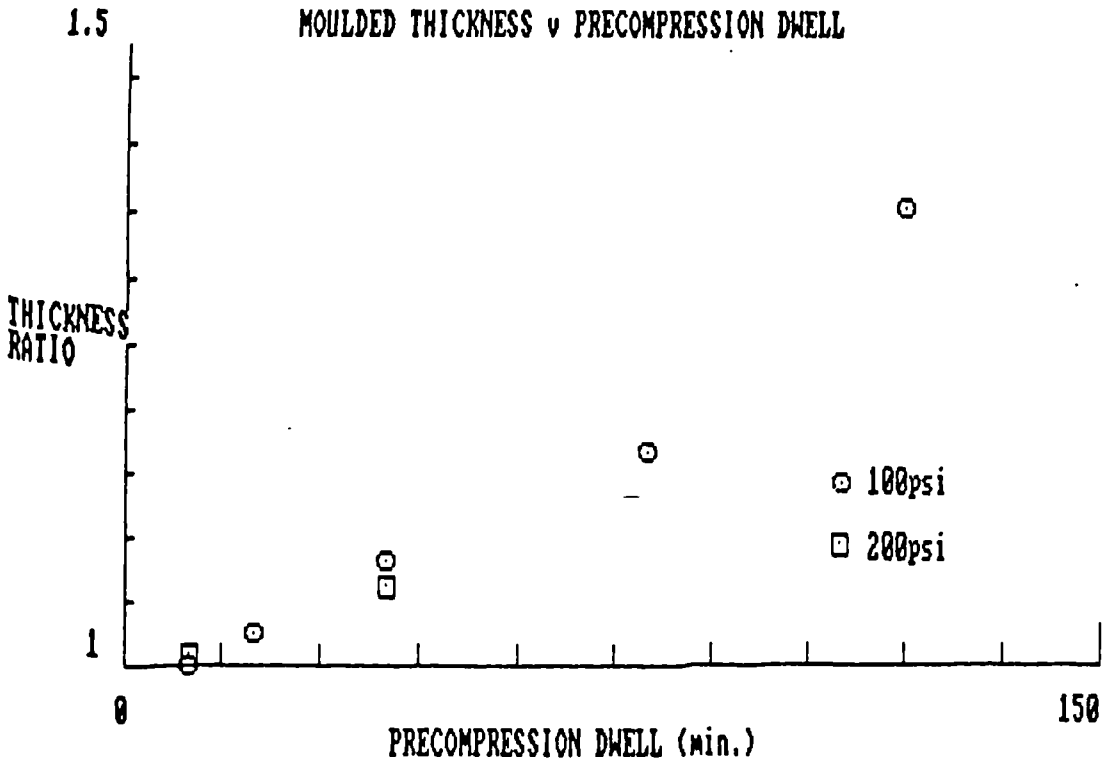

FIG.(102)

initial resin viscosity in the range 126 to 138 Poise.

Two further panels were moulded in an identical manner to above but with reduced times under compaction pressure in order to estimate the time required for consolidation. Thus for a precompression dwell of 20 minutes for both panels but with pressure application times of 7.5 and 15 minutes respectively the final thickness ratios were 1.064 and 1.096. These ratios are only slightly higher than the value of 1.028 obtained for the pressure application time of 1 hour in the initial set of experiments.

It is therfore clear that most of the compression occurs within times of the order 10 to 20 minutes under pressure.

Two other panels were moulded with precompression dwells of 10 and 40 minutes respectively but with the consolidation pressure increased from 100 to 200psi maintained for the 1 hour pressure duration at 125°C. No significant improvement in the amount of consolidation due to this increased pressure was observed however and similar thickness ratios at the low and high

pressure levels were obtained as shown in Fig.(102). This behaviour is attributed to the higher resistance to resin flow presented by the more compressed bleed pack in the higher consolidation pressure case.

From the above experiments therefore it is concluded that the viscosity of the resin has to be below values of the order of 150 Poise for adequate resin outflow to be obtained. At these low viscosity levels most of the compaction occurs within the first 10 to 20 minutes under a consolidation pressure in the range 100 to 200psi.

7.2.1 Voids.

The void content in the initial set of five experiments with variable precompression dwells were measured by means of image analysis equipment and the values obtained are as shown in Fig.(103).

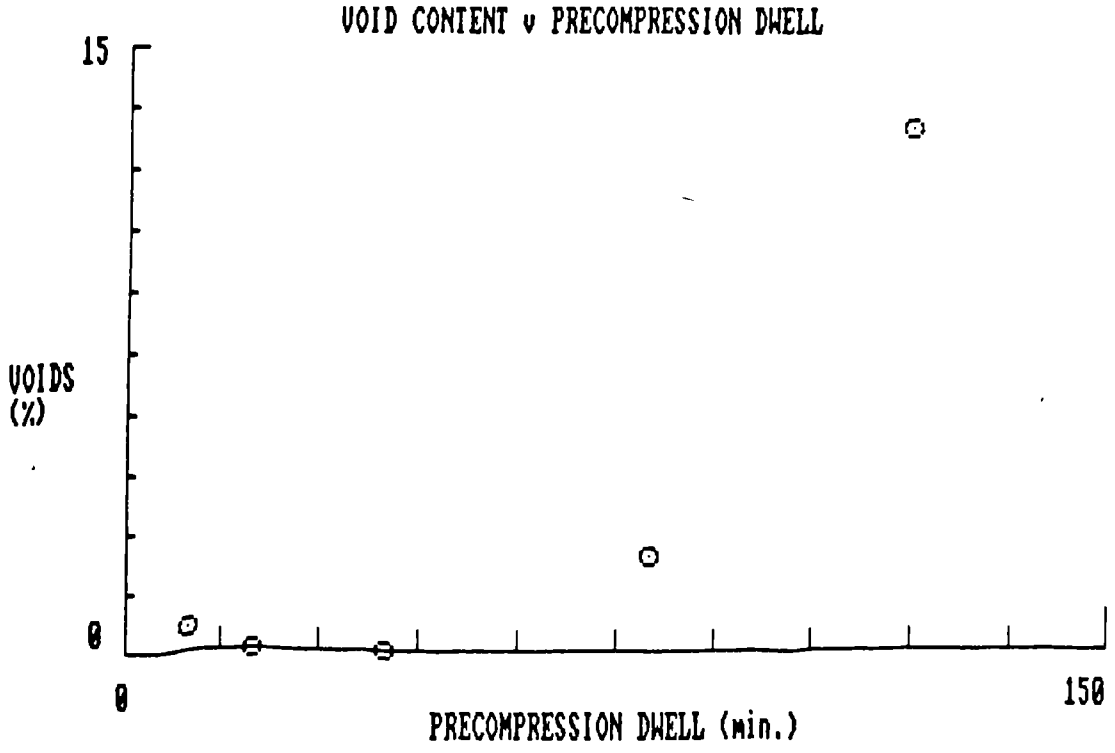

FIG.(103)

It is observed that the void content is a minimum value, of the order of 0.05% maximum for the panels with 20 to 40 minutes precompression dwells

corresponding to viscosities in the range 138 to 186 Poise. For the panels with longer precompression dwells than 40 minutes the occurrence of increased void content is explained by the lack of consolidation achieved at the higher viscosities.

The increased void content of 0.63% at the 10 minute dwell condition is attributed to excessive outflow of resin at the lower viscosity of 126 Poise which resulted in a lower hydrostatic pressure capability during the remainder of the compaction period.

Under these experimental conditions it is concluded that for effective void elimination the viscosity of the resin has to be greater than 126 Poise.

To achieve void free mouldings therefore the pressurisation conditions have to be carefully chosen in any moulding cycle in order to balance the conflicting requirements of a low viscosity for compaction and a high viscosity for void collapse.

7.3 Moulding Under Temperature Ramps.

Returning to the original problem posed in section 7.2 it is necessary to test the above principles under the ramp condition of 0.611°C/min. The output of the 'VISICURE' program for this ramp rate is shown in Fig.(104). As the temperature increases from 110°C the viscosity decreases so that at approximately 130°C its value is 150 Poise. The viscosity remains below the 150 Poise level until a temperature of approximately 146°C is attained i.e. for a total time of 26 minutes as shown in between the two outer arrows in Fig.(104).

Since,from the isothermal experiments described in section 7.2, the panel may be effectively moulded within 10 minutes of pressure application then a pressurisation region between the temperatures 133 and 139°C was chosen i.e. the region in between the two inner arrows in Fig.(104) with equivalent duration of 9.8 minutes.

Two panels were therefore moulded as per the following cycle under compaction pressures of 100 and

200psi respectively:-

(1) Lay-up inserted in autoclave at 110°C.

(2) Ramp from 110 to 133°C at 0.611°C/min. with no evacuation and no pressure.

(3) Ramp from 133 to 139°C at 0.611°C/min. with evacuation and pressure.

(4) Ramp from 139 to 190°C at 3.5°C/min. with evacuation but no pressure.

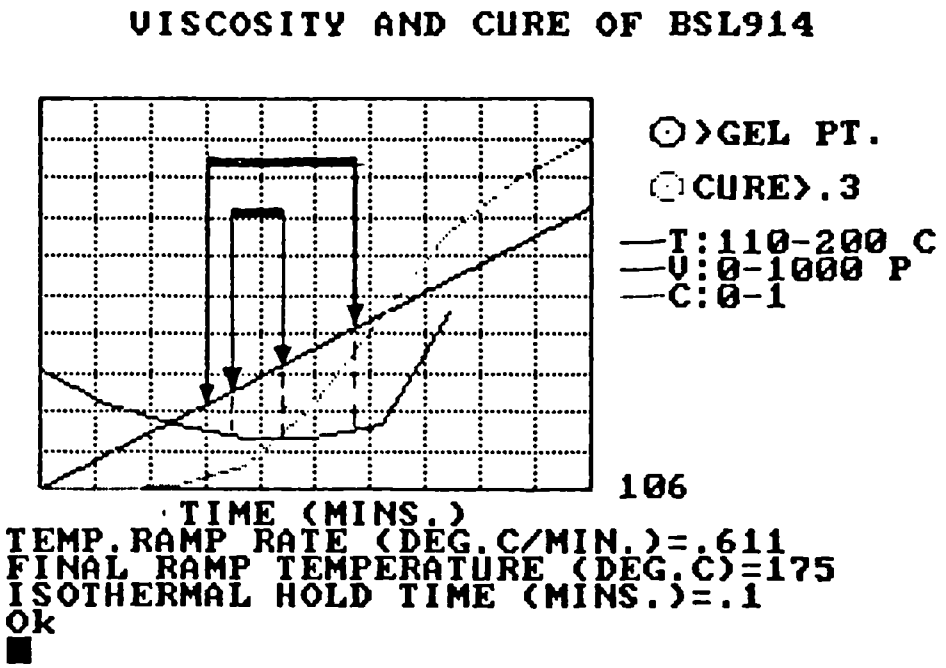

FIG.(104)

The thickness ratios for the moulded panels in this case were 1.044 and 1.048 for the respective pressures of 100 and 200psi. These ratios are substantially the same as those obtained for the 7.5 and 15 minute pressurisation times as described in section 7.2 for the 125°C isothermal conditions.

Thus similar moulded thicknesses are obtained under either isothermal or dynamic conditions for the

same time of pressurisation in the appropriate viscosity range. Also the effect of increasing the consolidation pressure from 100 to 200psi has a negligible effect on the moulded thickness in both the isothermal and dynamic case.

By applying pressure (100psi) within the temperature range 130 to 146°C for the same ramp condition i.e. between the two outer arrows in Fig.(104) (equivalent to a time of 26.2 minutes) the moulded thickness ratio of the resulting panel was 1.052. Thus increasing the time of consolidation does not significantly lead to an improvement in mouldability under these conditions.

Thus the panels under a ramp of 0.611°C/min. may be moulded to result in a composite with a fibre volume fraction of the order of 0.55.

The above example has demonstrated the use of the 'VISICURE' program for the design of a moulding cycle at a specific ramp rate.Clearly for the ramp rate of 0.611°C/min. it is difficult to achieve the design fibre volume fraction of 0.58 and the moulding cycle has to be optimised.

7.4 Optimisation Procedures.

On analysing several 'VISICURE' outputs as in Fig.(104) but at different temperature ramp rates the times during which the resin viscosity is below 150 Poise can be obtained for each ramp condition. These times are shown plotted versus ramp rate in Fig.(105).

It is observed that at ramp rates less than 0.3°C/min. the resin viscosity is not below 150 Poise for any length of time. Theoretically therefore moulding is not possible with such low ramp rates.

The available time however increases rapidly in the range of ramp rates from 0.3 to 0.5°C/min. to reach a plateau region in the ramp rate range of 0.5 to 1.25°C/min. At higher ramp rates than 1.5°C/min. however the available time progressively decreases.

The corresponding temperature range over which

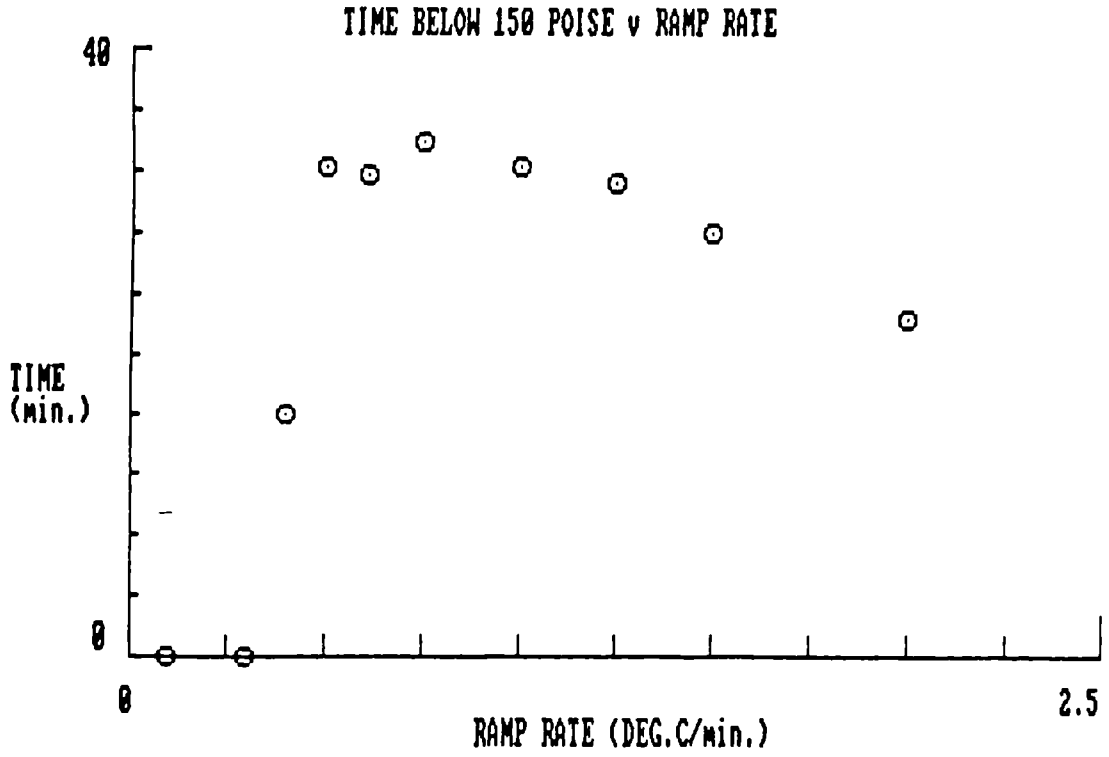

FIG.(105)

pressure may be applied is as shown in Fig.(106) where the hatched region represents the temperatures at which the resin viscosity is below 150 Poise.

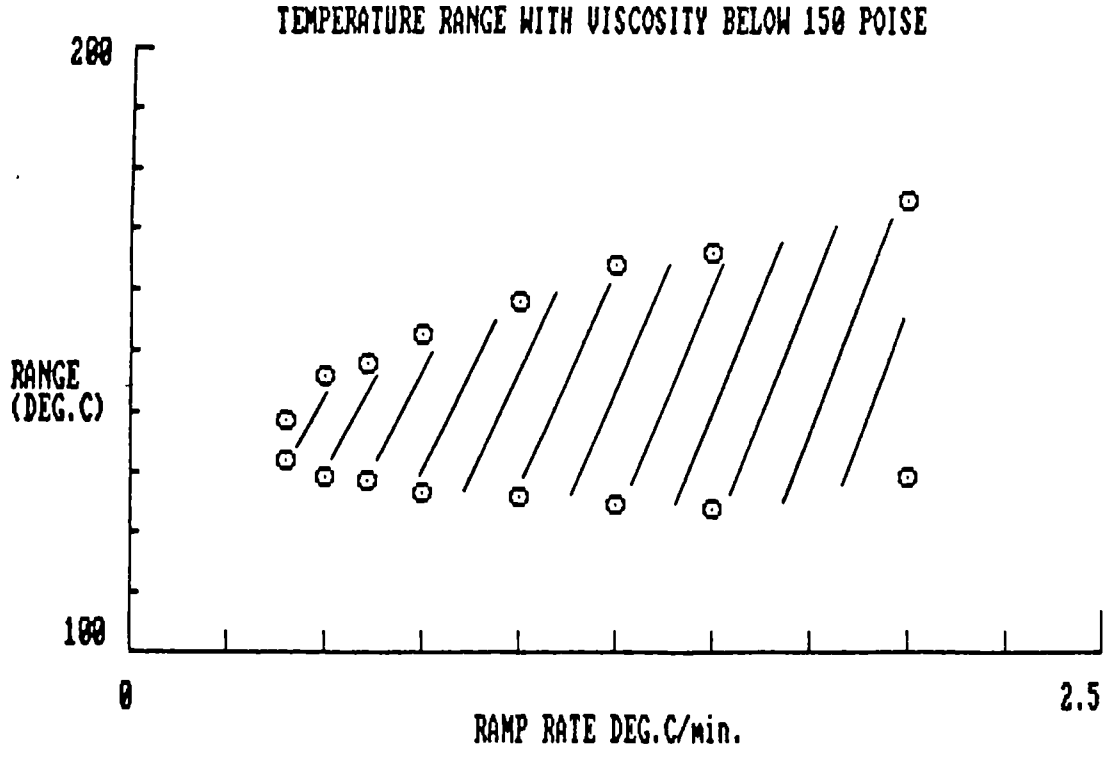

FIG.(106)

The minimum viscosities achieved with varying ramp rates are as shown in Fig.(107) where it is observed that the minimum viscosity approaches a lower limit in an asymptotic manner.

On consideration of the above figures it is concluded that 1.25°C/min. may be the optimum ramp rate for consolidation since pressurisation would be effective for a period of 31 minutes in the temperature range 125 to 164°C/min. Further, the minimum viscosity attained during the ramp is 88 Poise and efficient compaction would thus be expected. The model output for this ramp rate is shown in Fig.(108).

The available consolidation time will be further increased marginally by the introduction of an isothermal dwell during the temperature rise at 1.25°C/min. The effect of a dwell at 135°C is shown in Fig.(109) and it is observed that the time during which the resin viscosity is below 150 Poise is of the order of 33 minutes.

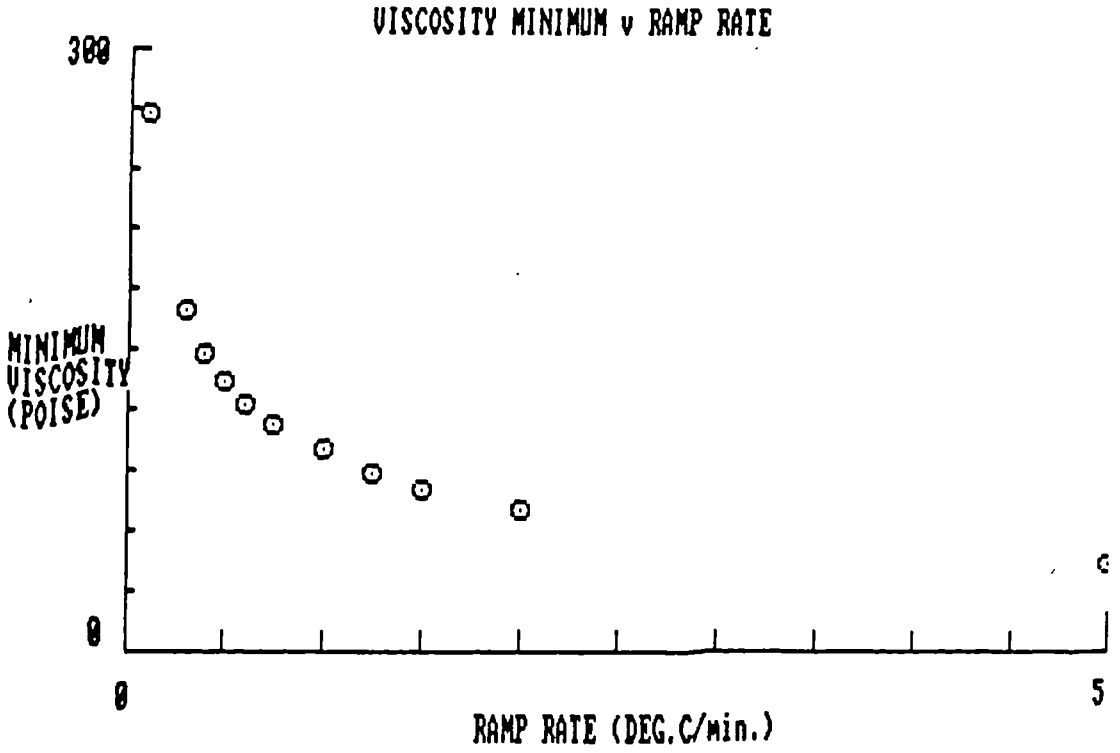

FIG.(107)

VISCOSITY AND CURE OF BSL914

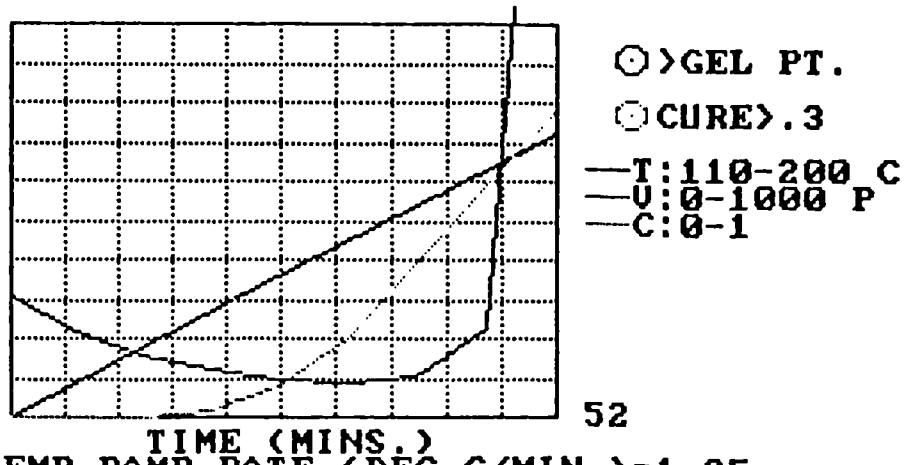

TEMP.RAMP RATE (DEG.C/MIN.)=1.25
FINAL RAMP TEMPERATURE (DEG.C)=175
ISOTHERMAL HOLD TIME (MINS.)=.1
Ok
■

FIG.(108)

VISCOSITY AND CURE OF BSL914

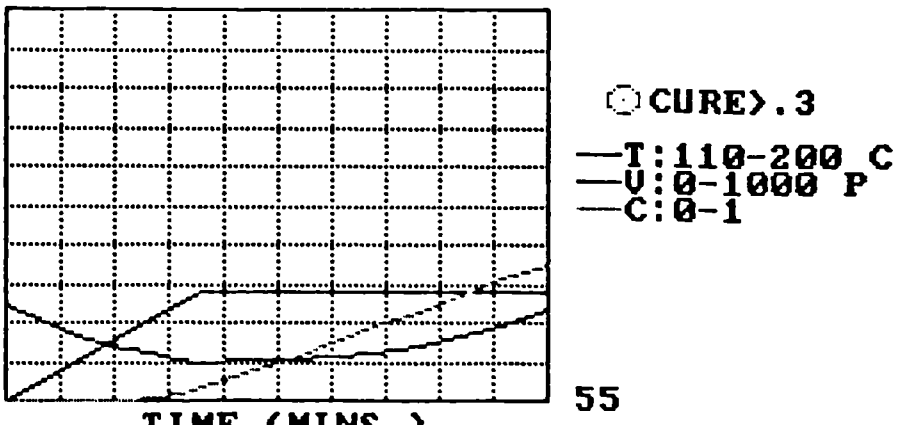

TEMP.RAMP RATE (DEG.C/MIN.)=1.25
FINAL RAMP TEMPERATURE (DEG.C)=135
ISOTHERMAL HOLD TIME (MINS.)=35
Ok
■

FIG.(109)

Due to the limitations of the current laboratory autoclave the nearest available ramp rate to the optimum was 1.611°C/min. The viscosity profile for this ramp rate including a dwell at 135°C is shown in Fig.(110).

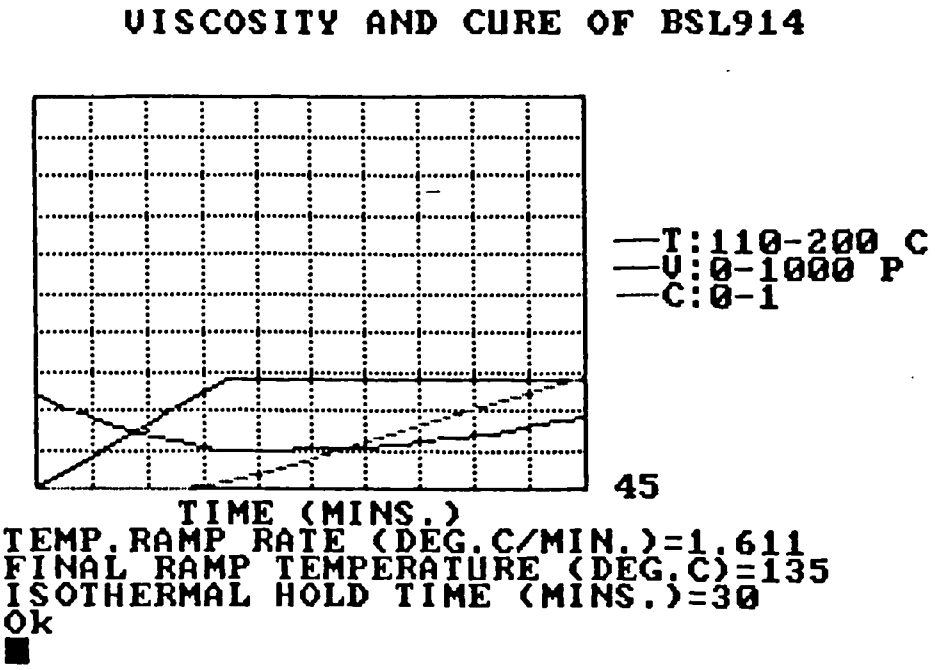

FIG.(110)

From a series of mouldings conducted with this ramp rate and a dwell of 35 minutes at 135°C it has been found that when a consolidation pressure of 100psi is applied at the beginning of the dwell period then a moulded thickness ratio of 1.018 is obtained. If pressure is applied at 125°C during the initial ramp however a moulded thickness ratio of 1 is obtained with the panel hence moulded to size.

From these experiments it is concluded that a minimum viscosity of 100 Poise is desirable and that consolidation pressure has to be applied from 125°C onwards in the moulding cycle for the attainment of a composite panel with a fibre volume fraction of 0.58. The time for consolidation to occur is estimated to be no greater than 30 minutes from Fig.(110).

7.5 Break In Cycle.

The second problem in section 7.1 arises due to the fact that from time to time in the production of composite material artefacts in the autoclave difficulties are encountered such as vacuum bag failure or resin lock-off in the evacuation pipes. Such failures may occur at any time in a moulding cycle.

In the event of such a failure the question arises as to how to proceed further with the moulding operation and there are three main options:-

1) The job may be cooled to ambient temperature and extracted from the autoclave with repair being effected prior to recycling to finalise consolidation and cure.

2) The moulding cycle may be continued to the postcure stage in the normal manner.

3) The job discontinued and the composite component scrapped.

Clearly undesirable component cost increases are associated with options 1) and 3) but option 3) is extremely costly especially in the case of large components such as those depicted in Fig.(1). It is therefore of paramount importance to have some guidelines, preferably quantitative, to establish which option is to be followed if such a catastrophic failure occurs in any moulding cycle.

Some boundary conditions may be applied from consideration of Fig.(106). Consider a moulding cycle with a temperature ramp in the range covered in the figure. As temperature increases from ambient the prepreg eventually becomes mouldable at the lower bound of the hatched region. Below the lower bound temperature therefore no consolidation (and hardly any cure advancement) would have occurred. Thus in this case option 1) should suffice if a failure occurs at temperatures below the lower limit for the relevant ramp

rate.

Similarly it can be concluded that if failure occurs at temperatures above the upper bound of the hatched region at the relevant ramp rate then option (2) above may be taken up since the material is fully consolidated at the upper bound temperature.

Unfortunately however the most likely incidence of failure occurs when the resin viscosity is in the region corresponding to the hatched area in Fig.(106) and this is due to the accelerated bag movement and resin outflow at these low viscosities. The hatched region also represents the most difficult conditions under which to assess the choice of options to follow due to the rapidly changing material properties in the same region.

The reason for these difficulties lies in the fact that if the prepreg is cooled from a temperature within this region then it is partially converted and thus more viscous than in the initial moulding action. After re-bagging etc.therefore the matrix resin has to be considered as a new material for which no model exsists to predict its behaviour in a subsequent moulding cycle.

Further, should recycling provide a sufficiently consolidated product there is no evidence to suggest that the material itself in such a case is equivalent in its physical and mechanical properties to that which would have been produced with a standard moulding cycle.

Initial experiments were therefore conducted to clarify some of these topics and to assess the possibility of raising the lower bound of mouldability for recycled material.

7.6 DSC Experiments.

In order to obtain a working model for the recycled material analysis of the residual exotherms generated by partially converted resin samples was required. For this purpose samples of resin were placed in the DSC pan and heated for various times at different isothermal temperatures so that known amounts of

preconversion were obtained at these temperatures. The required times were calculated by means of the cure sub-model and were as shown in Table 42. The residual exotherms associated with each of these preconverted samples were then determined on the DSC in the normal manner under isothermal conditions at 125, 135 and 150°C.

The typical thermal behaviour of preconverted resin may be explained by reference to Fig.(111). The isothermal exotherms at 125, 135 and 150°C for material preconverted at 135°C to the given conversions are shown. On observing the exotherm form in the first column i.e. the exotherms at 125°C then it is clear that as the amount of preconversion increases from 10% to 50% that the reaction apparently progresses from an autocatalytic form as defined by eq.3.10 to a n-th order reaction which is defined by eq.3.4. Also it is observed that as the isothermal temperature increases from 125 to 150°C for any preconversion up to 30% that the peak maximum drifts towards the commencement of the reaction.

This latter behaviour of each preconverted material is similar to that of virgin material in that the ratio m/n increases with increased temperature as in Fig.(20). This same trend of inreasing m/n ratio with isothermal temperature is observed in views of the exotherms for samples preconverted to 30% at the different temperatures as shown in Fig.(112).

Also it is observed that the reaction appears similar in each column irrespective of the preconversion temperature i.e. all reactions in the 125°C column appear to be autocatalytic and all reactions in the 150°C appear n-th order.

The implication of this latter observation is that the thermal behaviour of the resin is independent of the temperature at which the preconversion of 30% was obtained.

This thermal behaviour would be expected from the time-shift principle described in section 4.2 if similar cure reactions occur under all conditions. Further evidence of material equivalence under these varying preconversion conditions is obtained by

Residual Isothermal Exotherms for Material Preconverted to the Levels Shown at 135°C

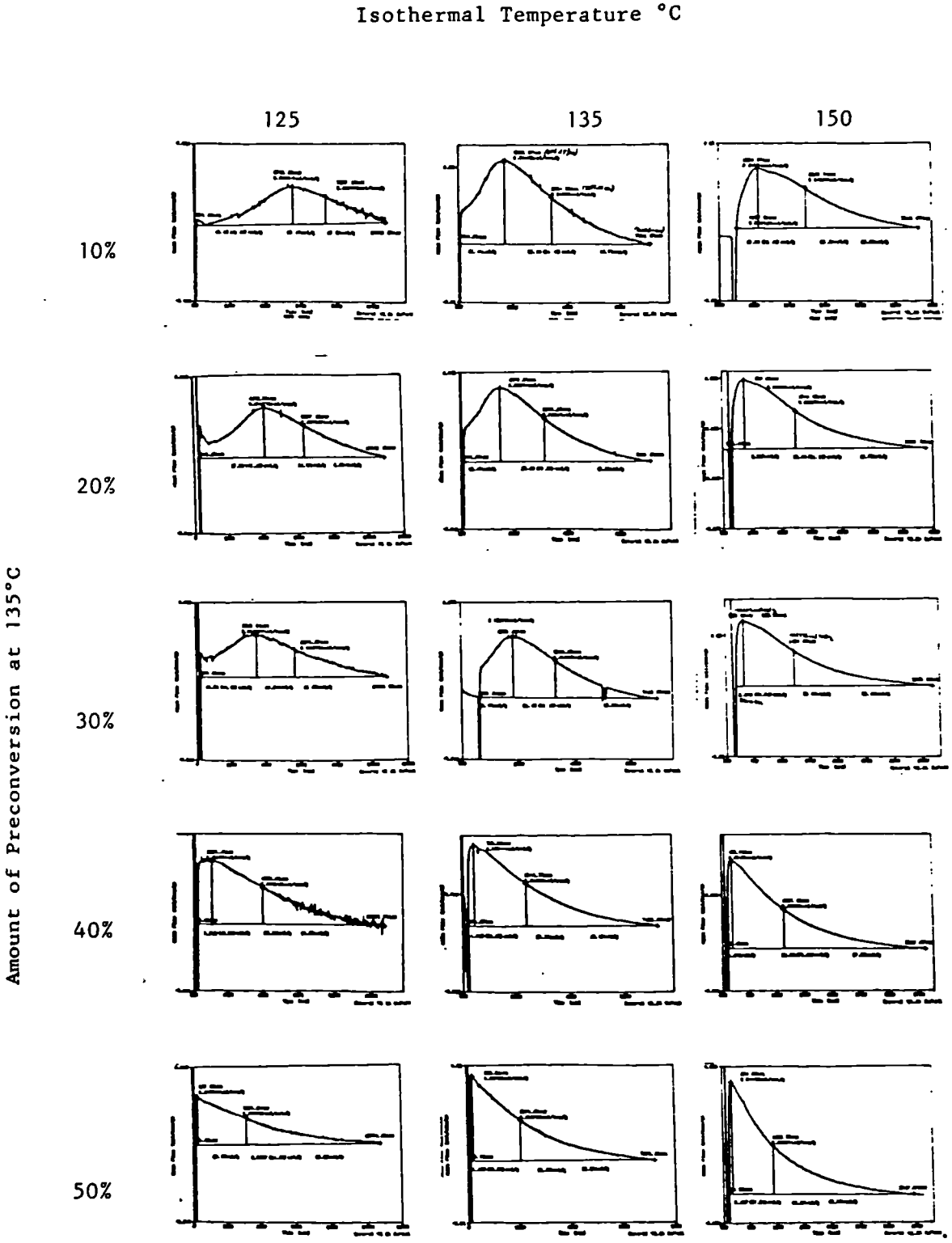

NB. Graphical scales not constant

FIG.(111)

Residual Isothermal Exotherms for 30% Preconverted Material

Isothermal Temperature °C

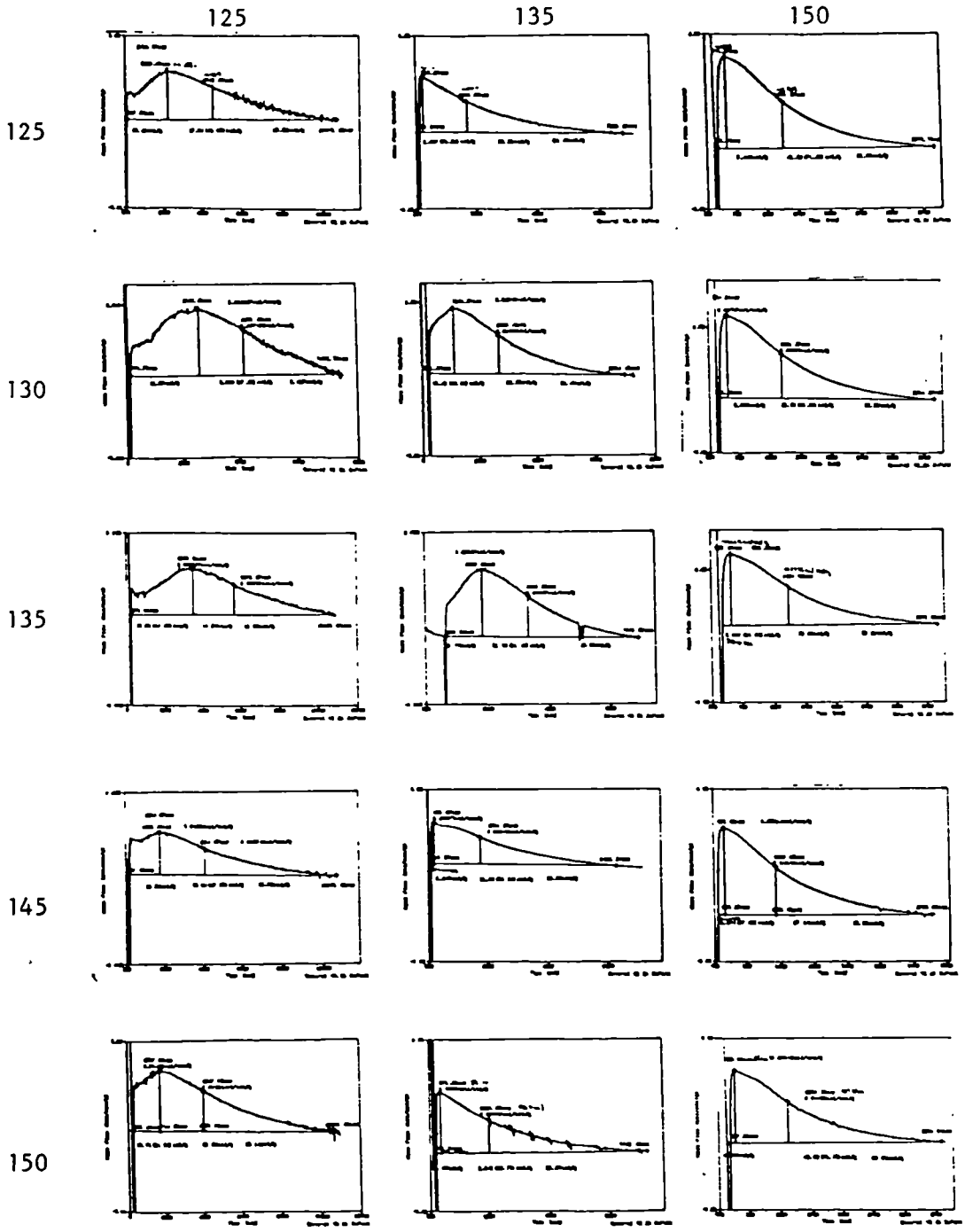

NB Graphical scales not constant

FIG.(112)

consideration of the rate constants of the individual reactions.

7.6.1 Rate Constants.

In Fig.(111) some of the reactions are autocatalytic as already described. The rate constant, k and the indices m and n in eq.(3.10) may therefore be evaluated by methods already described in previous Chapters. If the ratio r = m/n however exeeds 5 then, dependent on the value of n, the reaction is deemed to follow n-th order kinetics and the order of the reaction and the rate constant may be solved by rearrangement of eq.(3.4) to give

$$\ln(d\alpha/dt) = \ln k + m\ln(1-\alpha) \qquad (7.1)$$

Values of $d\alpha/dt$ and α were obtained at two points in the reaction corresponding to the two ordinates at peak maximum and approximately half peak height respectively.

The values of the ratio r, the autocatalytic rate constant K(AUTO) and the n-th order rate constant K for the exotherms obtained for resin preconverted at 135°C are shown in Table 43. Where appropriate (at $r < 5$) it will be observed that K(AUTO) and K are of similar values.

Of more interest however is the plot of the K values obtained at the isothermal temperature of 150°C against preconversion for three preconverted materials as shown in Fig.(113).

This plot is to be compared with that for the rate and conversion obtained from a single exotherm at 150°C for virgin material as in Fig.(50).

Bearing in mind the possible experimental errors and a change of model then it can be inferred from the close proximity of these two curves that an interrupted cure reaction will, on reheating, proceed according to the initial model for the cure reaction.

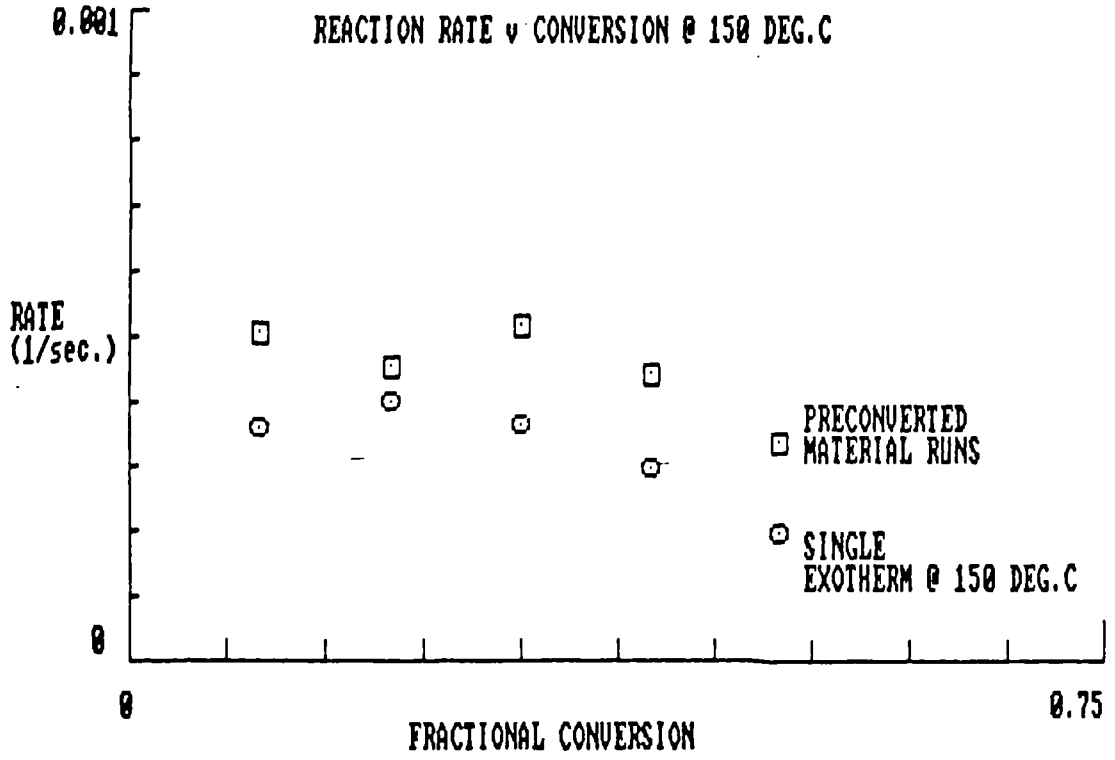

FIG.(113)

7.6.2 n-th Order Activation Energy.

From the above if the ratio r exceeds 5 then an autocatalytic model cannot be obtained. Both an activation energy and the reaction order may be evaluated from the n-th order kinetics model however when applied to the exotherms in Fig.(112). Values of k and m are shown in Table 44. Since the material is assumed to be constant, independent of preconversion temperature, then mean values of k and m may be obtained for each isothermal temperature column. The residual exotherms i.e. total area under the peaks at the respective isothermal temperatures are shown in Table 45 from which mean values at each temperature may be obtained.

From the mean values a linear dependence of m on temperature is obtained as shown in Fig.(114) and given by

$$m = (-1.435E\text{-}02)(T°K) + (7.192) \qquad (7.2)$$

Also from the Arrhenius plot of lnk versus reciprocal temperature is shown in Fig.(115) where the

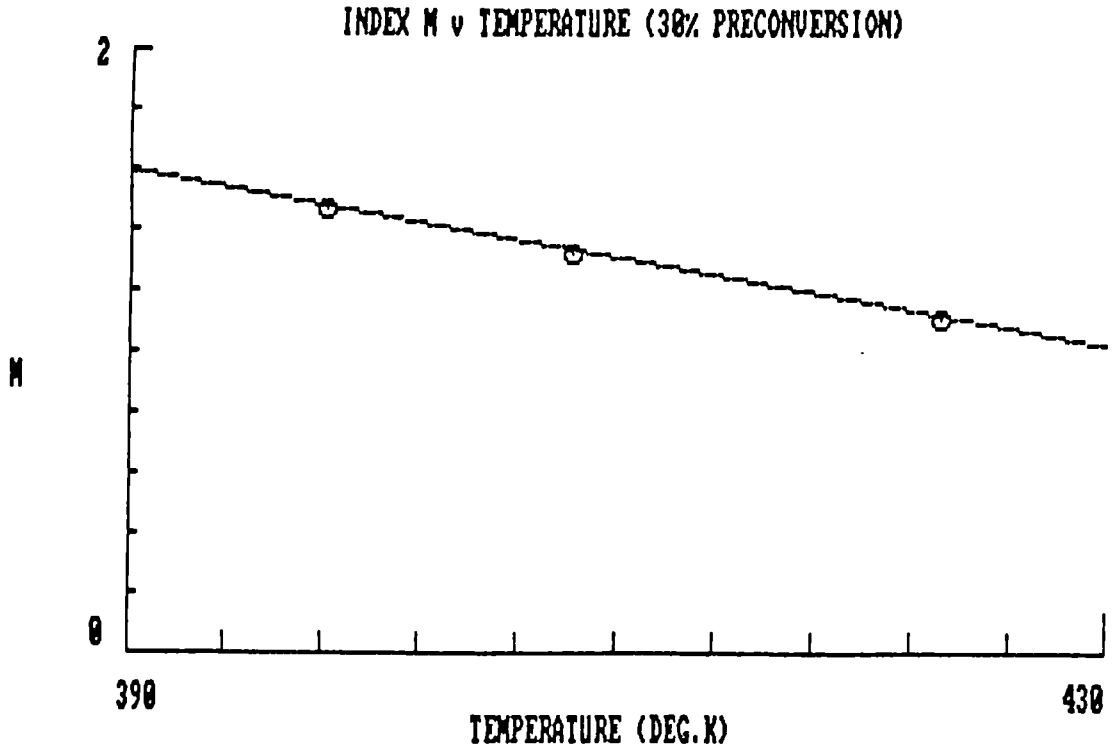

FIG.(114)

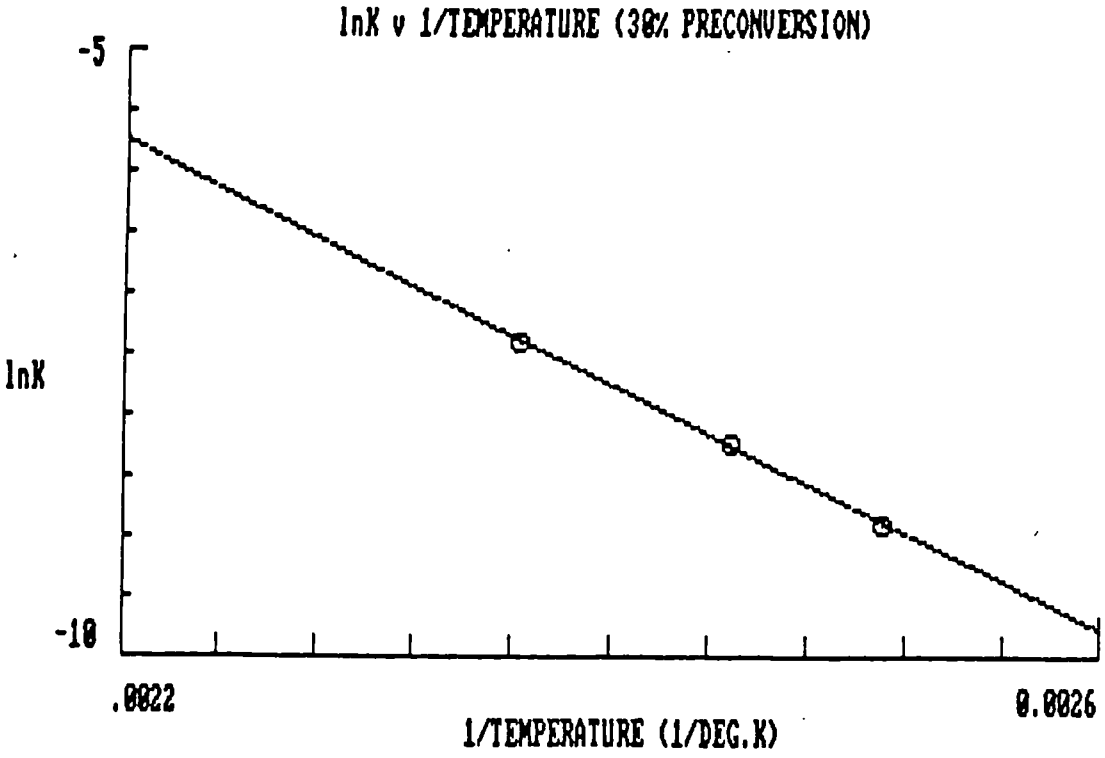

FIG.(115)

equation of the line is

$$\ln k = (-10094.59)(1/T°K) + (16.472) \qquad (7.3)$$

Hence the activation energy of 20.06 kcal/mol (83.9 kJ/mol) for the reaction compares favourably with those listed in Table 21.

7.6.3 Verification Of Model.

In order to verify the model for use in an interrupted cure situation the following DSC run was executed:-

1) Ramp at 1°C/min. from 110 to 145°C.

2) Cool to 110°C to simulate a break in a planned cycle.

3) Re-ramp at 1°C/min. from 110 to 150°C.

4) Isothermal hold at 150°C for 1 hour.

The DSC exotherm profile for this run is shown in Fig.(116).

The model prediction, obtained by modification of the 'VISICURE' program is shown in Fig.(117).

It will be observed that during the second ramp the resin does cure at a faster rate than during the initial ramp. The minor vertical displacement between the theoretical and the experimental curves is due to the small amount of cure that occurred during the cooldown period and which is not taken account of in the model.

At conversion levels up to 0.3 the viscosity of the resin during the second ramp is assumed to follow the chemorheological model defined by eq.(5.13). Above 0.3 conversion however only an approximate fit is so far available for the computer simulation shown in Fig.(118).

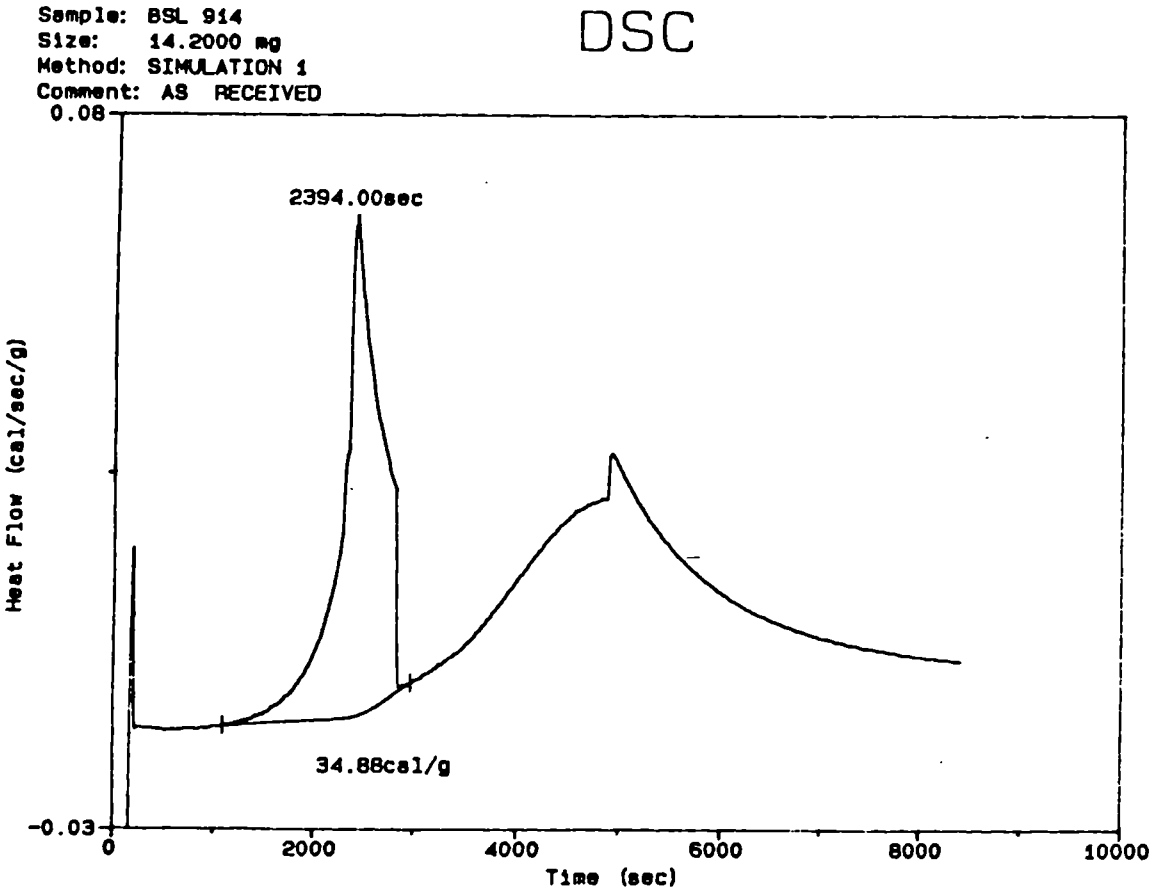

FIG.(116)

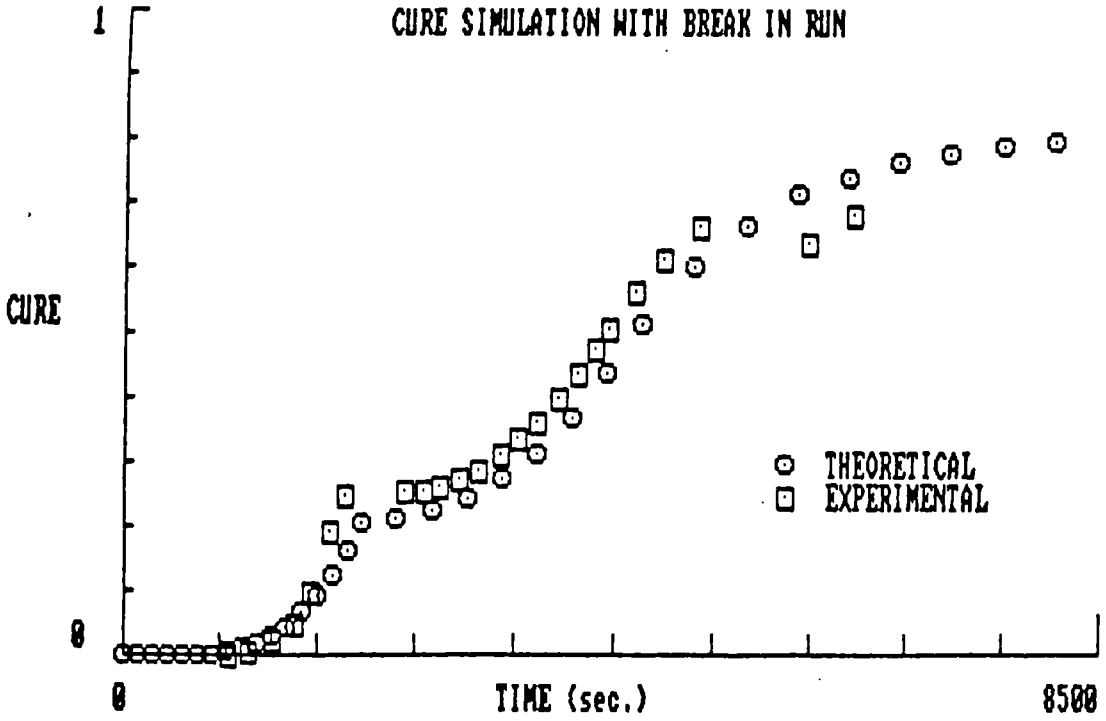

FIG.(117)

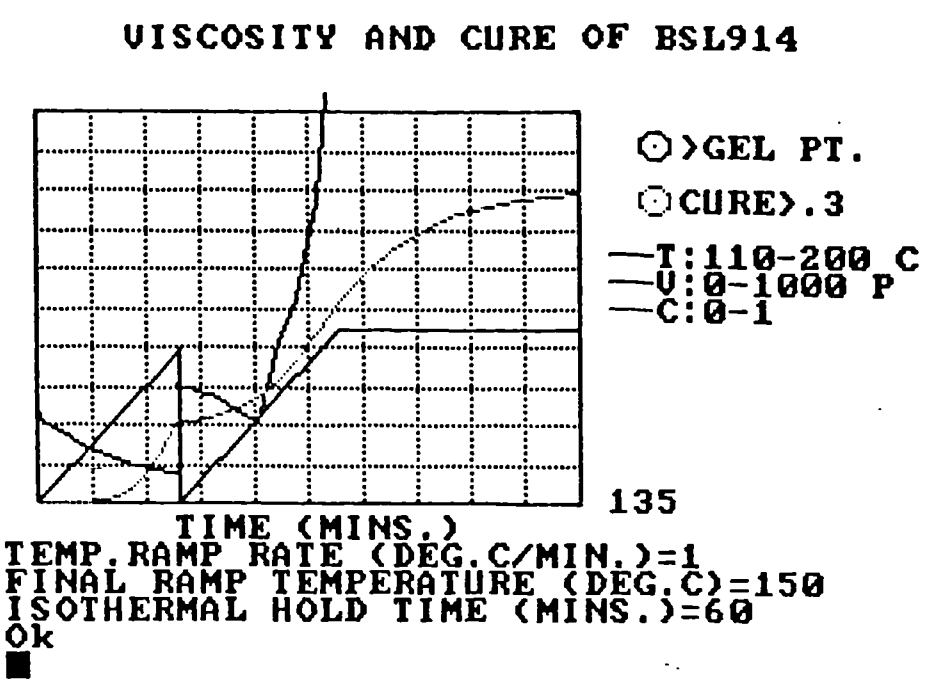

FIG.(118)

7.7 Tg Measurements.

In order to assess whether or not the thermomechanical properties of the resin are dependent on the manner in which conversion is achieved samples of resin were preconverted to the times shown in Table 42. These samples were then further heat treated so that maximum cure at each isothermal condition was realised. The Tg of each sample was then evaluated by means of TMA.

Typical results are as shown in Table 46 for resin preconverted to 30% at the preconversion temperatures indicated, ref.60.

Within experimental error it is concluded that irrespective of preconversion temperature the Tg at each isothermal cure condition is constant with mean Tg values of 87.84, 95.23 and 98.54°C being obtained at the corresponding isothermal cure temperatures of 125, 135 and 150°C.

Additional results for 50% converted material are as follows:-

After preconversion at 125°C	Tg = 49.44°C
After preconversion at 150°C	Tg = 47.54°C
Preconverted at 125°C + 4 hours at 190°C	Tg = 177.6°C
Preconverted at 150°C + 4 hours at 190°C	Tg = 179.5°C

- These results further indicate that the Tg following cure is only dependent on the amount of conversion and independent of the manner in which conversion is achieved for matrix resin in the above temperature range.

Further testing is required however to assess composite material performance under varying conditions of cure since the fibre-matrix interface properties may depend on the manner in which full cure is achieved.

7.8 Region Of Mouldability.

From the above the two main conclusions reached are:-

1) that modifications to the 'VISICURE' program based on the principle of repeat model application following a break in a moulding cycle may be used to evaluate resin conversion and viscosity on re-run.

2) that the thermomechanical properties of the resin are substantially independent of the path followed to a specific conversion within the range of mouldability of the resin.

Tentative initial guidelines as to the boundary conditions for the moulding of preconverted material may thus be obtained by means of the model.

By analysis of a number of simulation cycles with breaks as in Fig.(118) the times for which the viscosity is below 150 Poise during both the initial conditions before the incidence of failure and

the conditions appertaining to re-run may be established. On the assumption that a minimum time of 10 minutes at which the viscosity is below 150 Poise would be required during the second cycle for effective moulding then a region as shown hatched in Fig.(119) within which remoulding of the material is not possible may be determined. For any ramp rate therefore there exsist upper and lower temperature limits within which option (3) in section 7.5 would have to be taken up and the moulding operation discontinued.

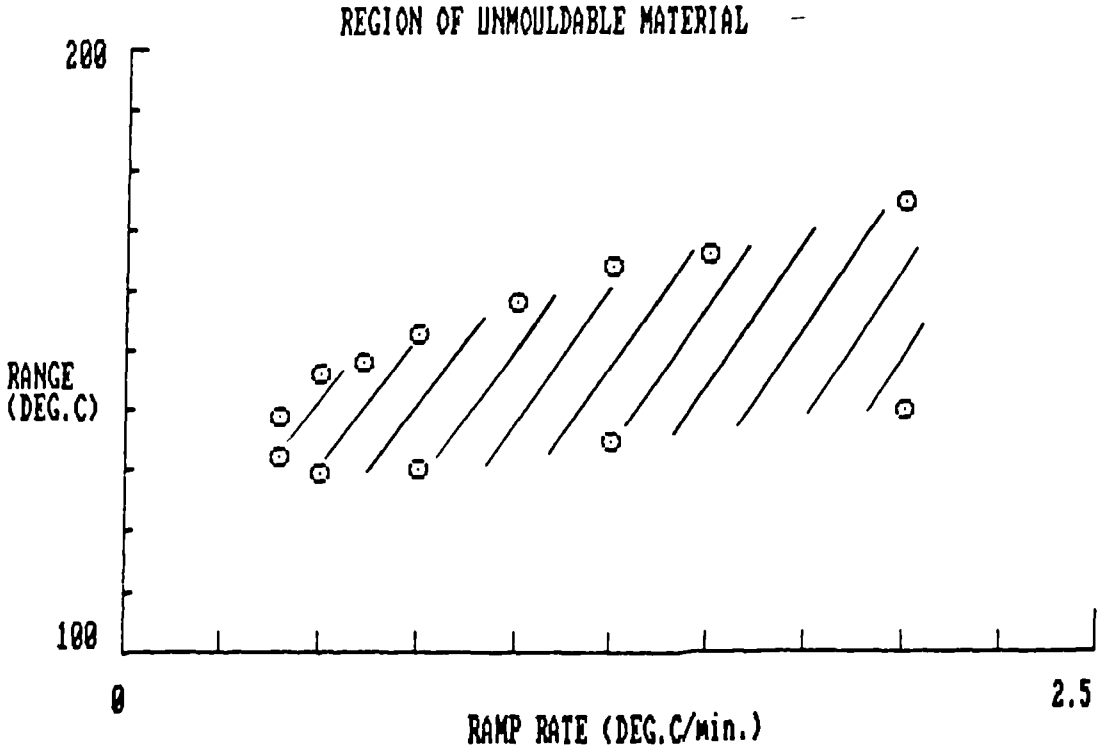

FIG.(119)

CONCLUSIONS

In the current work the reaction kinetics and viscosity behaviour of the BSL 914 resin system during cure by the application of heat have been studied and mathematically modelled.

In its cure behaviour the resin behaves in an autocatalytic manner whereby the reaction kinetics equation includes two reaction orders which have been found to be temperature dependent. The rate constant in the kinetic formula can be described by an equation of the Arrhenius form and two methods for the determination of the apparent activation energy from isothermal differential scanning calorimeter experimental results have been developed.

The activation energies obtained by these methods have compared favourably with those determined from master cure curves and Fourier Transform Infra-Red analysis.

By the incorporation of the reaction orders and activation energy in an autocatalytic function a mathematical model has been generated by means of which the cure at any time during an isothermal dwell can be predicted. Further, by appropriate integration of the rate equation, the cure with time during a linear temperature ramp can be evaluated.

It has been found that the viscosity behaviour of the resin under isothermal conditions can be adequately represented by quadratic equations with time as the independent variable. The coefficients of the quadratic equations at different temperatures can be related by an expression of the Arrhenius type. By appropriate integration the viscosity changes that occur with time during a linear temperature ramp can also be mathematically described. The modelled viscosity behaviour has been found to compare favourably with

experimental results.

By the use of these two mathematical models a program for use on a personal computer has been written in BASIC by means of which viscosity changes and cure advancement of the resin can be simulated for isothermal and dynamic temperature conditions.

The computer program has been found of use for the design of moulding cycles for carbon fibre prepreg consolidation in an autoclave manufacturing process.

It is envisaged that continued development of this program will be its incorporation in a totally integrated cure simulation of the process which will include not only the resin chemorheological behaviour but also the fibre dominated property models that affect laminate movement during consolidation.

The established procedures for model generation together with the auxiliary computer programs written during the course of this work will be invaluable for the generation of similar models for other resin systems in future should the need arise.

REFERENCES

(1) W.R.Jones,J.W.Johnson "A resin injection technique for the fabrication of aero engine components." Symposium Fabrication Techniques for Advanced Reinforced Plastics,University of Salford,April 1980.

(2) W.R.Jones "Investigations of resin injection techniques and their application in composite fabrication." MSc Thesis,University of Salford,1984.

(3) D.Purslow,R.Childs "Autoclave moulding of carbon fibre-reinforced epoxies." Composites,Vol.17,April 1986.

(4) A.C.Loos,G.S.Springer "Curing of graphite/epoxy composites." U.S.Govt.report AD-A130071.

(5) G.S.Springer "A Model of the Curing Process of Epoxy matrix Composites." Progress in Science and Engineering of composites,ICCM-IV,Tokyo 1982.

(6) A.C.Loos,G.S.Springer "Curing of Epoxy Matrix Composites." J.of Comp.Matls.,Vol.17,March 1983.

(7) R.Dave,J.L.Kardos,M.P.Dudukovic "Process Modelling of Thermosetting Matrix Composites:A guide for Autoclave Cure Cycle Selection." Amer.Soc.for Comp. 1st Technical Conf. Dayton Ohio 7-9 Oct.1986.

(8) L.Nicolais,A.Apicella "Processing of composite structures." Pure and Appl.Chem.,Vol.57,No.11,1985.

(9) A.R.Mallow,F.R.Muncaster,F.C.Campbell "Science based cure model for Composites." Amer.Soc.for Comp. 1st Technical Conf. Dayton Ohio,7-9 Oct.1986.

(10) J.W.Johnson "Resin matrices and their contribution

to composite properties."
Phil.Trans.R.Soc.London,A294,1980.

(11) J.W.Johnson "Processing and property relationships for fibre composites."Composites,Vol.14,No.2 April 1983.

(12) S.A.Zahir "The mechanism of the cure of epoxide resins by cyanamide and dicyandiamide." Sixth Int.Conf.in Organic Coatings Sci.and Techology,Technomics Pub.Co.Ltd.

(13) T.F.Saunders,M.F.Levy,J.F.Serino "Mechanism of the Tertiary Amine-Catalysed Dicyandiamide Cure of epoxy resins." J.of Poly.Sci.,Vol.5,1967.

(14) J.M.Barton "The application of Differential Scanning Calorimetry (DSC) to the study of Epoxy Resin Curing Reactions." Adv.Poly.Sci.,Vol.72,1985.

(15) "Thermal Characterization of Polymeric Materials." Edited by E.A.Turi, Academic Press,1981.

(16) K.Walsh,Rolls-Royce plc computer files.

(17) K.D.Tekchandani,Rolls-Royce plc computer files.

(18) J.M.Barton,D.C.L.Greenfield "Differential Scanning Calorimetry Cure studies of Tetra-N-glycidil diaminodiphenyl methane Epoxy Resins. 3-Reaction with Dicyandiamide." Brit.Poly.Journal,Vol.18,No.3,1986.

(19) N.S.Schneider,J.F.Sprouse,G.L.Hagnauer,J.K.Gillham "DSC and TBA studies of the curing behaviour of two DICY-containing epoxy resins." Poly.Eng.and Sci.,Vol.19,No.4 March 1979.

(20) E.Sacher "Kinetics of epoxy cure:3.The systems bisphenol-A epoxies/dicy." Polymer,Vol.14,March 1973.

(21) "Handbook of epoxy resins." by H.Lee and K.Neville,McGraw Hill Book Co.,1967.

(22) G.L.Hagnauer,D.A.Dunn "Dicyandiamide Analysis and solubility in epoxy resins." J.of App.Poly.Sci.,Vol.26,1981.

(23) J.Richards,Rolls-Royce plc computer files.

(24) G.Tydings,Rolls-Royce plc computer files.

(25) M.R.Kamal,S.Sourour "Kinetics and Thermal Characterisation of thermoset cure." Poly.Eng. and Sci.,Vol.13,Jan.1973.

(26) W.J.Sichina, Application Brief No.TA-93,DuPont publication.

(27) W.J.Sichina, Application Brief No.TA-98,DuPont publication.

(28) "General Chemistry." Edited by H.F.Holtzclaw,JR,W.R.Robinson and W.H.Nebergall. D.C.Heath and Co.

(29) C.C.Riccardi,H.E.Adahbo,J.R.Williams "Curing reaction of epoxy resins with diamines." J.of App.Poly.Sci., Vol.29,1984.

(30) P.Peyser,N.D.Bascom "Kinetics of epoxy resin polymerization using Differential Scanning Calorimetry." J.of App.Poly.Sci.,Vol.21,1977.

(31) R.B.Prime,E.Sacher "Kinetics of epoxy cure : 2 The system bisphenol-A diglycidil ether/polyamide." Polymer,Vol.13,1972.

(32) M.A.Acitelli,R.B.Prime,E.Sacher "Kinetics of epoxy cure :(1)The system bisphenol-A diglycidil ether/m-phenylene diamine." Polymer 12,1971.

(33) A.Dutta,M.E.Ryan "Effect of fillers on Kinetics of Epoxy cure." J.of App.Poly.Sci.,Vol.24,1979.

(34) K.A.Kasturiarachchi,G.Pritchard "Free dicyandiamide in crosslinked epoxy resins." J.of Mat.Sci.Letters 3,(1984).

(35) L.T.Pappalardo "DSC Evaluation of Epoxy and Polyimide-Impregnated Laminates (Prepregs.)" J.of App.Poly.Sci.,Vol.21,1977.

(36) S.Sourour,M.R.Kamal "Differential Scanning Calorimetry for characterisation of Thermoset Cure." Thermochim.Acta.14,41(1976).

(37) M.R.Kamal,S.Sourour,M.Ryan "Integrated thermo-rheological analysis of the cure of thermosets." SPE 31st Ann.Tech.Conf.Proc. 187(1973).

(38) C.D.Han,K.Lem "An experimental study of the injection moulding of thermosetting Polyester Resin." Poly.Eng.and Science,Vol.24,1984.

(39) M.R.Kamal "Thermoset characterization for Moldability Analysis." Poly.Eng.and Science,Vol.14,March 1974.

(40) M.E.Ryan,A.Dutta "Kinetics of epoxy cure : a rapid technique for kinetic parameter estimation." Polymer,Vol.20,1979.

(41) M.R.Keenan "Autocatalytic Cure Kinetics from DSC Measurements : Zero initial cure rate." J.of App.Poly.Sci.,Vol.33,1987.

(42) J.Mijovic.J.Kim,J.Slaby "Cure Kinetics of Epoxy formulations of the type used in Advanced Composites." J.of App.Poly.Sci.,Vol.29,1984.

(43) J.M.Barton,D.P.Bashford,Technical Report 77108,July 1977,R.A.E.publication.

(44) Tai-Shung Chung "Cure mechanism of a Modified Nitrile epoxy adhesive." J.of App.Poly.Sci.,Vol.29,1984.

(45) "Mathematics for Engineers and Scientists" by Alan Jeffrey,Thomas Nelson and Sons.Ltd.,1969.

(46) J.Higgins,Rolls-Royce plc computer files.

(47) "Encyclopedia of Polymer Science and Technology."Vols.8 and 14,Interscience Publishers,New York.

(48) A.Dinsdale,F.Moore "Viscosity and its measurement." published by The Inst.of Physics and The Phys.Soc.,1962.

(49) R.McKennell "The measurement and control of viscosity and related flow properties." Ferranti Instrument Manual,1960.

(50) J.M.Bai,T.H.Hore,N.Tiwar NASA-CR-176409,1985.

(51) J.F.Carpenter "Processing science for AS/3501-6 Carbon/Epoxy Composites." ADA 132323,1983.

(52) W.Engelmaier,M.B.Roller "Temperature-Viscosity-Time Profiles support empirical rules governing Multilayer Printed Wiring Board lamination." Insulation Circuits,1975.

(53) M.T.Aronhime,J.K.Gillham "The time-temperature-transformation (TTT) cure diagram of thermosetting systems." Office of Naval Res. DTIC AD-A162628,1985.

(54) J.K.Gillham "Structure-property relationships in Polymeric Matrix Materials." Office of Naval Res. DTIC ADA 153929,1985.

(55) W.I.Lee,A.C.Loos,G.S.Springer "Heat of reaction, Degree of cure and viscosity of Hercules 3501-6 Resin." J.of Comp.Matls.,Vol.16,Nov.1982.

(56) M.R.Dusi,W.I.Lee,P.R.Ciricioli,G.S.Springer, J.of Comp.Matls.,Vol.21,1987.

(57) S.Hill,Rolls-Royce plc computer files.

(58) E.Dean,Rolls-Royce plc log.

(59) C.Stewart,Rolls-Royce plc log.

(60) D.Maddock,Rolls-Royce plc computer files.

(61) D.J.Lind,Rolls-Royce plc Private communication.

APPENDIX 1

TABLES

GRAPH TITLE:- VARIATION OF H(iso) WITH TEMPERATURE

X-AXIS TITLE:-TEMPERATURE DEG.K
Y-AXIS TITLE:-H(iso) cal/g

COORDINATES OF POINTS IN GRAPH :-

PT.NO.	X	Y
1	398.2	62.93
2	403.2	93.28
3	408.2	87.93
4	408.2	79.2
5	413.2	94.35
6	418.2	84.83
7	423.2	102.3
8	423.2	110.6
9	428.2	92.06
10	433.2	106
11	438.2	117.4
12	443.2	106.6
13	448.2	137.4
14	450.2	108.1
15	453.2	90.05
16	463.2	103.9
17	483.2	89.31

TABLE 1

REACTION RATE v CONVERSION @ 140 DEG.C

X-AXIS TITLE= FRACTIONAL CONVERSION
Y-AXIS TITLE= RATE sec.-1

POINT NO	X	Y
1	.01434	1.0758E-04
2	.04684	1.6884E-04
3	.09642	2.5427E-04
4	.15542	3.4107E-04
5	.22021	3.7372E-04
6	.34295	3.5315E-04
7	.46314	3.1542E-04
8	.56121	2.6529E-04
9	.66741	.0002036
10	.74535	.0001575
11	.81913	1.1224E-04
12	.90055	6.8882E-05
13	.95925	3.4001E-05
14	.98839	1.6513E-05

TABLE 2

RATIO m/n v TEMPERATURE

X-AXIS TITLE= TEMPERATURE (DEG.K)
Y-AXIS TITLE= m/n

POINT NO	X	Y
1	398.2	1.6155
2	403.2	1.9984
3	408.2	2.398
4	408.2	1.4332
5	413.2	3.5404
6	418.2	4.16
7	423.2	5.4521
8	423.2	6.9297
9	428.2	7.2417
10	433.2	10.4403
11	438.2	9.9627
12	448.2	12.1998
13	453.2	10.3154
14	463.2	7.0644
15	483.2	3.8114

TABLE 3

AMOUNT AND RATE OF CURE

TIME(sec.)	FRACTIONAL CURE	EXPTL.REACT.RATE
1111.11	9.852174E-03	2.023478E-05
1904.76	2.126957E-02	.000038
2698.41	3.889565E-02	2.868696E-05
3492.06	6.790435E-02	4.466957E-05
4285.72	.1127217	6.837391E-05
4730.16	.1470087	8.578261E-05
5206.35	.1906261	1.018261E-04
6000	.2679826	9.486956E-05
6793.65	.3376174	7.970436E-05
7587.3	.3942	6.376522E-05
8380.96	.4395826	5.406087E-05
9174.611	.4743913	4.066957E-05
9968.26	.4998261	3.144348E-05
11555.56	.5300174	1.838261E-05

TABLE 4(a)

ISOTHERMAL RUN TEMPERATURE 125 DEG.C

TOTAL ISOTHERMAL EXOTHERM (OBTAINED FROM FORMULA)= 62.92749

RATIO = 1.448645

ln (F*ALPHA(1-F*ALPHA)^R)	ln (dALPHA/dt)
-4.043434	-10.80811
-3.304962	-10.17793
-2.750739	-10.45907
-2.278649	-10.01622
-1.914044	-9.59052
-1.767559	-9.363694
-1.674914	-9.192244
-1.688578	-9.263007
-1.873171	-9.437186
-2.174097	-9.660302
-2.574861	-9.825399
-3.064736	-10.11003
-3.635131	-10.36732
-5.045897	-10.90411

TABLE 4(b)

AMOUNT AND RATE OF CURE

TIME(sec.)	FRACTIONAL CURE	EXPTL.REACT.RATE
793.65	3.596522E-02	5.217392E-05
1587.3	8.776522E-02	9.556522E-05
2380.95	.1696957	.000126
3111.11	.2754348	1.553913E-04
3904.76	.3948261	1.404348E-04
4698.41	.4958696	1.125217E-04
5492.06	.5749043	8.663478E-05
6285.71	.6356435	6.68087E-05
7079.37	.6816261	5.010435E-05
8666.67	.7426609	2.882609E-05
11047.62	.7888521	1.417391E-05

TABLE 5(a)

ISOTHERMAL RUN TEMPERATURE 130 DEG.C

TOTAL ISOTHERMAL EXOTHERM (OBTAINED FROM FORMULA)= 71.84155

RATIO = 1.905145

ln (F*ALPHA(1-F*ALPHA)^R)	ln (dALPHA/dt)
-2.967699	-9.860928
-2.251046	-9.255702
-1.907133	-8.979229
-1.926641	-8.769564
-2.363443	-8.870768
-3.238661	-9.092364
-4.901526	-9.353809
0	-9.613677
0	-9.901402
0	-10.45423
0	-11.16411

TABLE 5(b)

AMOUNT AND RATE OF CURE

TIME(sec.)	FRACTIONAL CURE	EXPTL.REACT.RATE
99.20999	2.041739E-03	.0000326
198.41	5.970435E-03	4.459131E-05
357.14	1.389478E-02	5.353913E-05
674.6	3.294696E-02	6.613044E-05
1111.11	6.579913E-02	8.486956E-05
1488.09	.1013122	1.042609E-04
1884.92	.1475122	1.308696E-04
2264.9	.2017469	1.573044E-04
2757.94	.2833296	1.704348E-04
3253.97	.3632252	1.566087E-04
3750	.4349905	1.352174E-04
4246.03	.4962948	1.131304E-04
4682.54	.5411035	9.104348E-05
5138.89	.5790427	7.222609E-05
5595.24	.6083557	5.725217E-05
5992.06	.6285383	.0000448
6488.09	.6479122	3.586957E-05

TABLE 6(a)

ISOTHERMAL RUN TEMPERATURE 135 DEG.C

TOTAL ISOTHERMAL EXOTHERM (OBTAINED FROM FORMULA)= 79.83448

RATIO = 2.488738

ln (F*ALPHA(1-F*ALPHA)^R)	ln (dALPHA/dt)
-5.836307	-10.3312
-4.777456	-10.01797
-3.961584	-9.835098
-3.168889	-9.623881
-2.604	-9.374396
-2.317175	-9.168614
-2.143371	-8.941309
-2.090281	-8.757328
-2.201435	-8.677158
-2.491158	-8.76176
-2.919091	-8.908626
-3.458789	-9.086969
-4.011209	-9.304174
-4.652091	-9.535709
-5.333716	-9.768044
-5.967994	-10.0133
-6.807589	-10.23562

TABLE 6(b)

AMOUNT AND RATE OF CURE

TIME(sec.)	FRACTIONAL CURE	EXPTL.REACT.RATE
305.56	1.406957E-02	5.770435E-05
750	4.555653E-02	8.535652E-05
1194.45	9.411304E-02	1.355652E-04
1583.34	.158287	1.883478E-04
1909.47	.2235304	2.064348E-04
2381.69	.3184	1.936522E-04
2965.03	.4211826	1.583478E-04
3715.03	.5226609	1.132174E-04
4437.25	.5925304	8.162609E-05
5270.59	.6490782	5.492174E-05
6187.26	.6911477	3.697391E-05
7437.26	.726226	2.087826E-05

TABLE 7(a)

ISOTHERMAL RUN TEMPERATURE 135 DEG.C

TOTAL ISOTHERMAL EXOTHERM (OBTAINED FROM FORMULA)= 79.83448

RATIO = 2.488738

ln (F*ALPHA(1-F*ALPHA)^R)	ln (dALPHA/dt)
-3.949722	-9.760178
-2.892749	-9.368673
-2.360848	-8.906058
-2.122411	-8.57722
-2.100342	-8.485526
-2.306777	-8.549447
-2.822192	-8.750717
-3.762834	-9.086201
-4.939053	-9.413361
-6.869266	-9.809602
-13.50007	-10.2053
0	-10.7768

TABLE 7(b)

AMOUNT AND RATE OF CURE

TIME(sec.)	FRACTIONAL CURE	EXPTL.REACT.RATE
178.57	1.176522E-02	8.826088E-05
416.67	3.842609E-02	1.385218E-04
654.76	7.910435E-02	2.086087E-04
853.1701	.127513	2.798261E-04
1031.75	.1806696	3.066087E-04
1369.05	.2813653	2.897391E-04
1726.19	.379974	2.587826E-04
2063.49	.4604348	2.176522E-04
2519.84	.5475653	1.670435E-04
2956.35	.6115131	1.292174E-04
3511.91	.6720435	9.208696E-05
4464.29	.7388435	5.651305E-05
5793.66	.7870001	2.789565E-05
7222.23	.8109131	1.354783E-05

TABLE 8(a)

ISOTHERMAL RUN TEMPERATURE 140 DEG.C

TOTAL ISOTHERMAL EXOTHERM (OBTAINED FROM FORMULA)= 86.90747

RATIO = 3.230146

ln (F*ALPHA(1-F*ALPHA)^R)	ln (dALPHA/dt)
-4.213203	-9.335214
-3.147498	-8.884482
-2.614051	-8.475051
-2.376387	-8.181342
-2.31352	-8.089938
-2.49235	-8.14653
-2.944666	-8.259523
-3.530978	-8.432611
-4.487134	-8.697256
-5.562267	-8.954015
-7.226067	-9.292777
-12.30332	-9.781039
0	-10.48704
0	-11.20929

TABLE 8(b)

AMOUNT AND RATE OF CURE

TIME(sec.)	FRACTIONAL CURE	EXPTL.REACT.RATE
46.03	2.629565E-03	8.486086E-05
103.57	8.862608E-03	1.323478E-04
172.62	1.956696E-02	1.785218E-04
241.67	3.355826E-02	2.272174E-04
310.71	5.125391E-02	2.873913E-04
391.27	7.741043E-02	3.643478E-04
471.83	.1092278	4.190435E-04
552.38	.1438365	4.349566E-04
678.97	.1982713	4.226087E-04
794.0501	.2458626	4.044348E-04
920.63	.2960452	3.884348E-04
1093.25	.3603844	3.562609E-04
1265.87	.41808	3.126087E-04
1496.03	.4834887	2.572174E-04
1749.21	.5415409	2.025217E-04
2036.91	.5929756	1.570435E-04
2324.6	.6326452	1.205217E-04

TABLE 9(a)

ISOTHERMAL RUN TEMPERATURE 145 DEG.C

TOTAL ISOTHERMAL EXOTHERM (OBTAINED FROM FORMULA)= 93.0603

RATIO = 4.166357

ln (F*ALPHA(1-F*ALPHA)^R)	ln (dALPHA/dt)
-5.742814	-9.374498
-4.560112	-8.930077
-3.824209	-8.6308
-3.359251	-8.389602
-3.031893	-8.154666
-2.765879	-7.917402
-2.606764	-7.777536
-2.54278	-7.740264
-2.577422	-7.769064
-2.700172	-7.81302
-2.903144	-7.853386
-3.26461	-7.939848
-3.689361	-8.070559
-4.30642	-8.265589
-5.010817	-8.504664
-5.809099	-8.758988
-6.588714	-9.023681

TABLE 9(b)

AMOUNT AND RATE OF CURE

TIME(sec.)	FRACTIONAL CURE	EXPTL.REACT.RATE
55.56	1.081739E-02	2.773044E-04
111.11	2.896522E-02	3.72087E-04
152.78	4.593043E-02	4.396522E-04
208.33	7.298261E-02	5.329565E-04
250	9.632173E-02	5.842609E-04
291.67	.1210348	6.008696E-04
416.67	.1954783	6.099131E-04
597.22	.2961739	5.339131E-04
791.6701	.394087	4.722609E-04
1013.89	.4883479	3.789565E-04
1347.22	.5957391	2.714783E-04
1819.45	.6984348	1.74087E-04
2625	.7964348	8.517391E-05
3666.67	.8562869	3.851305E-05

TABLE 10(a)

ISOTHERMAL RUN TEMPERATURE 150 DEG.C

TOTAL ISOTHERMAL EXOTHERM (OBTAINED FROM FORMULA)= 98.29272

RATIO = 5.341704

ln (F*ALPHA(1-F*ALPHA)^R)	ln (dALPHA/dt)
-4.437655	-8.190396
-3.568839	-7.896384
-3.218696	-7.729527
-2.937327	-7.537071
-2.821762	-7.445163
-2.770342	-7.417133
-2.862479	-7.402194
-3.332386	-7.535278
-4.076298	-7.657979
-5.084839	-7.879089
-6.739079	-8.211629
-9.277992	-8.655956
-14.41544	-9.370815
0	-10.16451

TABLE 10(b)

AMOUNT AND RATE OF CURE

TIME(sec.)	FRACTIONAL CURE	EXPTL.REACT.RATE
83.32999	1.253044E-02	2.197391E-04
250	6.367826E-02	3.980869E-04
388.89	.1261304	.000486
583.33	.218913	4.647826E-04
888.89	.353	4.126957E-04
1388.89	.5296087	2.914783E-04
2083.33	.6844783	1.67913E-04
2777.78	.775	1.00087E-04
3472.22	.8312435	6.376522E-05
4166.67	.8687566	4.551305E-05
4861.11	.8946088	3.142609E-05
5555.55	.9134957	2.503478E-05

TABLE 11(a)

ISOTHERMAL RUN TEMPERATURE 150 DEG.C

TOTAL ISOTHERMAL EXOTHERM (OBTAINED FROM FORMULA)= 98.29272

RATIO = 5.341704

ln (F*ALPHA(1-F*ALPHA)^R)	ln (dALPHA/dt)
-4.301503	-8.42307
-3.010502	-7.828841
-2.766332	-7.629302
-2.942598	-7.673941
-3.730004	-7.7928
-5.641967	-8.140545
-8.841262	-8.692065
-12.76982	-9.209471
-19.23022	-9.660302
0	-9.997511
0	-10.36787
0	-10.59525

TABLE 11(b)

AMOUNT AND RATE OF CURE

TIME(sec.)	FRACTIONAL CURE	EXPTL.REACT.RATE
28.57001	6.848696E-03	3.871305E-04
66.67001	.02584	5.993044E-04
114.29	5.901392E-02	7.695653E-04
161.9	9.715304E-02	8.150435E-04
257.14	.1735704	7.772175E-04
361.9	.2512661	7.055652E-04
466.67	.3222487	6.488696E-04
609.52	.4075705	5.452174E-04
752.38	.4780227	4.454783E-04
895.24	.5353357	3.601739E-04
1161.9	.615727	2.513043E-04
1447.62	.6749443	.00017
1742.86	.71684	1.161739E-04
1980.95	.7410835	8.667826E-05
2219.05	.7591096	6.452174E-05

TABLE 12(a)

ISOTHERMAL RUN TEMPERATURE 155 DEG.C

TOTAL ISOTHERMAL EXOTHERM (OBTAINED FROM FORMULA)= 102.6055

RATIO = 6.808988

ln (F*ALPHA(1-F*ALPHA)^R)	ln (dALPHA/dt)
-4.922124	-7.856749
-3.741901	-7.419741
-3.181891	-7.169685
-3.002409	-7.11227
-3.110177	-7.159791
-3.519306	-7.256512
-4.069673	-7.340279
-4.938927	-7.514326
-5.849058	-7.716363
-6.749887	-7.928924
-8.347801	-8.288846
-9.897054	-8.679712
-11.29539	-9.060422
-12.27511	-9.353307
-13.11584	-9.648508

TABLE 12(b)

AMOUNT AND RATE OF CURE

TIME(sec.)	FRACTIONAL CURE	EXPTL.REACT.RATE
15.87	4.956522E-03	4.92087E-04
47.62	2.596522E-02	7.833913E-04
79.37	5.244348E-02	8.713043E-04
126.98	9.477391E-02	8.965217E-04
190.48	.1508174	8.663478E-04
333.33	.2669913	7.579131E-04
476.19	.3691652	6.664348E-04
634.92	.4652522	5.430435E-04
857.14	.5686435	3.946957E-04
1269.84	.6928173	2.261739E-04
1666.67	.7645305	1.412174E-04
2063.49	.8110174	9.539131E-05

TABLE 13(a)

ISOTHERMAL RUN TEMPERATURE 160 DEG.C

TOTAL ISOTHERMAL EXOTHERM (OBTAINED FROM FORMULA)= 105.9976

RATIO = 8.630825

ln (F*ALPHA(1-F*ALPHA)^R)	ln (dALPHA/dt)
-5.272073	-7.616855
-3.816106	-7.151879
-3.3721	-7.045519
-3.211209	-7.016989
-3.352325	-7.051224
-4.190951	-7.184942
-5.331306	-7.313568
-6.748761	-7.518321
-8.764785	-7.837396
-12.30779	-8.394206
-15.45318	-8.865211
-18.42022	-9.257522

TABLE 13(b)

AMOUNT AND RATE OF CURE

TIME(sec.)	FRACTIONAL CURE	EXPTL.REACT.RATE
19.04999	1.682609E-02	1.383478E-03
47.62	6.139131E-02	1.654783E-03
76.19	.1090696	1.673044E-03
142.86	.2158522	1.515652E-03
228.57	.3359391	1.30087E-03
352.38	.4798522	1.017391E-03
495.24	.6013304	7.171305E-04
647.62	.6940261	5.142609E-04
838.09	.7761391	3.597391E-04
1038.09	.8373479	2.596522E-04
1257.14	.8857392	1.865217E-04

TABLE 14(a)

ISOTHERMAL RUN TEMPERATURE 165 DEG.C

TOTAL ISOTHERMAL EXOTHERM (OBTAINED FROM FORMULA)= 108.4692

RATIO = 10.88109

ln (F*ALPHA(1-F*ALPHA)^R)	ln (dALPHA/dt)
-4.222221	-6.583154
-3.464345	-6.404086
-3.49445	-6.393111
-4.302366	-6.49191
-5.823449	-6.644722
-8.409962	-6.890514
-11.49258	-7.240253
-14.79054	-7.57278
-19.02866	-7.930132
-23.91757	-8.256168
-30.50814	-8.586962

TABLE 14(b)

AMOUNT AND RATE OF CURE

TIME(sec.)	FRACTIONAL CURE	EXPTL.REACT.RATE
13.89002	1.383478E-02	1.71913E-03
41.66998	7.442609E-02	2.377391E-03
55.56	.1076087	2.405218E-03
97.21997	.2036087	2.202609E-03
166.67	.3436087	1.851304E-03
236.11	.4620435	1.553913E-03
388.89	.6518696	9.747826E-04
597.22	.8056086	5.549565E-04
916.6701	.9340434	2.914783E-04
1263.89	1.012704	1.765218E-04

TABLE 15(a)

ISOTHERMAL RUN TEMPERATURE 175 DEG.C

TOTAL ISOTHERMAL EXOTHERM (OBTAINED FROM FORMULA)= 110.6528

RATIO = 17.0285

ln (F*ALPHA(1-F*ALPHA)^R)	ln (dALPHA/dt)
-4.488653	-6.365937
-3.930299	-6.041752
-4.210286	-6.030115
-5.601711	-6.118113
-8.552541	-6.291866
-11.87535	-6.466979
-19.65862	-6.933296
-31.0944	-7.496621
-60.16567	-8.140545
0	-8.642066

TABLE 15(b)

lnK(L) v 1/TEMPERATURE

X-AXIS TITLE= 1/TEMPERATURE (1/DEG.K)
Y-AXIS TITLE= lnK(L)

POINT NO	X	Y
1	2.511301E-03	-8.32849
2	2.480159E-03	-6.915367
3	2.449779E-03	-7.867867
4	2.449779E-03	-7.046865
5	2.420136E-03	-6.584628
6	.0023912	-6.394774
7	2.362949E-03	-6.129548
8	2.362949E-03	-6.071275
9	2.335357E-03	-5.824323
10	2.308403E-03	-5.921689
11	2.282063E-03	-5.527075
12	2.231147E-03	-3.721295

TABLE 16(a)

VARIATION OF n(L) WITH TEMPERATURE

X-AXIS TITLE= TEMPERATURE (DEG.K)
Y-AXIS TITLE= n(L)

POINT NO	X	Y
1	403.2	.83335
2	408.2	.6149505
3	413.2	.6005297
4	418.2	.4993788
5	423.2	.4982595
6	423.2	.4508438
7	428.2	.3909526
8	433.2	.3053416
9	438.2	.2362771

TABLE 16(b)

lnK(U) v 1/TEMPERATURE

X-AXIS TITLE= 1/TEMPERATURE (1/DEG.K)
Y-AXIS TITLE= lnK(U)

POINT NO	X	Y
1	2.511301E-03	-7.885327
2	2.480159E-03	-7.942618
3	2.449779E-03	-7.536442
4	2.449779E-03	-7.577486
5	2.420136E-03	-7.259516
6	.0023912	-6.715866
7	2.362949E-03	-6.99811
8	2.362949E-03	-6.716241
9	2.335357E-03	-6.329089
10	2.308403E-03	-6.486325
11	2.282063E-03	-5.995378
12	2.231147E-03	-5.740492

TABLE 17(a)

VARIATION OF n(U) WITH TEMPERATURE

X-AXIS TITLE= TEMPERATURE (DEG.K)
Y-AXIS TITLE= n(U)

POINT NO	X	Y
1	398.2	.4991208
2	403.2	.1958252
3	408.2	.3482437
4	408.2	.2824536
5	413.2	.2484659
6	418.2	.3153951
7	423.2	.1738993
8	423.2	.1944913
9	428.2	.222446
10	433.2	.1432376
11	438.2	.1000846
12	448.2	.0600623

TABLE 17(b)

lnK(D) v 1/TEMPERATURE

X-AXIS TITLE= 1/TEMPERATURE (DEG.K)
Y-AXIS TITLE= lnK(D) sec-1

POINT NO	X	Y
1	.0025113	-8.4354
2	.0024802	-8.4345
3	.0024498	-8.0889
4	.0024498	-8.1909
5	.0024201	-7.7639
6	.0023912	-7.311
7	.0023629	-7.484
8	.0023629	-7.204
9	.0023354	-6.8096
10	.0023084	-6.8573
11	.0022821	-6.3602
12	.0022311	-6.1425

TABLE 18(a)

VARIATION OF n(D) v TEMPERATURE

X-AXIS TITLE= TEMPERATURE (DEG.K)
Y-AXIS TITLE= n(D)

POINT NO	X	Y
1	398.2	.1978
2	403.2	.1551
3	408.2	.1532
4	408.2	.1493
5	413.2	.1455
6	418.2	.1395
7	423.2	.114
8	423.2	.087
9	428.2	8.560001E-02
10	433.2	.0819
11	438.2	.0563
12	448.2	.0683

TABLE 18(b)

lnK(LP) v 1/TEMPERATURE

X-AXIS TITLE= 1/TEMPERATURE (1/DEG.K)
Y-AXIS TITLE= lnK(LP)

POINT NO	X	Y
1	.0025113	-8.454799
2	.0024802	-8.4408
3	.0024498	-8.1121
4	.0024201	-7.8136
5	.0023912	-7.3711
6	.0023629	-7.488
7	.0023629	-7.1636
8	.0023354	-6.7963
9	.0023084	-6.8605
10	.002282	-6.3368

TABLE 19(a)

VARIATION OF n(LP) WITH TEMPERATURE

X-AXIS TITLE= TEMPERATURE (DEG.K)
Y-AXIS TITLE= n(LP)

POINT NO	X	Y
1	398.2	.1728
2	403.2	.1473
3	408.2	.1255
4	413.2	8.910001E-02
5	418.2	7.240001E-02
6	423.2	.1097
7	423.2	.1327
8	428.2	.0998
9	433.2	.0786
10	438.2	.0809

TABLE 19(b)

lnK(WH) v 1/TEMPERATURE

X-AXIS TITLE= 1/TEMPERATURE (1/DEG.K)
Y-AXIS TITLE= lnK(WH)

POINT NO	X	Y
1	.0025113	-8.4332
2	.0024498	-8.1717
3	.0023629	-7.1388
4	.0023354	-6.9044
5	.0023084	-6.8615

TABLE 20(a)

VARIATION OF n(WH) WITH TEMPERATURE

X-AXIS TITLE= TEMPERATURE (DEG.K)
Y-AXIS TITLE= n(WH)

POINT NO	X	Y
1	398.2	.2005
2	408.2	.1852
3	423.2	.1159
4	428.2	.1002
5	433.2	.0774

TABLE 20(b)

SUMMARY OF KINETIC PARAMETERS EVALUATION

ACTIVATION ENERGY, E kJ/mole	lnA sec-1	EQUATION FOR INDEX n		EQUATION IN TEXT	COMMENTS
		SLOPE	INTERCEPT		
92	-	-	-	3.5	From dynamic exotherm
88	-	-	-	3.7	From dynamic exotherm
108	24.58	-1.52E-2	6.87	3.27, 3.30	METHOD A-(L) values
70	13.03	-6.57E-3	3.00	3.31, 3.32	METHOD A-(U) values
76	14.28	-2.73E-3	1.27	3.44, 3.47	METHOD B-(D) values
78	15.04	-4.42E-3	1.98	3.48, 3.49	METHOD B-(LP) values
72	13.23	-4.83E-3	2.18	3.52, 3.53	METHOD B-(WH) values

TABLE 21

ARRHENIUS PLOT FOR ln(TIME SHIFT)

X-AXIS TITLE= 1/TEMPERATURE (1/DEG.K)
Y-AXIS TITLE= ln(SHIFT) sec.

POINT NO	X	Y
1	.0025113	1.8875
2	.0024498	.875
3	.0023912	0
4	.0023354	-.775
5	.0022821	-1.325
6	.0022311	-1.675

TABLE 22

ARRHENIUS PLOT FOR ln(TIME SHIFT)

X-AXIS TITLE= 1/TEMPERATURE (1/DEG.K)
Y-AXIS TITLE= ln(SHIFT)

POINT NO	X	Y
1	.0025113	1.895
2	.0024498	.895
3	.0023912	0
4	.0023354	-.78
5	.0022821	-1.555
6	.0022311	-1.8925

TABLE 23

GRAPH TITLE:-ln(REACTION RATE) v 1/TEMPERATURE
X-AXIS TITLE:-1/TEMPERATURE (1/DEG.K)
Y-AXIS TITLE:-ln(REACTION RATE) sec-1

POINT NO	X	Y
1	.0025113	-9.4121
2	.0024802	-8.8548
3	.0024498	-8.3349
4	.0023912	-7.4935

TABLE 24

ln(GELTIME) v 1/TEMPERATURE

X-AXIS TITLE= 1/TEMPERATURE (1/DEG.K)
Y-AXIS TITLE= ln(TIME) sec.

POINT NO	X	Y
1	.0024498	7.98616
2	.0023912	7.2724
3	2.36295E-03	6.95655
4	.0023084	6.04025

TABLE 25

ISOTHERMAL CURE RATE CALCULATED FROM THE
GENERALISED AUTOCATALYSED MODEL

ISOTHERMAL TEMPERATURE= 125

FRACTIONAL CONVERSION	THEORETICAL CURE RATE
.05	6.964175E-05
.1	8.535804E-05
.15	9.322221E-05
.2	9.654162E-05
.25	9.646456E-05
.3	9.343791E-05
.4	7.845895E-05
.5	4.584817E-05

TABLE 26

ISOTHERMAL CURE RATE CALCULATED FROM THE
GENERALISED AUTOCATALYSED MODEL

ISOTHERMAL TEMPERATURE= 130

FRACTIONAL CONVERSION	THEORETICAL CURE RATE
.05	1.064264E-04
.1	1.27278E-04
.15	1.370405E-04
.2	1.40656E-04
.25	1.399082E-04
.3	1.356151E-04
.4	1.176159E-04
.5	8.632042E-05
.6	3.178982E-05

TABLE 27

ISOTHERMAL CURE RATE CALCULATED FROM THE
GENERALISED AUTOCATALYSED MODEL

ISOTHERMAL TEMPERATURE= 140

FRACTIONAL CONVERSION	THEORETICAL CURE RATE
.05	2.36713E-04
.1	2.68754E-04
.15	2.801626E-04
.2	2.808965E-04
.25	2.745997E-04
.3	2.630736E-04
.4	2.280755E-04
.5	1.803455E-04
.6	1.214356E-04
.7	5.028288E-05

TABLE 28

ISOTHERMAL CURE RATE CALCULATED FROM THE
GENERALISED AUTOCATALYSED MODEL

ISOTHERMAL TEMPERATURE= 150

FRACTIONAL CONVERSION	THEORETICAL CURE RATE
.05	4.999349E-04
.1	5.386495E-04
.15	5.431745E-04
.2	5.311231E-04
.25	5.088604E-04
.3	4.795596E-04
.4	4.067182E-04
.5	3.215934E-04
.6	2.294375E-04
.7	1.345184E-04
.8	4.246021E-05

TABLE 29

ISOTHERMAL CURE RATE CALCULATED FROM THE
GENERALISED AUTOCATALYSED MODEL

ISOTHERMAL TEMPERATURE= 165

FRACTIONAL CONVERSION	THEORETICAL CURE RATE
.05	1.422508E-03
.1	1.433328E-03
.15	1.391436E-03
.2	1.326137E-03
.25	1.247566E-03
.3	1.16064E-03
.4	9.721993E-04
.5	7.744625E-04
.6	5.754612E-04
.7	3.817199E-04
.8	2.006694E-04
.9	4.586823E-05

TABLE 30

ISOTHERMAL CURE RATE CALCULATED FROM THE
GENERALISED AUTOCATALYSED MODEL

ISOTHERMAL TEMPERATURE= 175

FRACTIONAL CONVERSION	THEORETICAL CURE RATE
.05	2.758499E-03
.1	2.723029E-03
.15	2.643395E-03
.2	2.543478E-03
.25	2.431013E-03
.3	2.309478E-03
.4	2.045701E-03
.5	1.759043E-03
.6	1.450946E-03
.7	1.119404E-03
.8	7.576951E-04
.9	3.452301E-04

TABLE 31

GRAPH TITLE:-log v_o v TEMPERATURE
X-AXIS TITLE:-TEMPERATURE DEG.C
Y-AXIS TITLE:-log v_o

POINT NO	X	Y
1	109.6	2.2833
2	110	2.2923
3	110	2.3345
4	129	1.9823
5	129	1.8808
6	129	1.9823
7	129	1.9243
8	129	2.0792
9	129.5	1.9445
10	129.5	1.9638
11	129.5	2
12	129.5	2.0334
13	129.5	1.9031
14	129.5	1.9823
15	130	2.0645
16	138.2	1.8062
17	138.8	1.7482
18	139.2	1.8062
19	148.5	1.716
20	148.8	1.8062
21	149	1.8062
22	105.4	2.5563
23	109	2.2742
24	129.5	2.017
25	148.8	1.8062
26	138.8	1.8062
27	139.1	1.8062
28	149	1.9445
29	149	1.9031
30	126	1.9445
31	135	1.6466
32	127	1.5992
33	140	1.3452
34	145	1.4472
35	150	1.3802
36	100	2.4942
37	110	2.2041
38	120	2.0934
39	124.7	2.0492
40	129.5	1.9031
41	129.5	2.0334
42	129.5	2.017
43	129.8	1.9031
44	139	1.7482
45	139	1.7482
46	149	1.6812
47	149	1.7482

TABLE 32

GRAPH TITLE:-COEFFICIENT A v TEMPERATURE
X-AXIS TITLE:-TEMPERATURE DEG.C
Y-AXIS TITLE:-COEFFICIENT A

POINT NO	X	Y
1	109.6	9.485899E-06
2	110	9.3374E-06
3	110	2.6278E-05
4	129	.0002019
5	129	3.0515E-04
6	129	1.0545E-04
7	129	1.9858E-04
8	129	2.5091E-04
9	129.5	1.7386E-04
10	129.5	7.106801E-05
11	129.5	1.6866E-04
12	129.5	1.6046E-04
13	129.5	2.0407E-04
14	129.5	1.0116E-04
15	130	2.4729E-04
16	138.2	5.5528E-04
17	138.8	.0006786
18	139.2	6.1646E-04
19	148.5	.0033296
20	148.8	.0037398
21	149	.0028734
22	105.4	0
23	109	1.5476E-06
24	129.5	5.4574E-05
25	148.8	.0027553
26	138.8	.000718
27	139.1	6.4501E-04
28	149	.0048328
29	149	.0043495
30	126	1.952E-05
31	135	6.2596E-04
32	127	5.3892E-05
33	140	.0018313
34	145	.0042261
35	150	.0077095
36	100	1.8907E-05
37	110	4.501E-06
38	120	1.9937E-06
39	124.7	3.5917E-05
40	129.5	.0001542
41	129.5	6.6974E-05
42	129.5	1.1908E-04
43	129.8	2.4965E-04
44	139	.0013928
45	139	.0016968
46	149	.017652
47	149	.0041323

TABLE 33

GRAPH TITLE:-COEFFICIENT B v TEMPERATURE
X-AXIS TITLE:-TEMPERATURE DEG.C
Y-AXIS TITLE:-COEFFICIENT B

POINT NO	X	Y
1	109.6	8.0062E-04
2	110	7.8402E-04
3	110	4.5717E-04
4	129	.0029355
5	129	.0024803
6	129	.0078935
7	129	.0023527
8	129.5	.0037192
9	129.5	.0016405
10	129.5	7.189E-05
11	129.5	1.3349E-04
12	129.5	.0025115
13	129.5	8.0007E-04
14	130	3.1767E-05
15	138.2	.0034102
16	138.8	.0041284
17	148.5	.011
18	148.8	4.6126E-04
19	149	.0044725
20	105.4	0
21	1091	.0017943
22	129 5	.0020159
23	148 8	.0083374
24	149	.0068528
25	149	.03976
26	110	.0013451
27	120	.0034839
28	124.7	7.7982E-04
29	129.5	.003883
30	129.5	7.2558E-04
31	129.8	.0030755
32	139	.01618
33	139	.01313

TABLE 34

DYNAMIC MODEL RESULTS

TEMPERATURE RAMP RATE = 10000 DEG.C/MIN.
INITIAL RAMP TEMPERATURE = 110 DEG.C
FINAL RAMP TEMPERATURE = 175 DEG.C
ISOTHERMAL HOLD TIME AT 175 DEG.C = 20 MIN.

TIME (MIN.)	VISCOSITY (POISE)	CURE	HEAT OUTPUT (cal/g/s)
		RAMP CONDITIONS	
0	283.168	.0000001	0
6.499999E-04	216.2567	1.013282E-07	3.928701E-06
.0013	166.648	1.058936E-07	1.359055E-05
1.950001E-03	129.5223	1.209394E-07	4.550987E-05
.0026	101.49	1.709616E-07	1.561999E-04
3.249999E-03	80.1435	3.446154E-07	5.638542E-04
3.899998E-03	63.756	9.611799E-07	2.039227E-03
4.549996E-03	51.07827	3.037176E-06	6.799961E-03
5.199995E-03	41.19782	9.295325E-06	2.003755E-02
5.849994E-03	33.44308	2.593442E-05	5.199086E-02
		ISOTHERMAL CONDITIONS	
6.499992E-03	27.31558	6.5211E-05	.1200564
2.0065	47.80895	.3083767	.263163
4.0065	218.5684	.5425046	.1875358
6.0065	2610.158	.7050353	.1267299
8.0065	81420.41	.8124531	8.163166E-02
10.0065	10000	.8800372	4.991094E-02
12.0065	10000	.9202558	.0287022
14.0065	10000	.9426389	1.530194E-02
16.0065	10000	.9540895	7.398006E-03
18.0065	10000	.9593338	3.132872E-03
20.0065	10000	.9613951	1.096177E-03

TABLE 35

DYNAMIC MODEL RESULTS

TEMPERATURE RAMP RATE = 10000 DEG.C/MIN.
INITIAL RAMP TEMPERATURE = 110 DEG.C
FINAL RAMP TEMPERATURE = 111 DEG.C
ISOTHERMAL HOLD TIME AT 111 DEG.C = 60 MIN.

TIME (MIN.)	VISCOSITY (POISE)	CURE	HEAT OUTPUT (cal/g/s)
		RAMP CONDITIONS	
0	217.1399	.0000001	0
9.999999E-06	216.2564	1.000203E-07	3.904496E-06
.00002	215.3763	1.000411E-07	3.982035E-06
.00003	214.5011	1.000622E-07	4.060971E-06
.00004	213.6293	1.000838E-07	4.14136E-06
4.999999E-05	212.7616	1.001059E-07	4.223244E-06
5.999999E-05	211.898	1.001283E-07	4.306616E-06
7.000003E-05	211.0385	1.001512E-07	4.391482E-06
8.000011E-05	210.1827	1.001745E-07	4.477945E-06
9.000018E-05	209.331	1.001984E-07	4.565968E-06
		ISOTHERMAL CONDITIONS	
1.000003E-04	208.4829	1.002227E-07	4.655612E-06
6.0001	210.2212	3.711046E-04	2.239933E-04
12.0001	212.2412	1.372461E-03	4.132688E-04
18.0001	214.5506	2.945691E-03	5.903431E-04
24.0001	217.1583	5.059762E-03	7.591642E-04
30.0001	220.0748	7.69168E-03	9.213581E-04
36.0001	223.3114	1.082209E-02	1.077728E-03
42.0001	226.8813	1.443347E-02	1.228693E-03
48.0001	230.7987	1.850928E-02	1.374462E-03
54.0001	235.0795	.0230334	1.515117E-03
60.0001	239.7414	2.798984E-02	1.65066E-03

TABLE 36

DYNAMIC MODEL RESULTS

TEMPERATURE RAMP RATE = 1 DEG.C/MIN.
INITIAL RAMP TEMPERATURE = 110 DEG.C
FINAL RAMP TEMPERATURE = 175 DEG.C
ISOTHERMAL HOLD TIME AT 175 DEG.C = .1 MIN.

TIME (MIN.)	VISCOSITY (POISE)	CURE	HEAT OUTPUT (cal/g/s)
		RAMP CONDITIONS	
0	284.629	.0000001	0
6.5	219.5515	3.244295E-04	1.826251E-04
13	172.3091	3.102394E-03	1.163894E-03
19.5	138.3897	1.468848E-02	4.324485E-03
26	115.0278	4.851643E-02	.0116378
32.5	101.1441	.1237562	2.386073E-02
39	98.02626	.2522486	3.693257E-02
45.5	112.2917	.4183631	4.261212E-02
52	170.8708	.5845409	3.833922E-02
58.5	459.1123	.7263398	3.000778E-02
		ISOTHERMAL CONDITIONS	
65	6063.23	.8460181	2.245727E-02
65.01001	6063.241	.8463638	6.616072E-02
65.02002	6063.253	.8467085	6.599937E-02
65.03003	6063.265	.8470524	.0658383
65.04004	6063.279	.8473957	6.567738E-02
65.05005	6063.293	.8477378	6.551696E-02
65.06006	6063.307	.8480791	6.535676E-02
65.07007	6063.323	.8484199	.0651968
65.08008	6063.338	.8487596	.0650372
65.09009	6063.355	.8490984	6.487798E-02
65.1001	6063.372	.8494365	6.471895E-02

TABLE 37

DYNAMIC MODEL RESULTS

TEMPERATURE RAMP RATE = 1 DEG.C/MIN.
INITIAL RAMP TEMPERATURE = 110 DEG.C
FINAL RAMP TEMPERATURE = 160 DEG.C
ISOTHERMAL HOLD TIME AT 160 DEG.C = 50 MIN.

TIME (MIN.)	VISCOSITY (POISE)	CURE	HEAT OUTPUT (cal/g/s)
	RAMP CONDITIONS		
0	267.0397	.0000001	0
5	218.8111	1.991194E-04	1.448009E-04
10	181.054	1.536225E-03	7.182347E-04
15	151.5938	6.268718E-03	2.291049E-03
20	128.859	1.888212E-02	5.734351E-03
25	111.7952	4.662727E-02	1.199425E-02
30	99.85381	9.859349E-02	2.137546E-02
35	93.09319	.1818572	3.238126E-02
40	92.48789	.2951318	4.129353E-02
45	100.7747	.4255066	4.438182E-02
	ISOTHERMAL CONDITIONS		
50	125.0645	.5547739	4.132991E-02
55	156.8749	.6705843	3.514023E-02
60	414.0583	.744916	2.285726E-02
65	3874.465	.7938898	1.528507E-02
70	110940.8	.827061	1.050133E-02
75	10000	.8501236	7.396787E-03
80	10000	.8665451	5.328628E-03
85	10000	.8784911	3.917039E-03
90	10000	.8873498	2.931976E-03
95	10000	.894033	2.230564E-03
100	10000	.8991538	1.721936E-03

TABLE 38

DYNAMIC MODEL RESULTS

TEMPERATURE RAMP RATE = .1 DEG.C/MIN.
INITIAL RAMP TEMPERATURE = 110 DEG.C
FINAL RAMP TEMPERATURE = 160 DEG.C
ISOTHERMAL HOLD TIME AT 160 DEG.C = 50 MIN.

TIME (MIN.)	VISCOSITY (POISE)	CURE	HEAT OUTPUT (cal/g/s)
		RAMP CONDITIONS	
0	281.6267	.0000001	0
50	254.1368	1.484889E-02	1.107653E-03
100	248.3114	9.546419E-02	4.015586E-03
150	273.1323	.2819874	7.188129E-03
200	356.3957	.5029358	5.102011E-03
250	603.9233	.6226681	7.215208E-04
300	1727.236	.6931607	2.885645E-04
350	19889.57	.7530405	3.844194E-04
400	10000	.8043845	4.451949E-04
450	10000	.8479915	4.563567E-04
		ISOTHERMAL CONDITIONS	
500	10000	.8847582	4.212789E-04
505	10000	.8920666	2.432813E-03
510	10000	.8976393	1.869497E-03
515	10000	.9019502	1.456345E-03
520	10000	.9053288	1.14859E-03
525	10000	.9080079	9.161042E-04
530	10000	.9101556	7.381712E-04
535	10000	.9118941	6.004029E-04
540	10000	.9133141	4.925741E-04
545	10000	.9144834	4.073288E-04
550	10000	.915454	3.393028E-04

TABLE 39

DYNAMIC MODEL RESULTS

TEMPERATURE RAMP RATE = 10 DEG.C/MIN.
INITIAL RAMP TEMPERATURE = 110 DEG.C
FINAL RAMP TEMPERATURE = 160 DEG.C
ISOTHERMAL HOLD TIME AT 160 DEG.C = 50 MIN.

TIME (MIN.)	VISCOSITY (POISE)	CURE	HEAT OUTPUT (cal/g/s)
		RAMP CONDITIONS	
0	265.983	.0000001	0
.5	216.5003	3.375331E-06	2.082189E-05
1	177.2342	2.511013E-05	1.163479E-04
1.5	145.918	1.162113E-04	4.4938E-04
2	120.8261	4.115178E-04	1.380423E-03
2.5	100.6391	1.210222E-03	3.586044E-03
3	84.34286	3.086699E-03	8.157021E-03
3.5	71.1568	7.013578E-03	1.661231E-02
4	60.47997	.0144563	3.074123E-02
4.5	51.85438	2.737564E-02	5.219483E-02
		ISOTHERMAL CONDITIONS	
5	44.93924	4.807168E-02	8.185363E-02
10	76.74971	.3352842	9.313288E-02
15	333.9331	.5315871	5.940603E-02
20	3794.34	.6558711	3.765114E-02
25	110860.7	.7353658	2.438961E-02
30	10000	.7875174	1.623959E-02
35	10000	.8226918	1.111181E-02
40	10000	.8470519	7.79782E-03
45	10000	.8643358	5.598863E-03
50	10000	.8768692	4.103437E-03
55	10000	.8861372	3.063297E-03

TABLE 40

DYNAMIC MODEL RESULTS

TEMPERATURE RAMP RATE = 3 DEG.C/MIN.
INITIAL RAMP TEMPERATURE = 110 DEG.C
FINAL RAMP TEMPERATURE = 175 DEG.C
ISOTHERMAL HOLD TIME AT 175 DEG.C = 20 MIN.

TIME (MIN.)	VISCOSITY (POISE)	CURE	HEAT OUTPUT (cal/g/s)
		RAMP CONDITIONS	
0	283.6418	.0000001	0
2.166667	217.3095	4.275448E-05	6.96665E-05
4.333334	168.413	4.36902E-04	4.994085E-04
6.5	132.1776	2.300226E-03	2.123657E-03
8.666667	105.2928	8.553109E-03	6.651433E-03
10.83333	85.50037	.0250586	1.661649E-02
13	71.36555	6.085311E-02	3.420889E-02
15.16667	62.22885	.1256222	5.853973E-02
17.33333	58.42055	.2239055	8.356095E-02
19.5	62.14253	.3513502	.1019347
		ISOTHERMAL CONDITIONS	
21.66667	81.00922	.5018009	.1138488
23.66667	101.5026	.6773944	.1376139
25.66667	272.262	.7945601	8.951246E-02
27.66667	2663.852	.8690354	.0553369
29.66667	81474.1	.9138859	3.224722E-02
31.66667	10000	.9392139	1.748066E-02
33.66667	10000	.9524151	8.63823E-03
35.66667	10000	.9586136	3.770334E-03
37.66667	10000	.9611373	1.379537E-03
39.66667	10000	.9619724	3.848172E-04
41.66667	10000	.9621714	6.684165E-05

TABLE 41

Preconversion Times

Isothermal Preconversion Temperature °C	Preconversion 10%	20%	30%	40%	50%
125	38.9	66.7	93.9	122.9	159.2
130	21.8	37.3	52.5	68.9	88.4
135	13.2	22.8	32.5	42.7	55.1
145	5.5	9.9	14.5	19.6	25.8
150	3.7	6.8	10.1	14	18.6

Table 42

Preconversion at 135°C

Isothermal Temperature °C

Amount of Preconversion		125	135	150
10%	K	1.155×10^{-4}	2.555×10^{-4}	5.642×10^{-4}
	KAUTO	(1.170×10^{-4})	(2.592×10^{-4})	(5.719×10^{-4})
	r	1.239	1.868	4.360
20%	K	1.198×10^{-4}	2.396×10^{-4}	5.206×10^{-4}
	KAUTO	(1.117×10^{-4})	(2.122×10^{-4})	-
	r	1.387	2.142	6.136
30%	K	1.071×10^{-4}	2.658×10^{-4}	5.738×10^{-4}
	KAUTO	(8.704×10^{-5})	(2.895×10^{-4})	-
	r	1.430	2.244	9.257
40%	K	1.063×10^{-4}	2.087×10^{-4}	5.095×10^{-4}
	KAUTO	-	-	-
	r	5	11.391	12.990
50%	K	8.064×10^{-5}	1.619×10^{-4}	4.109×10^{-4}
	KAUTO	-	-	-
	r	35.466	25.041	16.700

Table 43

30% Conversions

K,m values

Preconversion Temperature °C		Isothermal Temperature °C		
		125	135	150
125	K	1.377×10^{-4}	2.836×10^{-4}	6.130×10^{-4}
	m	1.177	1.465	1.138
130	K	1.134×10^{-4}	2.004×10^{-4}	5.396×10^{-4}
	m	2.777	1.992	1.317
135		1.071×10^{-4}	2.658×10^{-4}	5.738×10^{-4}
		2.075	1.353	1.125
145	K	1.854×10^{-4}	2.728×10^{-4}) 2.645×10^{-4})	6.716×10^{-4}
	m	0.680	0.982) 1.068)	1.176
150	K	1.400×10^{-4}	3.207×10^{-4}	6.543×10^{-4} 6.371×10^{-4}
	m	0.684	1.096	0.961 1.045
Mean	K	1.367×10^{-4}	2.680×10^{-4}	6.149×10^{-4}
	m	1.479	1.333	1.120

Table 44

Residual Exotherms - 30% Conversion

Preconversion Temperature °C	Isothermal Temperature °C: 125	135	150
125	43.67	56.53	71.20 75.53
130	27.22	49.01	65.29
135	44.98	51.15	68.61
145	65.52	58.84 59.55	67.49
150	51.81	65.77	76.77 74.80
Mean	46.64	56.81	71.38

Table 45

Tg of 30% Preconverted Resin

Preconversion Temperature °C	Isothermal Cure Conditions		Tg °C
	Time (min)	Temperature °C	
125	180	125	79.99
	120	135	99.26
	60	150	111.51, 100.57
130	180	125	90.58
	120	135	93.37, 103.04
	60	150	93.69
135	180	125	85.17
	120	135	85.97
	60	150	91.80
145	180	125	87.58
	120	135	95.48, 91.22
	60	150	94.01
150	180	125	95.86
	120	135	98.25
	60	150	99.66

Table 46

APPENDIX 2

VISICURE PROGRAM

```
10 REM"VISICURE
20 GOSUB 21000
40 GOSUB 2000
50 GOSUB 3000
60 GOSUB 4000
70 GOSUB 5000
80 GOSUB 6000
90 GOSUB 7000
95 REC=0
100 GOSUB 24000
110 GOSUB 8000
120 GOSUB 26000
130 GOSUB 11000
500 END
2000 REM"DEFINE TITLE
2020 LOCATE 1,6
2030 PRINT "VISCOSITY AND CURE OF BSL914"
2500 RETURN
3000 REM"DEFINE CURVES
3010 VIEW (199,60)-(319,160)
3020 LINE (1,7)-(15,7),3
3030 LINE (1,15)-(15,15),2
3040 LINE (1,23)-(15,23),1
3045 PSET (3,31),2:CIRCLE (3,31),2,2
3046 PSET (12,31),2:CIRCLE (12,31),2,2
3050 LOCATE 9,28
3060 PRINT "T:110-200 C"
3070 LOCATE 10,28
3080 PRINT "V:0-1000 P"
3090 LOCATE 11,28
3100 PRINT "C:0-1"
3110 LOCATE 12,28
3120 PRINT "dH/dt:0-.3c/s"
3500 RETURN
4000 REM"DRAW GRAPH AXES"
4010 VIEW (0,20)-(199,160)
4020 LINE (10,5)-(190,120),3,B
4030 FOR I=1 TO 9
4040 YY=(120-INT(I*(115/10)))
4050 XX=(10+INT(I*(180/10)))
4060 LINE (10,YY)-(190,YY),3,,&HAAAA
4070 LINE (XX,120)-(XX,5),3,,&HAAAA
4080 NEXT I
4500 RETURN
5000 REM"INPUT PARAMETERS
5010 LOCATE 19,8
5015 PRINT "TIME (MINS.)"
5020 LOCATE 20,1
5030 INPUT "TEMP.RAMP RATE (DEG.C/MIN.)=",R
5050 INPUT "FINAL RAMP TEMPERATURE (DEG.C)=",TF
5070 INPUT "ISOTHERMAL HOLD TIME (MINS.)=",TH
5075 GOTO 5500
5080 LPRINT "R="R"  TF="TF"  TH="TH
5500 RETURN
```

```
6000 REM"SCALE FACTORS
6010 TX=((((TF-110)/R)*60)+(TH*60))
6020 TR=(((TF-110)*60)/R)
6030 TS=(TH*60)
6040 SX=180/TX
6045 ST=115/90
6050 SC=115/1
6060 SV=115/1000
6070 SH=115/.3
6500 RETURN
7000 REM"DRAW TEMP.PROFILE
7010 PP=((SX*TR)+10)
7015 MM=(120-(ST*(TF-110)))
7020 VIEW (0,20)-(199,160)
7030 LINE (10,120)-(PP,MM),3
7040 LINE (PP,MM)-(190,MM),3
7050 LOCATE 17,22
7060 PRINT INT((TR+TS)/60)
7070 LOCATE 23,1
7500 RETURN
8000 REM"EVALUATE VIS MODEL
8010 NR=((N/2)+1)
8020 NI=N/2
8030 NT=(NR+NI)
8040 DIM V(NT,2)
8050 VA=0
8060 TP=((TF-110)/(N/2))
8070 TV=(110-TP)
8080 FOR I=1 TO NT
8085 IF REC=1 THEN GOTO 8295
8090 IF I>NR THEN GOTO 8170
8100 SR=TP/R
8110 V(I,1)=((I-1)*SR*60)
8120 XO=(((-4400)*(1/(TV+273.2)))+8.2)
8130 XI=((2600*(1/(TV+273.2)))-4.45)
8140 XT=(((-11300)*(1/(TV+273.2)))+24.3)
8150 TV=(TV+TP)
8160 GOTO 8190
8170 SR=((TH/NI)*(I-NR))
8180 V(I,1)=(TR+(SR*60))
8190 Q=10^XT
8200 W=SR^2
8210 B=10^XO
8220 ZT=((Q*W)+(B*SR))
8230 VI=10^XI
8240 VT=10^(ZT+XI)
8250 IF I>NR THEN GOTO 8290
8260 VA=(VA+VT-VI)
8270 V(I,2)=(VI+VA)
8280 GOTO 8295
8290 V(I,2)=(VA+VT)
8295 IF V(I,2)>10000 THEN REC=1 ELSE IF REC=1 THEN V(I,2)=10000
8300 NEXT I
8500 RETURN
```

```
9000 REM"CURE WARNING
9005 FLAG=1
9010 VIEW (200,20)-(319,60)
9015 PSET (15,31),1
9020 CIRCLE (15,31),5,1
9030 PAINT (15,31),1
9050 LOCATE 7,29
9060 PRINT "CURE>.3"
9070 VIEW (0,20)-(199,160)
9400 LOCATE 23,1
9500 RETURN
10000 REM"GEL WARNING
10005 PLUG=1
10010 VIEW (200,20)-(319,60)
10015 PSET (15,15),2
10020 CIRCLE (15,15),5,2
10030 PAINT (15,15),2
10050 LOCATE 5,29
10060 PRINT ">GEL PT."
10070 VIEW (0,20)-(199,160)
10400 LOCATE 23,1
10500 RETURN
11000 REM"PRINTOUT
11010 LPRINT "DYNAMIC MODEL RESULTS":LPRINT
11020 LPRINT "TEMPERATURE RAMP RATE = "R" DEG.C/MIN."
11030 LPRINT "INITIAL RAMP TEMPERATURE = 110 DEG.C"
11040 LPRINT "FINAL RAMP TEMPERATURE = "TF" DEG.C"
11050 LPRINT "ISOTHERMAL HOLD TIME AT "TF" DEG.C = "TH" MIN."
11060 LPRINT
11070 LPRINT "TIME (MIN.)"TAB(15)"VISCOSITY (POISE)"TAB(35)"CURE"TAB(50)"HEAT OU
TPUT (cal/g/s)"
11080 FOR I=1 TO (N+1)
11085 IF I=1 THEN LPRINT TAB(27)"RAMP CONDITIONS"
11086 IF I=((N/2)+1) THEN LPRINT TAB(24)"ISOTHERMAL CONDITIONS"
11090 LPRINT (A(I,1)/60)TAB(15)V(I,2)TAB(35)A(I,2)TAB(50)H(I,2)
11100 NEXT I
11500 RETURN
21000 REM"SUBINIT
21020 CLS
21030 SCREEN 1
21040 KEY OFF
21050 WIDTH 40
21499 RETURN
```

```
24000 REM*SUBDIEQ
24040 XL=0
24050 YL=.0000001
24060 XH=(TR+TS)
24070 N=20
24080 NS=20
24090 DIM A((N+1),2)
24100 DIM C(N,(NS+1))
24105 DIM H((N+1),2)
24110 C=XL
24115 A(1,1)=C
24120 D=YL
24125 A(1,2)=D
24127 T=110
24134 FOR I=1 TO N
24135 L=I
24136 IF I>(N/2) THEN GOTO 24139
24137 H=(((TF-110)*60)/(R*NS*(N/2)))
24138 GOTO 24140
24139 H=((TH*60)/(NS*(N/2)))
24140 FOR J=1 TO (NS+1)
24142 IF I>((N/2)+1) THEN GOTO 24150
24145 GOSUB 30000
24150 IF I=1 AND J=1 THEN GOTO 24210
24160 IF J=1 THEN GOTO 24190
24161 IF (F*D)=>1 THEN TRAP=1 ELSE TRAP=0
24162 IF TRAP=1 THEN GOTO 24175
24164 GA=FNRAT(D)
24166 D=(D+(H*GA))
24167 IF (F*D)=>1 THEN GOTO 24175
24168 GB=FNRAT(D)
24170 GM=((GA+GB)/2)
24175 IF TRAP=0 THEN C(I,J)=(C(I,(J-1))+(H*GM)) ELSE C(I,J)=(C(I,(J-1)))
24180 GOTO 24220
24190 C(I,J)=C((I-1),(NS+1))
24200 GOTO 24220
24210 C(I,J)=YL
24220 C=C+H
24230 D=C(I,J)
24240 NEXT J
24250 C=C-H
24255 IF I>(N/2) THEN GOTO 24260
24257 T=(T+((NS*H*R)/60))
24260 A((L+1),1)=C
24270 A((L+1),2)=D
24272 IF TRAP=0 THEN H((L+1),2)=(115*FNRAT(D)) ELSE H((L+1),2)=0
24280 NEXT I
24300 RETURN
```

```
26000 REM*SUBMPLOT
26010 FLAG=0
26020 PLUG=0
26030 DIM B((N+1),2)
26035 DIM BV((N+1),2)
26037 DIM BH((N+1),2)
26040 FOR I=1 TO (N+1)
26050 FOR J=1 TO 2
26060 ON J GOTO 26070,26090
26070 B(I,J)=SX*(A(I,J))
26075 BV(I,J)=(SX*(V(I,J)))
26077 BH(I,J)=(SX*(A(I,J)))
26080 GOTO 26100
26090 B(I,J)=SC*(A(I,J))
26095 BV(I,J)=(SV*(V(I,J)))
26097 BH(I,J)=(SH*(H(I,J)))
26100 NEXT J
26110 NEXT I
26120 VIEW (0,20)-(199,160)
26240 FOR I=1 TO (N+1)
26250 FOR J=1 TO 2
26260 ON J GOTO 26270,26290
26270 X=10+INT(B(I,J))
26275 XV=10+INT(BV(I,J))
26277 XE=10+INT(BH(I,J))
26280 GOTO 26300
26290 Y=120-INT(B(I,J))
26295 YV=120-INT(BV(I,J))
26297 YE=120-INT(BH(I,J))
26300 NEXT J
26310 IF I=1 THEN PSET (X,Y),1
26320 IF I=1 THEN GOTO 26390
26321 LINE -(X,Y),1
26324 IF V(I,2)>=10000 THEN GOTO 26337
26326 AB=10+INT(BV((I-1),1))
26328 BC=120-INT(BV((I-1),2))
26333 PSET (AB,BC),2
26334 LINE (AB,BC)-(XV,YV),2
26337 IF FLAG=1 THEN GOTO 26350
26338 IF Y<(120-38) THEN GOSUB 9000
26350 IF PLUG=1 THEN GOTO 26380
26360 IF YV<5 THEN GOSUB 10000
26380 PSET (XE,YE),2
26383 CIRCLE (XE,YE),2,2
26385 PSET (X,Y),1
26387 FOR CC=1 TO 300:NEXT CC
26390 NEXT I
26399 RETURN
```

```
30000 REM"SUBFNACF
30010 REM"GENERALISED AUTOCATALYSED KINETICS MODEL FUNCTION"
30015 CU=(((1.204E-06)*((T+273.2)^2))+((-9.691656E-04)*(T+273.2))+.1950166)
30020 HT=(((-1.840437E-02)*((T+273.2)^2))+(16.53196*(T+273.2))-3601.842)
30022 IF D>CU THEN GOTO 30030
30024 NI=(((-1.515142E-02)*(T+273.2))+6.870618)
30026 GOTO 30040
30030 NI=(((-6.571918E-03)*(T+273.2))+2.994045)
30040 LR=(((-8796.092)*(1/(T+273.2)))+22.46026)
30050 RA=((2.718282)^LR)
30060 M=(NI*RA)
30070 F=115/HT
30072 IF D>CU THEN GOTO 30080
30074 LNK=(((-12989.99)*(1/(T+273.2)))+24.58238)
30076 GOTO 30090
30080 LNK=(((-8379.384)*(1/(T+273.2)))+13.02864)
30090 K=(((2.718282)^LNK)/F)
30100 DEF FNRAT(C)=(K*((F*C)^NI)*((1-(C*F))^M))
30199 RETURN
```

APPENDIX 3

FORMULAE AND CONVERSIONS.

The Arrhenius Equation and Conversion Factors

a) In the Arrhenius equation

$$k = A \exp E/RT \qquad (1)$$

k is the rate constant with units $sec.^{-1}$ in text.

A is the pre-exponential or frequency factor with units $sec.^{-1}$

R is the gas constant with dimensions

[R] = [ENERGY]/([DEGREES K] x [NO OF MOLES])

Units of R are $cal.deg.^{-1}mole^{-1}$ in text.

For the exponent to be a numerical factor the dimensions [X] of E can be obtained from

[E]/[RT] = [X]/([R] x [DEGREES K])

For the R.H.S. to be dimensionless the dimensions of [X] is given by

[X] = [ENERGY]/[MOLE]

E has therefore the dimensions of energy and is called the Activation Energy with units expressed in $cal.mole^{-1}$ or Joules $mole^{-1}$ in text

By taking natural logarithms of (1)

$$\ln k = (E/R)(1/T) + \ln A$$

in the form of the equations in the text.

From the slopes of the text equations therefore

$$\text{Activation Energy, } E = R \times \text{slope} \qquad (2)$$

Equation (2) applies to all the equations relating to the cure kinetics in the text.

The equivalent base 10 relation to eq (2) is given below.

Since $\log k = \ln k/\ln 10$

then $\log k = (\ln A + (E/R(1/T)))/\ln 10$

$= \ln A/(2.3026) + (E/(2.3026R))(1/T)$

b) Conversion Factors

1 Pascal	=	6894.76 psi (Pounds per square inch)
1 calorie	=	4.184 Joules
1 centipoise	=	$1 mN.s/m^2$